Systemphysiologische Untersuchungen zur Temperaturtoleranz des gemeinen Tintenfischs *Sepia officinalis*

Systemic investigations on the physiology of temperature tolerance in the common cuttlefish *Sepia officinalis*

Frank Melzner

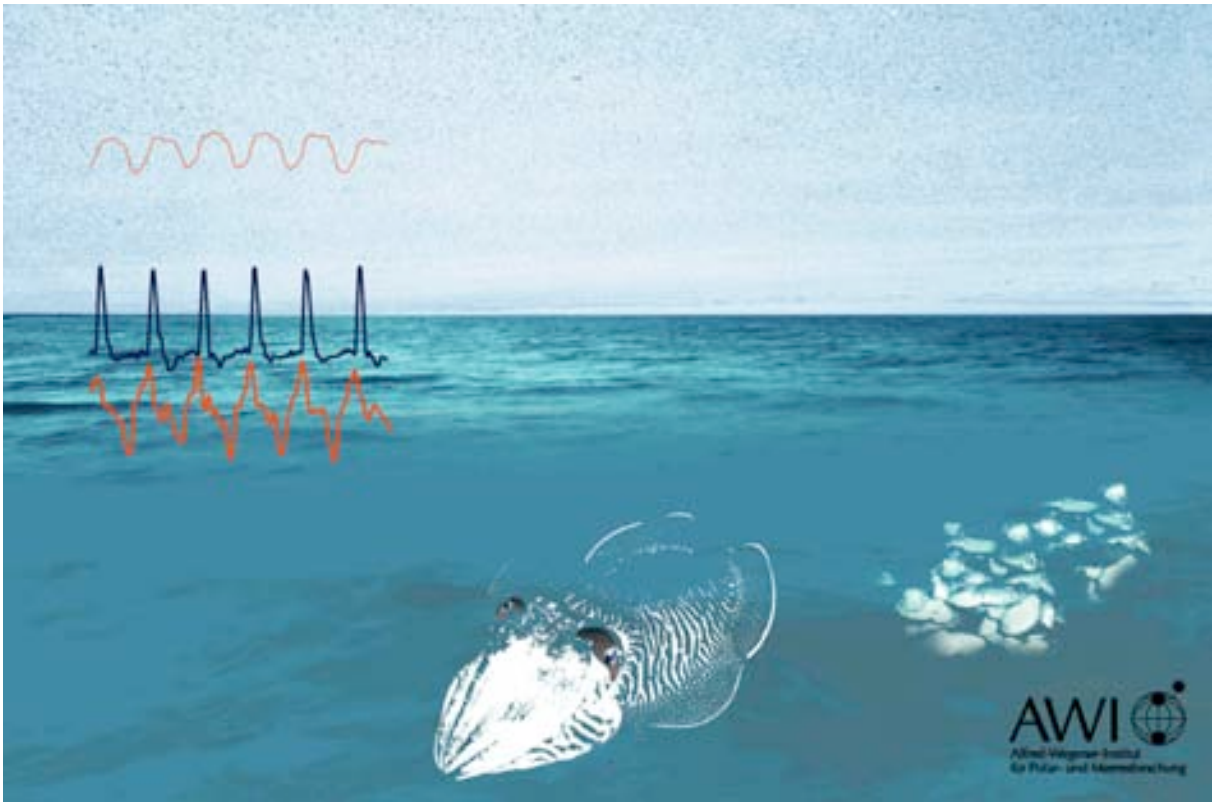

Systemphysiologische Untersuchungen zur Temperaturtoleranz des gemeinen Tintenfischs *Sepia officinalis*

Systemic investigations on the physiology of temperature tolerance in the common cuttlefish *Sepia officinalis*

Dissertation

Zur Erlangung des akademischen Grades

- Dr. rer. nat. –

dem Fachbereich 2 Biologie / Chemie

der Universität Bremen

vorgelegt von

Frank Melzner

Diplom-Biologe

Bremen 2005

I am strongly induced to believe that as in music, the person who understands every note will, if he also possesses a proper taste, more thoroughly enjoy the whole, so he who examines each part of a fine view, may also thoroughly comprehend the full and combined effect.

- Charles Darwin, The Voyage of the Beagle

Gutachter:

1. Gutachter: Prof. Dr. H.O. Pörtner, Universität Bremen
   Alfred-Wegener-Institut für Polar- und Meeresforschung
   Am Handelshafen 12, 27570 Bremen
2. Gutachter: Prof. Dr. G.O. Kirst, Universität Bremen
   FB II Biologie / Chemie Universität NW II A
   Leobener Strasse, 28359 Bremen

Contents

Summary

Mechanisms that affect thermal tolerance of ectothermic organisms have recently received much interest, due to global warming and climate change debates in both the public and in the scientific community. In physiological terms, thermal tolerance of several marine ectothermic taxa can be linked to oxygen availability, with capacity limitations in ventilatory and circulatory systems contributing to oxygen limitation at extreme temperatures. The present thesis set out to investigate the role of the systemic oxygen transfer apparatus in defining thermal tolerance in a cephalopod, the common cuttlefish *Sepia officinalis*. In an attempt to identify unifying principles of thermal tolerance, cephalopods make good comparative model species as, although being invertebrates, they have adopted a vertebrate-like high power lifestyle.

In a first approach, ventilatory mantle muscle metabolism was monitored in unrestrained animals subjected to acute thermal change, using non-invasive ^{31}P - NMR spectroscopy. Both at low (7°C) and high (26.6°C) extreme temperatures, utilization of muscle phosphagen (phospho-L-arginine) was observed to complement aerobic metabolism in animals of >100g body mass, indicating an oxygen limitation of aerobic metabolism.

Consequently, the role of the ventilatory system was investigated in more detail by measuring oxygen extraction from the ventilatory current and ventilatory pressure in combination with metabolic rate. Ventilatory power output could be modulated 83-fold over the entire thermal range studied (8-26°C), and calculated adjustments in ventilatory water flow were always found to be sufficient to ensure the high arterial PO_2 values (>14 kPa), necessary for efficient haemocyanin loading in the gills. Thus, it mostprobably is not the action of ventilatory muscles that becomes limiting for oxygen flux at extreme temperatures and causes the transition to anaerobic metabolism. This idea was further substantiated by the observation of lower than expected metabolic rates at temperatures of 11°C and 23°C already.

Therefore circulatory oxygen transport was examined in more detail. Measuring venous blood flow for the first time in a cephalopod, initial work focused on analyzing flow patterns under control and exercise conditions (15°C) in the most important cephalopod vein, the anterior vena cava (AVC). A tight coupling of AVC blood pulses to ventilatory pressure oscillations was observed under all conditions. Following exercise, blood flow could be elevated 2.2-fold above control. Subsequently testing the AVC system during temperature change revealed a circulatory capacity limitation at temperatures >22-23°C, going along with dramatic changes in blood pulse shape and a functional disintegration of the tight ventilatory – circulatory pulse coupling. Maximum patterns of blood flow at 22-23°C strikingly resembled those observed under recovery from exercise, suggesting that blood vessel mechanics limit higher blood flow rates, and, concomitantly tolerance of higher temperatures.

The transition to anaerobic metabolism in ventilatory muscles therefore is secondary to circulatory failure.

At temperatures < 11°C, blood pulse shape also changed characteristically from control patterns. However, probably more importantly, haemocyanin function was observed to be hampered by high blood pH, typical at low temperatures: Liberation of significant fractions of oxygen from the blood pigment is only possible at venous PO_2 values of < 1 kPa at < 11°C, permitting only low metabolic rates and probably causing the transition to anaerobic metabolism at 7°C.

An optimum in AVC function was identified at the acclimation temperature of 15°C. In addition, it also could be shown that *S. officinalis* can perform full metabolic acclimation of each, metabolic rate, AVC and ventilatory pulse rates, to an altered temperature of 20°C. This suggests, that the species can adapt cardiovascular function and scope to varying seasonal temperatures, thus shift its thermal tolerance window accordingly to match habitat temperatures.

In comparison to teleost species it became obvious that similar adaptations in life-style have resulted in similar system limitations during acute thermal change: In both high-power ecotypes, it is the circulatory system that eventually limits thermal tolerance on an organismic level, especially at high temperatures.

1. Introduction

In the context of current discussions of climate change (e.g. Hulme et al. 1999), effects of temperature on organisms and entire ecosystems has gained wide public interest. The present thesis will provide information on thermal tolerance mechanisms in a marine high power invertebrate, the cephalopod *Sepia officinalis*, adding yet another mosaic piece towards the understanding of unifying patterns of thermal tolerance in ectothermic marine animals (Pörtner et al. 2004).

1.1 Thermal tolerance in marine ectothermic animals

Researchers have intensively investigated heat and cold tolerance of several marine and freshwater fish species as fish aquaculture became more popular in the northern hemisphere in the first half of the 20th century (see Fry 1971 for a review). Early studies focused on short term lethal temperatures and the shift of these upon thermal acclimation, resulting in the construction of characteristic thermal tolerance diagrams for several species (Brett 1944, 1946, Fry et al. 1942, 1946). Later these were extended to also incorporate thermal ranges for activity and reproduction. Typically, thermal tolerance window widths were found to be greatest for animals at rest, while those for active animals and reproducing animals were found to be progressively narrower (see fig. 8 in Fry 1971 and Brett 1952, 1958, Brett and Alderdice 1958, Hoff and Westmann 1966). However, little research was devoted to the underlying mechanisms that cause ectothermic animals to experience such temperature dependent limitations.

Recent investigations on a number of marine ectothermic animals have shed some light on the mechanisms that limit thermal tolerance. Interestingly, invertebrate and vertebrate organisms may ultimately be constrained by oxygen availability, both at critically high and low temperatures. In annelid and sipunculid worms (Sommer et al. 1997, Zielinski and Pörtner 1996), a crustacean (Frederich and Pörtner 2000) and teleost species (Van Dijk et al. 1999), anaerobic metabolism was observed to set in at low and high extreme temperatures. Prior to the onset of anaerobic metabolism, detrimental changes in ventilatory and or circulatory performance could be observed in fish and crustacean species (Heath and Hughes 1973, Frederich and Pörtner 2000, Mark et al. 2002, Lannig et al. 2004), leading to the view that a second set of natural threshold temperatures may exist that characterizes initial limitations of the oxygen transport apparatus. Consequently, Frederich and Pörtner (2000), building on the conceptual framework of Shelford (1931) and Fry (1971), postulated a thermal tolerance model that defines threshold temperatures in relation to aerobic scope that is available to the animal (see fig 1.1).

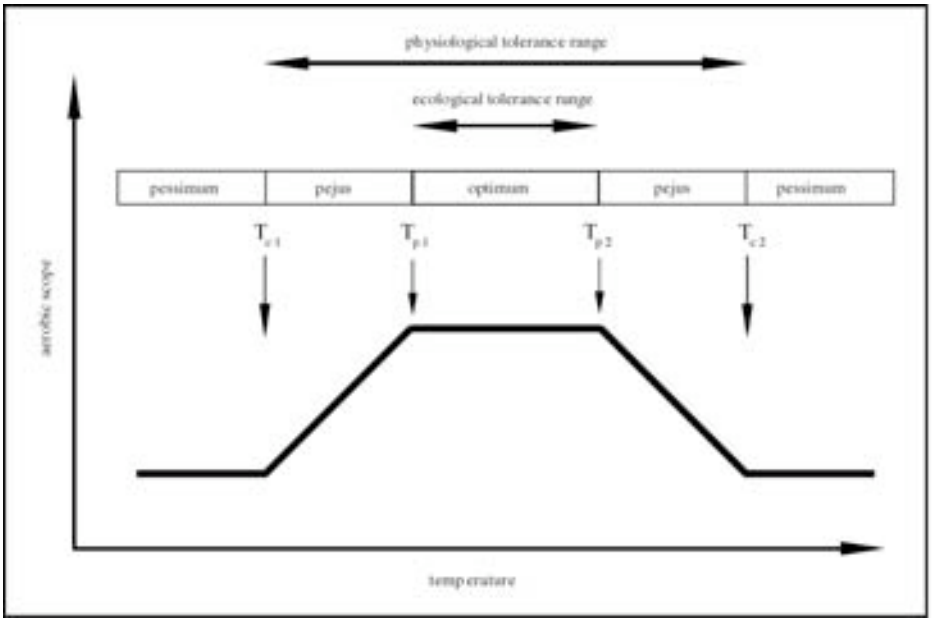

Fig 1.1: Oxygen limitation of thermal tolerance. Modified after Frederich and Pörtner (2000). See text for explanations.

As aerobic scope (AS) is the difference between maximum (sustainable) and standard metabolic rate (Fry 1947), the thermal interval in which AS is maximized was termed an optimum thermal range. In this range, enough AS is available to support all major oxygen consuming processes that ensure survival of the species on an ecological scale (i.e. growth, activity, reproduction). Those threshold temperatures above and below which aerobic scope declined were termed 'pejus' temperatures (T_{p1} and T_{p2} in fig 1.1). In these upper and lower pejus ranges, AS is not sufficient to sustain survival of the species on an ecological scale, however, residual AS may be sufficient to ensure short term survival. When AS drops to zero, critical temperatures are reached (T_{c1} and T_{c2}, fig. 1.1), anaerobic metabolism sets in to support standard metabolism and no scope for activity, growth and reproduction is left, therefore, T_{cs} indicate lethal limits due to a reliance on net use of anaerobic resources (Zielinski and Pörtner 1996, Sommer et al. 1997). The thermal interval between T_{p1} and T_{p2} (optimum) may determine the geographical distribution range of the species (Pörtner 2001). However, thermal acclimation was observed to shift entire thermal windows to lower or higher average temperatures, thus adding a certain degree of flexibility to the model (Sommer et al. 1997).

Choosing a cephalopod as a model organism, this thesis will mainly focus on the proposed unifying character of thermal tolerance mechanisms. Pörtner (2002a) introduced the concept of a systemic to molecular hierarchy of thermal tolerance mechanisms, indicating that any increase in the complexity of animal design may result in a decreased thermal sensitivity of the organism. Within organisms, the complex convection systems, the ventilatory and / or the circulatory systems, have been proposed to become limiting for tissue oxygen supply at pejus - temperatures in crustaceans and fish species (Frederich and Pörtner 2000, Mark et al. 2002, Lannig et al. 2004). As cephalopods are the only marine invertebrates that operate at comparable power as marine fish and have evolved similarly

efficient (and complex) oxygen transport systems, they represent a good model to test the proposed unifying mechanisms of thermal tolerance. Therefore, the present dissertation will investigate the systemic oxygen transport machinery of a model cephalopod organism and its response to changing temperatures. The following chapters will give a brief introduction of cephalopod metabolism and the design of cephalopod oxygen supply systems, to eventually lead to a set of questions that were addressed by carrying out adequate experiments.

1.2 Oxygen efficient energy metabolism

In comparison to marine teleosts, there are some marked differences in cephalopod muscle design that favor a more oxygen efficient mode of metabolism (see Hochachka 1994 for a review). Namely, cephalopods do not possess an intracellular oxygen carrier that would facilitate the diffusion of oxygen within cells (i.e. a myoglobin analogue, Wittenberg and Wittenberg 1990). Further, they are characterized by mitochondria being localized exclusively in the interfibrillar spaces, with no subsarcolemmal mitochondria being present in muscle tissues at all (Hochachka et al. 1978, Bone et al. 1981). Thus, characteristic localization of mitochondria in cephalopod muscles results in longer oxygen diffusion distances than in fish red muscles. Probably constantly operating at the verge of an oxygen limitation of muscle metabolism (Hochachka 1994), cephalopods have adopted some peculiar metabolic features: Most notably, squid mitochondria do not oxidize free fatty acids, but, rather, rapidly metabolize amino acids (especially proline and glutamate) and carbohydrates (Ballantyne et al. 1981, Mommsen and Hochachka 1981, Storey and Storey 1983). This may be of considerable significance, as β - oxidation of free fatty acids involves the formation of considerable amounts of $FADH_2$ (NADH to $FADH_2$ ratio = 1:1, Hochachka 1994), a reducing equivalent that results in less ATP production per mole oxygen than the carbohydrate or amino acid derived NADH does. That is, cephalopods avoid metabolic fuels that ‚waste' oxygen.

Consequently, and in analogy to insect flight muscle (Sacktor 1976), mainly proline stores are being utilized during high – intensity aerobic exercise in the squids *Loligo pealeii* (Storey and Storey 1978, Pörtner et al. 1993) and *Alloteuthis subulata* (Hochachka et al. 1983). As fig. 1.2 shows, one mole of proline, which is abundant at levels of up to 100 μmol g^{-1} wet $weight^{-1}$ in cephalopod muscles, can be oxidized to glutamate and be channeled into the Krebs cycle via α - ketoglutarate.

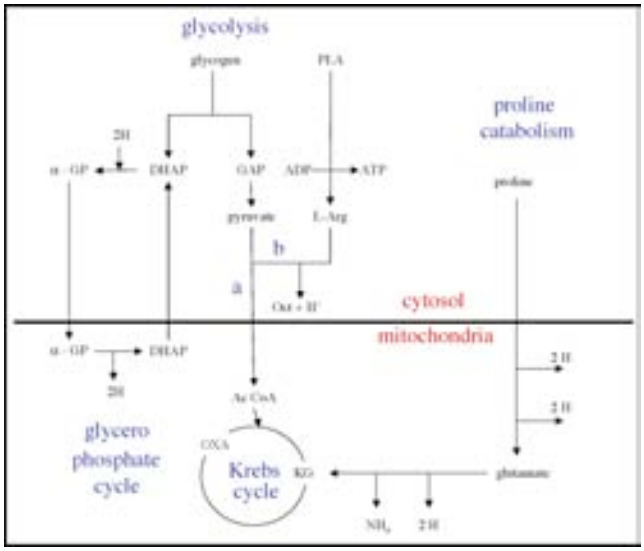

Fig. 1.2: Schematic illustration of aerobic and anaerobic metabolism in cephalopod molluscs, modified after Storey and Storey (1983) and Pörtner (1994). See text for explanations. Abbreviations: PLA = phospho L arginine, L-Arg = L arginine, Oct = octopine, GAP = glycerine aldehyde 3 phosphate, DHAP = dihydroxy acetone phosphate, α-GP = alpha glycerophosphate, AcCoA = acetyl coenzyme A, α-KG = alpha ketoglutarate, OXA = oxaloacetate. Note: For of clarity, Krebs cycle, respiratory chain and glycolysis reactions were largely omitted; a = aerobic pathway, pyruvate is channeled into the Krebs cycle, b = anaerobic pathway, pyruvate condenses with L arginine to form octopine.

It thereby leads to the production of 5 moles of NADH and 1 mole of $FADH_2$ (from proline to oxaloacetate, see fig 1.2), which can be used for the generation of approximately 17 moles of ATP in the respiratory chain (see Storey and Storey 1983). O'Dor and Wells (1978) have suggested that, in the absence of major lipid and carbohydrate storage in cephalopod muscle (Moon and Hulbert 1975), it is muscle protein that fuels cephalopod metabolism during periods of starvation. Aerobic carbohydrate metabolism resembles conditions found in vertebrates, with the exception that an α - glycerophosphate shuttle is being used to transport cytoplasmatic reducing equivalents into mitochondria (see fig 1.2).

A special feature of cephalopod metabolism is the high anaerobic capacity of certain muscle groups. Especially the central bulk of circular mantle muscle (see below and Bone et al. 1981) that is used for vigorously forcing water out of the mantle cavity during escape jetting or hunting, is progressively operating anaerobically at maximum exercise intensities (e.g. Pörtner et al. 1993, Finke et al. 1996). In cuttlefish *Sepia officinalis*, exercise and subsequent hypoxia led to depletion of both, muscle phospho - L – arginine (PLA) and glycogen stores, with PLA contributing about 33% and anaerobic glycolysis providing 66% to energy generation (Storey and Storey 1979, 1983). PLA is the cephalopod phosphagen and serves to buffer cellular ATP levels. In addition, L-arginine produced during transphosphorylation of PLA can condensate with accumulating glycolytic pyruvate to form octopine, the cephalopod anaerobic end product (e.g. Storey and Storey 1983). This is important to maintain redox balance during prolonged glycolytic energy production, as the condensation reaction results in the oxidation of NADH, thus regenerating NAD^+, which, in turn, is needed for the glyceraldehyde-3-phosphate dehydrogenase reaction of glycolysis (see fig 1.2). Muscular fatigue in

squid (*I. illecebrosus*, *L. pealeii*, *Lolliguncula brevis*) and cuttlefish (*S. officinalis*) during exercise or hypoxia is due to combined intensive PLA and / or ATP utilization along with changes in intracellular pH, manifesting itself in decreasing values of Gibb's free energy of ATP hydrolysis ($\Delta G/\Delta\xi$) (Storey and Storey 1979, Pörtner et al. 1993, 1996, Zielinski et al. 2000). Critical decreases in $\Delta G/\Delta\xi$ below the –45 to –50 kJ mol^{-1} that were found necessary for proper functioning of various cellular ATPases (Kammermeier et al. 1982, Combs and Ellington 1997, Jansen et al. 2003), were observed in all three squid species exercise or hypoxia induced fatigue.

Octopine production in cephalopods also goes along with an acidification of muscular tissues, helpful for eliciting transphosphorylation of PLA and ATP buffering during exercise, as observed in some squid species (*Illex illecebrosus, Lolliguncula brevis*, Pörtner et al. 1993, 1996). However, it could also be demonstrated that this acidification is constrained to muscular tissues, with little proton leakage into the blood stream (Pörtner et al. 1991). This is a necessary prerequisite for efficient gas transport in the blood, as will be explained below.

1.3 Blood oxygen transport

In contrast to the situation observed in fish, cephalopods do not posses an intracellular oxygen carrier. Rather, comparatively large haemocyanin (Hc) molecules with a molecular weight of 3.5 – 4.0 * 10^6 Dalton are being circulated, dissolved in the blood at concentrations ranging from approximately 60 to 145 g l^{-1} (Senozan et al. 1988, Pörtner 1990b, Zielinski et al. 2001). However, owing to the lower ratio of O_2 binding sites per unit molecular weight in haemocyanin as compared to fish haemoglobin (Miller 1994), as well as owing to viscosity and colloid – osmotic pressure constraints (Mangum 1990), oxygen carrying capacity of cephalopod bloods (1-3 mmol l^{-1}) is considerably lower than that of fish species (4-5 mmol l^{-1}; Mangum 1990). Consequently, cephalopod species have to pump much higher blood volumes to sustain even higher metabolic rates than their ectothermic high power competitors, the fishes (e.g. Wells et al. 1988, Shadwick et al. 1990 and see below). In addition, cephalopods have maximized the utilization (Ut = arterial Hc saturation – venous Hc saturation) of their haemocyanin oxygen shuttling capacities: While, under normoxic conditions, the pigment is typically fully saturated in gill vessels (S = 100%), venous haemocyanin saturation was found to be 20% or lower in several cephalopod species, giving a value for Ut of 80% or higher (Johansen et al. 1982, Houlihan et al. 1986, Mangum 1990, Pörtner, 1990b). Fish species are characterized by much lower Ut values under normoxic conditions, e.g. Ut = 30% for the rainbow trout, *Oncorhynchus mykiss* (Kiceniuk and Jones 1977).

High Ut values in cephalopods are a consequence of high Hc sensitivity to pH (=high Bohr and Haldane coefficients of < -1) and a high cooperativity of the pigment (see reviews by Mangum 1990, Pörtner 1994). In both, cuttlefish (*S. officinalis* Zielinski et al. 2001) and squid (*I. illecebrosus*,

L. pealeii, Pörtner 1990b), minor pH changes can liberate large fractions (>40% S / 0.1 pH units) of Hc bound oxygen. As, however, pH values recorded in venous and arterial vessels of cephalopods ususally did not differ under control conditions (e.g. Johansen et al. 1982), while in exercising squid (Pörtner et al. 1991) and hypoxic cuttlefish (Johansen et al. 1982) a slight venous alkalosis was observed, it was proposed that the main function of the large Bohr and Haldane effects would lie in a protection of blood pH and thus, arterial Hc saturation (e.g. Brix et al. 1981, 1989, Johansen et al. 1982). The analysis of Pörtner (1990b, fig. 1) illustrates, that upon a (putative) change in pH from 7.5 to 7.4 in *I. illecebrosus* arterial blood, Hc could not be fully saturated at a constant arterial PO_2 of 8 kPa. Rather, the pigment would be just about 50% saturated, forcing the animal to double blood perfusion rates to maintain levels of oxygen delivery to the tissues. This stresses the importance of protecting extracellular pH, likely by the combined means of proton retention in muscle tissues during exercise (see above) and by net proton export from the tissues via the blood stream, caused by high Haldane coefficients and (protein metabolism based) respiratory quotients (RQ) of < 1 (see Brix et al. 1981, Pörtner 1990b, Lee 1994 for details). Liberation of Hc bound oxygen likely depends on high cooperativity levels of the pigment, with maximized Hill coefficients (n_{50}) found between 5 and 10 at *in vivo* pH (Johansen et al., 1982, Pörtner 1990b, Pörtner et al. 1991).

Maintenance of arterial Hc saturation may indeed be the major problem for cephalopods during acute warming. Typically, cephalopod Hc oxygen affinity declines with rising temperatures (i.e. P_{50} values increase): Zielinski et al. (2001) demonstrated that haemocyanin P_{50} shifts at a rate of 0.12 kPa $°C^{-1}$ in the cuttlefish *S. officinalis*. In combination with decreasing Bohr coefficients (Φ) upon warming (Φ = -1.33 at 20°C, -0.99 at 10°C), this implies a decrease in haemocyanin oxygen affinity, indicating that at higher temperatures, progressively higher oxygen partial pressures are needed to ensure full saturation of the respiratory pigment in the gill vessels. A (putative) alpha stat pattern of extracellular pH regulation (decrease of pH at a rate of approximately 0.018 units $°C^{-1}$; Reeves 1972, Howell and Gilbert 1976, Burton 2002) stresses the importance of high mean oxygen partial pressures in gill vessels in order to maintain highly efficient shuttling of haemocyanin bound oxygen during acute warming.

During cold exposure, available data indicate a contrasting scenario of an oxygen transport limitation due to difficulties with Hc deoxygenation in the tissues: An *in vitro* oxygen binding study of cuttlefish (*S. officinalis*) haemocyanin suggested that from 20 to 10°C, oxygen isobars of a pH / saturation diagram (Pörtner 1990b) both shift to lower pH values and level off at higher haemocyanin oxygen saturations at low pH values, forming a progressively higher pH insensitive venous oxygen reserve (Zielinski et al. 2001). At 20°C and a blood oxygen partial pressure of 4.3 kPa (see fig 3 in the respective publication), haemocyanin molecules are fully saturated with oxygen above an extracellular pH (pH_e) of 7.6. Saturation strongly declines between blood pHs of 7.65 – 7.4, to finally level off at about 20% (i.e. an Ut of 80%) below pH_e 7.2. At 10°C and the same PO_2, decreases in haemocyanin saturation with declining pH are less steep, and, in addition, values level off at about 40% saturation at

pH values that are far lower (< pH 7.0) than those observed *in vivo* in cuttlefish venous vessels (Johansen et al. 1982, pH_e values ranged from 7.4 - 7.6 at 17°C water temperature). Thus, at a (putative) pH_e of 7.4 and a vein PO_2 of 4.3 kPa, cuttlefish haemocyanin would be about 30% saturated (Ut = 70%) at 20°C, but more than 80% saturated (Ut= 20%) at 10°C, implying that more than three times the amount of blood needs to be circulated to support the organism with an equal amount of oxygen at the lower temperature. In addition, the alpha stat theorem (see above) predicts pH_e values to be higher in the cold to ensure constant imidazole ionization. Howell and Gilbert (1976) suggested such a pattern to be relevant for squid blood. However, alpha stat pH regulation would decrease Ut even more and, in consequence, further enhance blood perfusion requirements in the cold.

1.4 Cephalopod ventilation

Cephalopods generate ventilatory currents in their mantle cavities to constantly engorge their gills in fresh seawater to facilitate gas exchange (Wells and Wells 1982, Wells 1990). The above (see 1.3) considerations of maximized haemocyanin utilization in cephalopods indicate that the ventilatory apparatus must always provide seawater with oxygen partial pressures high enough to ensure full Hc oxygenation in the gills. In general, there are two fundamentally different cephalopod ecotypes with differing ventilation systems: Active cephalopods (squids) that employ a jet propelled mode of locomotion, pump large volumes of water through their mantle cavities during swimming. This they do by contraction of (mainly aerobic) circular mantle muscle, which decreases mantle diameter and forces intramantle water out of the funnel at pressures between 0.3-1.0 kPa at rest. Refilling of the mantle cavity is aided by passive relaxation of mantle organ collagen springs in combination with the contraction of radial muscle fibres in this muscular hydrostat organ (see fig 1.3, Bone et al. 1981, 1994a, Webber and O'Dor 1986, Bartol 2001, Kier and Smith 1985, Milligan et al. 1997, Curtin et al. 2000, Wells 1990). Owing to high water perfusion requirements during swimming (seawater volumes equivalent to 20-35% of their own body mass min^{-1} are being moved), less than 20% of the available dissolved oxygen is extracted from the water stream during its passage through the mantle cavity. In squid species ventilation must clearly be considered a byproduct of locomotion (e.g. Webber and O'Dor 1986, Wells et al. 1988, Shadwick et al. 1990). The situation is different in cuttlefish and octopods. These cephalopods have managed to create a separate pumping system, operating at lower pressure heads (<0.2 kPa), transporting smaller volumes of water (seawater equivalents of 1-3% of their own body mass min^{-1}) and, consequently, displaying increased oxygen extraction rates from the ventilatory water stream of 50% and higher (Wells and Wells 1982, 1985, 1991). It could only recently be established that appendages of the funnel apparatus, the collar flaps, drive the respiratory water out of the mantle cavity of cuttlefish (*S. officinalis*). These thin muscular sheets of (mainly aerobic) muscle (Abbot and Bundgaard 1987) were previously thought to solely seal the mantle cavity

during expiration, while circular aerobic muscle layers were proposed to be active during expiration (Packard and Trueman 1974).

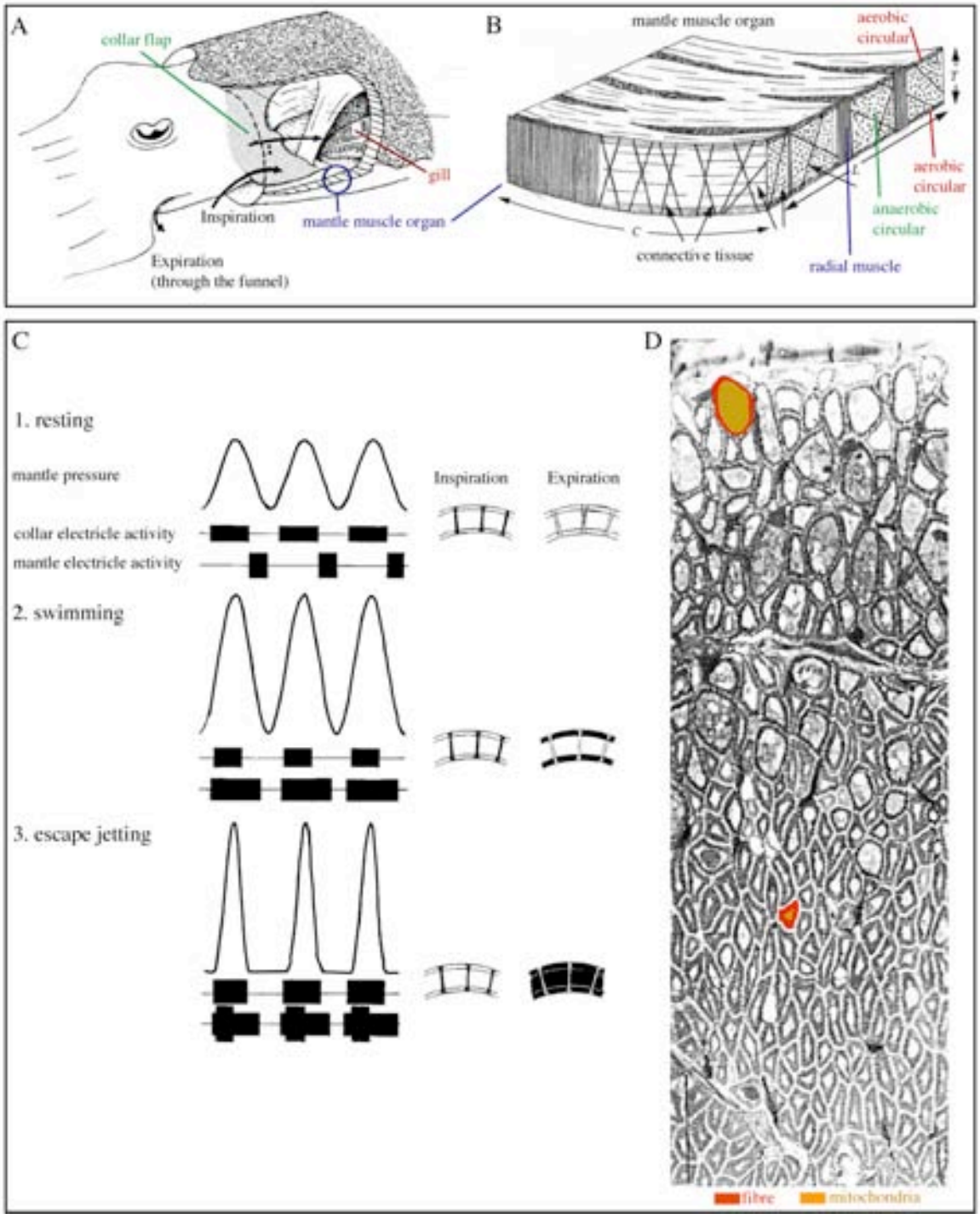

Fig. 1.3: The ventilatory apparatus of the cephalopod *Sepia officinalis* and its muscles. A) Schematic illustration of water flows in the cuttlefish mantle cavity. Collar flap muscles push water into the mantle cavity, past the gills and out through the muscular funnel (see bold arrows)(adapted from Bone et al. 1994a). B) A piece of cuttlefish mantle muscle organ: Thin layers of aerobic circular muscle embrace a thick, central layer of anaerobic circular fibres. Radial muscle fibres run perpendicular and connective tissue (collagen springs) runs in L – T and C – T planes (adapted from Curtin et al. 2000). C) Mantle pressure generation in the cuttlefish during 1. resting ventilation, 2. swimming and 3. escape jetting. While during 1. only radial mantle fibres are active, aerobic (2.)

and anaerobic (3.) circular fibres become progressively involved. In all three cases, collar flap electrical activity is present during expiration (=high mantle cavity pressure phases) (adapted from Bone et al. 1994a). D*) Alloteuthis subulata* (squid) mantle muscle transversal section (cut in plane L-T, see fig 1.3B). Large diameter mitochondria rich fibres of the inner mantle zone above, and smaller mitochondria – poor central fibres below. 60% of the cross sectional area of inner fibres are mitochondria, while central fibres only have a maximum mitochondrial area of 20% of the fibre profile (yellow insert = mitochondria, red insert = fibres)(adapted from Bone et al. 1981).

However, Bone et al. (1994a) could demonstrate that no circular mantle muscle fibres are active during resting ventilation. As in squids (see above), radial mantle muscle fibres aid during inspiration, contracting and thereby increasing mantle cavity diameter and sucking water into the mantle cavity through the lateral openings (see fig 1.3A).

Bone et al. (1994a) also investigated muscle tissue electrical activity during slow swimming and escape jetting (see fig 1.3C). While mantle cavity pressures during resting ventilation rarely exceed 0.005 - 0.15 kPa, pressures of 0.1 – 1 kPa were observed during slow swimming, which involves both, collar flap muscles and the thin aerobic layers of circular muscle on the mantle muscle organ periphery. Finally, highest pressures (up to 10 kPa), as generated during escape jetting, involve both aerobic and anaerobic circular muscle fibres. In all cases, inspiration is achieved by action of radial muscle fibres and elastic recoil of mantle organ collagen springs (Bone et al. 1994a, Curtin et al. 2000). Analogous to the situation in teleosts, cephalopods possess anaerobic or 'white' muscle, characterized by lower mitochondrial densities, higher myofibrillar densities, a lower capillarization and high phosphagen (PLA, see above) concentrations in combination with high levels of glycolytic enzymes (Mommsen et al. 1981). It is not surprising that the central bulk of circular mantle fibre, which is responsible for rapid escape movements, is of this type (see fig 1.3D): 'White' muscles in fish typically have high rates of activation and relaxation, as well as high shortening velocities, traits that are important during fast escape or hunting movements (e.g. Curtin and Woledge 1988). These advantages outweigh the main disadvantages, that is the inherent energetic inefficiency of anaerobic metabolism and rapid muscle fatigue due to phosphagen depletion and decreases in $\Delta G/\Delta\xi$ (see above). It is thus quite surprising to find that the radial mantle fibres, which are constantly engaged in routine ventilatory work are of the same type as the anaerobic fibres of the central mantle zone (Bone et al. 1994b). Whether these fibres are therefore prone to experience muscular fatigue at changing workloads (e.g. during acute thermal change) remains to be investigated. To date, no study has addressed the challenges that a cephalopod ventilation system has to undergo during thermal change.

1.5 Cephalopod circulation

Cephalopods are the only marine invertebrates with a true high pressure, fully closed circulation system, with a low blood volume (5-6% of body mass) and a circulation time of less than 2

minutes (Wells 1983, Schipp 1987a,b). However, there are two major features that distinguish cephalopod from fish circulation systems:

First, owing to its limited oxygen carrying capacity (see above), larger amounts of blood need to be circulated when compared with fish species. For example, resting cardiac outputs of 18 versus 42 ml kg^{-1} min^{-1} were determined for rainbow trout (*Oncorhynchus mykiss*) and common octopus (*O. vulgaris*) of comparable mass (see O'Dor and Webber 1986). Although cephalopod blood is characterized by a relatively low viscosity (approaching that of human plasma, Wells 1983), the high blood perfusion requirement likely has led to the evolution of a circulatory system equipped with multiple pumps moving the fluid. Coleoid cephalopod circulatory systems possess three hearts, paired branchial hearts to overcome the resistance of the gills and a systemic heart that distributes oxygenated blood across the body (see fig 1.4C and Wells 1983, Schipp 1987b for reviews). In addition, it was recognized early on that most peripheral blood vessels and all major veins propel blood peristaltically, thus potentially relieving the main systemic pumps (Bert 1867, v. Skramlik 1941, de Wilde 1955, Wells and Smith 1987, Schipp 1987a). A recent study (King et al. 2005) could demonstrate such peristaltic contractions of all major veins in unrestrained, resting cuttlefish (*S. officinalis*) *in vivo*. The organization of the entire circulatory system therefore is complex, with autonomous and non-autonomous contractile parts being under extensive nervous and humoral control (see Schipp 1987a,b and references therein).

Secondly, all circulatory organs are enclosed by the ventilatory pressure generation system. With pressures in the mantle cavity occasionally exceeding several kPa, there clearly is some potential for interaction of mantle cavity pressure with blood pressure patterns, especially in the major veins. Venous blood in cephalopods is led to the gills via large diameter, capacitance vessels (see Shadwick and Nilsson 1990, Schipp 1987a for a description of vessel characteristics). The most important one of these in coleoid cephalopods is the anterior vena cava (AVC), which receives numerous factors from the head and arms, funnel apparatus, retractor muscles of head and funnel and the hepatopancreas (see fig 1.4). In the cuttlefish *Sepia officinalis,* the AVC originates in a stout, valved muscular chamber located dorsally of the exhalant funnel roof, traverses the mantle cavity and splits up into paired lateral venae cavae at the anterior tip of the organ sac. Lateral venae cavae and inputs from the posterior parts of the animal feed the branchial hearts, which, in turn, generate the pressure to overcome gill vessel resistance (Tompsett 1939, fig. 47, 48 and text for a detailed description). Most peculiarly, the large diameter, thin walled (but muscular, see Schipp 1987a) AVC is fixed to the hepatopancreatic mass on its dorsal side, but is otherwise freely suspended in the mantle cavity, thus being under direct influence of ventilatory and locomotory pressure oscillations that are always present in the mantle cavity.

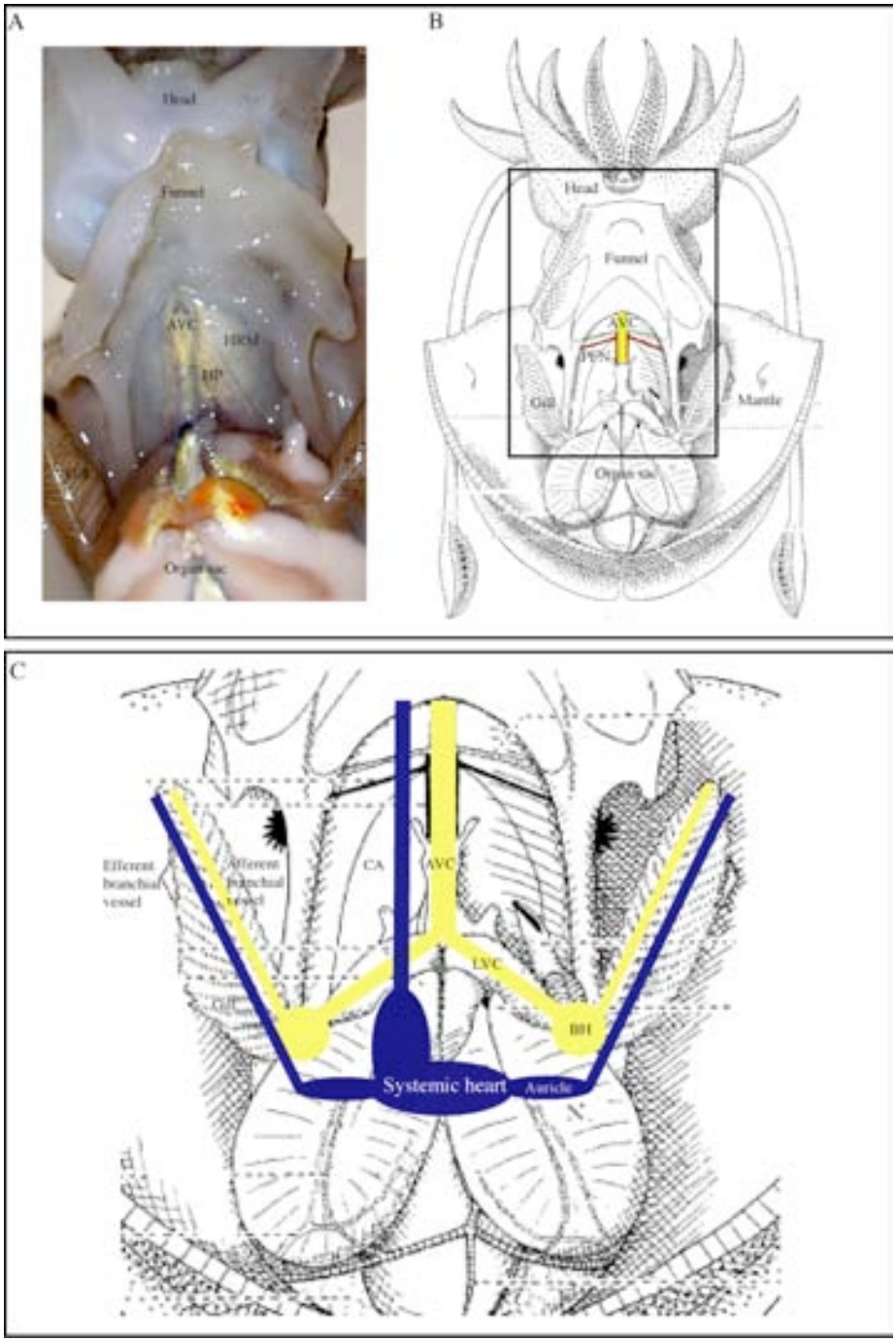

Fig. 1.4: The cuttlefish circulatory system. A) Photographic image of freshly killed, laboratory raised female specimen of approximately 300g wet mass with mantle and funnel cut open as depicted in B). Abbreviations: HRM = head retractor muscle, HP = hepatopancreatic mass. The anterior vena cava (AVC) is visible in the opened mantle cavity, filled with deoxygenated (therefore transparent) blood. B) schematic overview of female cuttlefish mantle cavity with AVC and posterior mantle nerves colored (Tompsett 1939). C) Schematic overview of major vessels and pumps of the anterior half of the animal: Venous blood (yellow) is transported via the AVC, through paired lateral venae cavae (LVC) into branchial hearts (BH) and to the gills (afferent branchial vessels). Oxygenated in the gills (blue), blood is transported to paired auricles of the systemic heart. The cephalic artery (CA) leads oxygenated blood towards the head. Posterior circulatory vessels not included, but see Tompsett 1939 for a detailed description).

Not surprisingly, a number of studies found pressure pulses in the AVC to be correlated with ventilatory mantle movements (e.g. Johansen and Martin 1962, Bourne 1982) and postulated that mantle cavity pressure conveyance could be responsible for blood propulsion in this vein. As ventilatory pressures in the mantle cavity and AVC blood pressure oscillations were not determined simultaneously in these studies, it is not clear, whether the outlined scenario is feasible. However, the close coupling between blood pressure pulse rates in major veins and ventilatory movements in general seems to be obligatorily present in all cephalopod ecotypes investigated to date, in octopods (Johansen and Martin 1962), squid (Bourne 1982) and nautilus (Bourne et al. 1978).

In peripheral arm veins peristaltic blood transport has been demonstrated to be closely coupled to ventilatory movements. This is apparently under reflectoric control of the subesophageal central nervous system (Mislin and Kauffmann, 1948, Mislin, 1950, Smith, 1962).

The two major convection systems in cephalopods, the circulatory and the ventilatory apparatus, are thus obligatorily coupled to one another functionally and form yet another level of higher total systemic complexity than two separate convection systems. How this integrated system is coordinated and how it reacts to acute thermal challenges has so far not been investigated.

1.6 Approaches and questions

From the afore-described unifying hypothesis of an oxygen limitation of thermal tolerance (1.1) and the particular organization of cephalopod metabolism with its specific oxygen transport cascade (1.2-1.5), a number of questions arise that will be approached in this thesis. The cuttlefish *Sepia officinalis* is being used as a cephalopod model organism throughout:

a) Is cuttlefish metabolism oxygen limited at critically high and low temperatures?

Using *in vivo* ^{31}P NMR spectroscopy and mantle cavity pressure recordings, mantle muscle energy metabolism were investigated during conditions of acute thermal change. The study focused on the constantly working, ventilatory radial fibres of the mantle muscle organ. It was hypothesized that radial fibres would progressively need to switch to an anaerobic mode of operation beyond critical temperatures, as indicated by phosphagen (PLA) utilization (publication 1). In addition, routine metabolic rate (rmr) was determined for cuttlefish of different body mass to investigate whether deviations from an expected exponential relationship with temperature (e.g. O'Dor and Wells 1987) would occur (publications 2 and 3).

b) Is the cuttlefish ventilatory system able to sustain oxygen demand of the organism during acute thermal change?

This question was addressed by measuring oxygen extraction rates from the ventilatory current with a microoptode placed in the cuttlefish exhalant stream. Metabolic rate and mantle cavity pressure oscillations were determined concomitantly. Power output and costs of ventilation were calculated and

discussed as to whether observed changes in ventilatory power output suffice to maintain high oxygen partial pressures in gill vessels across the entire temperature spectrum (publication 2).

c) Is the cuttlefish circulatory system able to sustain oxygen demand of the organism during acute thermal change?

In a first approach, we elaborated the relationships between blood flow patterns in the most important cephalopod venous vessel, the anterior vena cephalica (AVC) with respect to mantle cavity pressure oscillations, both during rest and spontaneous exercise (publication 4). In a second step, AVC blood flow parameters and ventilatory pressure patterns were observed during acute thermal change to investigate, whether maximum blood flow levels correlated with the metabolic rate increments observed. We hypothesized, that, owing to its high hierarchical position, the integrated circulatory and ventilatory convection system would be the first component of the oxygen transfer chain to become limiting for oxygen flux to tissues during thermal change (publication 5).

Two additional questions were addressed to complement the picture obtained in publications 1 - 5. This material is incomplete at present and will therefore only briefly be mentioned in the discussion section of this thesis (see 4):

d) Does low temperature impair haemocyanin oxygen transport?

In addition, a combined *in vitro* and *in vivo* study was carried out to investigate the suitability of the cuttlefish oxygen carrier haemocyanin to function properly at low temperatures. Previous *in vitro* studies on cuttlefish blood (Zielinski et al. 2001) indicated that at low temperatures, cephalopods may be unable to liberate large fractions of oxygen from the respiratory pigment, thereby greatly increasing relative blood perfusion requirements (see 1.2 and discussion).

e) Do cuttlefish have the ability to acclimate to altered thermal regimes?

In addition to routine metabolic rate, ventilation rate and ventilatory pressure determinations animals acclimated to 15°C (see above), the same set of variables was determined in animals raised at 20°C. According to the outlined hypothesis (1.1.), thermal acclimation is believed to shift the thermal window of an ectothermic species (see discussion).

2. Methods

2.1 Animals

European cuttlefish (*Sepia officinalis* L. 1758; class cephalopoda, subclass coleoidea, superorder decapodiformes, order sepiida) were used as a cephalopod model organism for work reported in this dissertation. The species is a neritic and demersal species, occurring on sandy grounds from the coastline to depths of 150 - 200m. It is distributed along the coasts of the eastern Atlantic and the Mediterranean Sea (Boletzky 1983), with breeding grounds extending from the Delta region of the Netherlands in the North (Oosterschelde, Yerseke 51°30'N 4°2'E; Paulij et al. 1990, 1991) to the Canary islands west of Africa in the South (28°N, 1°W; Boletzky 1983). *S. officinalis* is characterized by rapid growth rates (e.g. Pascual 1978, Forsythe et al. 1994) and a semelparous lifestyle, i.e. animals experience only a single breeding season and die thereafter (Boletzky 1983). The life span of the species varies from a two year life cycle in comparatively cold English Channel waters (Bouchaud-Camou and Boismery 1991, Dunn 1999, Denis and Robin 2001) to alternating one and two year cycles in the Bay of Biscay and the Mediterranean (Mangold-Wirz 1966, Le Goff and Daguzan 1991, Gauvrit et al. 1997).

Animals used in publications 1 through 5 all originated from the English Channel population. The life cycle, distribution and seasonal migrations of this stock are illustrated and summarized in fig 2.1. Briefly, English Channel (EC) cuttlefish spawn in inshore waters during the spring months. The offspring hatches in June and July and spends the summer in shallow coastal waters with high prey abundances, displaying rapid growth (Boucaud-Camou and Boismery 1991, Dunn 1999). In October, the animals start to migrate to deeper waters, progressively moving towards the central parts of the Channel (Hurd Deep). Bouchaud-Camou and Boismery (1991) have concluded that this migration is linked to declining temperature in the EC, as in autumn and winter, the animals always move westward, following the warmer water masses, exclusively staying at temperatures > 9°C. This conclusion is in agreement with laboratory studies performed by Richard (1971), who found *S. officinalis* to die at temperatures of 7°C, with animals displaying significant levels of physical activity only at temperatures above 10°C. Temperatures in the eastern part of the EC do drop considerably below 9°C during the winter months (Agoumi 1982, Wang et al. 2003).

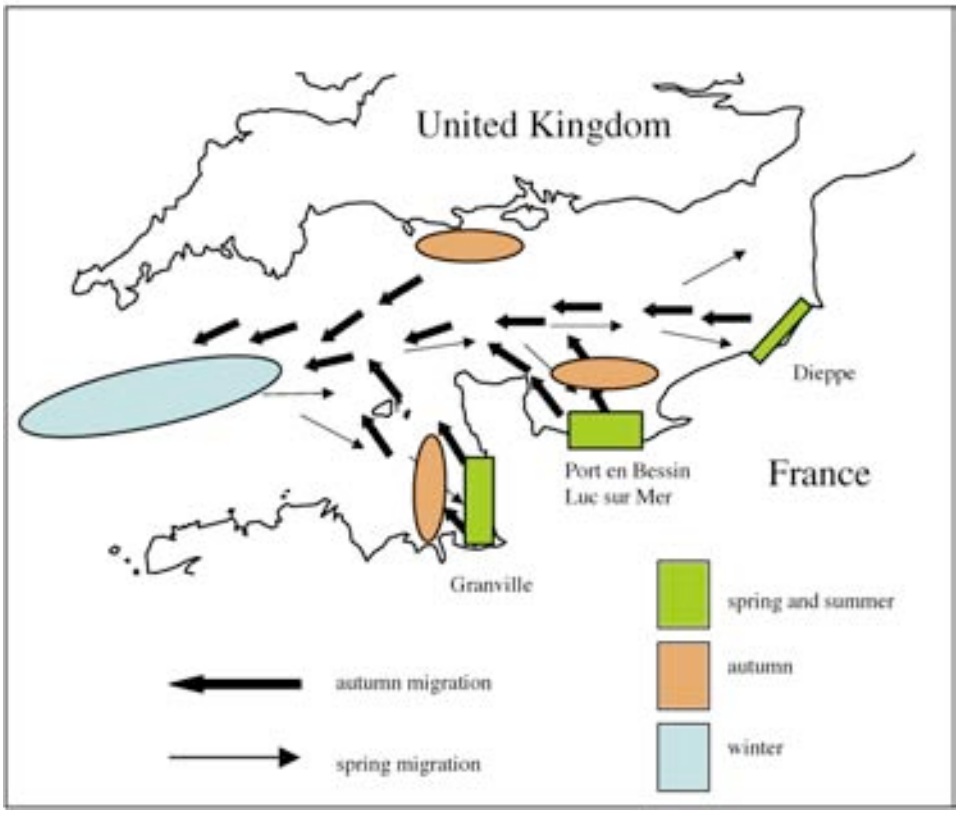

Fig 2.1. Cuttlefish *Sepia officinalis* habitat in the English Channel and seasonal migrations (adapted and modified from Bouchaud-Camou and Boismery 1991). From April to September, animals are located in coastal waters. Adult animals spawn and, subsequently, die in May and June. The new generation hatches about 1 month later and spends the summer in shallow (5-20m water depth), rocky and sandy coastal waters. In Normandy, there are three major spawning areas, located in the Bay of Seine (i.e. Port-en-Bessin, Luc-sur-Mer), in the Dieppe and the Granville areas. In October - November, animals move further offshore (10-30m water depth), and, finally, westward into the comparatively warm Hurd Deep, i.e. the central axis of the English Channel (60-100 m water depth) in the winter months (December-March) and, even further, into the offshore deeper waters off the northern part of the French Atlantic coast. The autumn migration (bold arrows in fig 2.1) is linked to temperature (and, potentially, food availability), with animals following the 9-10°C isotherms westward. Cuttlefish prefer winter temperatures of >9°C and sandy grounds, sharing the habitat with monkfish, gurnards, mullets, skates, dogfish and flatfish. The spring migration is more rapid (2 weeks duration) than the progressive autumn migration and is linked to reproduction (2nd year animals) or to feeding (1st year animals). Populations from the coast of Britain and the French coast mix in the winter (Bouchaud-Camou and Boismery 1991, Denis and Robin 2001, Wang et al. 2003).

Wild - laid cuttlefish eggs were obtained in May 2002 from Luc-sur-Mer, Bay of Seine (49°11'N, 359°38'W). Egg masses were split between two closed, recirculating aquaculture systems in the Alfred-Wegener-Institute and raised at constant temperatures of 20°C ± 0.2°C SD (warm acclimated animals, WA) and 15°C ±0.1°C SD (cold acclimated animals, CA). Animals were fed daily with live mysids (*Neomysis integer*) and live brown shrimp (*Crangon crangon*) for approximately 6 (WA animals) to 12 (CA animals) weeks. For the remainder of the time (08/2002-12/2003), animals were fed predominantly on frozen brown shrimp. Water quality parameters were determined three times weekly and maintained at levels suitable for cephalopod culture (e.g. Hanlon 1990).

In addition, some animals from a Bay of Biscay population (BB) were used for complementary studies of venous blood parameters (PO_2, pH) and of haemocyanin function. These animals were caught in traps by a local fisherman in La Rochelle (46°38'N, 358°30'W) in May and June 2003, kept for 1-2 weeks in tidal ponds at the CREMA, L'Houmeau, France, before being

transported in a cooling truck (10°C water temperature, 50 l seawater kg^{-1} animal, 50 g $MgCl_2$ 50 l^{-1} transport water) to Bremerhaven for experimentation. Animals were kept at 15°C in the aquaculture facilities of the Alfred-Wegener-Institute for approximately 1-2 weeks prior to experimentation.

Table 2.1 gives an overview of the experiments conducted with laboratory raised EC and wild caught BB animals, including number of replicates and mean masses of experimental animals:

Table 2.1. Experiments and animals used in the present dissertation:

#	*pop.*	*acclim. temp.*	*n*	*Mass (SD) [g]*	*parameters measured*	*publication*	*year*
1	EC	WA	5	12.5 (2.1)	MO_2	discussion	2002
2	EC	CA	5	15.0 (4.6)	MO_2	3, discussion	2002
3	EC	WA	5	98.5 (9.0)	ventilatory parameters	discussion	2002-2003
4	EC	CA	5	104 (7.4)	ventilatory parameters; *In vivo* ^{31}P NMR, *In vivo* MRI	1, 2, 5, discussion	2003
5	EC	CA	4	105 (7.0)	MO_2, oxygen extraction, ventilatory parameters	2, 3	2003
6	EC	CA	10	232 (30)	anterior vena cava (AVC) blood flow parameters, ventilatory parameters	4, 5	2003
7	EC	CA	4	238 (28)	MO_2	3	2003
8	EC	CA	4	495 (157)	MO_2	3	2003
9	BB	15°C*	19	444 (71)	*In vitro* blood oxygen binding	discussion	2004
10	BB	15°C*	6	470 (58)	*In vivo* blood pH, PO_2, haemocyanin oxygen saturation	discussion	2004

= experiment number in chronological order; pop. = population, either English Channel (EC) or Bay of Biscay (BB); acclim. = accclimation temperature, either 15°C (CA) or 20°C (WA); n = animals used for experiments; mass = animal wet mass and SD; parameters = measurements performed in respective experiments; publication = publication the results appear in; year = year the experiments were performed. MO_2 = routine metabolic rate. Experiments 1-8 and 10 all followed the same time sequel, i.e. acute warming and cooling at an average rate of 1°C h^{-1}; * animals kept at 15°C for 1-2 weeks, prior temperature regime unknown, but probably around 20°C for several weeks (G. Claireaux, pers. comm.).

2.2 General experimental procedures and setup

The experimental protocol was largely identical between experiments # 1- 8 and 10 (tab 2.1). Briefly, experimental animals were starved for 24 hours, and then transferred to the experimental set-ups. Surgery (if necessary) was conducted on the first day, followed by an overnight acclimatization period within the experimental chamber. On the second day, animals were cooled from control temperature (15°C) to 8°C (5°C), then warmed to and kept at control temperature over night, after which time they were finally warmed to 26°C (29°C) on the third day. Temperature was changed in a stepwise procedure at an average rate of 1°C h^{-1}. Specifically, a three - degree temperature change was accomplished during the first hour of a three hour period, while during the two subsequent hours temperature was kept constant for measurements. Assay temperatures were 14°C / 11°C / 8°C (5°C) on the second day, and 17°C / 20°C / 23°C / 26°C (29°C) on the third experimental day. Two experiments were slightly modified: In experiment # 4, temperature was changed continuously at a

rate of ±1°C h^{-1} at temperatures <8°C and >26°C to identify critical temperatures (T_c), and in experiment # 6 temperature was modified continuously at 1°C h^{-1} throughout.

Two experimental setups were used: Setup 1 (experiments # 3 and 4, NMR setup) was a perspex perfusion chamber analogous to the one used by Mark et al. (2002) for eelpout (fig 1a, publication 1). Plastic sliders within the chamber could be adjusted to the animals‘ dimensions and used to restrict the space available for roaming activity. The chamber was connected to a closed recirculation seawater system and placed within the magnet as described in Bock et al. (2002). Water quality was maintained with a protein skimmer (Aqua care, Germany) and a nitrification filter (Eheim Professional 2, Eheim, Germany).

Setup 2 (all other experiments): Animals were placed in an experimental recirculated aquarium system with a total water volume of 130 liter. This system consisted of a small animal chamber (20 l), which was suspended into a thermostatted water bath. The animal chamber was perfused at a rate of approximately 5 l min^{-1}. Water quality was maintained with a protein skimmer (Aqua care, Germany) and a nitrification filter (Eheim Professional 2, Eheim, Germany). A cryostat (Julabo, Germany) kept water temperature constant at ± 0.1 °C. Instead of the small animal chamber, an open respirometer was used in experiments # 1 and 2 (see tab 2.1, publication 3).

2.3 *In vivo* ^{31}P NMR and *in vivo* MRI

In vivo ^{31}P – NMR spectroscopy experiments were conducted in a 47/40 Bruker Biospec DBX system with a 40 - cm horizontal wide bore and actively shielded gradient coils (50 mT/m). A 5 cm ^{1}H / ^{31}P / ^{13}C surface coil was used for excitation and signal reception. The coil was placed directly under the animal chamber in such a manner as to gain maximum signal from the posterior mantle muscle section (fig 1b, publication 1). A calculated 80 – 90 % of sensitive coil volume was filled by mantle muscle tissue, and about 10 - 20% by tissues from the organ sac and coelomic fluid. As *Sepia officinalis* mantle muscle tissue is characterized by high phosphagen (PLA) concentration (about 34 μmol g^{-1} ww^{-1}, Storey and Storey, 1979) it is quite likely that the *in vivo* ^{31}P -NMR spectra almost exclusively represent the adenylate pool and intracellular pH (pH_i) of the mantle musculature.

In vivo ^{31}P – NMR spectra [sweep width, 5,000 Hz; flip angle, 45° (pulse shape bp 32; pulse length 200 μs); repetition time (TR) 1 s; scans, 256; duration, 3 min 40 s] were acquired once every 21.3 minutes to measure pH_i and its changes represented by the position of the P_i signal relative to the position of the PLA signal. pH_i was calculated using the PLA vs. P_i shift equation obtained by Doumen and Ellington (1992), using a pK_a value determined by Pörtner (1990a) for an ionic strength of I = 0.16. pK_a values were adjusted according to temperature (Kost, 1990). ^{31}P - NMR spectra were processed automatically using TopSpin V1.0 software (BrukerBioSpin MRI GmbH, Germany) and a

macro (written by R.- M. Wittig, AWI) to finally yield integrals of all major peaks within the spectrum (Bock et al. 2001), as these correlate with the amount of substance within the detection volume (=sensitive volume) of the ^{31}P - NMR coil (fig 1b). Flow weighted images to examine blood flow in major blood vessels were also generated directly before and after the collection of ^{31}P – NMR spectra but will be treated separately. Concentrations of metabolites (ATP, PLA, P_i) were expressed as percentages of the total ^{31}P – signal intensities. This was found necessary, as animals were free to move to some extent in the chamber both vertically and horizontally (for a maximum of 5 mm in either direction, to assure unrestrained ventilatory movements), thus altering overall *in vivo* ^{31}P – NMR signal intensities:

$$[Met] = ([Met] ([PLA]+ [\alpha ATP]+ [\beta ATP]+ [\gamma ATP] + [P_i])^{-1}) 100 \quad (1)$$

with [Met] in % being the relative concentration of metabolite (ATP, PLA, P_i) and ([PLA]+ [αATP]+ [βATP]+ [γATP] + [P_i]) being the sum of the five major ^{31}P - NMR peak integrals that constituted >98% of the overall ^{31}P signal (see fig 5a, publication 1). As a precondition for such an approach, it is necessary that no major phosphate export from the mantle muscle takes place. Finke et al. (1996) could demonstrate that the sum of adenylates and inorganic phosphate (ATP, ADP, AMP, PLA, P_i) in squid mantle muscle (*Lolliguncula brevis*) was similar in control and exercised animals, as was the sum of all arginine containing metabolites (PLA, Octopine, L Arginine). Storey and Storey (1979) also found the sum of arginine containing metabolites to be relatively stable in cuttlefish mantle muscle following hypoxia and exhaustive exercise (decreases of less than 10%, minor releases of octopine in the blood stream), but they did not determine inorganic phosphate concentrations. Still, both studies suggest that anaerobic metabolites mostly remain in the mantle muscle organ in cephalopods, thus giving validity to our approach. For better visualisation, percentages of concentrations were transformed into molar quantities assigning [PLA] control values found in cuttlefish mantle muscle (Storey and Storey 1979, [PLA] = 33,6 μmol g^{-1} ww^{-1}) to [PLA] controls in our study (see table 1, publication 1) and evaluating the other metabolite concentrations accordingly. Free energy change of ATP hydrolysis ($dG/d\zeta$, kJ mol^{-1}) was estimated from NMR visible metabolites as described by Pörtner et al. (1996), with apparent equilibrium constants of arginine kinase and myokinase adjusted to changing temperatures. Concentrations of L-Arginine (Arg) and octopine (Oct) were estimated using published values (Storey and Storey 1979) and assuming that a decrease in 1 μmol g^{-1} ww^{-1} [PLA] results in a concomitant 0.67 μmol g^{-1} ww^{-1} increase in [Arg] and a 0.33 μmol g^{-1} ww^{-1} increase in [Oct] (Storey and Storey 1979; as witnessed during moderate and severe hypoxia and during exercise).

In vivo magnetic resonance imaging (MRI) measurements were performed with a 4.7 Tesla Bruker Biospec 47/40 imaging spectrometer (Bruker, Germany) equipped with a mini imaging unit with gradient field strength of up to 200 mT m^{-1} (see publication 4). Flow weighted images were generated in the transversal plane at a position just prior to the forking of the anterior vena cava (AVC), enabling us to investigate pulse rates in afferent and efferent branchial vessels, cephalic artery

and vein simultaneously (see fig 1.4 for a schematic illustration of the cephalopod circulation system). Image acquisition was performed using the gradient echo Snapshot FLASH technique (Haase, 1990). Imaging parameters were as follows: matrix size 128 x 128, resulting in an in plane resolution of 312 μm; repetition time 6.7 ms, echo time 2.1 ms; 22.5° sinc3 pulse; pulse length 2,000 μsec; 1 slice, slice thickness 2 mm; field of view 4 x 4 cm; dummy scans = 4. Sequences of 20 – 32 images were generated in quick succession, resulting in a temporal image resolution of 0.986 sec. Regions of high flow appear bright in Snapshot FLASH generated MR images, with brightness being proportional to flow (see fig. 6 a-x, publication 4). Mean signal intensities were calculated by an operator controlled analysis of various regions of interest (ROIs) for the determination of relative blood flow changes. As 20 – 32 images were generated after one another at the same position, pulse rates for the various vessels of interest could be derived simultaneously and compared with ventilatory pressure oscillations. Such image sequences were acquired every 25 minutes for each of the five experimental animals.

2.4 Respiration

Oxygen consumption was recorded at each temperature by using the animal chamber of setup 2 (see 2.2) as an intermittent flow respirometer (in experiments # 5,7 and 8, see table 2.1). An oxygen microsensor (PreSens GmbH, Germany, oxygen microoptode NTH-L2.5-NS(35+1.2mm)-TF-COB2-NOP, temperature compensated) which was connected to the inflow tube of a small internal circulation pump (flow: 2 l min^{-1}) was used to measure the oxygen partial pressure in the chamber water. This pump and the animal's ventilatory action caused sufficient mixing of the water to record a linear decline in oxygen partial pressure over time, once the inflow of fresh seawater was blocked. During the two - hour measurement period at each temperature step (see 2.2), two or three oxygen consumption runs of 20 – 40 minutes duration were completed. Each run was terminated when the oxygen partial pressure in the respirometer water had declined to about 80 % air saturation. Successive runs were only started when the oxygen partial pressure in the animal chamber had returned to approximately 98-100% air saturation for more than 15 minutes. Two experiments (#1 and 2, see table 2.1) were performed in an open respirometer, identical to the one described in and used by De Wachter et al. (1997). In these experiments, oxygen partial pressures were measured at the in- and outflow of small, ca. 30 cm^3 cylindrical respiratory chambers, using polarographic oxygen electrodes (Eschweiler, Germany) that were calibrated at each temperature step according to the manufacturers instructions. The flow of seawater through the system was adjusted to always maintain oxygen saturations of >85% in the out flowing water. Measurements were performed continuously for two hours at each temperature step.

Both respirometers were cross – checked, errors between methods resulted in differences of < 5 % of MO_2 values. Respiration rates were corrected for bacterial respiration. Oxygen consumption was calculated using the formula (1) for the intermittent closed respirometer and (2) for the open respirometer:

$$MO_2 = (\Delta PO_2\ \beta O_2\ V1)\ t^{-1}\ m^{-1} \quad (1)$$

$$MO_2 = (\Delta PO_2\ \beta O_2\ V2)\ m^{-1} \quad (2)$$

with MO_2 = oxygen consumption rate (μmol O_2 g wet weight^{-1} min^{-1}), βO_2 = oxygen capacity of seawater (for a salinity of 33-35), according to Boutilier et al. (1984), V2 = flow rate through the respirometer (l min^{-1}), V2 = respirometer seawater volume (l), ΔPO_2 = difference in water oxygen partial pressure between start and end of experimental run (closed respirometer) or difference in oxygen partial pressure between in- and out flowing water (open respirometer).

2.5 Ventilatory patterns and oxygen extraction

To implant a catheter for ventilatory monitoring, animals were anaesthetized with a 0.4 mol l^{-1} $MgCl_2$ solution that was mixed 1:1 with seawater (Messenger, 1985) at 15°C for 3 – 3.5 minutes, then placed (ventral side up) on a wet leather cloth to prevent skin injuries. During surgery, animals were perfused with aerated seawater (0.04 mol l^{-1} $MgCl_2$) through the funnel aperture. A PE cannula, required to record postbranchial pressure, was connected to a 23 gauge hypodermic needle, led through the entire mantle cavity and then fed through the posterior ventro-lateral section of the mantle muscle. Cannulae (Portex PE tubing, i.d. 0.58 mm o.d. 0.96 mm, flared at the opening) were held in place by two 4 mm diameter plastic washers on the in and outside, embracing the mantle muscle in a sandwich-like fashion. PE tubes were connected to MLT-0699 disposable pressure transducers, signals amplified with a ML-110 bridge amplifier and further fed into a PowerLab/8SP data acquisition system (AD Instruments, Australia). Pressure transducers were calibrated daily. See publications 1 and 2 for a detailed description of pressure pattern analysis.

For determining oxygen extraction rates from the ventilatory current, an oxygen micro-optode (PreSens, Germany; implantable oxygen microsensor IMP-900/5-600/6-140/10-TS-COB2-YOP; tip diameter 50μm) was placed into the funnel opening to measure oxygen partial pressure in the ventilatory exhalant stream. To support the fragile fibre optic oxygen sensor and to secure its position, a PE catheter (Portex PE tubing, i.d. 0.98 mm) was implanted into the ventro-lateral part of the funnel tube (about 2.5 cm from the tip), secured with plastic disks (glued to the catheter) on both the inner and outer side of the tissue. Subsequently, the microoptode was fed through the tubing such that the sensor tip reached approximately 3 mm into the animal's exhalant water stream. Finally, the optode was glued to the distal end of the PE tubing with high viscose cyanacrylate glue (Hylo Gel, Marston Oelchemie, Germany). The sensor was connected to an oxygen meter (Microx TX2-A, PreSens,

Germany) whose analog output was fed into the PowerLab system. Prior to surgery, the sensors were calibrated (while placed within the PE tube) in a saturated ascorbate solution (0% dissolved oxygen) and aerated seawater (100% dissolved oxygen). Further calibration during experimental temperature changes was not necessary, since the oxygen meter automatically compensated for temperature. At the end of the experiments, animals were narcotized (see above), killed and optodes checked for drift. Usually drift amounted to 0.5 - 1% oxygen saturation per day (measured at 15°C). Thus, oxygen values were corrected by means of linear interpolation.

2.6 Circulation

Animals were anaesthetized and pressure catheters implanted as described above. In a second step, a miniature Doppler sensor was implanted to record blood velocity and blood volume flow with a directional pulsed Doppler flowmeter (Iowa Doppler Products, USA) after AVC maximum diameter (fully relaxed under anaesthesia) had been determined with calipers. Doppler sensors (Iowa Doppler Products, USA, model E cuff type transducers, 20 MHz), were stripped bare of all plastic and rubber, incorporated into a plastic piece, which subsequently was fixed in a bridge like arrangement around the AVC (see fig 1, publication 4 for bridge details and positioning). Bridges were made of plastic fittings (polyethylen). Great care was taken in choosing bridges with an AVC matching diameter, as we wanted to record blood velocity and flow in a relatively undisturbed vessel (while at the same time, minimally disturbing animals). Bridges were carefully positioned approximately 2-3 mm posterior of the posterior funnel nerves (see fig. 1.4 and Tompsett 1939) by sewing the bridge superficially to the head retractor muscle using Ethicon #N271H (Johnson and Johnson, USA) sterile silk ligature. Ligatures were glued to the bridge arms using high viscose cyanacrylate glue (Hylo Gel, Marston Oelchemie, Germany). The thin sensor wiring was fed through the mantle cavity and led, analogues to the pressure catheter, through the posterior mantle muscle using a surgical needle. Subsequently, the wiring was connected to the pressure catheter using silk ligature and high viscose cyanacrylate glue. Pure ethanol was used for disinfection. Total sensor mass (sensor + bridge) was 0.2 g, wiring total mass was 0.28 g (see fig 1, publication 4 for sensor dimensions). Analog outputs of the Doppler flow meter and the pressure transducer were fed into the PowerLab/8SP data acquisition system (AD Instruments, Australia). Mantle pressure and venous blood flow data were collected at a sampling rate of 100 – 400 Hz to investigate the phase relationships between both processes in detail. Pressure and blood flow traces were smoothed (smoothing type: triangular (Bartlett); window width 21 – 33 points for pressure recordings, 7 – 11 points for flow recordings). Great care was taken to not alter pulse amplitudes and phase relationships of curves by choosing inappropriate smoothing window sizes. See publications 4 and 5 for a detailed account of analysis methods performed on raw blood flow data and correlated pressure patterns.

2.7 *In vitro* haemocyanin oxygen binding

Prior to taking blood samples, Bay of Biscay animals (n=19) were anaesthetized in a 2% pure ethanol 98% seawater mixture for 15 – 20 minutes at 15°C (experiment # 9, tab 2.1). Blood was drawn from the AVC, the branchial hearts and the great mantle veins (see Tompsett 1939). Samples were immediately stored on ice, subsequently spun for 5 minutes at 3000 g in a cooled (0-4°C) centrifuge to remove blood cells. Supernatant blood from all 19 animals was pooled, mixed and then frozen at –20°C for about 1 - 2 months prior to analysis.

For the construction of haemocyanin oxygen binding curves at 11 and 17°C, blood samples were equilibrated in a tonometer (model 237, Instrumentation Laboratory, Italy) with humidified gas mixtures of varying PO_2 (between 0 and 21 kPa), provided by two gas mixing pumps (Wösthoff, Bochum, Germany). Whole blood pH was altered by changing the PCO_2 in the tonometer. pH was measured for each data point through an opening in the lid of the tonometer, using a conventional pH electrode (WTW multiline P4, calibrated daily). 50 or 100 μl blood samples of blood were analysed for oxygen content using a modified Tucker chamber (Tucker 1967). Injection of a blood sample into the chamber containing a 6 g l^{-1} KCN solution leads to the release of haemocyanin – bound oxygen (Bridges 1979) and an increase in PO_2. From these changes in PO_2, haemocyanin saturation can be calculated at specific PO_2s and pH values. Fig 2.2C-E illustrates the modified Tucker chamber, with a microoptode (Presens GmbH, Germany) instead of a polarographic electrode to record changes in PO_2. PO_2 was recorded on a PC, using Presens software. Typically, new PO_2 equilibria in the cyanide solution were reached after 1-5 minutes post injection of blood samples. The cyanide solution was replaced after 1-2 measurements. Results were displayed in pH saturation diagrams, as introduced by Pörtner (1990b). Changes in cooperativity (n_{50}, Hill-coefficients) could be derived from these diagrams using formula (4) in Pörtner (1990b).

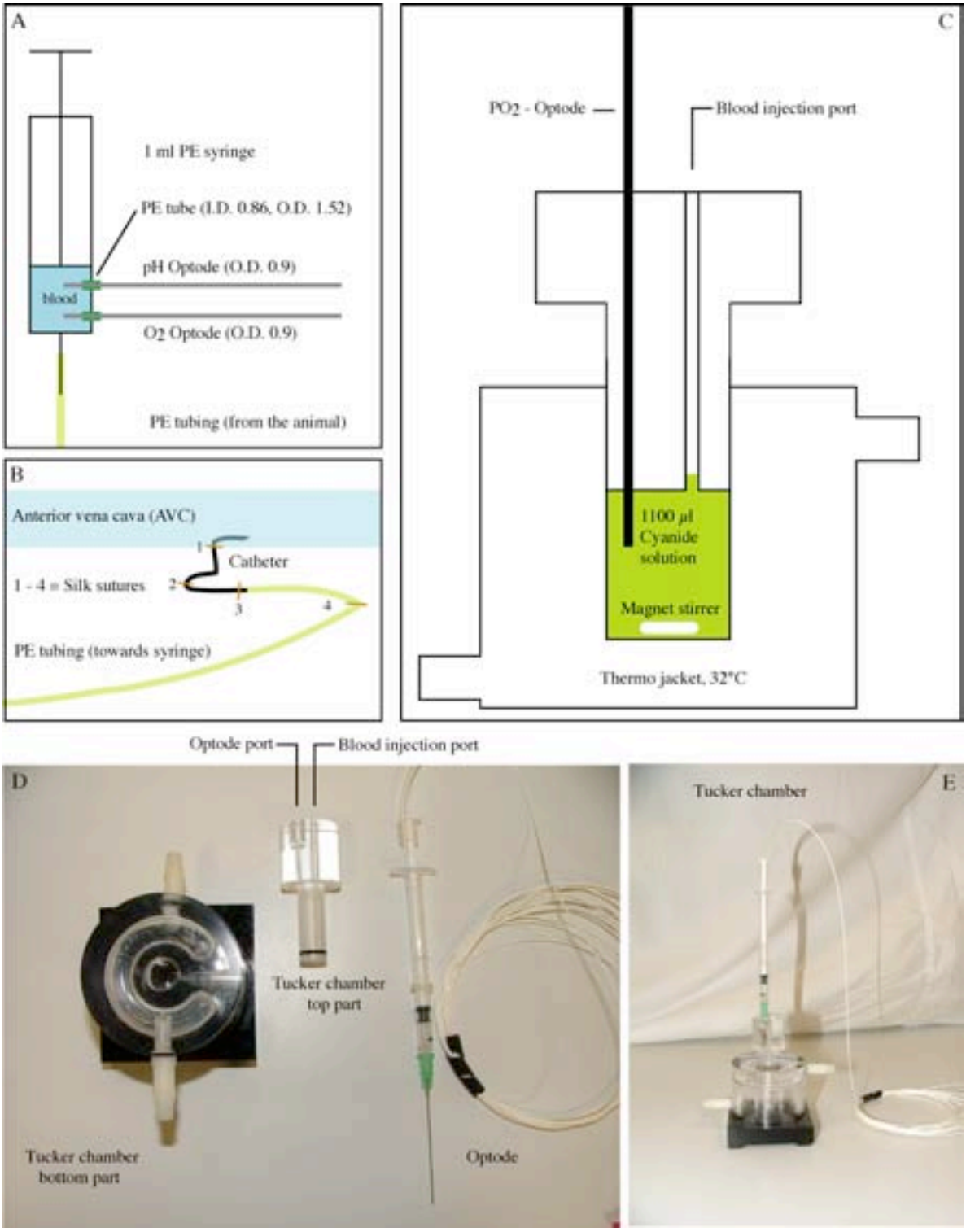

Fig. 2.2: *In vitro* and *in vivo* blood measurements. A) Syringe used for *in vivo* blood pH and PO_2 measurements. Oxygen and pH fibreoptic sensors were incorporated into 1 ml plastic syringes. B) Positioning of catheter in the cuttlefish AVC for *in vivo* blood pH, PO_2 and Hc saturation determinations. See text for explanations. C)-E) Modified Tucker chamber. Instead of a polarographic oxygen electrode, oxygen optodes (Presens GmbH, Germany, have been used for PO_2 measurements. The thermostated perspex chamber was filled with a 32°C cyanide solution (1100 μl, oxygen saturation between 40 and 50%). Blood samples of 50 or 100 μl volume were added with air tight glass syringes on the bottom of the chamber, thereby displacing a tantamount volume of cyanide solution into the blood injection port. Liberation of Hc bound oxygen results in an increase in cyanide solution PO_2, reaching a new equilibrium after 1-5 minutes.

2.8 *In vivo* blood pH, PO_2 and haemocyanin saturation

Wild caught animals from the Bay of Biscay population (experiment # 10, tab 2.1) were anaesthetized and a pressure catheter was implanted according to the procedure described above (2.5). A second catheter was inserted into the readily accessible part of the anterior vena cava (AVC) between its anterior muscular chamber and the forking into the two lateral venae cavae (Tompsett 1939). The vessel was exposed by "unsnapping" the funnel from the ventral mantle and was punctured by use of a modified syringe needle (23 gauge; see fig 2.2B) that was connected to a PE cannula (Portex PE tubing, I.D. 0.58 mm; O.D. 0.96 mm). Two holes at the needle's tip prevented blocking of the cannula by blood cells. The catheter was bent 2-4 cm from the front end (depending on the size of the animal) by about 140° and was completely filled with filtered seawater to avoid air bubbles entering the vessel. To fix the needle that extended into the AVC lumen, it was tied to the wall of the vessel with sterile silk ligature (Ethicon #N271H, Johnson and Johnson, USA). Three additional sutures were made along the course of the tubing to further stabilize the implanted catheter on the underlying musculature (head retractor muscle, muscular capsule of the digestive glands, Tompsett 1939). All sutures were sealed with cyanacrylate glue (Hylo Gel, Marston Oelchemie, Germany). The schematic drawing of fig 2.2B shows the exact positioning of the sutures, necessary to prevent the animal from removing the catheter. The PE cannula left the mantle cavity at its lateral anterior end carefully avoiding a possible interference with the activity of the collar flaps, which are engaged in ventilatory movements. Surgery procedures lasted for about 30 min.

pH and PO_2 measurements were performed using fibreoptical sensors (‚microoptodes' PreSens, Regensburg, Germany), coated with pH or oxygen sensitive fluorescence dyes. The microoptodes (implantable pH microsensor IMPL-900/2.5-600/5-140/10-TF-HP5-OIW and implantable PO_2 microsensor IMP-900/5-600/6-140/10-TS-COB2-YOP) were laterally inserted into commercially available 1 ml plastic syringes such that their tips reached two to three mm into the solution inside the syringe (fig 2.2A). The positions were chosen as close as possible to the front end of the syringe as to minimize the volume necessary for obtaining measurements. Temperature control was achieved simply by submerging the syringe with the connected catheter in the thermostatted water bath adjacent to the animal chamber. Using this system it was possible to reliably determine pH in a very small volume of only 200-400 μl of blood. Data recording was carried out by a Microx TX2-A device for PO_2 (PreSens, Germany, sampling rate: 1 sec^{-1}) and a μPDD3470 device for pH (Presens, Germany, sampling rate: 12 h^{-1}) both connected to a PC. pH calibration curves used to calculate pH values from the measured raw data (phase angles) were created for the blood of every studied individual. Blood collected after termination of experiments was titrated to different pH values by increasing CO_2 partial pressures in a tonometer (model 237, Instrumentation Laboratory, Italy; at each, 8, 11 and 17°C). Measured phase angles were correlated with pH values measured in the tonometer

with a conventional pH electrode (WTW multiline P4). PO_2 optodes were calibrated in air saturated seawater (100% air saturation) and in a saturated ascorbate solutions (0% air saturation) at constant temperature (oxygen optodes are temperature compensated).

Measurements on n = 6 animals were performed at 17°C and 11°C, measurements for n = 2 animals were obtained at 8°C. At each temperature step and within a time period of 2 hours, the syringe with PO_2 and pH sensors incorporated was slowly filled 4 times with AVC blood (at a rate of approximately 100 μl 10 sec^{-1}). Following a 20 min measurement period within the syringe, blood was slowly pushed back into the blood vessel. For the analysis of PO_2, data points obtained during the first 20 seconds of each syringe filling cycle were averaged. Later readings were constrained by blood cell respiratory activity.

In addition, 50 or 100μl blood samples were taken from the animal twice at each temperature step to measure haemocyanin saturation in the Tucker chamber setup (see above).

2.9 Statistics

Appropriate statistical techniques were employed using STATISTICA 95 software: ANOVA, tests for heterogeneity of slopes in combination with ANCOVA, Student-Newman-Keuls *post hoc* tests, paired t-tests. Regression analyses were performed using either STATISTICA 95 (multifactorial linear regression analysis) or Sigmaplot 9.0 (single factorial and non-linear regression analysis). All differences were considered significant if $p < 0.05$. See respective publications for detailed descriptions. If not stated otherwise, data are typically presented as mean values ± standard deviation (SD).

3. Publications

List of publications and declaration of my contribution towards them.

All experiments were developed and planned by myself with the second and third authors. Novel experimental and surgery techniques were developed by the second author and myself. All experiments were carried out either by myself alone (publication 3), or in close collaboration with the second author (publications 1,2,4,5). All manuscripts were written by myself, revised together with the coauthors.

Publication 1

MELZNER, F., BOCK, C. AND PÖRTNER, H.O. Critical temperatures in the cephalopod *Sepia officinalis* investigated using *in vivo* ^{31}P NMR spectroscopy.
Journal of Experimental Biology (submitted).

Publication 2

MELZNER F., BOCK C. AND PÖRTNER, H.O. Temperature dependent oxygen extraction from the ventilatory current and the costs of ventilation in the cephalopod *Sepia officinalis*.
Journal of Comparative Physiology B (submitted).

Publication 3

MELZNER F., BOCK C. AND PÖRTNER H.O. Allometry of thermal limitation in the cephalopod *Sepia officinalis*.
Comparative Biochemistry and Physiology A (submitted)

Publication 4

MELZNER F., BOCK C. AND PÖRTNER H.O. Coordination between ventilatory pressure oscillations and venous return in the cephalopod *Sepia officinalis*.
Journal of Comparative Physiology B (submitted)

Publication 5

MELZNER F., BOCK C. AND PÖRTNER H.O. The circulatory system limits thermal tolerance in the cephalopod *Sepia officinalis*.
Journal of Comparative Physiology B (submitted)

Critical temperatures in the cephalopod *Sepia officinalis* investigated using *in vivo* ^{31}P NMR spectroscopy.

Frank Melzner*, Christian Bock, Hans - O. Pörtner

Alfred-Wegener-Institute for Marine and Polar Research, Am Handelshafen 12, 27570 Bremerhaven, Germany

Short title: critical temperatures in cuttlefish

Key words: anaerobic metabolism, ventilation, exercise, cephalopoda, mollusca, mantle muscle, mantle cavity pressure

* Author to whom correspondence should be addressed:
phone: +49-471-4831-1331; fax: +49-471-4831-1149;
email: fmelzner@awi-bremerhaven.de

1. Summary

The present study was designed to test the hypothesis of an oxygen limitation defining thermal tolerance in the European cuttlefish (*Sepia officinalis*). Mantle muscle organ metabolic status and pH_i were monitored using *in vivo* ^{31}P NMR spectroscopy, mantle muscle performance was determined by recording mantle cavity pressure oscillations during ventilation and spontaneous exercise.

Under control conditions (15°C), changes in muscle phospho - L - arginine (PLA) and inorganic phosphate (P_i) levels could be linearily related to frequently occurring, high pressure mantle contractions with pressure amplitudes (MMPA) > 0.2 kPa. Accordingly, mainly MMPA > 2 kPa affected muscle PLA reserves, indicating that contractions with MMPA < 2 kPa only involve the thin layers of aerobic circular mantle musculature. On average, no more than 20% of muscle PLA was depleted during spontaneous exercise under control conditions.

Subjecting animals to acute thermal change at an average rate of 1°C h^{-1} led to significant P_i accumulation (equivalent to PLA breakdown) and decrements in the free energy of ATP hydrolysis ($\Delta G/d\zeta$) at both ends of the temperature window, starting at mean critical temperatures (T_c) of 7.0 and 26.8°C, respectively. Frequent groups of high pressure mantle contractions could not (in the warm) or only partially (in the cold) be related to net PLA breakdown in mantle muscle, indicating an oxygen limitation of routine metabolism rather than exercise related phosphagen use. We hypothesize that it is mainly the constantly working radial mantle muscles that become progressively devoid of oxygen. Estimates of very low $\Delta G/d\zeta$ values -44 kJ mol^{-1} in this compartment, along with correlated stagnating ventilation pressures in the warm support this hypothesis. In conclusion, we found evidence for an oxygen limitation of thermal tolerance in the cuttlefish *Sepia officinalis*, as indicated by a progressive transition of routine mantle metabolism to an anaerobic mode of energy production.

2. Introduction

An oxygen limitation of thermal tolerance was proposed to be a unifying principle in ectothermic water – breathing animals (Pörtner 2001, 2002a) and has been supported by the studies on several invertebrates (*Arenicola marina*, Sommer et al. 1997, *Maja squinado*, Frederich and Pörtner 2000, *Sipunculus nudus,* Zielinski and Pörtner 1996, *Littorina littorea*, Sokolova and Pörtner, 2003, *Laternula elliptica*, Peck et al., 2002) and fish species (*Rutilus rutilus*, Cocking 1959, *Pachycara brachycephalum*, Mark et al. 2002, *Gadus morhua*, Sartoris et al. 2003, Lannig et al. 2004). According to this hypothesis, ectothermic animals subjected to acute temperature change first experience a loss in aerobic scope and secondly, oxygen deficiency beyond low and high critical temperature thresholds (T_c), ultimately leading to a transition to an anaerobic mode of energy production and time-limited survival. It was further proposed, that oxygen limitation mechanisms first set in at high levels of organismal complexity, namely the integrated function of the major convection systems of the oxygen delivery apparatus.

Accordingly, previous studies have identified both ventilatory and circulatory (where present) systems in invertebrates to be limiting for oxygen transport during acute temperature change (Zielinski and Pörtner 1996, Frederich and Pörtner 2000), while circulatory insufficiency was suggested to be the first limiting process in fish species acutely subjected to high and low temperature extremes (Heath and Hughes 1973, Mark et al. 2002, Lannig et al. 2004).

The present study, working with the cuttlefish *Sepia officinalis*, will focus on an animal model that, although being an invertebrate, is characterised by several vertebrate-like features. Namely, sophisticated behaviours, a closed, high pressure blood convection system with low blood volume and a highly efficient counter – current gill gas exchange system similar to that of fish (Wells and Wells, 1982, 1991). These features make the cuttlefish an ideal candidate to road – test the proposed universal character of thermal tolerance limitation mechanisms (Pörtner 2002a).

An obvious first step is the evaluation of whether or not cuttlefish will display oxygen - limited thermal tolerance upon acute exposure to low and high temperature extremes, as evidenced by transition to an anaerobic mode of energy production at rest. Advent of mitochondrial anaerobiosis in

highly aerobic liver tissue determined high critical temperature (T_c) in fish (*Pachycara brachycephalum* and *Zoarces viviparus*), while the onset of anaerobic metabolism in white muscle only occurred shortly before death (van Dijk et al. 1999). Choice of tissues therefore seems to be crucial when investigating critical temperatures. Continuously working, aerobic organs with a permanently high oxygen demand are the first to suffer from oxygen deficiency and functional failure. Accordingly, we decided to monitor cephalopod mantle muscle energy status.

Cephalopod mantle tissue is permanently active and involved in ventilatory work, but also in jet propelled locomotion: As a result, the mantle muscle evolved as a complex organ that contains thin outer layers of aerobic circular muscles, which aid during slow swimming contractions, and thick layers of anaerobic muscle fibres in the central part of the mantle muscle organ, which produce the high pressure amplitude contractions during fast swimming (Bone et al. 1994a,b, Bartol 2001). The inner and outer layers of circular fibres possess high densities of mitochondria (Bone et al., 1981, Mommsen et al. 1981) leading to enhanced baseline oxygen demand. Approximately 30% of the mantle volume consists of radial muscle fibres that have a key role in ventilation (Milligan et al. 1997). By contracting, these radial muscle fibres decrease mantle muscle organ diameter to aid in refilling the mantle cavity with fresh seawater during each ventilation cycle. Funnel collar flap movements in combination with a passive relaxation of radial fibres aid during exhalation of the respiratory water. Contractions of circular muscle fibres are not involved in exhalation (Bone et al. 1994a).

Due to their permanent workload, muscle tissues active in ventilation are probably a good indicator tissue for the determination of critical temperatures. Other organs / tissues, that are less vital during short term stresses (i.e. digestive system, reproductive system) may even be temporarily shut down while essential fuels (nutrients, oxygen) are reallocated towards the organs which are maintained in continuous operation. Examples for such selective energy allocation towards certain organs and metabolic depression within other organs / tissues during acute environmental stressors are manifold in the animal kingdom (e.g. the mammalian diving response, Hochachka 2000, associated with cellular metabolic depression, e.g. Buck et al., 1993). If during thermal stress anaerobic metabolism is needed

to fuel ventilatory muscle contractions, obviously time limited survival has set in, critical temperatures are being reached.

Using *in vivo* ^{31}P - NMR spectroscopy, we had a technique available to continuously monitor concentrations of mantle muscle intracellular high energy phosphate compounds and pH_i in unrestrained animals. Net utilization of the phosphagen (phospho –L- arginine, PLA) to fuel muscle contractions is a sign of beginning anaerobiosis in molluscs. We could simultaneously monitor *in vivo* performance of the very muscle fibres observed with the NMR setup by recording mantle cavity pressure oscillations. Such pressure oscillations in the mantle cavity are a consequence of rhythmic action of the mantle muscle organ's ventilatory and locomotory muscles (Bone et al. 1994a,b).

The complexity of mantle muscle structure and the complexity of various, ventilatory and locomotory functions may be confounding factors in the analysis. It thus was necessary to first learn more about the various mantle cavity pressure patterns present and their influence on muscle tissue energy status under control conditions, to later use the acquired knowledge to distinguish between (putative) effects of high pressure mantle contractions related to spontaneous exercise and those of ventilatory pressure cycles on tissue energy status at thermal extremes.

We hypothesized that at both, high and low temperatures, mantle muscle metabolism would need to switch to anaerobic metabolism during resting conditions to sustain ventilatory activity. This report therefore concentrates on muscle energy status and the effects of ventilatory activity on mantle metabolism. It will at the same time address the possibly interfering effects of spontaneous, exercise related high pressure circular muscle contractions on muscle energy status. In a companion study (Melzner, Bock, Pörtner, submitted) we analyse how the pressure patterns generated during resting ventilation relate to oxygen extraction from the ventilatory stream, metabolic rate and the costs of ventilatory movements.

3. Material and Methods

3.1 Animals

European cuttlefish (*Sepia officinalis*) used in the present study were grown from egg clusters trawled in the Bay of Seine (France) in May 2002. The animals were raised in a closed re-circulated aquaculture system (20m^3 total volume, protein skimmers, nitrification filters, UV – disinfection units) at the Alfred–Wegener–Institute on a diet of mysids (*Neomysis integer*) and brown shrimp (*Crangon crangon*) under a constant dark–light cycle (12 – 12) and constant temperature regime (15°C +/- 0.1°C). Water quality parameters were monitored three times per week. Concentrations of ammonia and nitrite were kept below 0.2 mg l^{-1}, nitrate concentrations below 80 mg l^{-1}. Salinity was maintained between 32 and 35‰, and water pH between 8.0 and 8.2. All animals were raised in the same 3 m^3 volume tank. Five animals (104.2 g wetmass, 7.4 g SD) were used for experimentation.

3.2 Experimental protocol

Experimental animals were starved for 24 hours, and then transferred to the experimental set-up. Surgery was conducted on the first day, followed by an overnight acclimatization period within the experimental chamber (control 1). *In vivo* ^{31}P - NMR – spectra showed that anaesthesia during surgery resulted in a transient accumulation of inorganic phosphate (P_i), which could be fully reversed within 4-6 hours of recovery under control conditions. On the second day, animals were cooled from control temperature (15°C) to a lower critical temperature, then warmed to and kept at control temperature over night (control 2), after which they were finally warmed until an upper critical temperature was reached on the third day. Temperature was changed in a stepwise procedure at an average rate of 1°C h^{-1}. Specifically, a three degree temperature change was accomplished during the first hour of a three hour period, while during the two subsequent hours temperature was kept constant for *in vivo* ^{31}P - NMR spectroscopy and mantle cavity pressure measurements. Assay temperatures were 14°C / 11°C / 8°C on the second day, and 17°C / 20°C / 23°C / 26°C on the third experimental day. Temperatures were changed further at a rate of 1°C h^{-1}, if critical temperatures were not reached within the outlined temperature window. As the accumulation of P_i due to phosphagen utilization indicates limited energy production by aerobic metabolism, the appearance of significant P_i peaks in *in vivo* ^{31}P – NMR spectra and their persistence over an extended time period (>60 min) defined critical temperatures.

3.3 *In vivo* ^{31}P – NMR spectroscopy and mantle pressure oscillations

To implant a catheter for ventilatory monitoring, animals were anaesthetized with a 0.4 mol l^{-1} $MgCl_2$ solution that was mixed 1:1 with seawater (Messenger, 1985) at 15°C for 3 – 3.5 minutes, then placed (ventral side up) on a wet leather cloth to prevent skin injuries. During surgery, animals were perfused with aerated seawater (0.04 mol l^{-1} $MgCl_2$) through the funnel aperture. A PE cannula, required to record postbranchial pressure, was connected to a 23 gauge hypodermic needle, led through the entire mantle cavity and then fed through the posterior ventro-lateral section of the mantle muscle. Cannulae (Portex PE tubing, i.d. 0.58 mm o.d. 0.96 mm, flared at the opening) were held in place by two 4 mm diameter plastic washers on the in and outside, embracing the mantle muscle in a sandwich-like fashion. PE tubes were connected to MLT-0699 disposable pressure transducers, signals amplified with a ML-110 bridge amplifier and further fed into a PowerLab/8SP data acquisition system (AD Instruments, Australia). Pressure transducers were calibrated daily.

Following surgery, animals were placed in a perspex perfusion chamber analogous to the one used by Mark et al. (2002) for eelpout (fig 1a). Plastic sliders within the chamber could be adjusted to the animals‘ dimensions and used to restrict the space available for roaming activity. The chamber was connected to a closed recirculation seawater system and placed within the magnet as described in Bock et al. (2002). Water quality was maintained with a protein skimmer (Aqua care, Germany) and a nitrification filter (Eheim Professional 2, Eheim, Germany). Water quality was monitored daily and parameters were kept within the limits indicated above.

In vivo ^{31}P – NMR spectroscopy experiments were conducted in a 47/40 Bruker Biospec DBX system with a 40 - cm horizontal wide bore and actively shielded gradient coils (50 mT/m). A 5 cm ^{1}H / ^{31}P / ^{13}C surface coil was used for excitation and signal reception. The coil was placed directly under the animal chamber in such a manner as to gain maximum signal from the posterior mantle muscle section (fig 1b). A calculated 80 – 90 % of sensitive coil volume was filled by mantle muscle tissue, and about 10 - 20% by tissues from the organ sac and coelomic fluid. As *Sepia officinalis* mantle muscle tissue is characterized by high phosphagen (PLA) concentration (about 34 μmol g^{-1} ww^{-1},

Storey and Storey, 1979) it is quite likely that the *in vivo* ^{31}P -NMR spectra almost exclusively represent the adenylate pool and intracellular pH (pH_i) of the mantle musculature.

In vivo ^{31}P – NMR spectra [sweep width, 5,000 Hz; flip angle, 45° (pulse shape bp 32; pulse length 200 μs); repetition time (TR) 1 s; scans, 256; duration, 3 min 40 s] were acquired once every 21.3 minutes to measure pH_i and its changes represented by the position of the P_i signal relative to the position of the PLA signal. pH_i was calculated using the PLA vs. P_i shift equation obtained by Doumen and Ellington (1992), using a pK_a value determined by Pörtner (1990) for an ionic strength of I = 0.16. pK_a values were adjusted according to temperature (Kost, 1990). ^{31}P - NMR spectra were processed automatically using TopSpin V1.0 software (BrukerBioSpin MRI GmbH, Germany) and a macro (written by R.- M. Wittig, AWI) to finally yield integrals of all major peaks within the spectrum (Bock et al. 2001), as these correlate with the amount of substance within the detection volume (=sensitive volume) of the ^{31}P - NMR coil (fig 1b). Flow weighted images to examine blood flow in major blood vessels were also generated directly before and after the collection of ^{31}P – NMR spectra but will be treated separately. Concentrations of metabolites (ATP, PLA, P_i) were expressed as percentages of the total ^{31}P – signal intensities. This was found necessary, as animals were free to move to some extent in the chamber both vertically and horizontally (for a maximum of 5 mm in either direction, to assure unrestrained ventilatory movements), thus altering overall *in vivo* ^{31}P – NMR signal intensities:

$$[Met] = ([Met] ([PLA]+ [\alpha ATP]+ [\beta ATP]+ [\gamma ATP] + [P_i])^{-1}) 100 \quad (1)$$

with [Met] in % being the relative concentration of metabolite (ATP, PLA, P_i) and ([PLA]+ [αATP]+ [βATP]+ [γATP] + [P_i]) being the sum of the five major ^{31}P - NMR peak integrals that constituted >98% of the overall ^{31}P signal (see fig 5a). As a precondition for such an approach, it is necessary that no major phosphate export from the mantle muscle takes place. Finke et al. (1996) could demonstrate that the sum of adenylates and inorganic phosphate (ATP, ADP, AMP, PLA, P_i) in squid mantle muscle (*Lolliguncula brevis*) was similar in control and exercised animals, as was the sum of all arginine containing metabolites (PLA, Octopine, L Arginine). Storey and Storey (1979) also found the sum of arginine containing metabolites to be relatively stable in cuttlefish mantle muscle following

hypoxia and exhaustive exercise (decreases of less than 10%, minor releases of octopine in the blood stream), but they did not determine inorganic phosphate concentrations. Still, both studies suggest that anaerobic metabolites mostly remain in the mantle muscle organ in cephalopods, thus giving validity to our approach. For better visualisation, percentages of concentrations were transformed into molar quantities assigning [PLA] control values found in cuttlefish mantle muscle (Storey and Storey 1979, [PLA] = 33,6 μmol g^{-1} ww^{-1}) to [PLA] controls in our study (see table 1) and evaluating the other metabolite concentrations accordingly. Free energy change of ATP hydrolysis ($dG/d\zeta$, kJ mol^{-1}) was estimated from NMR visible metabolites as described by Pörtner et al. (1996), with apparent equilibrium constants of arginine kinase and myokinase adjusted to changing temperatures. Concentrations of L-Arginine (Arg) and octopine (Oct) were estimated using published values (Storey and Storey 1979) and assuming that a decrease in 1 μmol g^{-1} ww^{-1} [PLA] results in a concomitant 0.67 μmol g^{-1} ww^{-1} increase in [Arg] and a 0.33 μmol g^{-1} ww^{-1} increase in [Oct] (Storey and Storey 1979; as witnessed during moderate and severe hypoxia and during exercise).

3.4 Mantle cavity pressure analysis

Pressure oscillations in the cephalopod mantle cavity are generated to create both a ventilatory water stream past the gills (mainly by concerted action of the collar flap muscles of the funnel apparatus and radial mantle muscles) and a jet stream to elicit swimming and escape movements (mainly by action of circular and radial mantle muscles). While the former are associated with low pressure amplitudes, the latter can cause amplitudes of up to 25 kPa (Wells and Wells 1991). According to Bone et al. (1994), slow swimming in cuttlefish starts with pressure amplitudes of 0.1 – 1 kPa, while maximum ventilation pressure amplitudes (at rest) were 0.15 kPa. For an analysis of the interfering influence of spontaneous activity on temperature dependent muscle energetics we set a pressure threshold of 0.2 kPa as the starting point for non-ventilation related mantle pressure generation. All such pressure oscillations will be termed ‘swimming jets’ (SJ) hereafter. For all five animals, frequencies of SJs > 0.2 kPa amplitude were analysed at all temperatures. In addition, mean

mantle pressure amplitudes of these SJs ($MMPA_{SJ}$) were recorded (and grouped into twelve amplitude classes, i.e. 0.2-1 kPa, 1-2 kPa, […], 11-12 kPa).

3523 randomly chosen SJs from all temperatures and animals were used to develop a relationship of SJ duration vs. measurement temperature to calculate the fraction of experimental time spent with non – ventilation pressure generation. Also, the relationship of swimming jet amplitude ($MMPA_{SJ}$) vs. swimming jet mean pressure (MMP_{SJ} = pressure integral of SJ peaks) was determined to convert $MMPA_{SJ}$ to MMP_{SJ} at all temperatures. Routine ventilation pressures were analysed in similar ways. Thus we could calculate total mean mantle pressure as the sum of routine ventilation pressures (MMP_{rout}) and MMP_{SJ}:

$$MMP_{tot} = MMP_{SJ} + MMP_{rout} \quad (2)$$

3.5 Spontaneous exercise impacts on mantle metabolism

Mantle contractions associated with high amplitude pressure pulses were present at all temperatures. The major challenge in the present study was thus to distinguish between the effects of spontaneous exercise and the effects of routine ventilatory mantle muscle activity (related to ventilation only) on muscle metabolic status. Vast quantities of control ^{31}P NMR - spectra at 15°C were available to investigate activity patterns and patterns of metabolite change in the mantle organ:

First, consecutive *in vivo* ^{31}P - NMR spectra were analysed for changes in [PLA] and [ATP] parallel to changes in $[P_i]$:

$$\Delta [Met] = [Met]_{n+1} - [Met]_n \quad (3)$$

where Δ [Met] = concentration change of a given metabolite, $[Met]_{n+1}$ = concentration of the given metabolite obtained with spectrum n+1, $[Met]_n$ = concentration of metabolite obtained with spectrum n. Changes in pH_i were calculated in a similar fashion. A total of 282 intervals from all 5 animals were used for such comparisons. This was done to elaborate patterns of correlated concentration changes between the respective metabolites and pH_i and to investigate the degree to which phosphagen resources are commonly used under control conditions.

As a second step, an attempt was made to correlate metabolic changes observed within the mantle muscle with non – ventilatory muscle contractions (of pressure amplitudes >0.2 kPa). It is known from previous work that such mantle muscle contractions are fuelled in part by phosphagen breakdown, as aerobic metabolism cannot provide sufficient amounts of ATP to match demand at very high ATP fluxes (e.g. Pörtner et al. 1993, Finke et al. 1996). For this, *in vivo* ^{31}P - NMR spectra were scanned for relative increases in [P_i] (which is equivalent to a net phosphagen breakdown). A total of 30 intervals from all 5 animals were randomly selected, and all associated mantle contractions within each interval analysed. To find a (putative) causal relationship between spontaneous exercise and metabolite changes in the mantle organ, it was necessary to identify those suitable time intervals and pressure amplitudes that actually have an effect on muscle phosphagen stores. In an exercise study on squid (*Illex illecebrosus*) it could be demonstrated that mantle phosphagen levels returned close to control levels within 10 minutes after fatiguing exercise, where PLA had decreased by -22.5 μmol g^{-1} ww^{-1} from an initial concentration of >30 μmol g^{-1} ww^{-1} (Pörtner et al. 1993). Thus, in our case, a major spontaneous exercise event, occurring 20 minutes prior to ^{31}P NMR spectrum acquisition, might not be reflected in the latter due to a putative rapid recovery phase of PLA stores.

Consequently, intervals (21 minutes 20 seconds between the acquisition of two ^{31}P NMR spectra plus the acquisition time of the second spectrum; thus a total of 25 minutes) were divided into 11 two minute segments and one 3 minute segment (s1 – s12, see fig 1c). Both the frequency and amplitude of SJs greater than 0.2 kPa were determined for each segment. Pressure amplitudes were grouped into classes with the following class means: 0.6 kPa (=0.2-1kPa), 1.5 kPa (= 1kPa - 2kPa) [...] up to 11.5 (= 11kPa – 12kPa) and a jet index (JI, in kPa $segment^{-1}$) obtained for each segment by adding the products of class amplitude means and jet numbers within the respective amplitude classes. For example, five jets between two and three kPa and three jets between five and six kPa within one segment yield a JI of (5 * 2.5)+(3 * 5.5) = 29 kPa. 12 variables were created by adding JIs from segments within intervals a to l (see fig. 1c). Furthermore, each of these variables was split up by varying the pressure threshold used for JI calculation (only jets >0.2 kPa or >1kpa or >2 kpa […], >11 kPa used for calculations). Thus, for our example above, a JI calculated from jets >3 kPa would result in 3 * 5.5 = 16.5 kPa. This variation in duration of the interval and in the pressure amplitudes taken for

JI calculation created a total of 12 * 12 = 144 different variables that could be tested in an iterative linear regression analysis to explain a maximum of the variability observed in [P_i] changes as obtained by successive *in vivo* ^{31}P NMR spectra. In a similar fashion, maximum jet density (JD) of SJs > 0.2, > 1 [>...],> 11 kPa within segments of intervals a to l (fig 1c) was calculated (again, 144 possible variables) as a second factor that might influence [P_i] changes in mantle muscle tissue. For example, JD were 15 for jets > 1 kPa if we considered interval d (see fig 1c) and the density of jets > 1 kPa (in jets 2 min^{-1}) in segments s9, s10, s11 and s12 were 9, 12, 15 and 3.

3.6 Statistics

Simple linear, exponential and sigmoidal regression analyses were performed using SigmaPlot 8.0. Multiple linear regression analysis was also performed using STATISTICA, as were all other statistics. Comparisons between values grouped according to temperature or animal were conducted using one factorial ANOVA and subsequent post–hoc testing with Student–Newman–Keuls. T-tests were used to compare SJ frequencies obtained during the day with those obtained at night.

4. Results

4.1 Control conditions

4.1.1 Mantle pressure

Typical ventilation pressure amplitudes in all experimental animals were lower than 0.1 kPa, typically occurring during 57 or more minutes of each control hour. The remaining time was filled with spontaneous high pressure mantle contractions > 0.2 kPa. Occurrence of such SJs was observed in all animals, with pressure amplitudes distributed as shown in fig 2a. It appeared that roughly 73% of all non – routine ventilation pressure cycles >0.2 kPa were characterized by an amplitude lower than 2 kPa. Only 0.2% of all pressure cycles > 0.2 kPa showed pressure amplitudes of 11 – 12 kPa.

Mean SJ pressure amplitude of all SJs > 0.2 kPa was found to be 1.7 kPa. Frequencies of 108 (181) pressure cycles > 0.2 kPa h^{-1} during daily (nightly) control measurements were recorded, these did not appear to be evenly distributed over time, but rather were found to occur in groups of 3 – 50 SJs. A significant difference in high amplitude pressure cycle frequency between nighttime and daytime control measurements was also evident, with more jets observed at night ($t = 3.5$; df 4; $p<0.03$).

4.1.2 *In vivo* ^{31}P NMR spectroscopy

Concentrations of *in vivo* ^{31}P - NMR visible metabolites and pH_i were found to be as variable as mantle pressure recordings. Figure 3 gives an example: data are shown from 14 subsequent control ^{31}P NMR spectra taken from animal 4 between 23:22 and 04:47 hours during the second control phase of the experiment (at constant 15°C). While muscle ATP concentrations remained constant over the whole period, [PLA] decreased from 33.4 to 23.8 μmol g^{-1} ww^{-1} (Δ[PLA] = -29%) between 50 and 100 minutes. This was mirrored by a concomitant increase in $[P_i]$ from 0.8 to 11.6 μmol g^{-1} ww^{-1}. Recovery of the phosphagen pool in combination with a decrease in $[P_i]$ started at t = 100 minutes and lasted for 150 – 200 minutes. pH_i values followed a similar pattern when compared to [PLA], but were delayed by about 50 minutes. During the first 25 minutes of phosphagen utilization, pH_i increased from 7.43 to 7.49. Therafter, pH_i values decreased continuously to a minimum value of 7.32 at t = 150 minutes. A value close to control was reached again after 325 minutes. The observed P_i accumulation of 11.6 μmol g^{-1} ww^{-1} was the highest observed in any of the 5 animals under control conditions (tab 1).

Patterns of metabolite concentration changes and correlated pH_i changes appeared to be comparable between all animals. To elaborate these patterns, changes in metabolite concentration and pH_i were analysed from *in vivo* ^{31}P - NMR spectra over time (fig 4). As would be expected from figure 3, Δ[PLA] changed linearily with $\Delta[P_i]$, with a negative slope close to one (fig 4b), while ATP concentrations remained stable at about 7-9 μmol g^{-1} ww^{-1} (ANOVA, $F_{(7,272)} = 1.83$; $p<0,07$; fig 4d). pH_i changed linearily with increasing $\Delta[P_i]$ between <-3 and 3 μmol g^{-1} ww^{-1} (fig 4a), but deviated significantly from this relationship once [Pi] accumulated > 3 μmol g^{-1} ww^{-1}. pH_i fell back to 7.44

(control pH was 7.45; see table 1) at those higher inorganic phosphate accumulations. From 282 intervals analysed for fig 4, only 9 intervals (3%) were characterized by such a high increase in $[P_i]$. Correspondingly, intracellular $\Delta[H^+]$ changed linearily in the respective range of $\Delta[P_i]$ values (fig 4c). Increases in $[P_i] > 3$ μmol g^{-1} ww^{-1} did not result in a further proton buffering but rather led to a net increase in $[H^+]$ by 3 nmol l^{-1}.

It seemed obvious that fluctuations observed in the concentrations of high energy phosphates and in pH_i should be related to the frequency of high amplitude swimming jets. In a first iterative step of univariate linear regression analysis, 36 different jet index (JI) variables were identified that could explain significant fractions of variability in $\Delta[P_i]$. These differed in the length of the time interval as well as in the pressure threshold chosen for JI calculation. 12 of these are shown in table 2. Intervals of 13 – 15 minutes for JI calculation (corresponding to intervals f and g in fig. 1c) resulted in regressions with the highest R^2. Omitting mantle pressure cycles below 2 kPa also resulted in better regressions, while JIs exclusively calculated from swimming jets greater than 3 kPa failed to explain a similar amount of variability in $\Delta[P_i]$ (tab 2). The best single variable identified was a JI constructed from mantle pressure cycles greater than 2 kPa during the last 15 minutes of each 25 min interval:

$$\Delta[P_i] = 0.0387\ JI \qquad (4)$$

with $\Delta[P_i]$ in μmol g^{-1} ww^{-1} and JI in kPa calculated from SJs > 2kPa within interval g (see fig. 1c). This regression could explain 84% in $\Delta[P_i]$ variability. Accordingly, 20 jets of an amplitude between two and three kPa (JI = 50) would result in a $\Delta[P_i]$ of roughly 2 μmol g^{-1} ww^{-1}, which is equivalent to a 6% decline in mantle muscle phosphagen reserves. Inclusion of a second variable, jet density (JD), into the model significantly enhanced the fraction of explainable $\Delta[P_i]$ variability to 89%:

$$\Delta[P_i] = 0.0335\ JI + 0.1555\ JD \qquad (5)$$

with $\Delta[P_i]$ in μmol g^{-1} ww^{-1} and JI calculated from SJs >2 kPa within interval g and jet density (JD) calculated from jets > 5 kPa within interval g (see fig 1c).

As high spontaneous swimming jets could be related to the accumulation of inorganic phosphate observed in mantle muscle, true control values for [ATP], [PLA] and pH_i were calculated only from spectra with $[P_i] < 1.5$ μmol g^{-1} ww^{-1}, as this was the maximum $[P_i]$ found during prolonged routine ventilation sequences (table 1, only sporadic,< 10, jets of pressure amplitudes < 1 kPa for at

least 30 minutes). Mean pH_i values were comparable between animals, except for animal three which showed a significantly higher mean muscle pH_i. Variability in $[H^+_i]$ was low under control conditions, with a relative standard deviation (CV) of about ±15% at a mean concentration of 36.1 nmol l^{-1}. ATP concentrations were comparable between animals two through five, while animal one had a significantly lower muscle [ATP] than animals two, four and five. Although there were significant differences found in [PLA] between animals, it has to be considered that all mean concentrations were found within a range of -1.6% to +2.8% of the mean value of 33.6 μmol g^{-1} ww^{-1}. The ratio of [PLA] over [ATP] proved to be relatively stable between animals (4.0-4.6), with ratios being comparable from animals two through five and only animal one being characterised by a significantly higher ratio (table 1).

4.2 Acute temperature change

4.2.1 mantle pressure

Bouts of spontaneous mantle muscle activity (SJs > 0.2 kPa) could be observed at all temperatures (fig 2b), with no significant differences between temperatures ($F_{(6,28)}$=1.5; p<0.22). A trend towards a higher frequency of spontaneous swimming jets is evident with rising temperature between 8 and 23°C. Examination of swimming jets at all temperatures yielded a linear regression for the duration of individual swimming jets in relation to temperature:

SJ duration = -0.0225 T + 1.3025 (6)

R^2 = 0.89, n=3523 Sjs, with SJ duration in s and T = temperature in °C. Mean mantle pressure (MMP_{SJ}) and mean mantle pressure amplitude ($MMPA_{SJ}$) were also linearily related:

MMP_{SJ} = 0.2723 $MMPA_{SJ}$ (7)

R^2 = 0.81; n = 3523 SJs, with both MMPA and MMP in kPa. The frequency distribution of amplitudes of swimming jets at all investigated temperatures was comparable to the one obtained during control conditions (fig 2a). Between 36 and 110 SJs per hour were recorded (8-26°C range), corresponding to about 1 and 3% of the total experimental time spent performing high pressure swimming jets. With a

mean SJ amplitude of 1.7 kPa (see above), the impact of relatively few high pressure cycles constituted a significant fraction of total mantle pressure (MMP_{tot}): Between 20 –36% of MMP_{tot} were produced by high pressure swimming jets (fig 2c) in the investigated temperature range. Owing to the high variability in SJ frequency (see fig 2b) these differences were not significant, although a trend towards reduced pressure generation by SJs is evident between 23 and 26°C.

4.2.2 *In vivo* ^{31}P NMR spectroscopy

In vivo - ^{31}P - NMR spectra (fig 5a) revealed that despite the changes in metabolic rate and ventilatory power output observed over the entire temperature range (Melzner, Bock, Pörtner, submitted), muscle [ATP] remained constant (ANOVA: $F_{(6,28)}$=0.13; p<0.99) at around 8 μmol g^{-1} ww^{-1} (Fig 5b). The situation was different for the other metabolites: Although we could not detect significant differences in muscle [PLA] (ANOVA: $F_{(4,20)}$ = 1.48; p<0.25) and [P_i] (ANOVA: $F_{(4,20)}$= 1.68; p<0.20; fig 5b,c) between 11 and 23°C , there was a trend towards decreasing [PLA] values between 17 and 23°C, which was mirrored by increasing [P_i] values in this respective interval. Intracellular pH decreased with rising temperature in a linear fashion:

$$pH_i = 7.528 – 0.0061\ T \quad (8)$$

R^2=0.87; $F_{(1,5)}$ = 33.4; p<0.007, with T = temperature in °C, fig 5d. All animals started accumulating [P_i] (= net utilization of phosphagen reserves) in their mantle muscle organ at some point of time in both the cold and the warm. A huge standard deviation at 8 and 26°C indicated that the start point for this apparent failure of aerobic metabolism to sustain high cellular ATP fluxes differed between animals.

Therefore, grouping animals into pre – P_i accumulation (group A, means of *in vivo* ^{31}P - NMR spectra 60 minutes prior to P_i accumulation) and P_i accumulation (group B, means of *in vivo* ^{31}P - NMR spectra during P_i accumulation (60 minutes duration); with the start of accumulation defined as at least 2 successive spectra with a [P_i] > 1.5 μmol g^{-1} ww^{-1}) enabled us to improve the resolution of metabolic patterns at both ends of the temperature window (tab 3): In the cold, phase B mean temperature was 7°C. From phase A to B, [PLA] had decreased to 30.9 μmol g^{-1} ww^{-1} while [ATP]

remained constant. pHi was also comparable between phases A and B. At the warm end of the temperature spectrum, the picture was similar: At a mean temperature of 26.8°C, [PLA] decreased to 30.5 μmol g^{-1} ww^{-1}, while [ATP] and pHi did not change from phase A to B. Looking at the last ^{31}P - NMR spectra taken at each temperature (called $B_{extreme}$ in tab 3) illustrates that at high temperatures, pH_i is significantly decreased as compared to Phase A. A trend towards decreased pH_i values is also visible at the low temperature $B_{extreme}$, although it is not (yet) significant. Free energy changes of ATP hydrolysis $|\Delta G/\Delta\xi|$ decreased by 3.3 kJ mol^{-1} at the low $B_{extreme}$, by 5.1 kJ mol^{-1} at the high $B_{extreme}$. Mean values did not drop below 50 kJ mol^{-1}, if one assumes that phosphagen utilization is distributed evenly among all muscle fibre types (radial and circular fibers; (r+c) in table 3) present in the sensitive volume of the ^{31}P - NMR coil.

Having established that changes in [PLA] and [Pi] can be caused by swimming jets under control conditions, it was necessary to investigate whether changes at extreme temperatures were also due to locomotory exercise or due to routine ventilation activity. Regression models were tested to establish a link between SJs and inorganic phosphate accumulation in the mantle muscle organ at extreme temperatures (phase B). Testing the same set of variables as for the control situation (see above), a significant regression model could be established for the low extreme temperature situation

$$\Delta[P_i] = 0.022\ JI + 2.66\ JD \quad (9)$$

$R^2 = 0.49$; $F_{(2,29)} = 14.3$; $p<0.001$, with $\Delta[P_i]$ in μmol g^{-1} ww^{-1}, JI calculated within interval 1 (fig 1c) from jets > 2kPa, JD calculated in interval 1 from jets > 5 kPa. While this significant model could explain roughly half of the encountered variability in $\Delta[P_i]$ at low temperatures, we could not identify a single significant regression model at high temperatures.

In a second step, we looked at $[P_i]$ variability during 25 min intervals with no high pressure jets >0.2 kPa present. At both low and high extreme temperatures (phase B), a mean accumulation of $[P_i]$ could be found (high temp: $\Delta[P_i]$ = 1.15 μmol g^{-1} ww^{-1} (SD = 0.3 μmol g^{-1} ww^{-1}), n = 8 intervals; low temp.: $\Delta[P_i]$ = 0.53 μmol g^{-1} ww^{-1} (SD = 0.43 μmol g^{-1} ww^{-1}), n = 9 intervals), while during (randomly) chosen control intervals with no high pressure cycles present, no inorganic phosphate increases could be found at all ($\Delta[P_i]$ = -1.65 μmol g^{-1} ww^{-1} (SD = 1.9 μmol g^{-1} ww^{-1}), n = 8 intervals).

Rather, negative $\Delta[P_i]$ values dominated under control conditions, as periods without any SJs at all predominantly were found during recovery times from (spontaneous) exercise.

In summary, we have found significant increases in $[P_i]$ (= phosphagen use) in the mantle muscle organ at both, high and low temperature extremes, in all five animals investigated. At a control temperature of 15°C, $[P_i]$ variability could almost completely (89%) be explained by the occurrence of high pressure SJs. At high extreme temperatures, SJs could not be related to the observed increases in $[P_i]$. Inorganic phosphate accumulation was also observed during intervals without any SJs present, and thus was likely caused by elevated levels of routine ventilation alone. At low extreme temperatures, apparently both processes (routine ventilation energy demands and spontaneous exercise energy demands) contributed to $[P_i]$ accumulation.

5. Discussion

Using non-invasive *in vivo* ^{31}P – NMR spectroscopy we were able to continuously monitor key components of the *S. officinalis* mantle muscle energy system in unrestrained animals subjected to acute temperature changes. Our aim was to identify potential threshold temperatures, below or above which aerobic metabolism would insufficiently provide the energy required for muscle maintenance, routine activity (ventilatory contraction of radial fibres) and facultative exercise (high pressure contractions performed by aerobic and anaerobic circular fibres). A number of invasive studies on cephalopod mantle organ tisssue has provided the neccessary information to interpret the observed changes in NMR visible metabolites ([PLA], $[P_i]$, [ATP]) and pH_i , following the advent of anaerobic metabolism, both in mitochondria and the cytosol (Storey and Storey 1979, Gaede 1980, Finke et al. 1996, Pörtner et al. 1991, 1993, 1996, Zielinski 1999, Zielinski et al. 2000).

5.1 Control conditions

During control conditions we had the unique possibility to study the effects of facultative mantle muscle exercise on the animals' intracellular energy status. We could show that animals

displayed a higher activity (as evidenced by the occurrence of swimming jets with an amplitude >0.2 kPa) during 1-3% of the total time. Similar levels of activity were recently found for a tropical cuttlefish in its natural habitat (*S. apama* was found to be active (as estimated from elevated mantle pressures) approximately 3% of a days time; Aitken et al. 2005).

Control mantle muscle organ adenylate levels obtained in our study, as witnessed by the ratio of [PLA] over [ATP], are comparable to other studies that analysed metabolite concentrations invasively. Our ratio of 4.2 (0.4 SD) compares well with a value of 3.9 for *S. officinalis* (Storey and Storey 1979), 4.4 for the squid *Lolliguncula brevis* (Finke et al. 1996) or 3.5 for the squid *Loligo pealei* (Pörtner et al. 1993). We were able to clearly demonstrate that PLA stores were being utilized during high pressure swimming jets and could establish a quantitative relationship between exercise levels and decreases in [PLA] or increases in [P_i], respectively. The best relationship obtained suggests that SJs with a MMPA of > 2 kPa cannot be fuelled entirely by means of aerobic energy production, similar to findings in the squid, *L. brevis* (Finke et al. 1996). This fits the picture that slow swimming ('cruising') mantle pressure amplitudes in *S. officinalis* seem to not exceed 1.5 - 2 kPa (Wells and Wells 1991, their fig 1b). Bone et al. (1994a) could demonstrate that during slow swimming at pressure amplitudes between 0.1 – 1.0 kPa, (aerobic) circular fibres become involved in the pressure generating process. Thus it is quite likely that slow swimming at < 2 kPa can be fuelled entirely by metabolism of the thin aerobic muscle layers of the mantle periphery. More extreme exercise with pressure amplitudes > 2 kPa progressively involves central anaerobic fibres (Bone et al. 1994b) that exploit their phosphagen reserves in order to propel the animal at higher speeds. Gradual involvement of central (mainly) anaerobic fibres (rather than an all – or – nothing transition) to support aerobic fibres at an increasing workload has been recently demonstrated for swimming squid (*L. brevis*, Bartol 2001).

The fact that we found a linear relationship between jet indices constructed from mantle pressure amplitudes multiplied with jetting frequencies and phosphagen use is not surprising, as pressure production should be a direct function of circular mantle muscle fibre force generation. Muscle fibre force has been found to depend on the number of crossbridges in the force generating state per cross sectional area (e.g. Wannenburg et al. 1997), thus mantle cavity pressure in

cephalopods should be directly proportional to ATP flux rates in working mantle muscle. This corresponds to results of Webber and O'Dor (1986) who found correlated changes in mantle pressure integral and whole animal MO_2 during various levels of exercise in a squid (*I. iIllecebrosus*).

The inclusion of a second variable into the regression model (jet density, JD) significantly enhanced the fraction of explainable variation in inorganic phosphate concentration changes. This implies that high amplitude jets > 5 kPa pose a higher threat to cellular phosphagen reserves when they occur in quick succession, rather than distributed over a longer time interval. This could be due to oxygen depletion or aerobic fibre fatigue at high jet density, resulting in pressure generation exclusively by anaerobic fibres during high - jet density, high – pressure time intervals.

It should be emphasized that PLA stores were never used extensively under control conditions (15°C) and during facultative, spontaneous exercise. Mean maximum decreases in [PLA] (=increases in [Pi], see table 1) under control conditions amounted to 6.66 μmol g^{-1} ww^{-1}, which corresponded to roughly 20% of phosphagen reserves, although one animal (replicate 4, fig 3) depleted 35% of its phosphagen reserves on one occasion.

Figure 3 demonstrated that, during initial phosphagen transphosphorylation and P_i accumulation, pH_i can be buffered and remains unchanged. pH_i decreased only during prolonged phosphagen utilization, likely due to glycolysis and concomitant octopine formation (Storey and Storey 1979, Pörtner, 1987, 2002b). Work on *in vitro* preparations of scallop (*Argopecten irradians*) contracting phasic adductor muscles suppports this conclusion (Chih and Ellington 1985). While during initial exercise (40 muscle contractions) proton consumption by phosphagen utilization exceeded proton production by octopine formation, resulting in a net alkalosis of about 0.09 pH units ($\Delta[H+]$ = -16 nmol l^{-1}), further exercise (40 – 200 contractions) led to progressively declining pH_i values due to glycolytic proton production outmatching proton consumption by the phosphagen. Figure 4 provides a more quantitative picture and shows clearly, that anaerobic metabolism is seldomly employed to a degree that net cellular acidification occurs. Only 3% of all (randomly chosen) intervals analysed for fig. 4 showed a $[P_i]$ accumulation of > 3 μmol g^{-1} ww^{-1}. Such a degree of phosphagen utilization goes along with the onset of muscle acidosis, suggesting that glycolytic proton production outmatches proton buffering by phosphagen use.

Apparently, cuttlefish avoid intracellular acidification by terminating exercise in most cases as soon as glycolytic proton production equals phosphagen proton buffering capacity. Upon removal of inorganic phosphate during recovery, a glycolytic proton surplus, that cannot be buffered, results in a slight decrease in pH_i (fig 4a,b). Potentially adverse effects of decreased pH_i values on muscle function (see review by Fitts 1994) are thus shifted into recovery phases. Absolute changes in intracellular proton activities are low (in the nmol range, fig 4b), a feature also observed by Chih and Ellington (1985). A recent *in vivo* ^{31}P - NMR spectroscopy study on forced scallop exercise (Bailey et al. 2003) confirmed the metabolic patterns obtained in the older *in vitro* study on stimulated adductor muscle preparations.

5.2 Acute temperature change

Figure 5 depicts the changes in mantle organ metabolite levels with temperature. Despite the dramatic changes in ventilatory power output over the entire temperature range, [ATP] is strictly conserved (fig 5a), a phenomenon commonly encountered in studies on muscles of marine ectothermic animals subjected to acute temperature change (i.e. Mark et al. 2002, Sartoris et al. 2003, Zielinski 1999) and generally referred to as the ‚stability paradox' (Hochachka and Somero 2002). [PLA] was also constant between 11 and 23°C.

We could not find any evidence for an alphastat pattern of pH_i regulation (Reeves 1972, see Burton 2002 for a review) in the investigated temperature range. Typically, changes of around – 0.018 pH units $°C^{-1}$ are expected to ensure constant levels of imidazol and protein ionization. For fish species, such a pattern could be demonstrated in white muscle (Borger et al. 1998, Van Dijk et al. 1997, 1999, Bock et al. 2001). As for molluscs, an alphastat pattern of pH_i regulation was absent in the stenothermal marine bivalve *Limopsis marionensis* (Pörtner et al. 1999). Despite confounding effects of mantle muscle exercise at all temperatures, we found a decrease in pH_i with temperature by about –0.006 pH units $°C^{-1}$ over the full temperature range examined. Omitting pH_i values at 8 and 26°C, as phosphagen utilization was observed to start at these temperatures, gives an even lower rate of change of –0.004 pH units $°C^{-1}$. Between 11 and 17°C (the typical natural temperature range of this population

of cuttlefish in the English Channel, Boucaud – Camou and Boismery 1991), pH_i values are nearly identical. The absolute temperature dependent changes in pH_i are < 0.05 units between 11 and 23°C, which is lower than the range of change observed during facultative exercise at control temperature. Future studies should address the time dependence of intracellular pH regulation in response to temperature. Our study focused on short term temperature effects and may not have allowed mantle intracellular pH to fully reach new steady state values after each thermal challenge. As it stands, the question of temperature dependent pH_i regulation in cephalopods must remain open.

Patterns of metabolite changes observed at extreme temperatures exactly mirrored those during exercise under control conditions. The start of phosphagen utilization was observed in all 5 animals at both temperature extremes during phase B. Mean temperatures during this phase were 26.8°C and 7°C.

5.2.1 High T_c

The analysis of mechanisms at the high end of the temperature spectrum proved to be easier than at the low end: As no relationship between the few SJs (see fig 2b,c) and the use of the phosphagen could be established and also, since $[P_i]$ increases could be found during periods of ventilation at rest, obviously aerobic metabolic limitation had set in independent of effects of spontaneous SJ exercise at warm temperatures. Still, the results are difficult to interpret as mantle muscle is a complex organ that consists of different muscle fibre types with different functions (Bone et al. 1981, Bone et al. 1994a,b, Bartol 2001). Radial muscle fibres aid in refilling the mantle cavity during ventilation by contracting and thus enlarging mantle cavity volume. Bone et al. (1994a) were the first to demonstrate that expiration in the cuttlefish under control conditions (18°C) and at rest (mantle pressure amplitudes of 0.05 - 0.15 kPa), is not brought about by contraction of the outer, aerobic layers of circular fibres, but rather by the movements of the collar flaps (muscular funnel appendages, see Tompsett 1939) that expel water rhythmically from the mantle cavity. Maximum resting ventilation MMPA recorded in our experimental animals were lower than 0.15 kPa (Melzner, Bock, Pörtner, submitted), thus we assume that during our entire experimental series, radial fibres had

been the only constantly working myofilaments within the sensitive volume of our ^{31}P - NMR coil (fig 1b). Our companion study revealed that ventilation pressures stagnate at temperatures beyond 26°C. Fig. 6a shows ventilation pressure amplitudes (at rest) at temperatures close to the upper Tc for two experimental animals (the ones with the highest and the lowest T_cs), while fig 6b gives correlated increases in $[P_i]$ (circles). It is quite evident from this figure that declining ventilation pressures and phosphagen use are tightly coupled (all other experimental animals showed similar patterns). We thus conclude that an energetic limitation of radial muscle fibres is responsible for the observed increases in $[P_i]$ and the correlated decreases in ventilation pressures once phosphagen usage starts. Radial fibres have a mitochondrial content as low as central ‚anaerobic' circular fibres (Bone et al. 1981, Mommsen et al. 1981), thus may be especially sensitive to enduring ventilation exercise at high intensities. Considering that radial fibres constitute about 30% of total mantle volume in the cuttlefish (Milligan et al. 1997), and assuming that solely radial fibres deplete their phosphagen stores as ventilation pressures increase, while, on the other hand, circular fibre energy status remains constant, it is possible to estimate metabolite changes for the radial fibre compartment. Based on such considerations, radial fibre $|dG/d\zeta|$ for animals one and five would drop severely as phosphagen use proceeds (fig 6b). Following such a rationale, metabolite changes were recalculated for phase B (denoted r in table 3) for all five animals. Thus, mean [PLA] reserves would decrease by 75% from 33 to 8.5 μmol g^{-1} ww^{-1}, mirrored by an increases in $[P_i]$ in the same range and a 25% reduction in [ATP]. pH_i would be significantly decreased to 7.19 and $|\Delta G/d\zeta|$ would drop to below 44 kJ mol^{-1} in the radial fibre compartment of the mantle organ. These calculations correspond to similar $|\Delta G/d\zeta|$ values for mantle muscle of three species of squid following fatiguing exercise, which ranged from 42 to 47 kJ mol^{-1} (Pörtner et al. 1996), while values for two species of exercise fatigued eelpout (*P. brachycephalum, Z. viviparus*, Hardewig et al. 1998) white muscle ranged from 46.6 to 48 kJ mol^{-1}. Possibly, reductions in the free energy of ATP hydrolysis as calculated for cuttlefish radial muscle could contribute to muscle fibre fatigue in that vital muscle due to functional impairments of ATPase functions. Kammermeier et al. (1982) found a drop in contractile performance of perfused rat hearts (38°C) below a $|\Delta G/d\zeta|$ of 48 kJ mol^{-1}. He calculated threshold values of $|\Delta G/d\zeta|$ required for proper function of the various

ATPases engaged in muscular work to range from 45 – 53 kJ mol^{-1} (Kammermeier 1987, 1993). Only recently, Jansen et al. (2003) found maintenance of $[Na^+_i]$ homeostasis prevented by $|\Delta G/d\zeta|$ values below 50 kJ mol^{-1} due to a limitation of the sodium pump (Na^+/K^+ - ATPase) in perfused rat hearts. Less information on critical $|\Delta G/d\zeta|$ values for muscle function is available for ectothermic animals: Combs and Ellington (1995) calculated an energy requirement of 41 kJ mol^{-1} for blue mussel (*Mytilus edulis*) sarcolemmal Ca^{2+} - ATPase. A minimum $|\Delta G/d\zeta|$ value of 46 kJ mol^{-1} for the sodium pump of crayfish abdominal muscle was calculated by the same authors (Combs and Ellington 1997), although they found changes in $[Na^+_i]$ homeostasis well above 50 kJ mol^{-1} already. They speculated that global $|\Delta G/d\zeta|$ might not reflect the $|\Delta G/d\zeta|$ close to the sodium pump.

Also, both elevated intracellular proton and inorganic phosphate concentrations have frequently been connected with muscular fatigue independent of $|\Delta G/d\zeta|$ (Allen and Westerblad 2001, Fitts 1994). Increased $[P_i]$ is thought to reduce muscle force by reversing the force generating P_i release step by mass action (Hibberd et al. 1985). According to Debold et al. (2004, rat muscle fibres) the $[P_i]$ dependency of muscle fatigue is temperature related, with a more pronounced effect of $[P_i]$ at low temperatures. For ectothermic (marine) animals such studies have, to our knowledge, not been undertaken.

Judging from the presented results and literature data, it appears that progressive phosphagen usage indeed is causative of the observed stagnation in ventilatory pressure generation at high temperature extremes, although the exact mechanisms still need to be elucidated.

5.2.2 Low T_c

At low temperatures, we could demonstrate that SJs contributed significantly to increases in $[P_i]$. 50% of variability in $\Delta[P_i]$ could be attributed to facultative exercise of circular anaerobic fibres, while the other half remained unexplained. As neither SJ frequency nor the fraction of MMP_{SJ} on MMP_{tot} increased at lower temperatures (similar frequencies / pressures were observed between 8 and 11°C, fig. 2b,c) and no P_i accumulation occurred at 11°C (fig 5b), a major loss in aerobic scope for

spontaneous activity had evidently occurred towards low temperature extremes, resulting in the net use of phosphagen stores for spontaneous activity. The other 50% of variability that could not be explained by the linear regression is likely due to a limitation in oxygen flux towards radial muscles thus limiting their active role in ventilation. It seems that at low temperatures, all muscle fibre types might suffer from phosphagen breakdown. Accordingly, we calculated $|\Delta G/d\zeta|$ values assuming that mantle phosphagen depletion took place more homogeneously. In $B_{extreme}$, $|\Delta G/d\zeta|$ had dropped from 55 to 51 kJ mol^{-1}. This does not exclude the existence of heterogeneity or even of putative intracellular $|\Delta G/d\zeta|$ gradients. Hubley et al. (1997) calculated distinct intracellular concentration gradients of the vertebrate phosphagen, creatine phosphate (PCr), and free energy of ATP hydrolysis in working fish white muscle, depending on the maximum distance from the nearest mitochondrion. Maximum intracellular $|\Delta G/d\zeta|$ gradients of 7 kJ mol^{-1} were calculated. Interestingly, the study suggests, that in fish white muscle such $|\Delta G/d\zeta|$ gradients will be less pronounced in animals acclimated to high temperature (25°C) and acutely exposed to low temperature (5°C). This is mainly due to differing temperature relationships of metabolic rates and intracellular diffusion coefficients for ATP and PCr (i.e. Q_{10} for D_{PCr} was only found to be 1.28, while, typically, Q_{10} values for metabolism are >2). If this holds true for cuttlefish muscle as well, we can expect drops in $|\Delta G/d\zeta|$ to have less severe impact on intracellular ATPase function, and, thus, muscle function, during oxygen limitation developing at acute exposure to low temperatures.

However, although oxygen limitation of thermal tolerance in the cold likely progresses at a slower pace, phosphagen usage during periods without spontaneous activity is a certain sign of a cellular energy limitation, leading to time limited survival of the organism.

5.2.3 Perspectives: thermal limitation in cephalopods vs. fish

Van Dijk et al. (1999) found no changes in fish (*Pachycara brachycephalum*, *Zoarces viviparus*) white muscle energy status at high critical temperatures ($|\Delta G/d\zeta|$ did not drop below 60 kJ mol^{-1}), while in liver, an accumulation of succinate indicated a progressive switch to mitochondrial

anaerobiosis. Furthermore, two recent *in vivo* ^{31}P NMR studies on *P. brachycephalum* (Mark et al. 2002) and *Gadus morhua* (Sartoris et al. 2003) white muscle confirmed that only moribund animals displayed a drop in pH and $|\Delta G/d\zeta|$ in this respective tissue at temperatures beyond T_c. Sartoris et al. (2003) noted that even immediate cooling could not reverse detrimental changes in tissue energy status.

In our experiments, cuttlefish survived exposure to the high T_c, when rapidly cooled to control temperatures (Melzner and Bock, personal observation), suggesting that the observed net use of the phosphagen reflects an energetic limitation of actively working muscle sections rather than an energetic limitation of all muscle, including the resting bulk of circular and anaerobic ('white') muscle fibres. This emphasizes that active tissues are the first to be affected by temperature induced oxygen deficiency. Effects in white or passive muscle set in at the end of a progressive oxygen limitation cascade and thus only occur, once severe damage to other organs, especially those involved in driving blood circulation has already set in, leading to ventilatory and circulatory failure as in fish (Van Dijk et al. 1999, Mark et al. 2002). Accordingly, progressive radial fibre fatigue of the cephalopod mantle characterizes an early limitation in response to temperature. It will eventually affect all other tissues, as oxygen uptake and distribution will likely be negatively affected by decreasing ventilatory pressures (fig 6a,b). However, whether radial muscle fatigue observed in our study results from limited ventilatory muscle power output per se, or is caused by a progressively limited oxygen supply through the blood circulation or by a combination of both processes, yet remains to be established.

6. Acknowledgements

This study was carried out in support of the project: The cellular basis of standard and active metabolic rate in the free-swimming cephalopod, *Sepia officinalis* (NERC Grant PFZA/004). The authors wish to thank Rolf Wittig and Timo Hirse for their excellent technical support, Raymond and Marie - Paule Chichery (Université de Caen) for providing cuttlefish eggs in 2002 and 2003 and all student helpers that were engaged in raising the animals in our lab.

7. References

AITKEN, J. P., O'DOR, R. K. AND JACKSON, G. D. (2005). The secret life of the giant cuttlefish *Sepia apama* (Cephalopoda): Behaviour and energetics in nature revealed through radio acoustic positioning and telemetry (RAPT). *J. Exp. Mar. Biol. Ecol.* **320**, 77-91.

ALLEN, D. G. AND WESTERBLAD, H. (2001). Role of phosphate and calcium stores in muscle fatigue. *J. Physiol.* **536**, 657-665.

BAILEY, D. M., PECK, L. S., BOCK, C. AND PÖRTNER, H. O. (2003). High-energy phosphate metabolism during exercise and recovery in temperate and antarctic scallops: an in vivo ^{31}P-NMR study. *PBZ* **76 (5),** 622-633.

BARTOL, I. K. (2001). Role of aerobic and anaerobic circular mantle muscle fibers in swimming squid: Electromyography. *Biol. Bull.* **200**, 59-66.

BOCK, C., SARTORIS, F., WITTIG, R-M. AND PÖRTNER, H. O. (2001). Temperature-dependent pH regulation in stenothermal antarctic and eurythermal temperate eelpout (Zoarcidae): an *in vivo* NMR study. *Polar Biol.* **24**, 869-874.

BOCK, C., SARTORIS, F.J. AND PÖRTNER, H.O. (2002). In vivo MR spectroscopy and MR imaging on non – anaesthetized marine fish: techniques and first results. *Magnetic Resonance Imaging*. **20**, 165-172.

BONE, Q., PULSFORD, A. AND CHUBB, A.D. (1981). Squid mantle muscle. *J. mar. Biol. Ass. U.K.* **61**, 327-342.

BONE, Q., BROWN, E. R. AND TRAVERS, G. (1994a). On the respiratory flow in the cuttlefish *Sepia officinalis*. *J. Exp. Biol.* **194**, 153-165.

BONE, Q., BROWN, E. R. AND USHER, M. (1994b). The structure and physiology of cephalopod muscle fibres. In *Cepahlopod Neurobiology* (ed. N.J. Abbot, R. Williamson and L. Maddock), pp. 301-329. Oxford: Oxford University Press.

BORGER, R., DE BOECK, G., VAN AUDERKE, J., DOMMISSE, R., BLUST, R. AND VAN DEN LINDEN, A. (1998). Recovery of the energy metabolism after a hypoxic challenge at different temperature conditions: a ^{31}P nuclear magnetic resonance spectroscopy study with common carp. *Comp. Biochem. Physiol. A* **120**, 143 – 150.

BOUCAUD – CAMOU, E. AND BOISMERY, J. (1991). The migrations of the cuttlefish (*Sepia officinalis* L.) in the English Channel. In: E. Boucaud-Camou (Ed.), La Seiche. 1st International Symposium on the cuttlefish *Sepia*, pp. 179-189. Centre de publications, Université de Caen.

BUCK, L.T., HOCHACHKA, P.W., SCHON, A. AND GNAIGER, E. (1993). Microcalorimetric measurement of reversible metabolic suppression induced by anoxia in isolated hepatocytes *Am. J. Phys.* **265**: R1014-R1019

BURTON, R. F. (2002). Temperature and acid-base balance in ectothermic vertebrates: the imidazole alphastat hypothesis and beyond. *J. Exp. Biol.* **205**, 3587-3600.

CHIH, C. P. AND ELLINGTON, W. R. (1985). Metabolic correlates of intracellular pH change during rapid contractile activity in a molluscan muscle. *J. Exp. Zool.* **236**, 27-34.

COCKING, A. W. (1959). The effects of high temperature on roach (*Rutilus rutilus*). 1. The effects of temperature increasing at a known constant rate. *J. Exp. Biol.* **36**, 217-226.

COMBS, C. A. AND ELLINGTON, W. R. (1997).Intracellular sodium homeostasis in reaction to the effective free-energy change of ATP hydrolysis: studies of crayfish muscle fibers. *J. Comp. Physiol. B* 167, 563-569.

COMBS, C. A. AND ELLINGTON, W. R. (1995). Graded intracellular acidosis produces extensive and reversible reductions in the effetive free energy changes of ATP hydrolysis in a molluscan muscle. *J. Comp. Physiol.* **165**, 203-212.

DEBOLD, E. P., DAVE, H. AND FITTS, R. H. (2004). Fiber type and temperature dependence of inorganic phosphate: imlications for fatigue. *Am. J. Physiol.* **287**, C673-C681.

DOUMEN, C. AND ELLINGTON, W. R. (1992). Intracellular free magnesium in the muscle of an osmoconforming marine invertebrate: measurement and effect of metabolic and acid-base pertubations. *J. Exp. Zool.* **261**, 394-405.

FINKE, E., PÖRTNER, H.O., LEE, P.G. AND WEBBER, D.M. (1996). Squid (*Lolliguncula brevis*) life in shallow waters: oxygen limitation of metabolism and swimming performance. *J. Exp. Biol.* **199**, 911-921.

FITTS, E. (1994). Cellular mechanisms of muscle fatigue. *Physiol. Rev.* **74**, 49-94.

FREDERICH, M. AND PÖRTNER, H. O. (2000). Oxygen limitation of thermal tolerance defined by cardiac and ventilatory performance in spider crab, *Maja squinado*. *Am. J. Physiol.* **279**, R1531-R1538

GÄDE, G. (1980). Biological role of octopine formation in marine molluscs. *Mar. Biol. Lett.* **1**, 121-135

HARDEWIG, I., VAN DIJK, P. L. M. AND PÖRTNER, H. O. (1998). High energy turnover at low temperatures: recovery from exhaustive exercise in Antarctic and temperate eelpouts. *Am. J. Physiol.* **274**, R1789 – R1796.

HEATH, A, G. AND HUGHES, G. M. (1973). Cardiovascular and respiratory changes during heat stress in the rainbow trout (*Salmo gairdneri*). *J. Exp. Biol.* **59**, 323-338.

HOCHACHKA, P.W. (2000). Pinniped diving response mechanisms and evolution: A window on the paradigm of comparative biochemistry and physiology. Comp. Physiol. Biochem. 126A: 435-458.

HOCHACHKA, P.W. AND SOMERO, G.N. (2002). Biochemical adaptation. Oxford University Press, Oxford, 466 pp.

HUBLEY, M. J., LOCKE, B. R. AND MOERLAND, T. S. (1997). Reaction – diffusion analysis of the effects of temperature on high – energy phosphate dynamics in goldfish skeletal muscle. *J. Exp. Biol.* **200**, 975-988.

JANSEN, M. A., SHEN, H., ZHANG, L., WOLKOWICZ, P.E. AND BALSCHI, J. A. (2003). Energy requirements for the Na^+ gradient in the oxygenated isolated heart: effect of changing the free energy of ATP hydrolysis. *Am. J. Physiol.* **285**, H2437-H2445.

KAMMERMEIER, H., SCHMIDT, P. AND JÜNGLING, E. (1982). Free energy change of ATP-hydrolysis: a causal factor of early hypoxic failure of the myocardium? *J. mol. Cell. Cardiol.* **14**, 267-277.

KAMMERMEIER, H. (1987). High energy phophate of the myocardium: concentration versus free energy change. *Basic Res. Cardiol.* **82**, Suppl. 2, 31-36.

KAMMERMEIER, H. (1993). Efficiency of energy conversion from metabolic substrates to ATP and mechanical and chemiosmotic energy. *Basic Res. Cardiol.* **88**, 15-20.

KOST, G. J. (1990). PH standardization for phosphorus – 31 magnetic resonance heart spectroscopy at different temperatures. *Magn. Res. Med.* **14**, 496-506.

LANNIG, G., BOCK, C., SARTORIS, F. J. AND PÖRTNER, H. O. (2004). Oxygen limitation of thermal tolerance in cod, *Gadus morhua* L. studied by magnetic resonance imaging (MRI) and on-line venous oxygen monitoring. *Am. J. Physiol.* **287**, R902-R910.

MARK, F. C., BOCK, C. AND PÖRTNER, H. O. (2002). Oxygen – limited thermal tolerance in Antarctic fish investigated by MRI and ^{31}P – MRS. *Am. J. Physiol.* **283**, R1254-R1262.

MELZNER F., BOCK C. AND PÖRTNER, H.O. Temperature dependent oxygen extraction from the ventilatory current and the costs of ventilation in the cephalopod *Sepia officinalis*. *J. Comp. Physiol. B*, submitted.

MESSENGER, J. B., NIXON, M. AND RYAN, K. P. (1985). Magnesiumchloride as an anaesthetic for cephalopods. *Comp. Biochem. Physiol. C* **82**, 203-205.

MOMMSEN, T.P., BALLANTYNE, J., MACDONALD, D, GOSLINE, J. AND HOCHACHKA, P. W. (1981). Analogous of red and white muscle in squid mantle. *Proc. Natl. Acad. Sci. U.S.A.* **78**, 3274-3278.

MILLIGAN, B. J., CURTIN, N. A. AND BONE, Q. (1997). Contractile properties of obliquely striated muscle from the mantle of squid (*Alloteuthis subulata*) and cuttlefish (*Sepia officinalis*). *J. Exp. Biol.* **200**, 2425-2436.

O'DOR, R. K. AND WELLS, M. J. (1987). Energy and nutrient flow. In: Boyle, P. R. (Ed.), Cephalopod life cycles, Comparative reviews. (Vol 2) Academic Press, London, pp.109-133.

Peck, L.S., Pörtner, H.O., Hardewig, I. (2002) Metabolic demand, oxygen supply and critical temperatures in the Antarctic bivalve, *Laternula elliptica*. Physiol. Biochem. Zool. 75, 123-133.

PÖRTNER, H.O. (1987). Contributions of anaerobic metabolism to pH regulation in animal tissues: theory. *J. Exp. Biol.* **131**, 69-87.

PÖRTNER, H.O. (1990). Determination of intracellular buffer values after metabolic inhibition by fluoride and nitrilotriacetic acid. *Respir. Physiol.* **81**, 275-288.

PÖRTNER, H.O. (2001). Climate change and temperature dependent biogeography: oxygen limitation of thermal tolerance in animals. *Naturwissenschaften* **88**, 137-146.

PÖRTNER, H.O. (2002a). Climate change and temperature dependent biogeography: systemic to molecular hierarchies of thermal tolerance in animals. *Comp. Biochem. Physiol.* **132A**, 739-761.

PÖRTNER, H. O. (2002b). Environmental and functional limits to musclular exercise and body size in marine invertebrate athletes. *Comp. Biochem. Physiol. A* **133**, 303-321.

PÖRTNER, H. O., WEBBER, D. M., O´DOR, R. K. AND BOUTILIER, R. G. (1993). Metabolism and energetics in squid (*Illex illecebrosus*, *Loligo pealei*) during muscular fatigue and recovery. *Am. J. Physiol.* **265**, R157-R165.

PÖRTNER, H. O. (1994). Coordination of metabolism, acid-base regulation, and haemocyanin function in cephalopods. *Physiology of Cephalopod Molluscs-Lifestyle and Performance Adaptations*, edited by H. O. Pörtner, R. K. O´Dor, and D. MacMillan. Basel: Gordon and Breach. 131-148.

PÖRTNER, H. O., FINKE, E. AND LEE, P. G. (1996), Metabolic and energy correlates of intracellular pH in progressive fatigue of squid (*L. brevis*) mantle muscle. *Am. J. Physiol.* **271**, R1403-R1414.

PÖRTNER, H. O., PECK, L., ZIELINSKI; S. AND CONWAY, L. Z. (1999). Intracellular pH and energy metabolism in the highly stenothermal antarctic bivalve *Limopsis marionensis* as a function of ambient temperature. *Polar Biol.* **22**, 17-30.

REEVES, R. B. (1972). An imidazole alphastat hypothesis for vertebrate acid – base regulation: tissue carbon dioxide content and body temperature in bullfrogs. *Respir. Physiol.* **14**, 219-236

SARTORIS, F. J., BOCK, C., SERENDERO, I., LANNIG, G. AND PÖRTNER, H. O. (2003). Temperature – dependent changes in energy metabolism, intracellular pH and blood oxygen tension in the Atlantic cod. *J. Fish. Biol.* **62**, 1239-1253.

SOKOLOVA, I.M. AND PÖRTNER, H.O. (2003) Metabolic plasticity and critical temperatures for aerobic scope in a eurythermal marine invertebrate (*Littorina saxatilis*, Gastropoda: Littorinidae) from different latitudes. *J. Exp. Biol.* **206**, 195-207.

SOMMER, A., KLEIN, B. AND PÖRTNER, H. O. (1997). Temperature induced anaerobiosis in two populations of the polychaete worm *Arenicola marina* (L.*). J. comp. Physiol. B* **167**, 25-35.

STOREY, K. B. AND STOREY, J. M. (1979). Octopine metabolism in the cuttlefish, *Sepia officinalis*: octopine production by muscle and ist role as an aerobic substrate for non-muscular tissues. *J. Comp. Physiol.* **131**, 311-319.

TOMPSETT, D.H. (1939). Sepia. LMBC Memoirs, Liverpool University Press, 184 pp.

VAN DIJK, P. L. M., HARDEWIG, I. AND PÖRTNER, H.O. (1997). Temperature dependent shift of pHi in fish white muscle: contributions of passive and active processes. *Am. J. Physiol.* **272**, R84-R89.

VAN DIJK, P. L. M., TESCH, C., HARDEWIG, I. AND PÖRTNER, H. O. (1999). Physiological disturbances at critically high temperatures: a comparison between stenothermal antarctic and eurythermal temperate eelpouts (zoarcidae). *J. Exp. Biol.* **202**, 3611-3621.

WANNENBURG, T., JANSSEN, P. M. L., FAN, D. AND DE TOMBE, P. P. (1997). The Frank Starling mechanism is not mediated by changes in rate of cross-bridge detachment. *Am. J. Physiol.* **273**, H2428-H2435.

WEBBER, D. M. AND O'DOR, R. K. (1986). Monitoring the metabolic rate and activity of free – swimming squid with telemetered jet pressure. *J. Exp. Biol.* **126**, 205-224.

WELLS, M. J. (1990). Oxygen extraction and jet propulsion in cephalopods. *Can. J. Zool.* **68**, 815-824.

WELLS, M. J. AND WELLS, J. (1982). Ventilatory currents in the mantle of cephalopods. *J. Exp. Biol.* **99**, 315-330.

WELLS, M. J. AND WELLS, J. (1991). Is *Sepia* really an octopus? In Boucaud-Camou, E. (Ed.), La Seiche, 1st International symposium on the cuttlefish *Sepia*. Center of publications , Universite de Caen. pp. 77-92.

ZIELINSKI, S. AND PÖRTNER, H. O. (1996). Energy metabolism and ATP free - energy change of the intertidal worm *Sipunculus nudus* below a critical temperature. *J. Comp. Physiol. B* **166**, 492-500.

ZIELINSKI, S. (1999). Consequences of high metabolic rates in cephalopods from different geographical latitudes. *Ber. Polarforsch.* **338** 198pp.

Figure captions

Figure 1

(A) Animal in chamber in front of the magnet, connected to a seawater perfusion system. Sliders restrict the space available to the animal to a minimum. A grey box indicates the positioning of the ^{31}P surface coil below the animal's thick ventral mantle muscle. The pressure catheter (not visible) leaves the animal's mantle cavity and passes through the lid on the right towards a pressure transducer (see text). (B) Schematic illustration of the surface coil and its sensitive volume (grey semicircle). Metabolite changes within radial and circular muscles of the mantle muscle organ can be recorded. Circular muscle consists of a central bulk of anaerobic fibres and two thin layers of outer, aerobic fibres. (C) Schematic illustration of intervals defined between the acquisition of successive *in vivo* NMR spectra. One complete 25 min interval is illustrated (n), which is divided into 12 segments ($s1_n$-$s12_n$). For each segment, SJ pressure amplitudes and frequencies were determined, allowing us to calculate jet indices for variable time intervals (by summing up segment JI within intervals a to l, e.g. interval g consists of JIs from segments $s6_n$ – $s12_n$). For further explanations see text.

Figure 2

Swimming jets (SJ) amplitude distribution and frequency. (A) Pressure amplitude (MMPA) distribution of spontaneously occurring high pressure mantle cavity oscillations (SJs) > 0.2 kPa under control conditions (15°C). Amplitudes grouped into 1 kPa classes, frequencies expressed as % percent of total SJ frequency. The insert gives cumulative frequencies within selected intervals. (B) Frequency

of SJs >0.2 kPa at all experimental temperatures, expressed in incidences h^{-1} N=5 animals per temperature. Error bars represent standard deviation. (C) SJ contribution to total mantle pressure generation in % of total mean mantle pressure (MMP_{tot}) at all experimental temperatures, see text for calculations.

Figure 3

Metabolite changes due to spontaneous activity under control conditions (animal 4). *In vivo* ^{31}P - NMR spectra were acquired every 25 minutes, each data point represents concentration information for the respective metabolite obtained from a single spectrum (acquisition time = 3 min 40 sec).

Figure 4

Metabolite changes under control conditions. Information from n = 282 intervals of 25 min duration from all five animals. Intervals were grouped according to change in inorganic phosphate between successive NMR spectra. Groups were: $\Delta[P_i]$ = 0 to 0.99 μmol g^{-1} ww^{-1} (N=88 cases), $\Delta[P_i]$ = 1 to 1.99 μmol g^{-1} ww^{-1} (N=25 cases), $\Delta[P_i]$ = 2 to 2.99 μmol g^{-1} ww^{-1} (N=9 cases) and $\Delta[P_i]$ = > 3 μmol g^{-1} ww^{-1} (N=9 cases) on the positive side, $\Delta[P_i]$ = 0 to -0.99 μmol g^{-1} ww^{-1} (N=90 cases), $\Delta[P_i]$ = -1 to -1.99 μmol g^{-1} ww^{-1} (N=31 cases), $\Delta[P_i]$ = -2 to -2.99 μmol g^{-1} ww^{-1} (N=18 cases) and $\Delta[P_i]$ = < -3 μmol g^{-1} ww^{-1} (N=9 cases) on the negative side. Number of cases per group (displayed in fig 3B) are a direct measure of the probability of occurrence, as all intervals were picked randomly. Linear regression equations: (A) $pH_i = 7.444 + 0.022\ \Delta[P_i]$; R^2= 0.96; $F_{(1,5)}$=121; p<0.001 (for the range <-3 – 3 μmol g^{-1} ww^{-1}); (B) $\Delta[PLA]_i = -0.88\ \Delta[P_i]$; $R^2 = 0.99$; $F_{(1,6)}$=; p<0.001; (C) $\Delta H^+_i = -0.41 - 1.58\ \Delta[P_i]$; $R^2 = 0.94$; $F_{(1,5)}$=88; p<0.001 (for the range <-3 – 3 μmol g^{-1} ww^{-1}); (D) [ATP] for ANOVA, see text. All concentrations in μmol g^{-1} wet $weight^{-1}$ (=ww^{-1})

Figure 5

Mantle organ metabolic status vs. temperature. (A) A set of spectra obtained on animal one at different temperatures. Note increases in P_i peak area towards high and low temperatures. (B) ATP and inorganic phosphate concentrations; (C) PLA concentration; (D) pH_i. N=5 animals per temperature. Error bars represent standard deviation. Data derived from *in vivo* ^{31}P NMR spectra. Concentrations of metabolites are proportional to the area under their respective peaks in the ^{31}P NMR spectrum.

Figure 6

Mantle metabolic status and mean mantle pressure amplitude (MMPA) vs. temperature. (A) MMPA maxima encountered in animals one and five; (B) concomitant changes in $[P_i]$ and $\Delta G/d\zeta$ in the radial muscle compartment, based on the assumption that observed changes in *in vivo* ^{31}P - NMR spectra solely represent the situation in working radial muscles (see text). Animal 1 had the lowest, animal 5 the highest thermal tolerance of all animals investigated. Still, both show a tight correlation between stagnating and, eventually, decreasing, pressure amplitudes once $|\Delta G/d\zeta|$ decreases (the other 3 animals show similar patterns, data not shown).

Table 1. Control parameters (15°C) of cellular high energy phosphates and pH_i as determined using *in vivo* ^{31}P - NMR spectroscopy. Statistical comparisons between animals in: ANOVA and Student-Newman-Keuls post –hoc test. Significant differences between animals marked (e.g. sig $p<0.05$ = 1 = animal differs from animal 1). All results as means and standard deviations. $[P_i]_{max}$ = maximum inorganic phosphate concentration observed; $pH_{i\ lowest\ /\ highest}$ = highest / lowest pH_i values observed under control conditions; replicates = individual animals; S.D. in brackets.

parameter	*replicate 1*	*replicate 2*	*replicate 3*	*replicate 4*	*replicate 5*	*Mean*
$[P_i]_{max}$ μmol g^{-1} ww^{-1}	5.27	5.72	5.46	11.65	5.25	6.66 (2.79)
$pH_{i\ lowest}$	7.31	7.28	7.39	7.31	7.34	7.32
$pH_{i\ highest}$	7.56	7.52	7.69	7.56	7.58	7.58
$pH_{i\ range}$	0.25	0.24	0.3	0.25	0.24	0.256 (0.025)
$[H^+_i]_{range}$ [nmol/l]	21.4	22.3	20.3	21.4	19.4	20.96 (1.12)
pH_i mean	7.43(0.05)	7.38(0.06)	7.50(0.06)	7.43(0.07)	7.44(0.06)	7.45 (0.07)
sig $p<0.05$	3	3	1;2;4;5	3	3	
$[H^+_i]$ [nmol/l]	37.2 (4.38)	42.4 (5.9)	31.5 (4.0)	37.2 (6.1)	35.9 (4.4)	36.1 (5.3)
sig $p<0.05$	3	3	1;2;4;5	3	3	
[PLA] μmol g^{-1} ww^{-1}	33.0 (0.6)	34.5 (0.8)	33.4 (0.6)	33.8 (0.9)	33.8 (0.9)	33.6 (0.6)
sig $p<0.05$	2;5	1;3	2		1	
[ATP] μmol g^{-1} ww^{-1}	7.3 (0.6)	8.6 (0.6)	7.9 (0.4)	8.2 (0.9)	8.1 (0.6)	8.0 (0.8)
sig $p<0.05$	2;4;5	1		1	1	
PLA/ATP	4.6 (0.4)	4.0 (0.4)	4.2 (0.2)	4.1 (0.5)	4.2 (0.4)	4.2 (0.4)
sig $p<0.05$	4;5			1	1	

Table 2: Selected significant linear regressions of jet index (JI) vs. change in inorganic phosphate concentration ($\Delta[P_i]$). First six regressions: variable time intervals for jet index (JI) calculation, fixed pressure threshold (only jets > 2 kPa MMPA included). Regression 7 through 12: variable jet amplitudes used for JI calculation, fixed time interval (25 minutes, interval l, fig. 1). Regression 13 (two factorial linear model): best model obtained, using a JI calculated for an interval of 15 minutes (interval g, fig 1) and exclusively with jets with a pressure amplitude > 2 kPa (variable X1), the second variable being jet density (JD) >5 kPa amplitude within interval g (variable X2, see text for further explanations). R^2 *100 indicates the percentage of explained variance in $\Delta[P_i]$ employing the respective regressions.

#	*X*	*regression*	*Analysis of variance*	*R^2 *100*
1	$JI_{i;\ >2kPa}$	$\Delta[P_i]=0.0318X$	$F_{(1,28)}=73.69$; $p<0.001$	72.46
2	$JI_{h;\ >2kPa}$	$\Delta[P_i]=0.0352X$	$F_{(1,28)}=106.2$; $p<0.001$	79.14
3	$JI_{g;\ >2kPa}$	$\Delta[P_i]=0.0387X$	$F_{(1,28)}=149.9$; $p<0.001$	84.26
4	$JI_{f;\ >2kPa}$	$\Delta[P_i]=0.0422X$	$F_{(1,28)}=88.88$; $p<0.001$	76.04
5	$JI_{e;\ >2kPa}$	$\Delta[P_i]=0.0430X$	$F_{(1,28)}=44.11$; $p<0.001$	62.22
6	$JI_{d;\ >2kPa}$	$\Delta[P_i]=0.0639X$	$F_{(1,28)}=35.96$; $p<0.001$	56.22
7	$JI_{l;\ >0,2\ kPa}$	$\Delta[P_i]=0.0159X$	$F_{(1,28)}=13.65$; $p<0.001$	30.38
8	$Ji_{l;\ >1\ kPa}$	$\Delta[P_i]=0.0258X$	$F_{(1,28)}=27.13$; $p<0.001$	47.39
9	$JI_{l;\ >2\ kPa}$	$\Delta[P_i]=0.0515X$	$F_{(1,28)}=67.64$; $p<0.001$	69.67
10	$JI_{l;\ >3\ kPa}$	$\Delta[P_i]=0.0909X$	$F_{(1,28)}=52.90$; $p<0.001$	64.15
11	$JI_{l;\ >4\ kPa}$	$\Delta[P_i]=0.1289X$	$F_{(1,28)}=27.48$; $p<0.001$	47.73
12	$JI_{l;\ >5\ kPa}$	$\Delta[P_i]=0.1635X$	$F_{(1,28)}=16.65$; $p<0.001$	35.05

	Ind. Variables (X_n)	Analysis of variance	*R^2 *100*
13	$X_1 = JI_{15\ min;\ >2kPa}$ $X_2 = JD_{15\ min;\ >5kPa}$	$F_{(2,27)}=110.7$; $p<0.001$ $\Delta[P_i] = 0.0335X_1 + 0.1555X_2$	89.13

Table 3. Cellular energy status at extreme temperatures. See text for definition of phases and abbreviations. Differences between phase mean values were detected using ANOVA and Student-Newman-Keuls tests. Only results from post hoc comparisons between group A and each other group are displayed in this table. n.s. = non significant. (r+c) = metabolite levels and pH_i values assuming a homogenuous distribution over the whole mantle organ (radial and circular muscle fibres); (r) = metabolite levels and pH_i values assuming a heterogenuous distribution of metabolite levels in that phosphagen depletion only took place in radial muscle fibres; extr = extreme = values obtained with the last *in vivo* ^{31}P NMR spectrum prior to termination of cooling or heating.

	low extreme temperature			*high extreme temperature*				
	A (r+c)	B (r+c)	extr (r+c)	A (r+c)	B (r+c)	extr (r+c)	A (r)	extr (r)
pH_i	7.47 (0.04)	7.48 (0.07) n.s.	7.44 (0.06) n.s.	7.38 (0.07)	7.35 (0.04) n.s.	7.29 (0.03) p<0.001	7.38	7.19
[PLA] μmol g^{-1} ww^{-1}	34.5 (1.2)	30.9 (2.1) p<0.006	30.7 (2.3) p<0.006	33.1 (1.2)	30.5 (2.1) p<0.04	28.1 (3.5) p<0.001	33.1	8.5
[P_i] μmol g^{-1} ww^{-1}	1.3 (0.3)	4.5 (1.9) p<0.004	4.6 (1.8) p<0.004	1.2 (0.3)	4.5 (1.1) p<0.001	7.5 (1.2) p<0.001	1.2	25.6
[ATP] μmol g^{-1} ww^{-1}	7.7 (1.0)	7.9 (0.5) n.s.	8.0 (1.2) n.s.	8.0 (0.4)	7.8 (1.0) n.s.	7.5 (1.2) n.s.	8.0	5.8
temp	9.02 (1.4)	6.97 (0.81)	6.3 (1.1)	23.1 (2.3)	26.78 (1.9)	27.2 (1.6)	23.1	27.2
[Oct] μmol g^{-1} ww^{-1}	0.2	1.4	1.5	0.2	1.06	1.9	0.2	8.2
[Arg] μmol g^{-1} ww^{-1}	30.4	32.8	32.9	29.1	30.8	32.4	29.1	45.5
$dG/d\xi$ kJ mol^{-1}	-54.7	-51.3	-51.4	-55.8	-52.2	-50.7	-55.8	-43.9

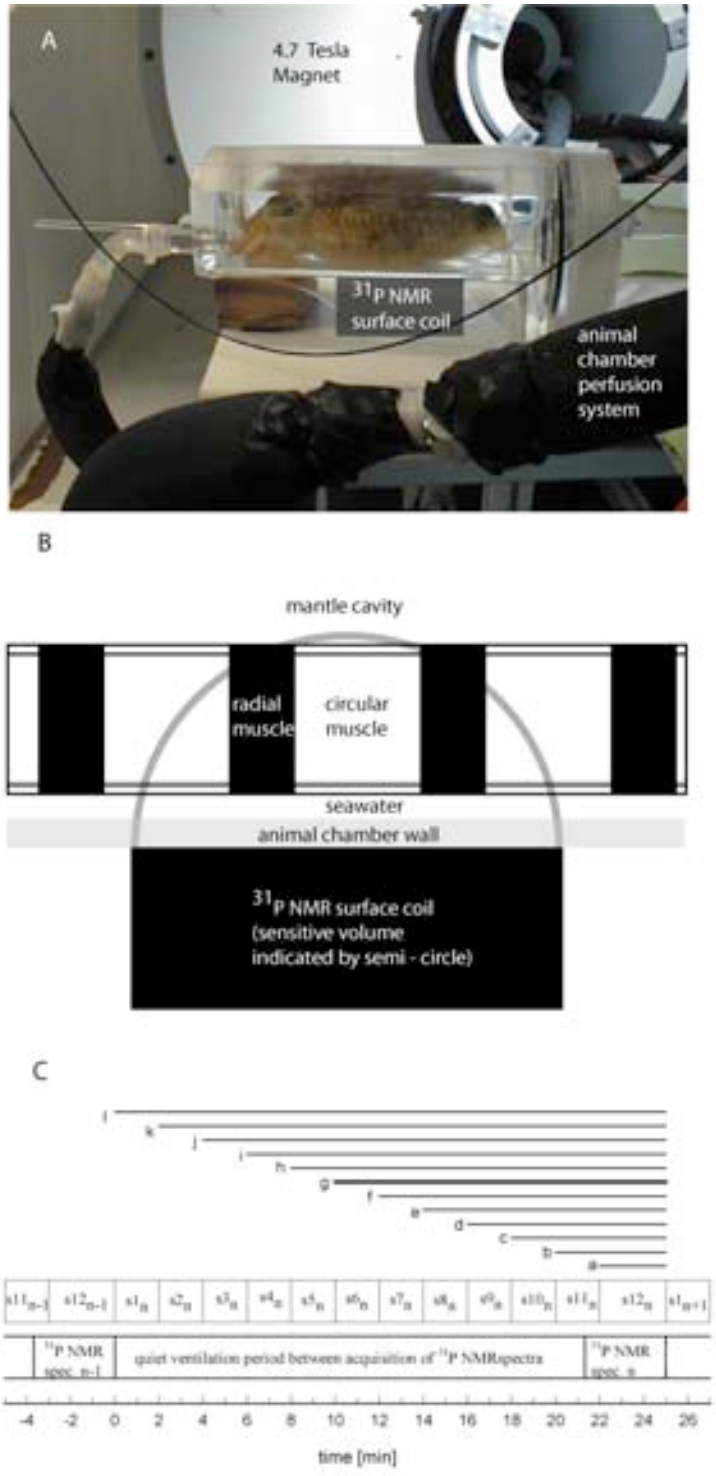
A
4.7 Tesla
Magnet
31P NMR
surface coil
animal
chamber
perfusion
system
B
mantle cavity
radial
muscle
circular
muscle
seawater
animal chamber wall
31P NMR surface coil
(sensitive volume
indicated by semi - circle)
C
time [min]

Figure 1

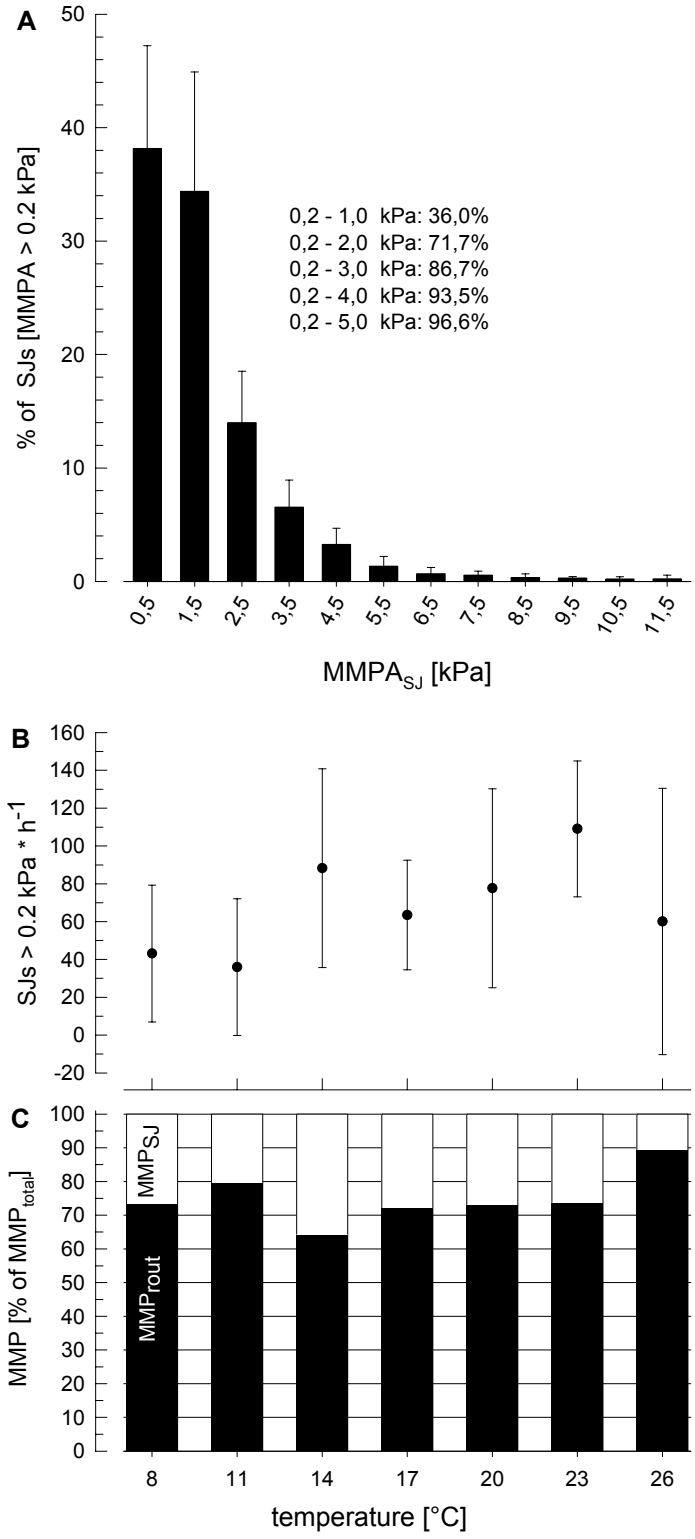
A
% of SJs [MMPA > 0.2 kPa]
0,2 - 1,0 kPa: 36,0%
0,2 - 2,0 kPa: 71,7%
0,2 - 3,0 kPa: 86,7%
0,2 - 4,0 kPa: 93,5%
0,2 - 5,0 kPa: 96,6%
0,5
1,5
2,5
3,5
4,5
5,5
6,5
7,5
8,5
9,5
10,5
11,5
MMPA$_{SJ}$ [kPa]
B
SJs > 0.2 kPa * h^{-1}
C
MMP [% of MMP$_{total}$]
MMP$_{SJ}$
MMP$_{rout}$
8
11
14
17
20
23
26
temperature [°C]

Figure 2

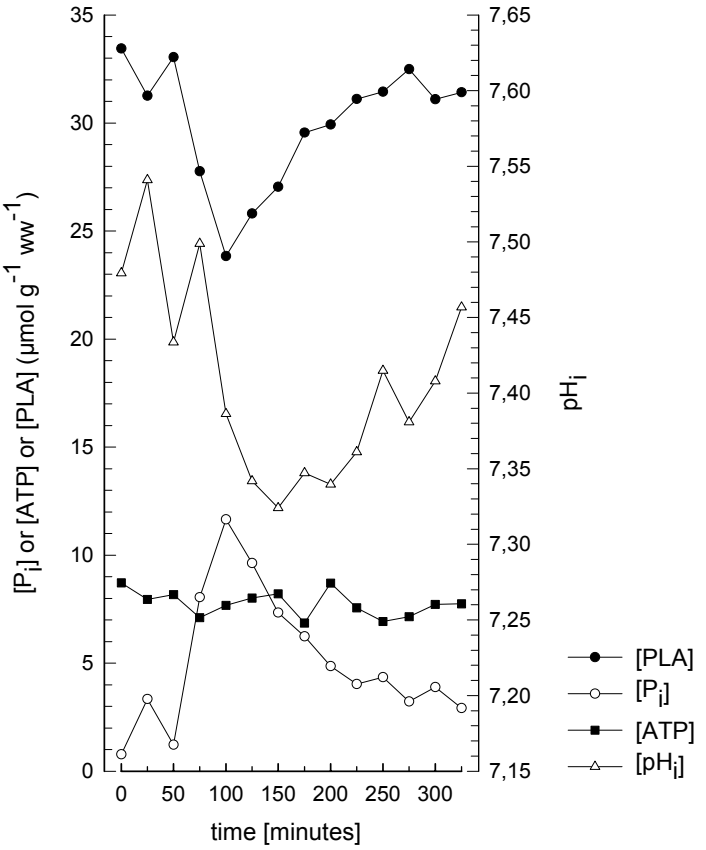
35
30
25
20
15
10
5
0
7,65
7,60
7,55
7,50
7,45
7,40
7,35
7,30
7,25
7,20
7,15
0
50
100
150
200
250
300
time [minutes]
[Pi] or [ATP] or [PLA] (µmol g-1 ww-1)
pHi
[PLA]
[Pi]
[ATP]
[pHi]

Figure 3

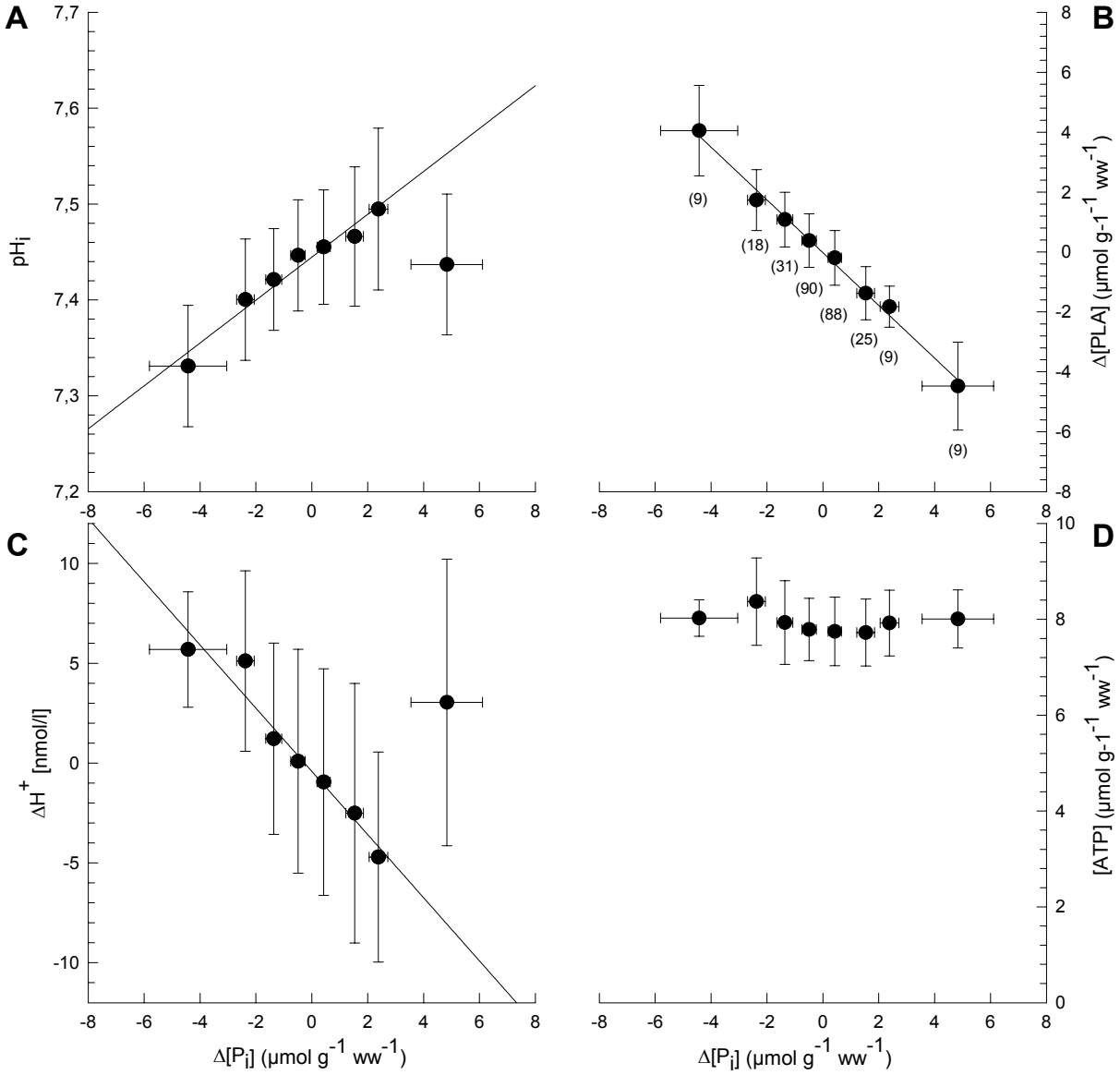
A
B
C
D
pH$_i$
Δ[PLA] (μmol g-1 ww-1)
ΔH+ [nmol/l]
[ATP] (μmol g-1 ww-1)
Δ[P$_i$] (μmol g^{-1} ww^{-1})
Δ[P$_i$] (μmol g^{-1} ww^{-1})
(9)
(18)
(31)
(90)
(88)
(25)
(9)
(9)

Figure 4

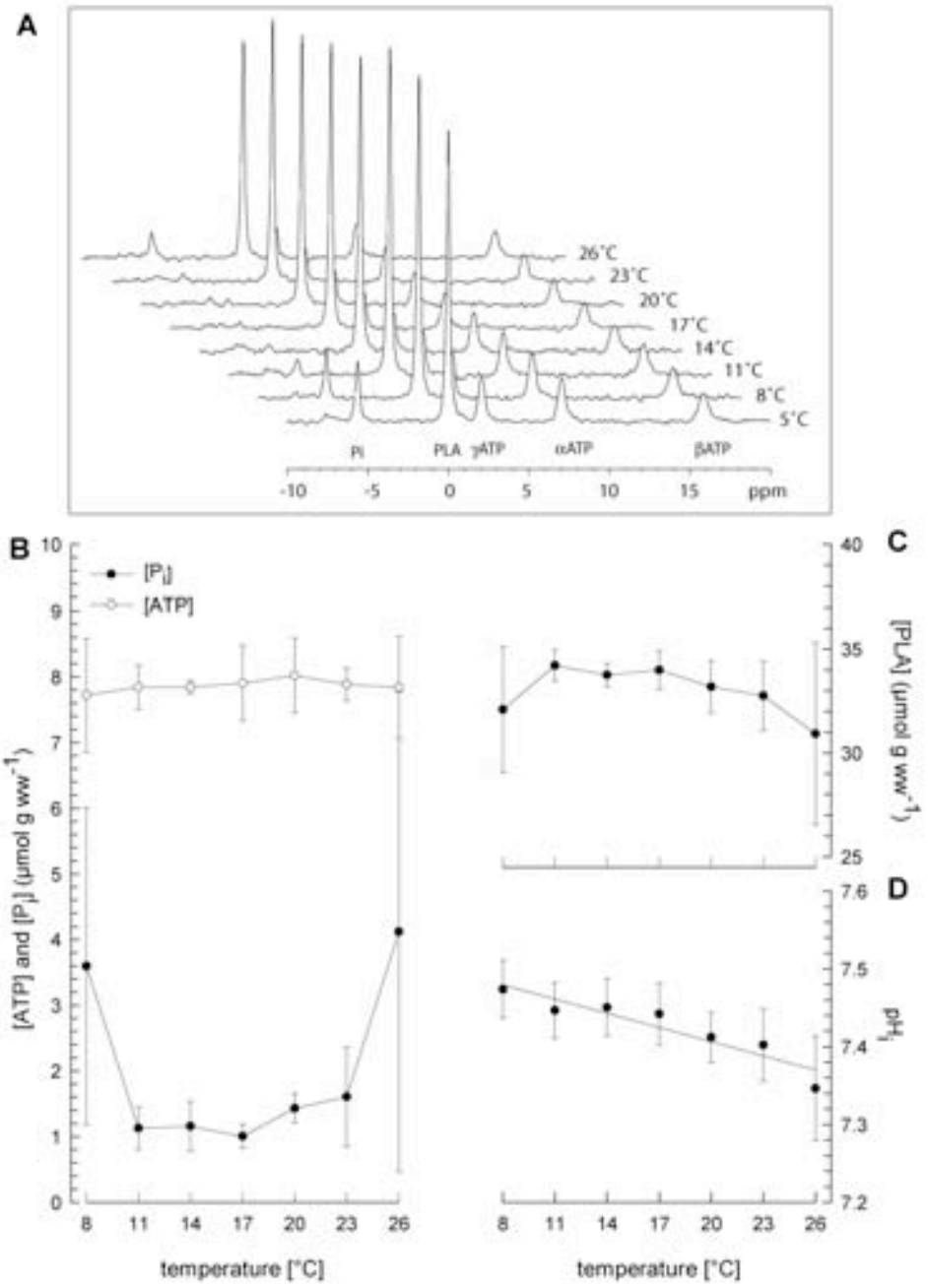
A
26°C
23°C
20°C
17°C
14°C
11°C
8°C
5°C
Pi
PLA
γATP
αATP
βATP
-10
-5
0
5
10
15
ppm
B
[Pi]
[ATP]
[ATP] and [Pi] (µmol g ww-1)
temperature [°C]
C
[PLA] (µmol g ww-1)
D
pHi
temperature [°C]

Figure 5

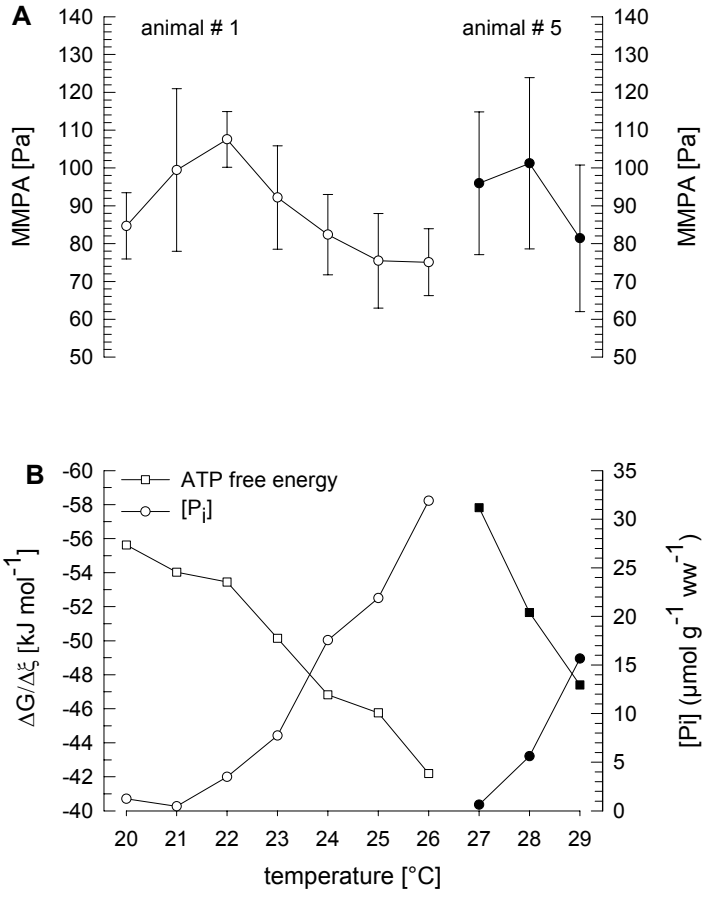
A
animal # 1
animal # 5
MMPA [Pa]
MMPA [Pa]
140
130
120
110
100
90
80
70
60
50
B
ATP free energy
[Pi]
ΔG/Δξ [kJ mol-1]
[Pi] (µmol g-1 ww-1)
-60
-58
-56
-54
-52
-50
-48
-46
-44
-42
-40
35
30
25
20
15
10
5
0
20
21
22
23
24
25
26
27
28
29
temperature [°C]

Figure 6

Temperature dependent oxygen extraction from the ventilatory current and the costs of ventilation in the cephalopod *Sepia officinalis*

Frank Melzner*, Christian Bock, Hans - O. Pörtner

Alfred-Wegener-Institute for Marine and Polar Research, Am Handelshafen 12, 27570 Bremerhaven, Germany

Short title: oxygen extraction in cuttlefish

Key words: cephalopoda, ventilation, mantle cavity pressure, oxygen consumption, cuttlefish

* Author to whom correspondence should be addressed:
phone: +49-471-4831-1331; fax: +49-471-4831-1149;
email: fmelzner@awi-bremerhaven.de

1. Summary

Earlier work found cuttlefish (*Sepia officinalis*) ventilatory muscle tissue to progressively switch to an anaerobic mode of energy production at critical temperatures (T_c) of 7.0 and 26.8°C. These findings suggested that oxygen availability limits thermal tolerance. The present study was designed to elucidate, whether it is the ventilatory apparatus that sets critical temperature thresholds during acute thermal stress. Routine metabolic rate (rmr) rose exponentially between 11 and 23°C, while below (8°C) and above (26°C) this temperature range, rmr was significantly depressed. Ventilation frequency (v_f), and mean mantle cavity pressure (MMP) followed an exponential relationship within the entire investigated temperature range (8-26°C). Oxygen extraction from the ventilatory current (EO_2) decreased in a sigmoidal fashion with temperature, falling from >90% at 8°C to 32% at 26°C. Consequently, ventilatory perfusion requirement (v_{MV}) increased by a factor of 20 from 7 to 150 % body weight min^{-1} in the same temperature interval. Increases in MMP and v_{MV} resulted in ventilatory muscle power output (P_{out}) increasing by a factor of 83 from 0.04 – 3.2 mW kg^{-1} animal. Nonetheless, costs for ventilatory mechanics remain below 2% rmr in the natural thermal window of the population (English Channel, 9 – 17°C), owing to very low MMPs of <0.05 kPa driving the ventilatory stream, and may maximally rise to 11.5% rmr at 26°C. Model calculations suggest that the ventilatory system can maintain high arterial PO_2 values of >14 kPa over the entire temperature interval. We therefore conclude that the cuttlefish ventilation system is probably not limiting oxygen transfer during acute thermal stress. Depression of rmr well before critical temperatures are being reached, is likely caused by circulatory capacity limitations and not by fatigue of ventilatory muscle fibres.

2. Introduction

Available evidence across various aquatic phyla, namely annelids, sipunculids, molluscs (bivalves and gastropods), crustaceans, and fish, supports the view that impairment in the capacity for oxygen supply set the first line of thermal limitation at low and high temperatures in aquatic ectotherms (for review see Pörtner, 2001, 2002a, Pörtner et al., 2004). In a recent study (Melzner, Bock, Pörtner, submitted) we could demonstrate that this generalization is also applicable to cephalopods, as elaborated for the cuttlefish *Sepia officinalis*. Below 7°C and above 26.8 °C, anaerobic metabolism in mantle muscle organ progressively contributed to energy generation. Especially at high temperatures, accumulation of inorganic phosphate, as well as decreases in phosphagen levels and in the Gibb's free energy change of ATP hydrolysis, were observed in parallel with stagnating and, eventually, decreasing ventilation pressure amplitudes. Obviously, muscle fatigue became involved, resulting in a progressive failure of the ventilatory apparatus once critical temperatures were reached. In order to clarify whether the observed changes in muscle metabolic status were caused by modulations in ventilatory effort (exercise induced fatigue), or caused by a mismatch between oxygen demand and oxygen delivery by working ventilatory muscles (hypoxia induced fatigue), the present report examines performance and cost of the cuttlefish ventilatory apparatus in relation to whole animal metabolic rate during acute temperature change.

Owing to the vast amount of convergent developments in structural and functional organization of oxygen transfer systems between high power marine molluscs, the cephalopods, and high power marine ectothermic vertebrates, the fishes (Packard 1968, O'Dor and Webber 1986), it would not be entirely surprising to find similar processes to be limiting within the oxygen transfer network at approaching critical temperatures in both groups. In fish (rainbow trout, *Oncorhynchus mykiss*, Heath and Hughes 1973) stagnating metabolic rates beyond 24°C went along with stagnating heart rates, while ventilation frequency, and even more so, relative ventilation volumes could still be increased, suggesting circulatory failure rather than failure of oxygen uptake at the gills. Sartoris et al. (2003) also concluded that ventilatory effort should be fully sufficient to ensure constantly high $PO_{2\ a}$ in gill vessels during temperature change in cod (*Gadus morhua*). Farrell (2002) reinterpreted Heath

and Hughes (1973) rainbow trout data and postulated that a developing bradycardia and cardiac arrythmia observed between 23 and 26°C could be caused by declining $PO_{2\ v}$, as the teleost heart's oxygen demand is mainly (trout) or exclusively (cod) fuelled by venous blood return. Recent investigations of cod venous oxygen tension and blood flow (Lannig et al. 2004) provided some evidence for such a scenario of a developing systemic hypoxia when approaching thermal extremes. Apparently, the cod cardiovascular system can only maintain constantly high $PO_{2\ v}$ within a narrow optimum temperature range, whereas beyond this interval, full aerobic scope cannot be maintained. In summary, a negative feedback cycle of increasing cardiac hypoxia, elicited by heart power output itself, seems to be a bottleneck in the fish oxygen transfer network when exposed to acute temperature change.

Unlike most teleost hearts the cephalopod systemic heart is fuelled entirely by arterial blood coming directly from the gills. Consequently, cephalopod hearts encounter higher oxygen partial pressures under normoxic conditions than most fish. Values of 70% air saturation have been measured in the efferent branchial vessel of cuttlefish (Johansen et al. 1982). Under hypoxic conditions below a specific threshold, cardiac performance is hampered in cephalopods. Bradycardia and reduced stroke volume were encountered in octopus (*O. vulgaris*, Wells and Wells 1986), associated with a concomitant decrease in oxygen consumption rate. An *in vitro* study of isolated *O. vulgaris* ventricle also found decreasing cardiac power with developing hypoxia. Clearly, oxygen diffusion becomes limiting at low oxygen partial pressures and could limit cardiac performance. Depending on pH dependent oxygen affinity of the haemocyanin, this might happen despite >95% arterial hemocyanin saturation (Houlihan et al. 1982, Johansen et al. 1982). To compensate for this limitation, haemocyanin (Hc) oxygen loading and release should occur at progressively higher PO_2s with increasing temperature, as Hc oxygen affinity decreases with temperature (Zielinski et al. 2001). This mechanism may, however, support oxygen transport only within a limited thermal window. In the presence of a putative alpha stat pattern of blood pH regulation (Reeves 1972, Howell and Gilbert 1976), blood pH would decline with rising temperature, possibly not allowing for full Hc saturation once a critically high temperature threshold is reached. Conversely, increased oxygen affinity at low temperatures (Zielinski et al. 2001) would be beneficial for efficient Hc loading at the gills, but, on the

other hand, impede oxygen unloading on the venous side, leading to enhanced requirements for tissue perfusion.

Thus, a critical factor during thermal stress in cephalopods might be the maintenance of high arterial blood oxygen partial pressures within gill vessels to ensure maximum oxygen supply to the heart when circulatory performance increases at rising metabolic rates at higher temperatures. In contrast, oxygen loading may not become limiting at low temperatures. Given that high arterial PO_2s are a must for proper oxygen transfer system functioning, drastic adjustments in ventilation volume might be required to increase diffusion gradients at the water blood threshold (at constant gill oxygen diffusion capacity) and to thereby sustain metabolic rates, especially with rising temperature. It is known that both cuttlefish (Wells and Wells 1982, 1991) and octopods (Wells and Wells 1985) can extract high fractions (>50%) of the dissolved oxygen from the ventilatory water stream at rest. However, it is not known how extraction efficiencies change with increasing temperatures and associated oxygen demands. Probably, higher metabolic rates can only be realised by reducing extraction rates, and the associated increase in water – blood diffusion gradients at rising oxygen demands. We consequently subjected the cuttlefish ventilatory system to acute temperature change to clarify (1) whether ventilatory power output adjustments suffice to support diffusive oxygen flow at constantly high gill blood $PO_{2\ a}$s, and (2) whether ventilatory muscle fatigue plays a role in thermal limitation.

3. Material and Methods

Data from two experiments will be considered in the present paper. Ventilatory pressure patterns were analysed using pressure recordings in one group of animals (experiment 1), while determinations of oxygen extraction rates from the ventilatory water stream and of routine metabolic rate were performed on a second group of animals (experiment 2). Experimental conditions and animals in the two experiments were chosen in a similar manner such that both data sets provide fully complementary information.

3.1 Animals and experimental protocol

Animals used for oxygen extraction measurements and metabolic rate determinations in the present study originated from the same culture population as described elsewhere (Melzner, Bock, Pörtner, submitted). Animals were chosen according to body wet mass to ensure comparability between experiments. Mean body mass was 104.2 g (7.4 g SD, N = 5 animals) in experiment 1 as compared to 105g (7.0 g SD, N = 4 animals) in experiment 2. The experimental protocol was identical between experiments. In brief, experimental animals were starved for 24 hours, and then transferred to the experimental set-up. Surgery was conducted on the first day, followed by an overnight acclimatization period within the experimental chamber. On the second day, animals were cooled from control temperature (15°C) to 8°C, then warmed to and kept at control temperature over night, after which they were finally warmed to 26°C on the third day. Temperature was changed in a stepwise procedure at an average rate of 1°C h^{-1}. Specifically, a three degree temperature change was accomplished during the first hour of a three hour period, while during the two subsequent hours temperature was kept constant for measurements. Assay temperatures were 14°C / 11°C / 8°C on the second day, and 17°C / 20°C / 23°C / 26°C on the third experimental day.

3.2 Oxygen extraction from the ventilatory current (experiment 2)

Animals were placed in an experimental recirculated aquarium system with a total water volume of 130 liter. This system consisted of a small animal chamber (20 l) which was suspended into a thermostatted water bath. The animal chamber was perfused at a rate of approximately 5 l min^{-1}. Water quality was maintained with a protein skimmer (Aqua care, Germany) and a nitrification filter (Eheim Professional 2, Eheim, Germany). A cryostat (Julabo, Germany) kept water temperature constant at ± 0.1 °C.

Following a 24 h starvation and acclimatization period within the system, animals were anaesthetized with a 0.4 mol l^{-1} $MgCl_2$ solution that was mixed 1:1 with seawater (Messenger, 1985) at 15°C for 3 – 3.5 minutes, then placed (ventral side up) on a wet leather cloth to prevent skin injuries.

During surgery, animals were perfused with aerated seawater (0.04 mol l^{-1} $MgCl_2$) through the funnel aperture. A PE cannula, required to record post-branchial pressure, was connected to a 23 gauge hypodermic needle, led through the entire mantle cavity and then fed through the posterior ventro-lateral section of the mantle muscle. Cannulae (Portex PE tubing, i.d. 0.58 mm o.d. 0.96 mm, flared at the opening) were held in place by two 4 mm diameter plastic washers on the in and outside, embracing the mantle muscle in a sandwich-like fashion. PE tubes were connected to MLT-0699 disposable pressure transducers, signals amplified with a ML-110 bridge amplifier and further fed into a PowerLab/8SP data acquisition system (AD Instruments, Australia). Pressure transducers were calibrated daily.

Subsequently, an oxygen micro-optode (PreSens, Germany; implantable oxygen microsensor IMP-900/5-600/6-140/10-TS-COB2-YOP; tip diameter 50μm) was placed into the funnel opening to measure oxygen partial pressure in the ventilatory exhalant stream (see fig 1). To support the fragile fibre optic oxygen sensor and to secure its position, a PE catheter (Portex PE tubing, i.d. 0.98 mm) was implanted into the ventrolateral part of the funnel tube (about 2.5 cm from the tip), secured with plastic disks (glued to the catheter) on both the inner and outer side of the tissue. Subsequently, the microoptode was fed through the tubing such that the sensor tip reached approximately 3 mm into the animal's exhalant water stream. Finally, the optode was glued to the distal end of the PE tubing with high viscose cyanacrylate glue (Hylo Gel, Marston Oelchemie, Germany). The sensor was connected to an oxygen meter (Microx TX2-A, PreSens, Germany) whose analog output was fed into the PowerLab system. Prior to surgery, the sensors were calibrated (while placed within the PE tube) in a saturated ascorbate solution (0% dissolved oxygen) and aerated seawater (100% dissolved oxygen). Further calibration during experimental temperature changes was not neccessary, since the oxygen meter automatically compensated for temperature. At the end of the experiments, animals were narcotized (see above), killed and optodes checked for drift. Usually drift amounted to 0.5 - 1% oxygen saturation per day (measured at 15°C). Thus, oxygen values were corrected by means of linear interpolation. In parallel with measurements of mantle pressure oscillations and of oxygen partial pressure in the exhalant stream, oxygen consumption was recorded at each temperature by using the animal chamber as an intermittent flow respirometer. An oxygen microsensor (PreSens GmbH,

Germany, oxygen microoptode NTH-L2.5-NS(35+1.2mm)-TF-COB2-NOP) which was connected to the inflow tube of a small internal circulation pump (flow: 2 l min^{-1}) was used to measure the oxygen partial pressure in the chamber water. This pump and the animals‘ ventilatory action caused sufficient mixing of the water to record a linear decline in oxygen partial pressure over time.

During the two hour measurement period at each temperature, two or three runs of 20 – 40 minutes duration were completed. Each run was terminated when the oxygen partial pressure in the respirometer water had declined to about 80 % air saturation. Successive runs were only started when the oxygen partial pressure in the animal chamber had returned to approximately 98-100% air saturation for more than 15 minutes. Mean slopes of oxygen partial pressure declines in the animal chamber were used to calculate oxygen consumption. Values were corrected for rates of bacterial respiration, as analysed in empty chambers. Oxygen extraction from ventilatory currents was calculated only for normoxic periods with >98% water oxygen saturation (at least 30 minutes per temperature step) and during periods of resting ventilation pressure recordings, in the absence of high pressure oscillations related to spontaneous activity (see below for definitions). To prevent the animals from swimming in the chamber, a plastic slider was used to restrict the available chamber area to about 150-200 cm^2 (depending on the animals’ dimensions).

Oxygen extraction rate from the ventilatory current was calculated:

$$EO_2 = SO_{2\,I} - SO_{2\,E} \quad (1)$$

With EO_2 = % oxygen extraction rate from the ventilatory current, $SO_{2\ I}$ = animal chamber water oxygen saturation [%]. $SO_{2\ E}$ = exhalant stream water oxygen saturation [%]. Ventilatory minute volume (v_{MV}) was calculated using EO_2 and whole animal oxygen consumption (MO_2) data with (2a) and without (2b) consideration of potential skin respiration. Combined with ventilation frequency (v_f), ventilatory stroke volumes (v_{SV}) could be calculated. Due to the lack of experimental data on *in vivo* skin respiration in *Sepia* spp., skin respiration was estimated to account for 25% percent of total oxygen uptake. This value represents an intermediate percentage when compared to experimental data on *Octopus vulgaris in vivo* skin respiration (Madan and Wells 1996).

$$v_{MV} = (MO_2 - 0.25\ MO_2)\ (cO_2\ EO_2\ 0.01)^{-1} \quad (2a)$$

$$v_{MV} = MO_2\ (cO_2\ EO_2\ 0.01)^{-1} \quad (2b)$$

$$v_{SV} = v_{MV}\, v_f^{-1} \quad (3)$$

with v_{MV} = ventilatory minute volume (ml animal^{-1} min^{-1}), MO_2 = oxygen consumption (μmol animal^{-1} min^{-1}), cO_2 = oxygen content of animal chamber seawater (μmol ml^{-1}), v_{SV} = ventilatory stroke volume (ml stroke^{-1}) and v_f = ventilatory frequency (strokes min^{-1}). For better comparison with other studies, both v_{MV} and v_{SV} were also expressed as % fractions of the animals' body weight min^{-1} (1 g body weight ≈ 1 ml; density of cuttlefish can be actively modified by the animals, but is close to the density of seawater (Denton and Gilpin-Brown, 1961).

3.3 Mantle pressure and costs of ventilation (experiments 1 and 2)

Mantle pressure recordings were used to determine ventilatory frequency, v_f, at all examined temperatures, to gain insight into potential differences in ventilatory investment between experiments. As there were no differences in v_f between experiments (see fig 3a), we proceeded by solely analysing mantle pressures obtained from experiment 1 animals, as patterns of metabolite changes in the mantle muscle organ are available for this group (Melzner, Bock, Pörtner, submitted). Routine ventilation, mean mantle pressure amplitude ($MMPA_{rout}$, difference between maximum and minimum pressure during ventilatory pressure cycles, Pa) and routine mean mantle pressure (MMP_{rout}, integrated ventilation pressure pulses, Pa) were determined for each temperature step from ten pressure pulses per five minutes experimental time. Such analyses were only performed with ventilatory pressure pulses of an amplitude < 0.2 kPa. Pulses of an amplitude > 0.2 kPa were classified as swimming jets (SJs) (Melzner, Bock, Pörtner, submitted, Bone et al. 1994a) and not considered for resting ventilation pressure analysis. Also, maximum sustainable pressure amplitudes ($MMPA_{max}$) and frequencies ($v_{f\ max}$) were determined for ventilatory respiration of each animal, with "sustainable" defined as the maintenance of a maximum rate or pressure amplitude over a period of at least 30 minutes.

3.4 Ventilation costs

Power for the ventilatory system (only water transportation mechanics, not muscle maintenance) can be quantified as the product of average flow and average pressure (O'Dor and Webber 1991). We calculated power using measured postbranchial pressures (this study), and estimates of prebranchial pressure (prebranchial pressure = approximately twice postbranchial pressure, Wells and Wells 1991, fig 1a):

$$P_{out,\,a} = v_{MV}\ MMP_{rout} \quad (4a)$$

$$P_{out,\,b} = v_{MV}\ 2\ MMP_{rout} \quad (4b)$$

With P_{out}, (W kg^{-1}) = ventilatory power output calculated either from measured post- (a) or estimated prebranchial pressure (b); v_{MV} (m^3 sec^{-1}) = ventilatory minute volume, MMP_{rout} (Pa) = mean resting mantle pressure. Furthermore, ventilatory power input was estimated:

$$P_{in} = P_{out\ a,b}\ E^{-1} \quad (5)$$

with P_{in} (W kg^{-1}) = power invested in ventilatory mechanics, E (P_{out} P_{in}^{-1}) = efficiency of mantle muscle contraction (sensu Syme 1994; net efficiency = work done / net energy expenditure). We used E = 0.03, which is the lowest efficieny so far recorded for cuttlefish mantle muscle (O'Dor and Webber 1991). Thus, calculated P_{in} values likely represent high rather than low estimates. Whole animal oxygen consumption data were used to calculate animal total power:

$$P_{tot} = MO_2\ C \quad (6)$$

with P_{tot} (W kg^{-1} or J s^{-1} kg^{-1}) = animal total power; MO_2 (μmol O_2 kg^{-1} s^{-1}) = whole animal oxygen consumption; C (J μmol O_2^{-1}) = standard oxycaloric conversion (20.1 J ml^{-1} O_2 or 0.448 J μmol O_2^{-1}, Wells and Clarke 1996). Thus we estimated the fraction of total power invested in the mechanical work of ventilation at each temperature step:

$$v_C = 100\ P_{in}\ P_{tot}^{-1} \quad (7)$$

With v_C (%) = costs for ventilatory mechanics, expressed as percent of animal total power.

3.5 Gill oxygen diffusion rates

Potential maximum oxygen flow through cuttlefish gill epithelia into the circulation system was estimated using formula 5 in Eno (1994):

$MO_{2\ max} = \Delta PO_2\ D_{GO2}$ (8)

with $MO_{2\ max}$ (μmol O_2 min^{-1} g^{-1}) = maximum possible oxygen consumption via gill oxygen uptake; ΔPO_2 (kPa) = mean PO_2 difference between water and blood; D_{GO2} (μmol O_2 kPa^{-1} min^{-1} g^{-1}) = gill oxygen diffusing capacity.

As gill oxygen diffusion capacities have not yet been determined for adult cuttlefish, we used a value obtained for the octopod *Octopus vulgaris* (Eno 1994, D_{GO2} = 0.01674 μmol O_2 kPa^{-1} min^{-1} g^{-1}), a species that resembles *S. officinalis* in lifestyle and physiological properties (similar routine metabolic rate, similar oxygen extraction rate $EO_{2,}$, similar hypoxia tolerance thresholds; Johansen et al. 1982, Wells and Wells 1983, 1991). For a counter - current flow model of branchial gas transfer, ΔPO_2 can be estimated using the following formula (Piiper 1998):

$\Delta PO_2 = (0.5(PO_{2\ I} + PO_{2\ E})) - (0.5(PO_{2\ a} + PO_{2\ v}))$ (9)

with $PO_{2\ I}$ (kPa) = inhalant water oxygen partial pressure as measured in the animal chamber; $PO_{2\ E}$ (kPa) = exhalant water oxygen partial pressure as measured in the funnel (see above); $PO_{2\ a}$ (kPa) = arterial oxygen partial pressure; $PO_{2\ v}$ (kPa) = venous oxygen partial pressure. *S. officinalis* blood oxygen partial pressures were derived from data of Johansen et al. (1982b, their table 1, only data sets with $PO_{2\ I}$ > 133 mmHg ≅ 17.7 kPa considered; arterial oxygen saturation 70% of $PO_{2\ I}$, venous oxygen saturation 17% of $PO_{2\ I}$).

3.6 Statistics

Simple linear, exponential and sigmoidal regression analyses were performed using SigmaPlot 8.0. All other statistics were performed using STATISTICA software. Log transformed ventilation frequencies of experiments 1 and 2 were tested for homogeneity of slopes, neccessary for the conduction of ANCOVA. ANCOVA (independent variable: experiment, dependent variable: ventilation rate, covariable: temperature) was used to decide whether ventilatory performance was comparable between experiments. T-tests were employed to compare measured with expected

metabolic rates at extreme temperatures (8 and 26°C) which were determined by extrapolation from the exponential MO_2 temperature relationship observed within the thermal tolerance window.

4 Results

4.1 Control conditions (15°C)

Once acclimated to the experimental surroundings, cuttlefish typically settled down on the floor of the animal chamber, performing resting ventilatory movements. Quiet ventilation at rest is driven by mean routine mantle pressures (MMP_{rout}) of 19.7 Pa (±5.3 Pa SD) and corresponding mantle pressure amplitudes ($MMPA_{rout}$) of 33.3 Pa (±.7.5 Pa SD). V_f was found to be less variable with 30.7 (±3.7 SD) strokes per minute.

Figure 2a (first 20 seconds, last 20 seconds, see insert Fig 2c) shows control patterns of ventilation. During such phases, oxygen extraction rates from the ventilatory current were observed to be very high (approximately 80%). Thus, exhalant oxygen saturation ($SO_{2\ E}$) (Fig. 2b) amounted to only about 20% in the funnel. Periods of quiet ventilatory mantle muscle activity were frequently interrupted by bursts of spontaneous activity, with mantle cavity pressure exceeding routine ventilation pressure by a maximum factor of more than 350. Figure 2a (8:13:25 – 8:15:20) shows such a series of mantle pressure cycles with a maximum pressure amplitude of > 5 kPa. As pressure cycle amplitude increased, less oxygen was extracted from the ventilatory current, resulting in high $SO_{2\ E}$ values in the funnel (Fig 2b). Occurrence of such SJs was observed in all animals (see Melzner, Bock, Pörtner, submitted for a detailed analysis).

4. 2 Acute temperature change

In both experiments ventilation rate was strongly influenced by temperature (fig 3a). Mean ventilation rates (v_f) ranged from 23 to 87 strokes min^{-1} between 8 and 26°C. Exponential fits best

described the relationship between v_f and temperature. Tests for heterogeneity of slopes of log transformed v_f data from both experiments ($F_{(1,59)}$=0.2;p<0.65) and subsequent analysis of covariance (factor: experiment, variable: v_f, covariate: temperature; $F_{(1,60)}$=0.2; p<0.66) could not detect any differences in v_f between experiments. Thus we consider animals from both experiments fully comparable in terms of their ventilatory performance. Figure 3a also depicts v_f for individual animals from experiment 1 beyond 26°C. Essentially, maximum sustainable v_f for these five animals was >90 strokes min^{-1} (93.2 ±7), regardless of the temperature at which this rate was reached. In all cases, maximum sustainable ventilatory frequencies coincided with maximum sustainable $MMPA_{rout}$ and MMP_{rout} (see below).

The experiment 1 mean mantle pressure amplitude ($MMPA_{rout}$) relationship with temperature could best be described by a sigmoidal regression (fig 3b). $MMPA_{rout}$ ranged from 24 to 102 Pa between 8 and 26°C. All five animals reached a maximum sustainable mantle pressure amplitude between 100 and 120 Pa (107 ±11 Pa), four at temperatures around 26-29 degrees, one animal between 20 and 23°C. Animals experienced a period of relatively constant, high pressure mantle amplitudes just prior to a sharp decrease at high temperatures (see fig 3b). MMP_{rout} rose exponentially with temperature, ranging from 12 to 49 Pa between 8 and 26°C (fig 3c). Oxygen extraction rate (EO_2) also changed profoundly with temperature in a sigmoidal fashion (fig 4b). While EO_2 amounted to > 90% at low temperatures (8 and 11°C), it decreased rapidly and nearly linearly at a rate of approximately 5% $°C^{-1}$ between 14 and 23°C. A minimum EO_2 of 32% was found at 26°C. Data from one animal measured at 29°C (not included in fig 4b) confirmed that EO_2 may level off between 30 and 35%. Thus, the relative mantle cavity perfusion requirement (ml water transported per unit MO_2) tripled between 8 and 26°C. As whole animal oxygen consumption could be shown to increase by a factor of roughly six in the same temperature interval (fig 4d), changes in ventilatory mass stream are dramatic: While v_{SV} (estimates in brackets assume no skin respiration) increased from about 0.3 (0.4) to 1.8 (2.4) ml per ventilatory pressure cycle, ventilatory minute volume changed by a factor of >20 from 7 (10) ml at 8°C to 150 (199) ml at 26°C. As a consequence, animals had to transport seawater equivalents of roughly 150 – 200% their own body mass per minute through the mantle cavity when they were approaching upper thermal limits. Both v_{MV} and v_{SV} could best be approximated employing sigmoidal

fits (fig. 4a,c). High rates of v_{MV} change observed between 8 and 23°C (increases of 50 - 100% per 3 °C interval) were followed by a much smaller increase between 23 and 26°C (18%). Whole animal oxygen consumption rose from 0.026 to 0.128 μmol O_2 g^{-1} min^{-1} between 8 and 23°C, followed by a decline to 0.123 μmol O_2 g^{-1} min^{-1} at 26°C. An exponential fit best represented MO_2 values between 11 and 23°C. As below and above this temperature window P_i accumulation could be observed to start in mantle muscle (see Melzner, Bock, Pörtner, submitted), data points at 8 and 26°C were omitted from the regression. Extrapolation of the exponential regression line (11 to 23°C) to 8 and 26°C and subsequent testing of extrapolated MO_2 values for both temperatures against the measured oxygen consumption values revealed significant differences (26°C: $t = -2.7$, df 8, $p<0.04$; 8°C: $t = 3.4$; df 8, $p<0.02$). Q_{10} values for MO_2 were 6.0 (SD 3.4) between 8 and 11°C, 2.42 (SD 0.41) between 11 and 23°C and 0.88 (SD 0.67) between 23 and 26°C.

Using ventilatory volume (m^3 sec^{-1}) and MMP_{rout} (Pa) we were able to calculate the ventilatory muscle system power output (P_{out}). P_{out} rose with temperature in a sigmoidal fashion, with power increasing by a factor of 83 between 8 and 26°C, from 0.038 to 3.17 mW kg^{-1} $animal^{-1}$ in the most power consuming case, assuming that no skin respiration is taking place and that prebranchial MMP_{rout} is twice as high as postbranchial pressure (fig 4e, table 1). Different scenarios were employed to estimate the amount of total power consumed by ventilatory muscles to perfuse the gills with oxygenated seawater (table 1). Ventilation costs (V) rose dramatically (by a factor of 18) between 8 and 26°C, from 0.6 to 11.5 % of P_{tot} in the worst case (not allowing for skin respiration, prebranchial MMP_{rout} = 2 postbranchial MMP_{rout}).

Model calculations displayed in table 2 further demonstrate that under the assumption of constantly high $PO_{2\ a}$ values of 14.3 – 14.7 kPa and constant $PO_{2\ v}$ of 3.5 kPa (Johansen et al. 1982), modifications in ventilatory perfusion alone probably are sufficient to maintain proper ventilatory oxygen fluxes at all temperatures: $MO_{2\ max}$ (column 6) is an estimate of the maximum amount of oxygen that can diffuse into the bloodstream via gill epithelia (at the blood and water oxygen tensions denoted in columns 1-4). $MO_{2\ necc}$ (column 7) indicates the amount of oxygen that must necessarily diffuse via the gills at those metabolic rates measured in our experiment, assuming that 25% of oxygen consumption is provided by means of diffusion via skin surfaces. As $MO_{2\ max}$ is always greater than

$MO_{2\ necc}$, it follows that the ventilatory apparatus is able to provide the neccessary oxygen fluxes across the gill epithelia at all temperatures at largely unaltered blood oxygen tensions by exclusively altering $PO_{2\ E}$, i.e. oxygen extraction form the ventilatory water. Most notably, ventilatory perfusion adjustments are sufficient to not only sustain observed metabolic rates at extreme temperatures (8 and 26°C), but also those that were to be expected at these temperatures, would MO_2 follow the exponential relationship observed between 11 and 23°C (see fig 4d and text above).

5. Discussion

5.1 Oxygen consumption

Oxygen consumption rates found in this study were similar to those reported for *Sepia officinalis* in previous studies. Wells and Wells (1991) recorded a MO_2 of 0.087 μmol O_2 g^{-1} min^{-1} (scaled to a 105 g animal using a mass exponent b = 0.78, Johansen et al. 1982, Melzner, Bock, Pörtner, unpublished data, at 20°C), which is within 10% of the 0.094 μmol O_2 g^{-1} min^{-1} we determined at that temperature. Calculating MO_2 after Johansen et al. (1982, their mass specific VO_2 regression omitting small animals) yields a value of 0.08 μmol O_2 g^{-1} min^{-1} (scaled to a 105 g animal) at 17°C, which is similar to the 0.077 μmol O_2 g^{-1} min^{-1} we measured at 17°C. Still, such comparisons should be carried out with precaution as the above mentioned studies were performed on *S. officinalis* caught in the wild, with acclimatization temperatures being unknown. It is known from studies on fish (i.e. Jobling 1982) and, recently, cephalopods (Melzner, Bock, Pörtner, unpublished data), that acclimatization temperatures influence metabolic rates (standard metabolic rate of *P. platessa* acclimated to and measured at 10°C was found to be >70% higher than that of animals acclimated to 20°C and acutely measured at a temperature of 10°C (Jobling, 1982)).

5.2 Ventilation

Most records of *Sepia officinalis* ventilation rates match the rates determined in this study (Mislin (1966): 22-65 strokes min^{-1} in animals with 20-35 cm body length, 10-25°C; Bone et al. (1994): 48 – 60 strokes min^{-1} (at MMPAs of 50 to 150 Pa, animals 5-25 cm ML, 18°C; Boal and Ni (1996): 45 strokes min^{-1} (animals 80-200g, 19-21°C; Boal and Golden (1999): 39,9 strokes min^{-1}, animals 95-251g, 19-21°C; Terbeck (2003): 48 strokes min^{-1}; animals 82g, 16°C). Only those rates determined by Wells and Wells (1991) are considerably higher at 105 strokes min^{-1} (animals 273-326g, 20°C, normoxic conditions). Routine mean ventilation pressures (MMP_{rout}) and pressure amplitudes ($MMPA_{rout}$) under control conditions are in the same range (<0.12 kPa) as those determined by Wells and Wells (1991) for the same species and are lower than resting mantle pressure amplitudes of most other cephalopods (octopods 0.2 kPa, squids 0.3 – 0.75; Wells 1988). Pressures driving the ventilatory stream in the cuttlefish are located between those measured in the mantle cavities of bivalves, where pressures of 10 – 40 Pa can be generated by the combined action of cilia (as seen in the blue mussel, *Mytilus edulis*, Jørgensen et al. 1986), and those generated by marine fish species in their buccal cavities during routine ventilation (i.e. 0.2 – 0.3 kPa pressure amplitude in *Salmo salar* and *Squalus acanthias*, Perry and McKendry 2001).

5.3 Oxygen extraction rates from the ventilatory current

A mean oxygen extraction rate (EO_2) of roughly 80% at 15°C represents the highest rate recorded so far for a cephalopod species. Wells and Wells (1982, 1991) have also measured oxygen extraction from the ventilatory current, but found lower mean values of 51% (1982) and 33% (1991). The authors noted that in their first study, animals always hovered or swam above the ground and concluded that their measurements would probably not represent resting extraction rates. This corresponds to our observations that during higher pressure amplitudes of mantle cavity oscillations (spontaneous exercise), oxygen extraction rates dropped considerably (see fig 2). In the study by Wells and Wells (1991), v_f was unusually high. This may have contributed to their low reported extraction rates. High v_f in our experiment at high temperatures also went along with low extraction rates (see below). As suggested by Wells and Wells (1991), the decapod cephalopod *S. officinalis* has evolved

(in physiological terms) in the octopod direction, favouring a sedentary lifestyle in combination with higher oxygen extraction rates. This contrasts the patterns seen in constantly swimming decapods. Among various cephalopod species, EO_2 estimates under normoxic conditions range from <10% for squids (*Lolliguncula brevis*, *Illex illecebrosus*) and Nautilus (*Nautilus pompilius*) to >60% for *Octopus vulgaris* (Wells & Wells 1985, Webber & O'Dor 1986, Wells et al. 1986).

Consequently, respiratory perfusion requirements are very low in cuttlefish under control conditions. A mere 30 – 35% of its body weight in seawater has to be transported past its gills per minute at 15°C, while the small squid *L. brevis* (10g, Wells et al. 1988) needs to pump (at least) 9 times its own body weight per minute at the same temperature. *S. officinalis* EO_2 is more comparable to fish species that live in similar highly uniform (sandy and muddy bottom) environments, where, likely, selective pressures are on good camouflage, which includes the minimization of movements. In plaice (*Pleuronectes platessa*), and even more so, flounder (*Plathichthys flesus*) high EO_2 (plaice: 69%, flounder 78%, 10°C, normoxic conditions) minimizes ventilatory movements, as perfusion requirements are decreased (0.4% of body weight $stroke^{-1}$, 8.9% and 10.6% bw min^{-1}; Steffensen et al. 1982). Interpolating our data to 10°C yields a stroke volume v_{SV} of 0.48% bw min^{-1} and a minute v_{MV} of 12.6% bw min^{-1}, which is already close to flatfish performance, but then, we have not yet considered allometry effects which would lead to even lower numbers for our cuttlefish compared to the fish (the afore mentioned pleuronectids were five times heavier than our cuttlefish).

Low ventilation pressures and low ventilatory perfusion volumes are the basis for a relatively cheap ventilatory perfusion system in the cuttlefish. At control temperature (15°C) a maximum of less than 1.5% of animal power is consumed by ventilatory muscle pressure generation. Obviously, decoupling ventilation from the locomotory water flow has created two distinct pumping systems in the cuttlefish: The classical (see O'Dor and Webber 1986) high impedance, positive displacement pump employed during high amplitude jets (Vogel 1994) and a (cheap) low impedance, fluid dynamic pump. While both systems make use of radial mantle fibres during the refilling phase of the ventilatory cycle (Bone et al. 1994), the latter receives impetus from the collar flap muscles, thin sheets of muscle that propel water into the mantle cavity in a mode that reminds of beating flagellae arranged in parallel (in fact, many other fluid dynamic pumps are driven by cilia (e.g. bivalves) or

flagellae (e.g. sponges), see Vogel 1994 for examples). In consequence, our estimates of the cost of ventilation in the cuttlefish are lower than most estimates for fish resting ventilatory mechanics. Estimates range from 0.5% (Alexander 1970) to 43% (Schumann & Piiper 1966) of resting metabolic rate (rmr) for active gill ventilation, with most authors finding values of 10 - 15% rmr (Hughes 1973, Cameron & Cech 1970). This is partly related to the higher ventilation pressures in fish buccal cavities (see above), but is also a consequence of elevated metabolic rates in cephalopods (see O'Dor and Webber 1986). Thus, even if P_{in} were comparable between a fish and *S. officinalis*, ventilatory costs (in % of P_{tot}) were lower in the cuttlefish, as P_{tot} typically is higher in the molluscan high performance taxon. As mentioned, it is not possible to calculate ventilation costs for those cephalopods which extract oxygen from the locomotory water current. Still, table 3 gives estimates for *L. brevis* mantle muscle mechanics at 20°C (derived from Wells 1988, Wells et al. 1988) in comparison to our data for cuttlefish. At twice the v_f, three times the MMP_{rout} and 14 times the v_{MV} of the cuttlefish, the little squid consumes at least 18% of its total power for ventilatory / locomotory muscle mechanics (even at an optimistic 10% EO_2, estimates double at a more realistic 5% EO_2) whilst maintaining position in the water column. This comparison nicely illustrates how the employment of a separate ventilatory pumping system in sedentary cephalopods can cut down costs.

5.4 Acute temperature change

Temperature change resulted in an exponential increase in oxygen consumption rates (see fig 4) by 8.9% $°C^{-1}$ between 11 and 23°C, corresponding to a Q_{10} of 2.5. The squid *Lolliguncula brevis*, being subjected to temperatures between 14.5 and 28.5°C (Wells et al. 1988) also displayed an exponential increase in MO_2 with temperature (rates of increase: 4.34% $°C^{-1}$; Q_{10}: 1.47). Q_{10} values for MO_2 for various cephalopods (*Loligo* spp., *Octopus* spp., *Nautilus pompilius*) derived within narrower temperature ranges were usually found to range between 1.5 and 3 (Wells and O'Dor 1987). In the present study, the significant deviation from the exponential increase as observed at 8 and 26°C likely results from the onset of whole animal oxygen limitations and, possibly, associated metabolic depression. At both temperatures less oxygen was consumed than predicted by the Q_{10} relationship. In

an earlier study by Wells et al. (1988), deviations from the Q_{10} - relationship could not be found in *L. brevis* in a temperature range between 15 and 27 °C, but hypoxia tolerance was decreased at the highest temperature analysed. Three out of five animals died during progressive hypoxia at oxygen tensions which they would have survived at lower temperatures (Wells et al. 1988). These findings compare well with our results, as they also indicate an oxygen - limited loss in scope for survival and activity.

Elevated oxygen demand during warming in our cuttlefish could not be met by maintaining high EO_2, rather, v_{MV} needed to be increased at a rate of 20.4% $°C^{-1}$ (between 8 and 23°C) to compensate for MO_2 increasing at only 8.9% $°C^{-1}$. This corresponds to the exponential increase in ventilatory muscle power output (P_{out}) of 30.1% $°C^{-1}$ (8-23°C), resulting in a 83-fold increase in P_{out} over the whole temperature range. This does not neccessarily imply that individual muscle fibres need to cope with such a high workload increment. It has been shown that cephalopods gradually recruit more mantle muscle fibres at increasing workloads (Bartol 2001). Overall, power requirements for ventilation mechanics increase at the same high rate as muscle power output. This is equivalent to a shift in the overall energy budget of the animal: ventilation costs increase to a greater extent than whole animal power. Still, owing to the cheap fluid dynamic ventilation pump, maximum costs will not be greater than 12% of the animals' total power (table 1), since our estimates are based on two rather pessimistic assumptions: the absence of skin respiration and a very low efficiency of muscle contraction (E) of 0.03.

In vitro measurements on cuttlefish skin show that there is a considerable potential for skin respiration (Madan and Wells 1996), but *in vivo* measurements are not available. Estimates of up to 25% of total MO_2 (depending on the degree of skin exposure to water and flow around respiratory surfaces) seem reasonable (Madan and Wells 1996). Skin respiration would decrease ventilation costs (table 1). An efficiency of 0.03 was determined by O'Dor and Webber (1991) for locomotory mantle contractions at optimum swimming speeed, higher efficiencies of 0.07 and 0.38 were found at critical and maximum speeds. As fins also contribute to speed in cuttlefish, determined efficiencies are likely low estimates (P_{in} was determined by O'Dor and Webber from increases in oxygen consumption with swimming speed. As power needed for animal propulsion is allocated to both mantle muscles and fins

($P_{in} = P_{in\ mantle} + P_{in\ fins}$), P_{in} is likely an overestimation, leading to an underestimation of mantle muscle efficiency if P_{out} is solely calculated from mantle muscle performance. Higher efficiencies would lead to lower estimates of ventilation costs. In the range of temperatures typically encountered in the natural habitat of our experimental cuttlefish population in the English Channel (10 - 17.5°C, Boucaud – Camou and Boismery 1991) ventilation costs are always <2% of total power at rest.

Our model calculations (table 2) on maximum oxygen flow through gill epithelia demonstrated that at an assumed 25% contribution of skin respiration and D_{GO2} values similar to those of *O. vulgaris*, the witnessed increases in P_{out} and concomitant increases in ΔPO_2 between water and blood with temperature fully suffice to provide the required diffusive flow of oxygen into branchial vessels as needed for arterial oxygenation. Model calculations are based on arterial PO_2 values of 14-15 kPa, similar to those measured in the efferent branchial vessel *in vivo* by Johansen et al. (1982) at 17°C. This is important for two reasons: Firstly, blood from the efferent branchial vessel perfuses the systemic heart. Houlihan et al. (1987) have shown that the *O. vulgaris* heart reacts strongly to declining $PO_{2\ a}$ by reducing its power output. Secondly, haemocyanin oxygen binding properties are highly temperature dependent. Zielinski et al. (2001) demonstrated that haemocyanin P_{50} shifts at a rate of 0.12 kPa $°C^{-1}$ in the cuttlefish *S. officinalis*. In combination with decreasing Bohr coefficients upon warming (Φ = -1.33 at 20°C, -0.99 at 10°C), this implies a decrease in haemocyanin oxygen affinity, indicating that at higher temperatures, progressively higher oxygen partial pressures are needed to ensure full saturation of the respiratory pigment in the gill vessels. A (putative) alpha stat pattern of extracellular pH regulation (decrease of pH at a rate of approximately 0.018 units $°C^{-1}$; Reeves 1972, Burton 2002, Howell and Gilbert 1976) additionally stresses the importance of high mean oxygen partial pressures in gill vessels in order to maintain highly efficient shuttling of haemocyanin bound oxygen. These considerations support the hypothesis that cuttlefish probably optimize their oxygen transfer systems towards constantly high oxygen partial pressures in arterial blood, leaving it to the ventilatory apparatus to undergo many-fold changes in power output to modulate water PO_2s and thus, diffusive oxygen flux from water to blood. Wells and Wells (1995) demonstrated that cephalopods (*O. vulgaris*) can react immediately (within two or three ventilation cycles) to changing oxygen partial pressures in the ventilatory water stream by modulating v_{SV} and v_f.

They further concluded (from nerve cutting experiments) that principal oxygen receptors must be located in the gill complex and that ventilation parameters are controlled by the brain. Whether oxygen receptors monitor internal (blood) or external (water) conditions (or both, as in fish, Gilmour 2001) remains to be established. However, a control circuit with central nervous efferent and afferent fibres in the cuttlefish, with an internal oxygen sensor in the efferent branchial vessel could possibly steer ventilatory power output in order to keep arterial PO_2 at the desired high levels.

5.5 Critical temperatures and the ventilatory apparatus

In a parallel study (Melzner, Bock, Pörtner, submitted) we could demonstrate that a progressive switch to anaerobic metabolism is taking place in cuttlefish mantle muscle tissues at both ends of the thermal window, at 7 and 26.8°C, suggesting a thermal limitation of aerobic metabolism. At the high end of the temperature spectrum, use of muscle phosphagen and decreases in the Gibbs free energy of ATP hydrolysis ($\Delta G/d\xi$) were correlated with stagnating and decreasing ventilation pressure amplitudes. We proposed that this probably is due to fatigue of radial mantle muscle fibres, which are engaged in the work of ventilating the gills. Similarly, mantle phosphagen use and decreases in $\Delta G/d\xi$ in the cold may also be an indication of a beginning energetic limitation of working muscle fibres.

Consequently, we designed the present study to elucidate whether ventilatory action of the cephalopod mantle muscle organ itself is the reason for the observed switch to anaerobic metabolism or just secondary to stagnating or decreasing oxygen supply to the muscle due to circulatory capacity limitation.

Determinations of routine metabolic rate (rmr) in experiment 2 revealed significant deviations from the expected exponential relationship with temperature between 23 and 26°C in the warm and between 8 and 11°C in the cold, indicating oxygen transport capacity limitations on both sides of the temperature spectrum starting at temperatures well before critical.

The ventilatory apparatus functions to maintain high oxygen partial pressures in the arterial blood to ensure proper haemocyanin oxygen loading. Our investigations demonstrated that cuttlefish

are characterized by a relatively cheap ventilatory system that can undergo 83 – fold changes in power output to provide suitable oxygen diffusion gradients at varying whole animal oxygen demands. By increasing the amount of water channelled past the gills, mean water PO_2 is being raised, oxygen extraction rate (EO_2) drops, and diffusive oxygen flux into the blood is enhanced. Our model calculations (table 2) revealed that the ventilatory system is most likely able to fulfil its role within the entire temperature range investigated, i.e. between 8 and 26°C. It is not only able to sustain the observed oxygen flux at 8 and 26°C, rather, ventilatory effort would even be sufficient to sustain prognosed (see tab 2) oxygen consumption values at those temperatures. The unexpected drops in oxygen consumption rate below 11°C and above 23°C therefore likely do not result from low arterial oxygen partial pressures and concomitant incomplete haemocyanin oxygenation. Rather, circulatory capacity limitations or problems with oxygen extraction from the blood must be responsible for the observed deviations in routine metabolic rate at these thermal extremes.

Beyond the temperature interval of 8 – 26°C, onset of anaerobic metabolism in mantle muscle tissues therefore is most likely not due to exercise induced fatigue of mantle muscle but secondary to an oxygen deprivation of working ventilatory muscle fibres.

These results fit recent findings on thermal tolerance in the other ectothermic marine high performance taxon, the fishes (Heath and Hughes 1973, Mark et al. 2002, Sartoris et al. 2003, Lannig et al. 2004). Apparently, when being subjected to acute thermal stress, high power ectothermic life in ocean environments is ultimately constrained by the limited functional scope of high pressure, closed blood circulation machinery rather than by low pressure ventilation systems.

However, how exactly the circulatory system limits the European cuttlefish *Sepia officinalis* during acute thermal challenges, remains to be established.

6. Acknowledgements

This study was carried out in support of the project: The cellular basis of standard and active metabolic rate in the free-swimming cephalopod, *Sepia officinalis* (NERC Grant PFZA/004). The authors wish to thank Rolf Wittig and Timo Hirse for their excellent technical support, Raymond and

Marie - Paule Chichery (Université de Caen) for providing cuttlefish eggs in 2002 and 2003 and all student helpers that were engaged in raising the animals in our lab.

7. References

AITKEN, J. P., O'DOR, R. K. AND JACKSON, G. D. The secret life of the giant cuttlefish *Sepia apama* (Cephalopoda): Behaviour and energetics in nature revealed through radio acoustic positioning and telemetry (RAPT). *J. Exp. Mar. Biol. Ecol.*, in press.

ALEXANDER, R. McN. (1970). Functional design in fishes. Hutchinson, London, 160 pp.

BARTOL, I. K. (2001). Role of aerobic and anaerobic circular mantle muscle fibers in swimming squid: Electromyography. *Biol. Bull.* **200**, 59-66.

BARTOL, I.K., MANN, R. AND PATTERSON, M.R. (2001). Aerobic respiratory costs of swimming in the negatively buoyant brief squid *Lolliguncula brevis*. *J. Exp. Biol.* **204**, 3639-3653.

BOAL, J. G. AND NI, J. N. (1996). Ventilation rate of cuttlefish, *Sepia officinalis*, in response to visual stimuli. *The Veliger* **38**(4), 342-347.

BOAL, J. G. AND GOLDEN, D. K. (1999). Distance chemoreception in the common cuttlefish *Sepia officinalis* (Mollusca, Cephalopoda). *J. Exp. Biol. Ecol.* **235**, 307-317

BONE, Q., PULSFORD, A. AND CHUBB, A.D. (1981). Squid mantle muscle. *J. mar. Biol. Ass. U.K.* **61**, 327-342.

BONE, Q., BROWN, E. R. AND TRAVERS, G. (1994a). On the respiratory flow in the cuttlefish *Sepia officinalis*. *J. Exp. Biol.* **194**, 153-165.

BONE, Q., BROWN, E. R. AND USHER, M. (1994b). The structure and physiology of cephalopod muscle fibres. In *Cepahlopod Neurobiology* (ed. N.J. Abbot, R. Williamson and L. Maddock), pp. 301-329. Oxford: Oxford University Press.

BOUCAUD – CAMOU, E. AND BOISMERY, J. (1991). The migrations of the cuttlefish (Sepia officinalis) in the English Channel. In: Boucaud-Camou, E. (Ed.), La Seiche, 1st International symposium on the cuttlefish *Sepia*. Center of publications, Universite de Caen. pp. 179-189.

BURTON, R. F. (2002). Temperature and acid-base balance in ectothermic vertebrates: the imidazole alphastat hypothesis and beyond. *J. Exp. Biol.* **205**, 3587-3600.

CAMERON, J. N. AND CECH, J.R. (1970). Notes on the energy cost of gill ventilation in teleosts. *Comp. Biochem. Physiol.* **34**, 447-455.

DENTON, E.J. AND GILPIN-BROWN, J.B. (1961). The buoyancy of the cuttlefish, *Sepia officinalis* (L.). *J. mar. Biol. Ass. U.K.* **41**, 319-342.

ENO, C. N. (1994). The morphometrics of cephalopod gills. *J. mar. Biol. Ass. U.K.* **74**, 687-706.

FARRELL, A.P. (2002). Cardiorespiratory performance in salmonids during exercise at high temperature: insights into cardiovascular design limitations in fishes. *Comp. Biochem. Physiol. A* **132**, 797-810.

FREDERICH, M. AND PÖRTNER, H. O. (2000). Oxygen limitation of thermal tolerance defined by cardiac and ventilatory performance in spider crab, *Maja squinado*. *Am. J. Physiol.* **279**, R1531-R1538

GILMOUR, K.M. (2001). The CO_2 / pH ventilatory drive in fish. *Comp. Biochem. Physiol. A* **130**, 219-240.

HEATH, A, G. AND HUGHES, G. M. (1973). Cardiovascular and respiratory changes during heat stress in the rainbow trout (*Salmo gairdneri*). *J. Exp. Biol.* **59**, 323-338.

HOULIHAN, D. F., INNES, A. J., WELLS, M. J. AND WELLS J. (1982). Oxygen consumption and blood gases of *Octopus vulgaris* in hypoxic conditions. *J. Comp. Physiol.* **148**, 35-40.

HOULIHAN, D.F., AGNISOLA, C., HAMILTON, N. M. AND GENOINO, T. I. (1987). Oxygen consumption of the isolated heart of octopus: effects of power output and hypoxia. *J. Exp. Biol.* **131**, 137-157

HOWELL, B.J. AND GILBERT, D.L. (1976). pH - temperature dependence of the hemolymph of the squid, Loligo pealei. *Comp. Biochem. Physiol. A* **55**, 287-289.

HUGHES, G. M. (1973). Respiratory responses to hypoxia in fish. *Amer. Zool.* **13**, 475-489.

JOBLING, M. (1982). A study of some factors affecting rates of oxygen consumption of plaice, *Pleuronectes platessa* L. *J. Fish. Biol.* **20**, 501-516.

JOHANSEN, K., BRIX, O., KORNERUP, S. AND LYKKEBOE, G. (1982a). Factors affecting O_2-uptake in the cuttlefish, *Sepia officinalis*. *J. mar. Biol. Ass. U.K.* **62**, 187-191.

JOHANSEN, K., BRIX, O. AND LYKKEBOE, G. (1982b). Blood gas transport in the cephalopod, *Sepia officinalis*. *J. Exp. Biol.* **99**, 331-338.

JØRGENSEN, C.B. AND RIISGÅRD, H.U. (1988). Gill pump characteristics of the soft clam *Mya arenaria*. *Mar. Biol.* **99**, 107-109.

LANNIG, G., BOCK, C., SARTORIS, F. J. AND PÖRTNER, H. O. (2004). Oxygen limitation of thermal tolerance in cod, *Gadus morhua* L. studied by magnetic resonance imaging (MRI) and on-line venous oxygen monitoring. *Am. J. Physiol.* **287**, R902-R910.

MADAN, J. J. AND WELLS, M.J. (1996). Cutaneous respiration in *Octopus vulgaris*. *J. Exp. Biol.* **199**, 2477-2483.

MARK, F. C., BOCK, C. AND PÖRTNER, H. O. (2002). Oxygen – limited thermal tolerance in Antarctic fish investigated by MRI and ^{31}P – MRS. *Am. J. Physiol.* **283**, R1254-R1262.

MELZNER, F., BOCK, C. AND PÖRTNER, H.O. Critical temperatures in the cephalopod *Sepia officinalis* investigated using *in vivo* ^{31}P NMR spectroscopy, *J. Exp. Biol.*, submitted.

MISLIN, H. (1966). Über die Beziehungen zwischen Atmung und Kreislauf bei Cephalopoden (*Sepia officinalis* L.). Synchronregistrierung von Elektrokardiogramm (Ekg) und Atembewegungen am schwimmenden Tier. *Verh. Dtsch. Zool. Ges.* 175-181.

O'DOR, R.K. AND WEBBER, D.M. (1986). The constraints on cephalopods: why squid aren't fish. *Can. J. Zool.* **64**, 1591-1605.

O'DOR, R. K. AND WELLS, M. J. (1987). Energy and nutrient flow. In: Boyle, P. R. (Ed.), Cephalopod life cycles, Comparative reviews. (Vol 2) Academic Press, London, pp.109-133.

O'DOR, R. K. AND WEBBER, D. M. (1991). Invertebrate athletes: trade – offs between transport efficiency and power density in cephalopod evolution. *J. Exp. Biol.* **160**, 93-112.

PACKARD, A.(1972). Cephalopods and fish: limits of convergence. *Biol. Rev.* **47**, 241-307.

PERRY, S.F. AND MCKENDRY, J.E. (2001). The relative roles of external and internalCO_2 versus H^+ in eliciting the cardiorespiratory responses of *Salmo salar* and *Squalus acanthias* to hypercarbia. *J. Exp. Biol.* **204**, 3963-3971.

PIIPER, J. (1998). Branchial gas transfer models. *Comp. Biochem. Physiol.* **119A**, 125-130

REEVES, R. B. (1972). An imidazole alphastat hypothesis for vertebrate acid –base regulation: tissue carbon dioxide content and body temperature in bullfrogs. *Respir. Physiol.* **14**, 219-236

SARTORIS, F. J., BOCK, C., SERENDERO, I., LANNIG, G. AND PÖRTNER, H. O. (2003). Temperature – dependent changes in energy metabolism, intracellular pH and blood oxygen tension in the Atlantic cod. *J. Fish. Biol.* **62**, 1239-1253.

STEFFENSEN, J. F., LOMHOLT, J. P., JOHANSEN, K. (1982). Gill ventilation and O2 extraction during graded hypoxia in two ecologically distinct species of flatfish, the flounder (*Platichthys flesus*) and the plaice (*Pleuronectes platessa*). *Env. Biol. Fish.* **2**, 157-163.

TERBECK, S. (2003). Der Einfluss vopn Kalium auf die Aktivität von *Sepia officinalis*. Diploma thesis, University of Münster, 61 pp.

TOMPSETT, D.H. (1939). Sepia. LMBC Memoirs, Liverpool University Press, 184 pp.

VOGEL, S. (1994). Life in moving fluids: the physical biology of flow. Princeton University Press, 467 pp.

WELLS, M. J. (1990). Oxygen extraction and jet propulsion in cephalopods. *Can. J. Zool.* **68**, 815-824.

WELLS, M. J. AND CLARKE, A. (1996). The costs of living and reproducing for an individual cephalopod. *Phil. Trans. R. Soc. Lond. B* **351**, 1083-1104

WELLS, M. J. AND WELLS, J. (1982). Ventilatory currents in the mantle of cephalopods. *J. Exp. Biol.* **99**, 315-330.

WELLS, M. J. AND WELLS, J. (1983). The circulatory response to acute hypoxia in *Octopus*. *J. Exp. Biol.* **104**, 59-71.

WELLS, M. J. AND WELLS, J. (1985). Ventilation frequencies and stroke volumes in acute hypoxia in *Octopus*. *J. Exp. Biol.* **118**, 445-448.

WELLS, M. J. AND WELLS, J. (1986). Blood flow in acute hypoxia in a cephalopod. *J. Exp. Biol.* **122**, 345-353.

WELLS, M. J. AND WELLS, J. (1991). Is *Sepia* really an octopus? In Boucaud-Camou, E. (Ed.), La Seiche, 1st International symposium on the cuttlefish *Sepia*. Centre de publications, Universite de Caen. pp. 77-92.

WELLS, M. J. AND WELLS, J. (1995). The control of ventilatory and cardiac responses to changes in ambient oxygen tension and oxygen demand in octopus. *J. Exp. Biol.* **198**, 1717-1727.

WELLS, M.J., HANLON, R.T., LEE, P.G. AND DIMARCO, F.P. (1988). Respiratory and cardiac performance in *Lolliguncula brevis* (Cephalopoda, Myopsida): the effects of activity, temperature and hypoxia. *J. Exp. Biol.* **138**, 17-36.

ZIELINSKI, S., SARTORIS, F. AND PÖRTNER, H.O. (2001). Temperature effects on hemocyanin oxygen bnding in an Antarctic cephalopod. Biol. Bull. **200**, 67-76.

Figure captions

Figure 1

Positioning of the fibre optic oxygen sensor in the ventilatory stream. (A) A PE tube was first implanted into the funnel, subsequently the fragile oxygen sensor is advanced through the tube and approx. 3 mm into the ventilatory exhalant stream. (B) is a top view of the 50 μm diameter sensor tip from above, in the PE tube. In order to prevent damage to the sensor by movements of the funnel roof (the tube typically collapses during inspiration), small sections of the PE tube (marked black, parallel to water flow) were left as support along the distal 3 mm of the sensor.

Figure 2

Experiment 2. Routine ventilation and spontaneous exercise (animal 2, 15°C). (A) The first 20 sec. and the last 20 sec. represent control patterns of ventilation with pressure amplitudes < 0.1 kPa (see also insert c). Interspersed are groups of swimming jets (SJ) with amplitudes > 0.2 kPa. (B) Correlated recordings of $SO_{2\ E}$ (exhalant stream oxygen saturation, %) as measured in the funnel with a fibre optic oxygen sensor. MP = mantle pressure.

Figure 3

Experiment 1 and 2: Ventilation frequency (v_f) and ventilation pressures in relation to temperature (T, in °C). Some animals were heated above 26°C in experiment 1 (black circles, additional data points). All data points are means, error bars are standard deviations (SD). (A) v_f for experiments 1(N=5) and 2 (N=4). See text for ANCOVA of log transformed v_f data from both experiments. Regression (exp. 1, 8 – 26°C): v_f (strokes min^{-1}) = 13.04 exp (0.074 T); R^2 = 0.993; $F_{(1,5)}$ = 726; p<0.001. (B) Experiment 1 routine ventilation pressure amplitude ($MMPA_{rout}$) vs. temperature (T, in °C). Sigmoidal regression (8 – 26°C): $MMPA_{rout}$ (Pa) = 25.6 + (2967.1/(1 + exp(-(T – 41.4)/4.23))); R^2 = 0.997; $F_{(3,3)}$ = 985, p<0.001. (C) Experiment 1 routine mean pressure (MMP_{rout}) vs. temperature (T, in °C). Exponential regression (8 – 26°C): MMP_{rout} (Pa) = 6.02 exp (0.081 T); R^2 = 0.995; $F_{(1,5)}$ = 520; p<0.001.

Figure 4

Experiment 2. (A) Ventilatory minute volume (v_{MV}) expressed in ml $animal^{-1}$ $minute^{-1}$ or % body weight (bw) $animal^{-1}$ $minute^{-1}$. Sigmoidal regression (8 – 26°C): v_{MV} (ml $animal^{-1}$ $minute^{-1}$) = 11.9 + (151.9/(1 + exp(-(T – 21.05)/2.06))); R^2 = 0.994; $F_{(3,3)}$ = 172.1 p<0.001. (B) Oxygen extraction from the ventilatory current (EO_2). Sigmoidal regression (8 – 26°C): EO_2 (% of available oxygen) = 28.97 + (68.56/(1 + exp(-(T – 18.29)/-2.62))); R^2 = 0.999; $F_{(3,3)}$ = 985 p<0.001. (C) Ventilatory minute volume (v_{SV}) expressed in ml $animal^{-1}$ $stroke^{-1}$ or % bodyweight (bw) $animal^{-1}$ $stroke^{-1}$. v_{SV} (ml $animal^{-1}$ $stroke^{-1}$) = 0.22 + (1.83/(1 + exp(-(T – 19.0158)/4.11))); R^2 = 0.979; $F_{(3,3)}$ = 45.6 p<0.006. (D) Oxygen consumption (MO_2). Exponential regression (11 - 23°C), regression line extrapolated to 8 and 26°C, see text for explanation: MO_2 (μmol O_2 g^{-1} min^{-1}) = 0.018 exp (0.0847 T); R^2 = 0.995; $F_{(1,3)}$ = 520, p<0.001). (E) Ventilatory power output (P_{out}). Sigmoidal regression (8-26°C): P_{out} (mW kg^{-1} animal tissue) = 0.094 + (3.46/(1 + exp(-(T – 22.23)/1.78))); R^2 = 0.998; $F_{(3,3)}$ = 931 p<0.001.(F) Ventilation costs (v_C). Exponential regression (8-26°C): v_C (% of P_{tot}) = 0.1172 exp(0.1774 T); R^2 = 0.989; $F_{(1,5)}$ = 458, p<0.001). All data points are means ± SD. All regressions against temperature (T, in °C).

Table 1. *S. officinalis* ventilation power and ventilation cost estimates. P_{out} calculated from formula 4b; estimates based on postbranchial pressures (formula 4a) are 0.5 of listed table values. Values for v_C calculated using $P_{out\ b}$. See text for definitions and calculations.

	a) 25% skin respiration				*b) no skin respiration*			
temp [°C]	$P_{out\ b}$ [mW kg^{-1}]	SD	v_C [% of P_{tot}]	SD	$P_{out\ b}$ [mW kg^{-1}]	SD	v_C [% of P_{tot}]	SD
8	0.028	0.007	0.48	0.12	0.038	0.009	0.64	0.16
11	0.069	0.016	0.70	0.16	0.092	0.021	0.92	0.20
14	0.124	0.033	0.92	0.24	0.165	0.044	1.22	0.32
17	0.242	0.081	1.40	0.46	0.323	0.108	1.86	0.62
20	0.617	0.293	2.92	1.38	0.822	0.391	3.88	1.84
23	1.657	0.699	5.80	2.44	2.209	0.932	7.74	3.26
26	2.379	0.855	8.64	3.1	3.173	1.140	11.52	4.14

Table 2. *S. officinalis* maximum gill diffusion rate estimates in relation to neccessary oxygen diffusion rates. Maximum diffusion rate estimates ($MO_{2\ max}$) are based on oxygen saturation measured in cuttlefish blood by Johansen et al. (1982b; 70% $SO_{2\ a} \cong PO_{2\ a}$14.3 – 14.7 kPa, 17% $SO_{2\ v} \cong PO_{2\ v}$ 3.5 kPa at 17°C). Neccessary oxygen diffusion rates ($MO_{2\ necc}$) via gill epithelia were calculated using our exponential MO_2 vs. temperature regression (see fig 4d), assuming that 25% of consumed oxygen is supplied by skin respiration ($MO_{2\ exp}$). $PO_{2\ I}$ = inhalant water PO_2, $PO_{2\ E}$ = exhalant water PO_2, $PO_{2\ v}$ = venous blood PO_2, $PO_{2\ a}$ = arterial blood PO_2. See text for calculations.

T	$PO_{2\ I}$	$PO_{2\ E}$	$PO_{2\ v}$	$PO_{2\ a}$	ΔPO_2	$MO_{2\ max}$	$MO_{2\ necc}$
[°C]	*[kPa]*	*[kPa]*	*[kPa]*	*[kPa]*	*[kPa]*	*[µmol O_2 min^{-1} g^{-1}]*	*[µmol O_2 min^{-1} g^{-1}]*
	(1)	*(2)*	*(3)*	*(4)*	*(5)*	*(6)*	*(7)*
8	21.0	0.8	3.5	14.7	1.8	0.031	0.026
11	20.9	1.5	3.5	14.6	2.2	0.037	0.035
14	20.8	2.5	3.5	14.6	2.6	0.046	0.044
17	20.8	6.1	3.5	14.5	4.5	0.076	0.057
20	20.7	9.8	3.5	14.5	6.3	0.106	0.074
23	20.6	12.5	3.5	14.4	7.6	0.129	0.095
26	20.5	13.9	3.5	14.3	8.3	0.141	0.122

Table 3. Squid vs. cuttlefish ventilation mechanics. Data for squid (*Lolliguncula brevis*) from Wells et al. (1988), Wells and Wells (1991). Mean mantle pressure (MMP) for the squid estimated using a MMP vs. MMPA regression obtained in our companion paper (Melzner, Bock, Pörtner submitted, formula 7). Ventilation costs for the squid estimated with E = 0.03 (Bartol et al. 2001). Cuttlefish P_{out} derived from formula 4b, not allowing for skin respiration. See text for definitions and calculation of variables. A part of the difference in metabolic rate (P_{tot}) can be explained by different body masses of species. Squid v_C include costs for maintenance of position (animals hovering in midwater).

Variable	*L. brevis* *11 g (20°C)*	*S. officinalis* *105 g (20°C)*	*factor*
$MMPA_{rout}$ [Pa]	300	43.9	6.8
MMP_{rout} [Pa]	81	29.7	2.7
v_{SV} [% bw stroke^{-1}]	11.6	1.5	7.7
v_{MV} [% bw min^{-1}]	1210	84.2	14.4
v_f [strokes min^{-1}]	104	53.3	2
EO_2 [%]	10	52.5	5.3
Skin resp. [% of MO_2]	20	0	-
MO_2 [μmol O_2 g^{-1} min^{-1}]	0.402	0.094	4.3
P_{out} [mW kg^{-1}]	16.34	0.822	19.9
P_{in} [mW kg^{-1}]	544.7	27.4	19.9
P_{tot} [W kg^{-1}]	3.02	0.71	4.25
v_C [% of P_{tot}]	18.0	3.9	4.6

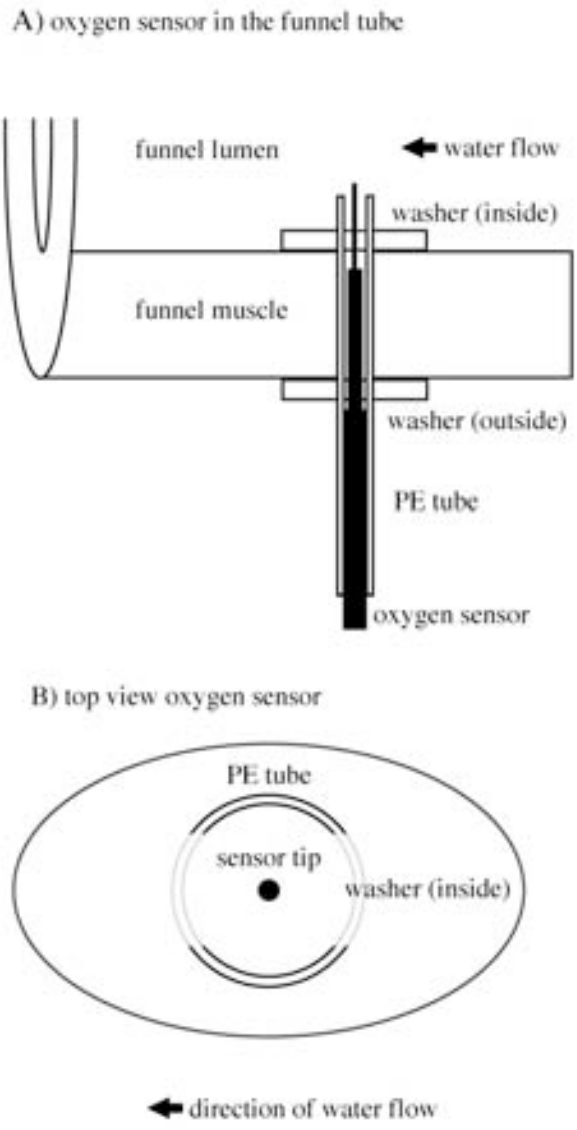
A) oxygen sensor in the funnel tube
funnel lumen
water flow
washer (inside)
funnel muscle
washer (outside)
PE tube
oxygen sensor
B) top view oxygen sensor
PE tube
sensor tip
washer (inside)
direction of water flow

Figure 1

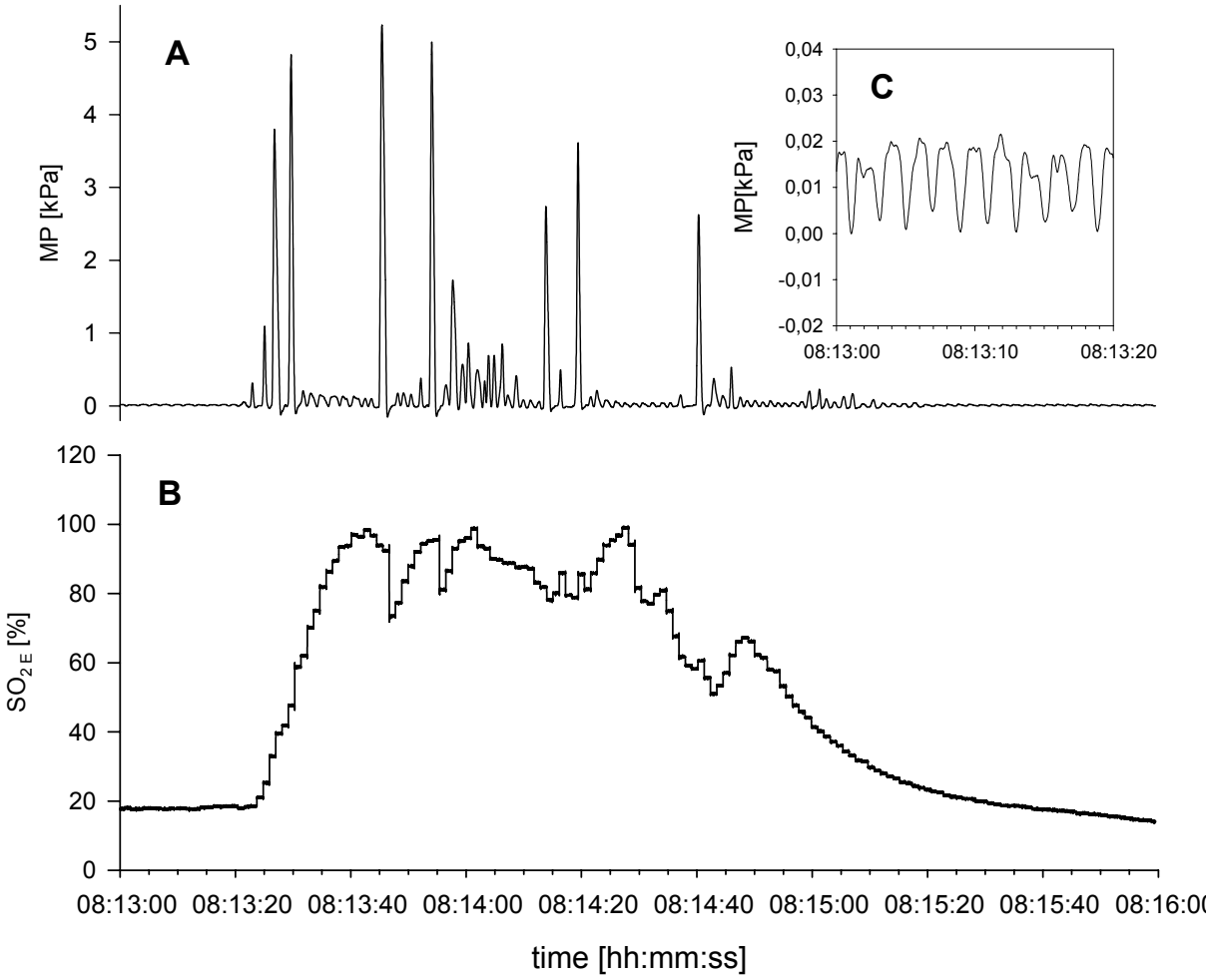
A
B
C
MP [kPa]
MP[kPa]
SO_{2E} [%]
time [hh:mm:ss]
08:13:00
08:13:10
08:13:20
08:13:40
08:14:00
08:14:20
08:14:40
08:15:00
08:15:20
08:15:40

Figure 2

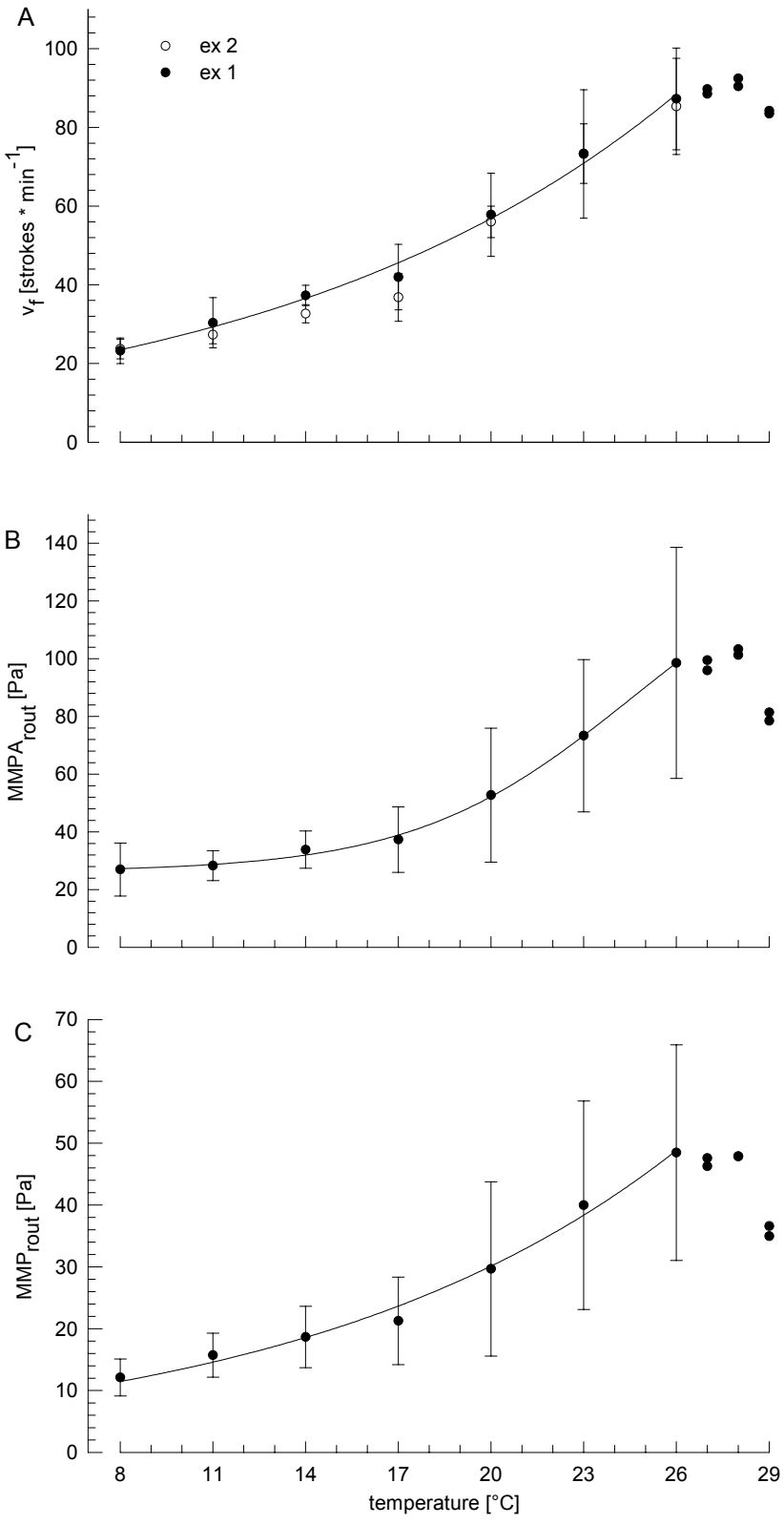
A
ex 2
ex 1
v_f [strokes * min^{-1}]
B
$MMPA_{rout}$ [Pa]
C
MMP_{rout} [Pa]
temperature [°C]

Figure 3

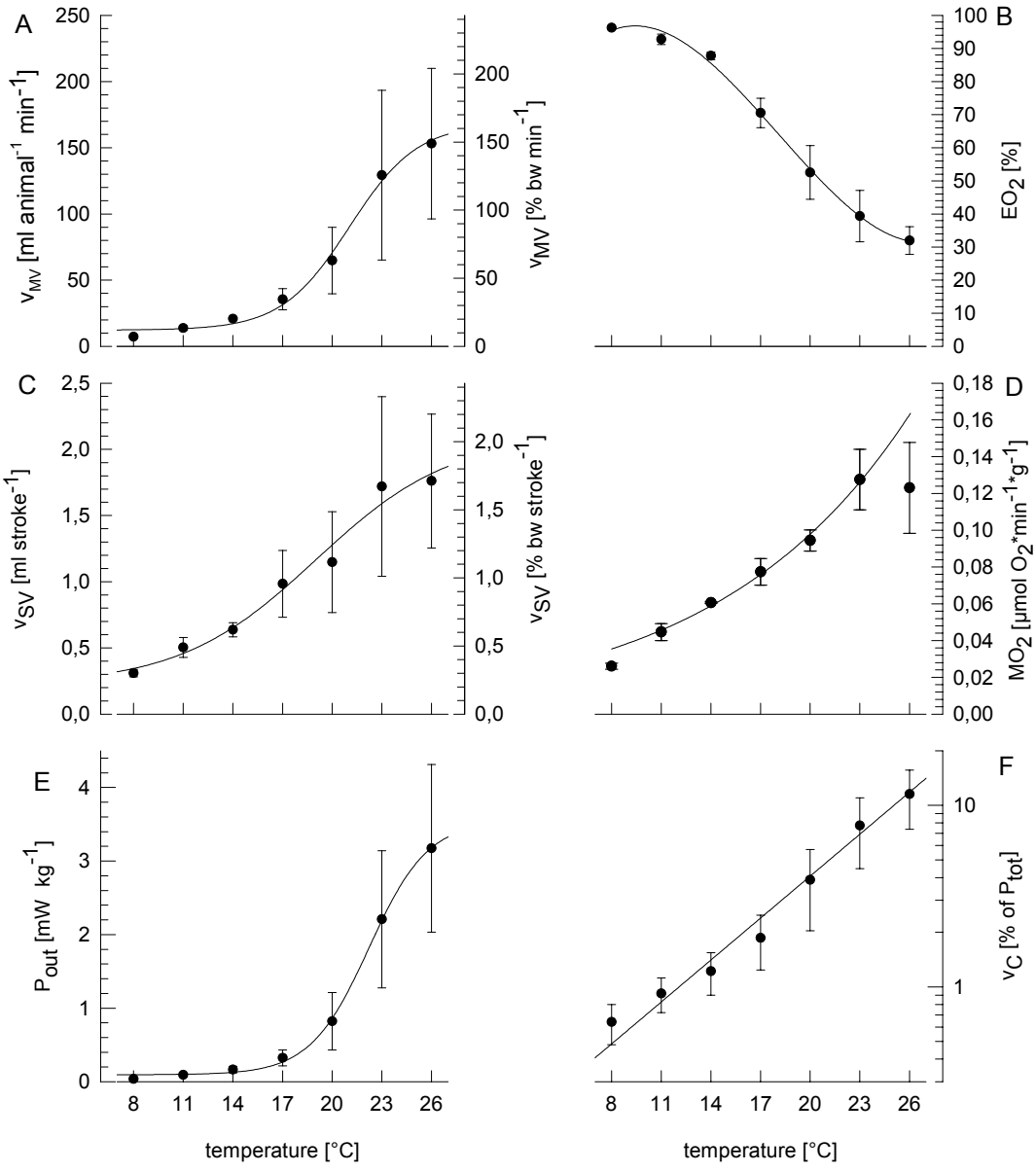
A
B
C
D
E
F
v_{MV} [ml animal^{-1} min^{-1}]
v_{MV} [% bw min^{-1}]
EO_2 [%]
v_{SV} [ml stroke^{-1}]
v_{SV} [% bw stroke^{-1}]
MO_2 [µmol O_2*min^{-1}*g^{-1}]
P_{out} [mW kg^{-1}]
v_C [% of P_{tot}]
temperature [°C]
temperature [°C]

Figure 4

Allometry of thermal limitation in the cephalopod *Sepia officinalis*

Frank Melzner*, Christian Bock, Hans – O. Pörtner

Alfred Wegener Institute for Marine and Polar Research, Am Handelshafen 12, 27570 Bremerhaven, Germany

short title: thermal limitation in cuttlefish

key words: cephalopoda, oxygen consumption, skin respiration, oxygen limitation, aerobic scope

* Author to whom correspondence should be adressed:
phone: +49-471-4831-1331; fax: +49-471-4831-1149;
email: fmelzner@awi-bremerhaven.de

Abstract

Cuttlefish *Sepia officinalis* routine metabolic rate was determined in response to acute thermal changes at a rate of 1°C h^{-1} for a variety of animal sizes (15 – 496 g wet mass). In a thermal frame of 11 to 23°C, oxygen consumption rates (MO_2, in μmol O_2 g^{-1} min^{-1}) were observed to rise with increasing temperature (T, in °C) and to decline with increasing body mass (m, in g), according to the formula: ln MO_2 = -3.3 + 0.0945T – 0.215 ln m (R^2 = 0.93). Outside the above thermal window, animals were not able to increase MO_2 at similar rates, indicating a beginning oxygen limitation of metabolism. Large animals (>100 g body mass) already displayed lower than expected MO_2 values at 8 and 26°C, while smaller animals (15 g wet mass) were characterized by a wider thermal window (MO_2 values deviated from expected rates at 5 and 29°C).

Morphometric data of cuttlefish mantle skin area was obtained to discuss size - related effects of skin respiration potential on thermal tolerance. Cuttlefish growth was observed to be isometric, as constant 'Vogel numbers' of 4.2 indicated (animal body masses: 11 to 401 g). In the same mass range, specific mantle surface area declined three - fold from 10.7 (0.24) (means ±SD) to 3.3 (0.52) cm^2 g^{-1}. Thus, increased thermal tolerance in smaller animals may be enabled by a higher skin respiration potential due to higher specific skin surface areas. An elevated fraction of MO_2 provided by means of skin respiration in small animals could relieve the cardiovascular system, which previously has been found a major limiting component during acute thermal stress in cuttlefish.

1. Introduction

Fitting the emerging picture of an oxygen limitation of thermal tolerance in marine ectothermic animals (Pörtner et al. 2004), we could recently demonstrate that cuttlefish (*Sepia officinalis*; Mollusca, Cephalopoda) metabolism is constrained by oxygen supply at extremely low and high temperatures (Melzner, Bock, Pörtner, submitted 1,2). This became evident through *in vivo* ^{31}P - NMR spectroscopy measurements which revealed a progressive transition to an anaerobic mode of energy production in mantle muscle tissues of resting animals (100g body mass, reared at 15.0°C) beyond temperatures of 26.8 and 7.0 °C, respectively. Prior to the onset of anaerobic metabolism (between 23 and 26°C or 11 and 8°C, respectively), oxygen consumption rates deviated significantly from the expected exponential relationship of MO_2 vs. temperature.

In the present study, we investigated oxygen consumption rates of cuttlefish ranging between 15 and 495 g body mass. We analysed, whether (1) deviations from an exponential relationship between MO_2 and temperature typically occur close to thermal limits (both in the warm and in the cold) over a wide range of body masses. We also evaluated, whether (2) oxygen limitation is influenced by body size, such that putative deviations from the exponential change in metabolic rate occur at similar temperatures in the different mass groups studied, and whether (3) the thermal response of metabolism, reflected in the slope of ln MO_2 vs. temperature, differs between mass groups. Another goal was the establishment of a regression model to explain MO_2 variability in relation to animal body mass and water temperature in order to accurately predict routine metabolic rates. Furthermore, we investigated whether (4) the specific mantle surface area available for skin respiration changes with body mass (between 11 and 400g body mass). This should allow to estimate the contribution of skin respiration to total oxygen uptake and its influence on whole animal aerobic scope for temperature dependent survival in cuttlefish.

2. Material and Methods

Four groups of animals were used in this study between August 2002 and August 2003. All animals originated from eggs trawled in the Bay of Seine (France) in May 2002. They were raised in our aquaculture facilities at constant temperature (15.0°C ±0.1°C), salinity (32 – 33‰) and pH (> 8.0) (see table 1 for group composition and body masses of experimental animals).

Respiration analyses were conducted in an intermittent flow respirometer (groups 2 - 4) (Melzner, Bock, Pörtner, submitted b) or in a flow-through respirometer (group 1) as used by De Wachter et al. (1997). In both cases, respiration rates were corrected for bacterial respiration. Initially, animal respiration was analysed in both respirometers, differences between methods resulted below 5 % of MO_2 values. Experimental protocols and water quality maintenance systems exactly resembled those of our previous investigation (Melzner, Bock, Pörtner, submitted 1,2). Briefly, 24h starved animals were transferred and acclimated to the respirometers for at least 24 hours at T = 15°C. On the following day, the water was cooled to 8 or 5°C, brought back to control temperatures over night and warmed to 26 or 29°C on the third experimental day. Average rates of temperature change were 1°C h^{-1}, temperature steps maintained for 2 h each were 5, 8, 11, 14, 17, 20, 23, 26, 29°C. Animals from group one were subjected to all experimental temperatures, those of groups two and four to temperatures between 8 and 26°C, while group three animals were exposed to temperatures between 17 and 26°C exclusively. Heating or cooling to a given temperature was achieved within 1 hour, leaving two hours for repeated measurements in the intermittent flow respirometer (two to three runs of 20 to 40 minutes) or two hours of continuous measurement in the flow through system.

Morphometric data were obtained for two laboratory-raised groups of animals originating from the same population as those used for oxygen consumption measurements. Data were collected for different animal sizes between 11.4 g and 400.8 g body wet mass following standard taxonomic measurement protocols (see O'Dor and Hoar, 2000). Mantle surface area was estimated by measuring mantle circumference and mantle width at 5 known positions along the mantle's longitudinal axis. Digital images of the respective animals were used to interpolate circumferences between measurement points. Subsequently, the outer surface area of the mantle was obtained by integration. Inner surface areas were calculated as outer surface areas minus the areas covered by the cuttlebones.

Fin area was calculated from direct measurements of fin width in combination with photograph analysis. All digital photography analysis was performed using public domain NIH Image software (source: http://rsb.info.nih.gov/nih-image). Total mantle area was calculated as the sum of outer and inner mantle surface area and two times fin surface area. Specific surface area was taken as a measure for skin respiration potential and calculated as total mantle area divided by total mantle mass. Following the rationale of O'Dor and Hoar (2000), differences in mantle muscle organ geometry between the two mass groups were compared using dimensionless ‚Vogel numbers'. These were calculated for the mantle muscle organ:

$$V_M = Ma^{1/2} / Mv^{1/3} \quad (1)$$

with V_M = Vogel number for the mantle organ, Ma = mantle organ skin area, Mv = mantle organ volume, converted from mantle mass, using a density of 1023 kg m^{-3} for cuttlefish muscle (Denton and Gilpin - Brown 1961).

Statistical analyses were carried out using STATISTICA software. Linear regression analysis was performed with ln MO_2 vs. temperature data. ANCOVA was carried out (independent variable: mass group, dependent variable: ln MO_2, covariable: temperature), following a test for heterogeneity of slopes. MO_2 values at extreme temperatures were compared to expected MO_2 values (by interpolating regression lines) with t-tests. Further, a two – factorial linear regression model was constructed, with ln mass and temperature explaining ln MO_2 variability.

3. Results

Figure 1a displays oxygen consumption rates vs. temperature for three size groups of animals (group one, 15g, group two, 105 g, and group four, 494.5 g). Significant linear regressions of ln transformed MO_2 data were obtained between 11 and 23°C for all mass groups. A test for heterogeneity of slopes confirmed that slopes did not differ significantly from each other ($F_{(4,55)}$ = 0.377; $p<0.83$). Thus, regardless of animal body mass, MO_2 increased at a rate of 9.5 – 9.9% $°C^{-1}$ in the respective temperature interval (corresponding to Q_{10} values of 2.5 – 2.6). Extending these regressions to extreme temperatures (5-8°C and 26-29°C) and comparing expected MO_2 values

(MO_{2exp}) to measured MO_2 values ($MO_{2\ meas}$) revealed significant differences in all mass groups studied (see table 2): In larger animals (grous 2 and 4, >100g), MO_2 values measured are significantly lower than those expected according to the elongated regression at both, exteme high and low temperatures (8 and 26°C). In contrast, the smallest animals (group 1, 15g) could still maintain expected rates of oxygen consumption at 8 and 26°C, but showed significantly decreased MO_2 values at 5 and 29°C.

Statistical analysis revealed a significant effect of body mass on oxygen consumption (ANCOVA; independent variable: mass group, dependent variable: ln MO_2, covariable: temperature; temperature interval 11 – 23°C; $F_{(4,59)}$=169; $p<0.001$). As temperature dependent slopes of ln MO_2 did not differ between mass groups, it directly followed that there is a temperature independent effect of body mass on oxygen consumption. Therefore, all oxygen consumption values for each animal were normalized to a common temperature of 0° C (using the regression equations obtained in fig 1a) and averaged to evaluate mass effects on oxygen consumption rates. A subsequent linear regression analysis of ln MO_2 vs. ln body mass yielded a significant relationship (see fig 1b) with a mass coefficient (= slope) of 0.785. Regressing ln MO_2 per unit body mass against ln body mass yielded a significant result with a slope of –0.215 (fig 1b).

Combining both temperature and mass effects on oxygen consumption rates in a single regression resulted in a two factorial linear model that could explain 93% of observed variability in MO_2:

$$\ln MO_2 = -3.3 + 0.0945\ T - 0.215 \ln m \quad (R^2 = 0.93;\ F_{(2,74)} = 492;\ p<0.001) \qquad (2)$$

With ln MO_2 = oxygen consumption rate in μmol O_2 g^{-1} min^{-1}, m = body mass in g, T = temperature in °C.

Table 3 displays morphometric parameters for two mass groups of cuttlefish raised at 15°C. Mantle mass constituted a constant fraction of total body mass (36 – 37%), at both low (11 g mean) and high (401 g mean) body mass. Although the mantle became slightly elongated in relation to width with increasing body size (a pattern also reflected in cuttlebone morphology, Table 3), mantle surface area only increased by a factor of 10.5, while mass increased 35 fold. Thus, mass-specific mantle

surface area declined three fold from 10.7 to 3.3 cm^2 g^{-1} mantle tissue between 11 and 401 g. Dimensionless ‚Vogel numbers' of 4.18 and 4.20 for small and big animals, respectively, indicate an isometric mode of growth for the cuttlefish mantle muscle organ in the mass range investigated (Vogel 1994, O'Dor and Hoar 2000).

4. Discusson

To our knowledge, the present study is the first to relate both body mass and acute exposure to a wide range of temperatures to oxygen consumption rates in a cephalopod species. The experimental animals used in this study originated from the same laboratory raised population and were kept at a constant temperature regime. This is probably important, as acclimation to a given temperature regime has been shown to influence tissue mitochondrial densities, and thus standard metabolic rate, in both ectothermic vertebrates (Sidell 1980, Egginton and Sidell 1989) and invertebrates (Sommer and Pörtner 2002). Low variability in MO_2 values encountered in our experiments likely is the consequence of controlled laboratory rearing conditions. Oxygen consumption values obtained in our study represent routine metabolic rates (rmr, Fry 1947) rather than standard metabolic rate (smr), as we could find that experimental animals typically spent roughly 1 - 3% of the experimental time performing high pressure mantle contractions (spontaneous activity), which, due to their high pressure amplitude, comprised 20 – 30% of total ventilation costs (Melzner, Bock, Pörtner, submitted 1).

Interestingly, a similar level of spontaneous activity has recently been documented for a tropical cuttlefish species in its natural habitat (*S. apama* was found to be active during approximately 3% of a days time; Aitken et al. 2005).

Typically, relationships between MO_2 and body mass follow a power formula, i.e. $MO_2 = am^b$, with m = bodymass, a and b being constants (Peters 1983). At present, there is only one other study available relating cuttlefish body mass to oxygen consumption. Johansen and coworkers (1982) obtained a regression for *S. officinalis* animals caught from the English Channel and combined those with measurements of hatchlings raised in the laboratory. Their mass exponent of b = 0.913 deviates from the one obtained in our study. The authors stated that by omitting the small animals from their

regression, they obtained b = 0.771, which comes closer to our value. However, variability in Johansen et al.'s (1982) MO_2 values is high and the effects of different (and, likely, unknown) acclimation temperatures may have influenced metabolic rates and thus, slopes of regression lines. Typical mass exponents for other cephalopods range from b = 0.61 to above 1, but, again, most studies have been performed on cephalopods caught in the wild which implies an unknown temperature and feeding regime (see Wells and O'Dor 1987 for a review). Our mass exponent b does not deviate significantly from the b = 0.75 found empirically for a variety of ectothermic invertebrates and vertebrates (Hemmigsen 1960). Such a mass exponent of 3/4 has recently been predicted to reflect a unifying principle for all living organisms on the basis of fractal geometric considerations (i.e. West et al. 1997, 1999).

Between 11 and 23°C, oxygen consumption rates increased exponentially at the same rate in all three mass groups examined, corresponding to Q_{10} values of 2.5 – 2.6 which fit previous studies on cephalopod metabolic rate (O'Dor and Wells, 1987). At extreme temperatures of 8 and 26°C in specimens with a body mass of 105 g, we could recently relate deviations from the MO_2 regression to the onset of oxygen limitations. *In vivo* ^{31}P - NMR spectroscopy measurements revealed that deviations from the normal Q_{10} relationship were early signs of a progressive switch to an anaerobic mode of energy production (Melzner, Bock, Pörtner, submitted a). Apparently, a similar pattern of lower than expected oxygen consumption rates at thermal extremes is present over the whole investigated mass range. While the chosen temperature steps of 3°C could not resolve putative differences between mass groups of 100 g and above, 15 g animals could adjust oxygen consumption according to Q_{10} up to a higher temperature of 26°C. This trend is also present at low temperatures, albeit less pronounced. A high standard deviation encountered at 8°C in the 15g mass group may mask the onset of a progressive deviation from the linear regression. Overall, these patterns indicate a wider thermal window at small body sizes.

Interestingly, Johansen et al. (1982) found small *S. officinalis* (0.12 – 1.5 g) to be more hypoxia tolerant than larger ones (100 g and greater). Smaller animals were able to regulate oxygen uptake down to water PO_2s of about 5.3 kPa (40 mm Hg), whereas larger specimens displayed a critical PO_2 of about 9.3 kPa (70 mm Hg). Similar results were obtained by De Wachter et al. (1988)

who found a positive linear relationship between critical water oxygen partial pressures and log wet mass in juvenile *S. officinalis* (0.2 – 154 g bodymass). It thus appears that smaller sized cuttlefish are able to extract ambient oxygen and cover their oxygen demand down to lower ambient oxygen levels. This improves their hypoxia tolerance. At the same time smaller individuals display elevated metabolic capacity (aerobic scope) which allows them to resist longer to the thermally induced development of functional (internal) hypoxia at extreme temperatures (Pörtner et al., 2004). In fact, *S. officinalis* juveniles from the English Channel are exclusively found in shallow coastal waters, which are subject to higher fluctuations in temperature and oxygen content than the deeper water habitats of larger animals (Boucaud-Camou and Boismery 1991).

Wells (1992) could demonstrate that cephalopod heart size (and, likely, cardiac output) scales with a mass exponent of 0.9, which clearly reflects adaptation to the elevated routine metabolic rates of smaller animals. But would circulatory adaptations also provide smaller animals with additional aerobic scope for survival of more extreme hypoxic or thermal challenges than their larger conspecifics? Eno (1994) found relatively high gill diffusion capacities in hatchling cuttlefish (0.5 ml O_2 min^{-1} $Torr^{-1}$ kg^{-1}, approximately 10 times above those that of 40 - 1000 g *Octopus vulgaris*), but data on larger animals does not exist. Skin respiration certainly also has to be taken into account. No *in vivo* measurements on *S. officinalis* skin respiration have been performed. Available estimates of skin respiration between 8 - 41% of total MO_2 for *Octopus vulgaris* (Madan and Wells 1996, *in vitro* and *in vivo* measurements) or 18 – 58% for squid *Illex illecebrosus* mantle muscle at rest (Pörtner 1994, theoretical analysis based on blood gas transport data) may indicate the general importance of skin respiration in cephalopods. Thus a decrease in surface area associated with increasing body mass likely contributes to the reduction in whole animal aerobic scope. We have shown in previous publications (Melzner, Bock, Pörtner, submitted 1, 2) that close to thermal limits, the circulatory system of *S. officinalis* fails to provide sufficient oxygen to tissues.

In fish, skin respiration predominates in early ontogenetic stages, but progressively loses importance as gill gas exchange becomes more efficient and mass-specific skin surface area declines (i.e. Rombough and Ure 1991, Wells and Pinder 1996). Furthermore, Rombough and Moroz (1997) found fish larvae to be characterized by excess diffusive oxygen exchange capacity (mainly due to

high specific skin area) and postulated that larvae should therefore be less affected by ambient hypoxia than adult specimens. O'Dor and Hoar (2000) calculated that fish (cod, *Gadus morhua*) grow isometrically, reflected in decreasing specific skin surface areas with increasing mass. Squid grow allometrically, as rising ‚Vogel numbers' indicate. However, O'Dor and Hoar's conclusion that squid skin surfaces would grow ‚faster' than body volumes needs to be specified. Below a certain positive slope in ‚Vogel number' increase with body volume, specific surface area declines with increasing tissue volume although growth is positively allometric. Whether the slope found for squid was high enough to support their conclusions remains to be demonstrated (see their fig. 4b). In contrast, we could demonstrate that *S. officinalis* mass-specific mantle surface area declined threefold from small to large animals (11 to 401 g total body wet mass, table 2). Using *in vitro* skin respiration data (Madan and Wells, 1996, *Sepia orbignyana* skin samples measured at T = 22°C) as well as mantle surface areas (table 2) and routine metabolic rates for 11 and 400 g wet mass *S. officinalis* (22°C using equation (1)), it is possible to roughly estimate the minimum fraction of total MO_2 taken up by mantle skin surfaces. Accordingly, 11 g animals could potentially take up 21%, 400 g animals 14% of their respective routine MO_2 through mantle skin alone (contributions of other skin surfaces on arms and head not even considered). *In vitro* skin respiration data used for our calculation may be low estimates, as Madan and Wells (1996) could also demonstrate, that *in vivo* skin respiration in *O. vulgaris* was 2 –3 times higher than *in vitro* estimates. Nonetheless, these model calculations suggest that smaller animals likely cover a higher fraction of MO_2 through skin respiration than larger specimens, potentially alleviating the work load of the main blood circulation system and contributing to a higher aerobic scope in smaller sized animals.

Calculated ‚Vogel numbers' suggest that cuttlefish mantle muscle organ growth is isometric, thus obeying the rules of conventional Euclidean geometrics (surface growth to the 2nd power, volume growth to the 3rd). Based on such considerations (and constant Vogel numbers of 4.2) we would expect specific mantle skin surface area to range between 37.5 cm^2 per g mantle tissue in hatchling animals with a mantle organ mass of 0.1 g and 1.8 cm^2 per g mantle tissue in a full grown animal with 800 g mantle mass, giving a factorial scope for mass-specific mantle skin area of 20 over the lifecycle of a typical English Channel *S. officinalis*. These figures illustrate the potential that may

exist for variable degrees of partitioning of oxygen uptake between gill and skin respiration during ontogeny and their possible implications for metabolic scope for growth, activity or survival in general.

In conclusion, by employing a two factorial regression model, we could explain most of the variabililty (93%) in routine metabolic rate of 15°C laboratory raised *S. officinalis* by variability in body mass and effects of acute temperature change within a temperature window of 11 – 23°C. Deviations from exponential relationships of MO_2 with body mass are characteristic for all mass groups outside this temperature envelope, with smaller animals apparently being characterized by a wider temperature window, especially on the warm side of the thermal envelope. Mass-specific mantle skin area declines rapidly with increasing body mass and a larger fraction of whole animal MO_2 may be supplied by skin respiration in smaller animals, thereby contributing to higher aerobic scopes for survival which are key in supporting the wider thermal windows seen in smaller individuals.

5. Acknowledgements

This study was carried out in support of the project: The cellular basis of standard and active metabolic rate in the free-swimming cephalopod, *Sepia officinalis* (NERC Grant PFZA/004). The authors wish to thank Timo Hirse for excellent technical support, Raymond and Marie - Paule Chichery (Université de Caen) for providing cuttlefish eggs in 2002 and 2003 and all student helpers that were engaged in raising the animals in our lab

6. References:

AITKEN, J. P., O'DOR, R. K. AND JACKSON, G. D (2005). The secret life of the giant cuttlefish *Sepia apama* (Cephalopoda): Behaviour and energetics in nature revealed through radio acoustic positioning and telemetry (RAPT). *J. Exp. Mar. Biol. Ecol.* **320**, 77-91.

BOUCAUD-CAMOU, E. AND BOISMERY, J. (1991). The migration of the cuttlefish (*Sepia officinalis* L.) in the English Channel. In Boucaud-Camou, E. (Ed.), La Seiche, 1st International symposium on the cuttlefish *Sepia*. Center of publications , Universite de Caen. Pp.179-189.

DENTON, E.J. AND GILPIN-BROWN, J.B. (1961). The buoyancy of the cuttlefish, *Sepia officinalis* (L.). *J. mar. Biol. Ass. U.K.* **41**, 319-342.

DE WACHTER, B., WOLF, G., RICHARD, A. AND DECLEIR, W. (1988). Regulation of respiration during juvenile development of *Sepia officinalis* (Mollusca: Cephalopoda). *Mar. Biol.* **97**, 365-371

DE WACHTER, B., SARTORIS, F.J. AND PÖRTNER, H.O. (1997). The anaerobic endproduct lactate has a behavioural and metabolic signalling function in the shore crab *Carcinus maenas*. *J. Exp. Biol.* **200**, 1015-1024

EGGINTON, S. AND SIDELL, B.D. (1989). Thermal acclimation of subcellular structure of fish muscle. *Am. J. Phys.* **256**, R1-R10.

ENO, C. N. (1994). The morphometrics of cephalopod gills. *J. mar. Biol. Ass. U.K.* **74**, 687-706.

FRY, F.E.J. (1947). Effects of the environment on animal activity. *University of Toronto Studies Biology Series* **55**, 1-62.

HEMMIGSEN, A.M. (1960). Energy metabolism as related to body size and respiratory surfaces, and its evolution. *Rep. Steno Mem. Hosp. And Nordisk Insulin Laboratorium*. **9**, 6-110.

JOHANSEN, K., BRIX, O., KORNERUP, S. AND LYKKEBOE, G. (1982). Factors affecting O_2-uptake in the cuttlefish, *Sepia officinalis*. *J. mar. Biol. Ass. U.K.* **62**, 187-191.

MADAN, J.J. AND WELLS, M.J. (1996). Cutaneous respiration in *Octopus vulgaris*. *J. Exp. Biol.* **199**, 2477-2483.

MELZNER, F., BOCK, C. AND PÖRTNER, H.O. Critical temperatures in the cephalopod *Sepia officinalis* investigated using *in vivo* ^{31}P NMR spectroscopy, *J. Exp. Biol.*, submitted a.

MELZNER F., BOCK C. AND PÖRTNER, H.O. Temperature dependent oxygen extraction from the ventilatory current and the costs of ventilation in the cephalopod *Sepia officinalis*. *J. Comp. Physiol.* B, submitted b.

O'DOR, R.K. AND WELLS, M.J. (1987).Energy and nutrient flow. In: Boyle, P.R. (Ed.), *Cephalopod life cycles, Comparative reviews (Vol 2).* Academic Press, London, pp. 1009-133.

O'DOR, R.K. AND HOAR, J.A. (2000). Does geometry limit squid growth? *ICES J. Mar. Sci.* **57**, 8-14.

PETERS, R.H. (1983). *The ecological implications of body size*. Cambridge University Press, Cambridge. 329 pp.

PÖRTNER, H.O. (1994). Coordination of Metabolism, acid-base regulation and haemocyanin function in cephalopods. In *Physiology of Cephalopod Molluscs: Lifestyle and Performance*

Adaptations, eds. H.O. Pörtner R. K. O'Dor and D. L. Macmillan, pp. 131-148. Basel: Gordon and Breach.

PÖRTNER, H.O., MARK, F.C. AND BOCK, C. (2004). Oxygen limited thermal tolerance in fish? Answers obtained by nuclear magnetic resonance techniques. *Respir. Physiol. Neurobiol.* **141**, 243-260.

ROMBOUGH, P.J. AND URE, D. (1991) Partitioning of oxygen uptake between cutaneous and branchial surfaces in young chinook salmon *Oncorhynchus tshawytscha*. *Physiol. Zool.* **64**, 717-727.

ROMBOUGH, P.J. AND MOROZ, B.M. (1997). The scaling and potential importance of cutaneous and branchial surfaces in respiratory gas exchange in larval and juvenile walleye *Stizostedion vitreum*. *J. Exp. Biol.* **200**, 2459-2468.

SIDELL, B.D. (1980). Response of goldfish (*Carassius auratus* L.) muscle to acclimation temperature: alterations in biochemistry and proportions of different fiber types. *Physiol. Zool.* **53**, 98-107.

SOMMER, A. AND PÖRTNER, H.O. (2002). Metabolic cold adaptation in the lugworm *Arenicola marina*: a comparison of a North Sea and a White Sea population. *Mar. Ecol. Prog. Ser.* **240**, 171-182.

VOGEL, S. (1994). *Life in moving fluids*. Second edition. Princeton, NJ: Princeton University Press. 467 pp.

WELLS, M.J. (1983). Circulation in cephalopods. In: Wilbur, K.M. (Ed.), The Mollusca. Physiology Vol 2. Academic Press, London, pp. 239 – 290.

WELLS, M.J. (1992). The cephalopod heart: The evolution of a high performance pump. *Experientia*. **48**, 800-808.

WELLS, P.R. AND PINDER, A.W. (1996). The respiratory development of Atlantic salmon. 2. Partitioning of oxygen uptake among gills yolk sac and body surfaces. *J. Exp. Biol.* **199**, 2737-2744.

WEST, G.B., BROWN, J.H. AND ENQUIST, B.J. (1997). A general model for the origin of allometric scaling laws in biology. *Science*. **276**, 122-126.

WEST, G.B., BROWN, J.H. AND ENQUIST, B.J. (1999).The fourth dimension of life: fractal geometry and allometric scaling of organisms. *Science*. **284**, 1677-1679.

Figure caption:

Figure 1. (A): Respiration rates of size groups 1, 2 and 4 (g1, 15 g, g2, 105 g, g4, 494.5 g) vs. temperature. Regressions are valid for temperatures 11 to 23°C, but were extended to illustrate deviations outside the analysed temperature window. Group 3 is not included, as measurements were only performed between 17 and 26°C. (B) ln MO_2 vs. mass for all 17 animals studied. Respiration rates for each animal were normalized to a temperature of 0°C, using regressions obtained in fig 1a. Regression equations give standard errors for mass exponents (in brackets).

Table 1. Experimental animal masses and temperature ranges investigated.

group	*Mass [g] (SD)*	*T range [°C]*	*n*
1	15.0 (4.6)	5 – 29	5
2	105.0 (7.0)	8 – 26	4
3	238.0 (28.0)	17 – 26	4
4	495.0 (157.0)	8 – 26	4

Table 2. Deviations from expected rates of oxygen consumption. Observed oxygen consumption rates ($MO_{2\,obs}$) were compared with expected rates of oxygen consumption ($MO_{2\,exp}$, as determined using exponential regressions in fig 1). Standard deviations (SD) were assumed to be comparable between observed and expected MO_2. $p < 0.05$ (bold) indicates significant differences between observed and expected MO_2 (t-tests).

group	*temperature*	*$MO_{2\,obs}$*	*SD*	*$MO_{2\,exp}$*	*p*
1	**5**	**0.005**	**0.009**	**0.039**	**<0.001**
1	8	0.038	0.015	0.05	<0.12
1	26	0.229	0.057	0.234	<0.46
1	**29**	**0.207**	**0.068**	**0.303**	**<0.03**
2	**8**	**0.026**	**0.002**	**0.035**	**<0.001**
2	**26**	**0.123**	**0.025**	**0.163**	**<0.04**
4	**8**	**0.015**	**0.003**	**0.022**	**<0.005**
4	**26**	**0.086**	**0.009**	**0.111**	**<0.003**

Table 3: Morphometric differences between small and large *S. officinalis* raised at 15°C.

TM = total body wet mass; M = mantle; CB = cuttlebone; ML = dorsal mantle length; Mv = mantle muscle organ volume (not cavity volume); Ma = mantle organ surface area (including fin surface area). Specific mantle area = mantle area (including fin area) divided by mantle (including fins) wet mass. See text for the calculation of dimensionless ‚Vogel numbers'; n = 9 small and n = 7 big animals used for comparisons; n = 5 animals from each group for surface area calculation and derived ‚Vogel number'.

Parameter	*Small animals*	*SD*	*Big animals*	*SD*	*Factorial change*
TM [g]	11.38	1.43	400.7	115.6	35.2
Total length [cm]	5.97	0.29	20.9	2.42	3.5
M mass [g]	4.31	0.69	144.2	39.2	33.5
M length [cm]	3.94	0.18	15.72	2.34	4.0
M thickness [cm]	0.23	0.02	0.73	0.08	3.1
Fin width [cm]	0.46	0.04	2.19	0.51	4.8
CB length [cm]	3.76	0.22	14.95	2.10	4.0
CB width [cm]	1.58	0.07	5.59	0.77	3.5
CB length / CB width	2.38	0.07	2.68	0.12	1.12
Gill mass [% of TM]	1.12	0.08	0.90	0.14	0.81
Gill length [% of ML]	37.3	2.3	34.6	2.5	0.93
M mass [% of TM]	37.7	2.0	36.3	3.8	0.96
M thickness [% of ML]	5.9	0.4	4.7	0.3	0.79
Ma [cm^2]	45.89	1.88	480.3	71.7	10.5
Specific Ma [$cm^2\ g^{-1}$]	10.7	0.24	3.3	0.52	0.31
V_M [$Ma^{1/2}$ / $Mv^{1/3}$]	4.18	0.06	4.20	0.20	0.995

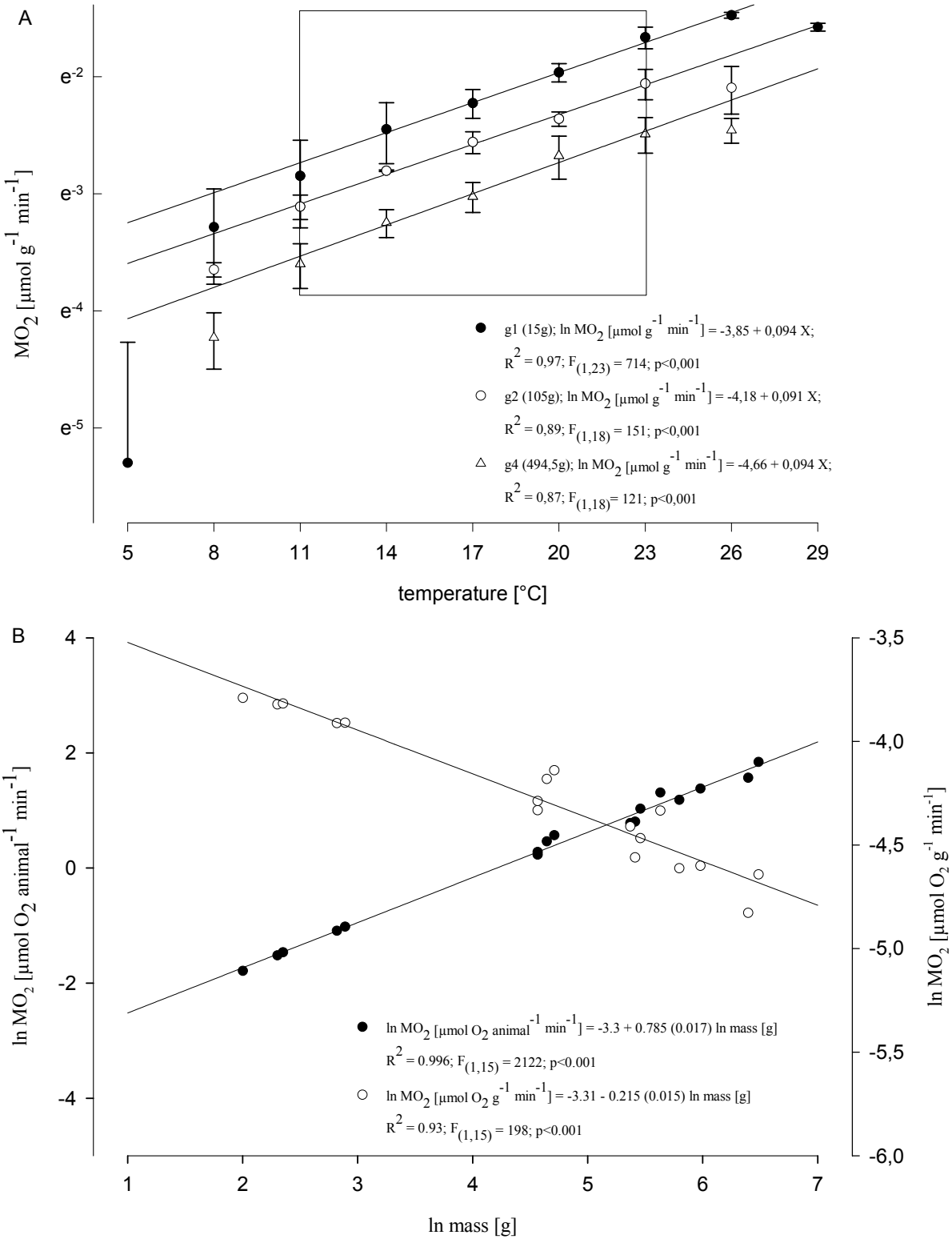
A
e-2
e-3
e-4
e-5
MO2 [µmol g-1 min-1]
g1 (15g); ln MO2 [µmol g-1 min-1] = -3,85 + 0,094 X;
R2 = 0,97; F(1,23) = 714; p<0,001
g2 (105g); ln MO2 [µmol g-1 min-1] = -4,18 + 0,091 X;
R2 = 0,89; F(1,18) = 151; p<0,001
g4 (494,5g); ln MO2 [µmol g-1 min-1] = -4,66 + 0,094 X;
R2 = 0,87; F(1,18)= 121; p<0,001
5 8 11 14 17 20 23 26 29
temperature [°C]
B
ln MO2 [µmol O2 animal-1 min-1]
ln MO2 [µmol O2 g-1 min-1]
ln MO2 [µmol O2 animal-1 min-1] = -3.3 + 0.785 (0.017) ln mass [g]
R2 = 0.996; F(1,15) = 2122; p<0.001
ln MO2 [µmol O2 g-1 min-1] = -3.31 - 0.215 (0.015) ln mass [g]
R2 = 0.93; F(1,15) = 198; p<0.001
4 2 0 -2 -4
-3,5 -4,0 -4,5 -5,0 -5,5 -6,0
1 2 3 4 5 6 7
ln mass [g]

Figure 1

Coordination between ventilatory pressure oscillations and venous return in the cephalopod *Sepia officinalis* under control conditions, spontaneous exercise and recovery.

Frank Melzner*, Christian Bock, Hans – O. Pörtner

Alfred Wegener Institute for Marine and Polar Research, Am Handelshafen 12, 27570 Bremerhaven, Germany

short title: circulation and ventilation in cuttlefish

key words: cephalopoda, blood flow, venous return, anterior vena cava, mantle pressure, ventilation, exercise, MRI

* Author to whom correspondence should be adressed:
phone: +49-471-4831-1331; fax: +49-471-4831-1149;
email: fmelzner@awi-bremerhaven.de

Abstract

Venous blood flow was measured for the first time in a cephalopod. Blood velocity was determined in the anterior vena cava (AVC) of cuttlefish *S. officinalis* with a Doppler – probe, while simultaneously, ventilatory pressure oscillations were recorded in the mantle cavity. In addition, magnetic resonance imaging (MRI) was employed to investigate pulsatile flow in other major vessels. Blood pulses in the AVC are obligatorily coupled to ventilatory pressure pulses, both in frequency and phase. AVC average maximum blood velocity ($AVC_{av\ max\ V}$) in animals of 232 (±30 SD) g wet mass at 15°C was found to be 14.2 (±7.1) cm s^{-1}, AVC stroke volume (AVC_{SV}) was 0.2 (±0.1) ml $stroke^{-1}$, AVC minute volume (AVC_{MV}) amounted to 5.5 (±2.8) ml min^{-1}. Intense exercise bouts of 1-2 min resulted in factorial increases of 2.2 in AVC_{MV}, enabled by 1.6 fold increments in both, AVC pulse frequency (AVC_f) and $AVC_{av\ max\ V}$. As increases in blood flow occurred delayed in time by 1.7 min with regard to exercise periods, we concluded that it is not mantle cavity pressure conveyance that drives venous return in this cephalopod blood vessel. However, during jetting at high pressure amplitude (>1 kPa), AVC blood flow and mantle cavity pressure pulse shapes completely overlap, suggesting that under these conditions, blood transport must be driven passively by mantle cavity pressure. MRI measurements at 15°C also revealed that under resting conditions, AVC_f and ventilation frequency (v_f) match at 31.6 (±2.1) strokes min^{-1}. In addition, rates of pulsations in the cephalic artery and in afferent branchial vessels did not significantly differ from AVC_f and v_f. It is suggested that these adaptations are beneficial for high rates of oxygen extraction observed in *S. officinalis* and the energy conserving mode of life of the cuttlefish ecotype in general.

1. Introduction

Extant cephalopods lead an expensive mode of life when compared to other marine invertebrates and even to teleosts (Wells 1994). High levels of energy turnover result, which are supported by high performance levels in all physiological systems including blood circulation. Little is known about the regulation of the circulatory system in general and blood flow in cephalopod molluscs in particular. Only two studies were successful to quantify blood flow in a major cephalopod blood vessel *in vivo*, the cephalic artery of common octopus (*Octopus vulgaris*, Wells and Wells 1986, Wells et al. 1987). Present knowledge of cephalopod hemodynamics is largely based upon blood pressure recordings in the three hearts and in arterial vessels, complemented by blood volume flow estimates based on the Fick principle (e.g. Johansen 1965, Wells and Wells 1983, Wells et al. 1988, Shadwick et al. 1990). Owing to the (potentially) large contribution of gas exchange via skin surfaces to total oxygen uptake (see Pörtner, 1994, Madan and Wells, 1996) these calculations may have led to erroneously cardiac output estimates (e.g. Shadwick et al. 1990). Even less information is available for the venous return system in cephalopods, probably owing to the delicate nature of these vessels in cephalopods (e.g. Schipp 1987). No direct estimates of either blood velocity or blood volume flow, and only few estimates of venous blood pressures are available to date for unrestrained coleoid cephalopods (Johansen and Martin, 1962 for *O. dofleini*, Bourne, 1982 for *Loligo pealei*).

Venous blood in cephalopods is led to the gills via large diameter capacitance vessels (see Shadwick and Nilsson 1990, Schipp 1987b for a description of vessel characteristics). The most important one of these in coleoids is the anterior vena cava (AVC), which receives numerous factors from the head and arms, funnel apparatus, retractor muscles of head and funnel and the hepatopancreas. In the cuttlefish *Sepia officinalis,* the AVC originates in a stout, valved muscular chamber located dorsally of the exhalant funnel roof. It traverses the mantle cavity and splits up into paired lateral venae cavae at the anterior tip of the organ sac. Lateral venae cavae and inputs from the

posterior parts of the animal feed into the branchial hearts, which, in turn, generate the pressure to overcome gill vessel resistance (Tompsett 1939, fig. 47, 48 and text for a detailed description). It is most peculiar that the large diameter, thin walled (but muscular, see Schipp 1987b) AVC is fixed to the hepatopancreatic mass on its dorsal side, but is otherwise freely suspended in the mantle cavity, thus being under direct influence of ventilatory and locomotory pressure oscillations that always occur in the mantle cavity.

A number of studies found pressure pulses in the AVC to be correlated with ventilatory mantle movements (e.g. Johansen and Martin 1962, Bourne 1982) and postulated that mantle cavity pressure conveyance might be responsible for blood propulsion in this vein. However, as ventilatory pressures in the mantle cavity were not determined in above mentioned studies simultaneously with AVC blood pressure, it is not clear, wheter the outlined scenario is feasible. In addition, it is not established, whether observed AVC blood pressure pulses are relevant for blood propulsion in the vein. A number of studies suggested that blood transport could also be achieved by means of peristaltic contractions of AVC circular muscles (Bert, 1867, v. Skramlik, 1941, de Wilde 1955, Wells and Smith, 1987, Schipp, 1987, King et al 2005). Such peristaltic blood transport has been demonstrated in peripheral arm veins (Mislin and Kauffmann, 1948, Mislin, 1950, Smith, 1962), closely coupled to ventilatory movements and apparently under reflectoric control of the subesophageal central nervous system. Whatever the exact mechanism of blood transport in the AVC, the close coupling between blood pressure pulse rates in major veins and ventilatory movements in general seems to be present in all cephalopod ecotypes investigated to date, in octopods (Johansen and Martin 1962), squid (Bourne 1982) and nautilus (Bourne et al. 1978).

The present study reports the first measurements of venous blood velocity and volume flow in a cephalopod. It also focuses on phase relationships between the pressures generated in the mantle cavity and blood flow patterns in the AVC in unrestrained cuttlefish to learn more about interactions between ventilatory and circulatory systems in cephalopods. Special emphasis is placed on blood flow during spontanoeus exercise, conditions under which mantle cavity pressure amplitudes can increase some 100 fold (Wells and Wells 1991, Melzner, Bock, Pörtner, submitted a). Exercise even has caused

cardiac arrest in octopods (Wells et al. 1987). Wells and coworkers suggested that high mantle cavity pressures during exercise might stall venous return and thus prevent proper systemic heart filling.

Furthermore, we aimed at a better understanding of the hemodynamic basis for high rates of oxygen extraction from the ventilatory stream encountered in those cephalopods that have successfully decoupled their ventilatory apparatus from locomotion, cuttlefish and octopods. Both ecotypes are able to extract more than 50% of the dissolved oxygen from their ventilatory streams (Wells and Wells 1982, 1985, 1991). Only recently we determined resting extraction rates of > 80% in the cuttlefish *S. officinalis* (Melzner, Bock, Pörtner, submitted b). In the light of such figures, one would surely expect tight matching of blood and water flow phases during counter-current gas exchange in gill vessels, especially as both water and blood flows are pulsatile rather than continuous. Pulsatility of counter-current flows in general was suggested to reduce gas exchange efficiency (Piiper and Scheid, 1984).

Two experiments were carried out: In a first experiment, we focused on the determination of blood pulse rates in major blood vessels (cephalic artery, afferent branchial vessels, AVC) of *S. officinalis* in relation to mantle cavity pressure oscillations, to investigate whether an absolute coupling between ventilatory and circulatory pulse rates is present in this cephalopod. This was done by employing non-invasive magnetic resonance imaging (MRI) techniques in combination with mantle cavity pressure measurements. In a second set of experiments, we used miniature Doppler sensors fitted around the AVC to determine blood flow and velocity, while simultaneously measuring pressures in the mantle cavity, to eventually elaborate patterns of ventilatory and circulatory integration on a high time resolution basis.

2. Material and Methods

2.1 Terminology

In agreement with a recent study of cuttlefish hemodynamics (King et al., 2005), we will make use of the term ‚anterior vena cava (AVC)' instead of ‚cephalic vein', as the respective vein is called in the standard treatise on cuttlefish anatomy (Tompsett, 1939). This makes sense, as in the octopod literature, the homologous vessel is also termed AVC, while ‚cephalic vein' refers to a circular vein in the octopod head that collects factors from the arms (Isgrove 1909, Smith 1962).

2.2 Animals

European cuttlefish (*Sepia officinalis*) used in the present study were grown from egg clusters trawled in the Bay of Seine (France) in May 2002, kindly provided to us by M.P. and R. Chichery. The animals were raised in a closed re-circulated aquaculture system (20m^3 total volume, protein skimmers, nitrification filters, UV – disinfection units) at the Alfred–Wegener–Institute on a diet of mysids (*Neomysis integer*) and brown shrimp (*Crangon crangon*) under a constant dark–light cycle (12 – 12) and constant temperature regime (15°C +/- 0.1°C). Water quality parameters were monitored three times per week. Concentrations of ammonia and nitrite were kept below 0.2 mg l^{-1}, nitrate concentrations below 80 mg l^{-1}. Salinity was maintained between 32 and 35‰, pH between 8.0 and 8.2. All animals were raised in the same 3 m^3 volume tank. Two consecutive experiments were carried out on cuttlefish originating from the same laboratory raised generation. Following measurements under control conditions, animals were subjected to acute temperature change. However, these results were treated separately (Melzner, Bock, Pörtner, submitted a, b, c). In experiment 1 (N = 5 animals; March - April 2003) *in vivo* MRI and mantle cavity pressure trials were carried out. In experiment 2 (N = 10; July – October 2003), flow was recorded in the AVC, again in combination with mantle cavity pressure determinations (see table 2 for animal masses).

2.3 Experimental protocol

Experimental animals were starved for 24 hours, then transferred to the experimental setup. Surgery was conducted on the first day, followed by an overnight acclimatization period within the experimental set-up at 15°C (±0.1°C). *In vivo* ^{31}P - NMR – spectra showed that anaesthesia during surgery resulted in a transient accumulation of inorganic phosphate (P_i) in the cuttlefish mantle muscle organ, which could be fully reversed within 4-6 hours of recovery under control conditions (Melzner, Bock, Pörtner, submitted a). In experiment 1, MRI measurements at 14 - 15°C were performed on the second day, at least during four subsequent hours between 07:00 – 13:00. In experiment 2, all data (starting one hour after implantation of Doppler sensors) were analyzed. However, true control values were obtained between 07:00-10:00 hours on day two.

2.4 Experiment 1

To implant a catheter for ventilatory monitoring, animals were anaesthetized with a 0.4 mol l^{-1} $MgCl_2$ solution that was mixed 1:1 with seawater (Messenger, 1985) at 15°C for 3 – 3.5 minutes, then placed (ventral side up) on a wet leather cloth to prevent skin injuries. During surgery, animals were perfused with aerated seawater (0.04 mol l^{-1} $MgCl_2$) through the funnel aperture. A PE cannula (connected to a 23 gauge hypodermic needle) was led through the entire mantle cavity and then fed through the posterior ventro-lateral section of the mantle muscle to record postbranchial pressure. Cannulae (Portex PE tubing, i.d. 0.58 mm o.d. 0.96 mm, flared at the opening) were held in place by two 4 mm diameter plastic washers on the in and outside, embracing the mantle muscle in a sandwich-like fashion. PE tubes were connected to MLT-0699 pressure transducers, signals amplified with a ML-110 bridge amplifier. Data were fed into a PowerLab/8SP data acquisition system (AD Instruments, Australia). Pressure transducers were calibrated daily.

Following surgery, animals were placed in a perspex perfusion chamber analogous to the one used by Mark et al. (2002) for eelpout. Plastic sliders within the chamber could be adjusted to the

animals‘ dimensions and were used to restrict the space available for roaming activity. The chamber was connected to a closed recirculation seawater system and placed within the magnet as described in Bock et al. (2002). Water quality was maintained with a protein skimmer (Aqua care, Germany) and a nitrification filter (Eheim Professional 2, Eheim, Germany). Water quality was monitored daily and parameters were kept within the limits indicated above.

In vivo MRI measurements were performed with a 4.7 Tesla Bruker Biospec 47/40 imaging spectrometer (Bruker, Germany) equipped with a mini imaging unit with a gradient field strength of up to 200 mT m-1. Flow weighted images were generated in the transversal plane at a position just prior to the forking of the AVC, enabling us to investigate pulse rates in afferent and efferent branchial vessels, cephalic artery and vein simultaneously. Image acquisition was performed using the gradient echo Snapshot FLASH technique (Haase, 1990). Imaging parameters were as follows: matrix size 128 x 128, resulting in an in plane resolution of 312 μm; repetition time 6.7 ms, echo time 2.1 ms; 22.5° sinc3 pulse; pulse length 2,000 μsec; 1 slice, slice thickness 2 mm; field of view 4 x 4 cm; dummy scans = 4. Sequences of 20 – 32 images were generated in quick succession, resulting in a temporal image resolution of 0.986 sec^{-1}. Blood vessels displayed variable degrees of brightness proportional to flow in Snapshot FLASH generated MR images (see fig. 6 a-x). Mean signal intensities were calculated by an operator controlled analysis of various regions of interest (ROIs) for the determination of relative changes in blood flow. As 20 – 32 images were generated consecutivey in the same position, pulse rates for the various vessels of interest could be derived simultaneously and compared with ventilatory pressure oscillations. Such image sequences were acquired once every 25 minutes.

2.5 Experiment 2

Animals were anaesthetized and pressure catheters implanted as described above. In a second step, a miniature Doppler sensor was implanted to record blood velocity and blood volume flow with a

directional pulsed Doppler flowmeter (Iowa Doppler Products, USA) after AVC maximum diameter (fully relaxed under anaesthesia) had been determined with callipers. Doppler sensors (Iowa Doppler Products, USA, model E cuff type transducers, 20 MHz), were stripped bare of all plastic and rubber, incorporated into a plastic piece, which subsequently was fixed in a bridge like arrangement around the AVC (see fig 1 for bridge details and positioning). Bridges were made of plastic fittings (polyethylen). Great care was taken in choosing bridges matching the diameter of the AVC, as we wanted to record blood velocity and flow in a relatively undisturbed vessel (while at the same time, minimally disturbing animals). Bridges were carefully positioned approximately 2-3 mm posterior of the ventral nerves (see Tompsett 1939, fig. 6) by sewing the bridge superficially to the head retractor muscle using Ethicon #N271H (Johnson and Johnson, USA) sterile silk ligature. Ligatures were glued to the bridge arms using high viscose cyanacrylate glue (Hylo Gel, Marston Oelchemie, Germany). The thin sensor wiring was fed through the mantle cavity and led, analogues to the pressure catheter, through the posterior mantle muscle using a surgical needle. Subsequently, the wiring was connected to the pressure catheter using silk ligature and high viscose cyanacrylate glue. Pure ethanol was used for wound disinfection. Total sensor mass (sensor + bridge) was 0.2 g, total mass of the wiring was 0.28 g (see fig 1 for sensor dimensions).

Following surgery, animals were placed in an animal chamber within a recirculated seawater bath as previously described in greater detail and with water quality parameter thresholds as indicated above (Melzner, Bock, Pörtner, submitted b). Animals were kept at constant 15°C in fully aerated seawater (salinity 33-35) during experimentation.

Analogue outputs of the Doppler flowmeter and the pressure transducer were fed into the PowerLab/8SP data acquisition system (AD Instruments, Australia). Mantle pressure and venous blood flow data were collected at a sampling rate of 100 – 400 Hz to investigate the phase relationships between both processes in detail. Pressure and blood flow traces were smoothed (smoothing type: triangular (Bartlett); window width 21 – 33 points for pressure recordings, 7 – 11 points for flow recordings). Great care was taken to not alter pulse amplitudes and phase relationships of curves by choosing inappropriate smoothing window sizes.

2.6 Data analysis

All experiment 2 pressure and Doppler data were analyzed using Chart 5.0 software (AD Instruments, Australia). Ventilation frequency (v_f) and cephalic vein pulse frequency (AVC_f) were determined during the entire experimental period by automatically counting pressure or flow peaks. Mean mantle pressure (MMP, Pa) was determined from the mantle pressure time integral. Control pressure ($MMP_{control}$) was exclusively determined from pulses <0.1 kPa pressure amplitude (10 pulses per 5 min interval experimental time were analyzed), as higher pressures are related to spontaneous activity and swimming (Bone et al. 1994). Resting venous flow pulses were integrated within the respective intervals to yield average blood velocity and average flow, using the Doppler equation ($V = (F_dC)\ (2F_0 \cos A)^{-1}$; with V = velocity in mm s^{-1}, F_d = Doppler shift frequency in kHz (the instrument was calibrated to 0.5 V phasic output = 1 kHz Doppler shift), C = velocity of sound in blood (1,565,000 mm s^{-1}), F_0 = transmitter frequency (20,000 kHz), A = angle between sound beam and velocity vector = 45°) and an average cephalic vein diameter of 2.8 mm (0.2 mm SD). Positive velocities correspond to forward flow events (=flow towards the gills), negative velocities to backward flow (=flow towards the head).

Phase relationships of the venous flow pulses relative to mantle cavity pressure pulses within representative sequences were analyzed for 8 animals for which both mantle pressure and blood flow recordings were of very good quality (15 pressure and blood flow cycles per animal were analyzed). All phase comparisons were expressed in relation to the mantle cavity pressure period, with one full cycle corresponding to 360° phase and 0° and 360° defined to be minimum mantle cavity pressures (see fig 2). Phase angles (ϕ) for maximum mantle cavity pressure increase were determined:

$$\phi_1 = T_{\text{max slope MP}} / v_p * 360° \quad (1)$$

and phase angles of main blood peak start (peak B, see fig 2 and text for definition)

$$\phi_2 = T_{\text{start peak B}} / v_p * 360° \quad (2)$$

Phase shifts (δ) between both events were calculated for each of the eight animals:

$$\delta = \phi_1 - \phi_2 \quad (3)$$

with $T_{max\ slope\ MP}$ = time point of maximum mantle cavity pressure increment (=maximum slope of the pressure curve), measured (in s) from the start of the corresponding mantle cavity pressure period; $T_{start\ peak\ B}$ = start of the main blood flow peak, measured (in s) from the start of the corresponding mantle cavity pressure period; v_p = duration of the respective mantle cavity pressure period (in s).

For each animal, periods of spontaneous exercise and recovery were analyzed to determine how increments in mantle pressure pulse amplitudes by factors > 100 influence blood flow in the cephalic vein. Data sets from 6 randomly chosen animals were analyzed for groups of high amplitude pressure cycles (termed swimming jets = SJ). Selection criteria were: at least 30 min of $MMP_{control}$ and control v_f prior to and following the exercise event, no more than 2 minutes of total exercise, a one minute exercise interval with a MMP of > 0.13 kPa (exercise). Of all suitable intervals identified, those with the highest MMP were selected for each animal. The following parameters were analyzed for pre - exercise, exercise and post – exercise one minute intervals: MMP (Pa), v_f (ventilatory strokes min^{-1}), AVC_f (AVC blood flow pulses min^{-1}), AVC average maximum blood velocity ($AVC_{av\ max\ V}$ in cm s^{-1}) and AVC stroke and minute volume (AVC_{SV} in ml blood $pulse^{-1}$ and AVC_{MV} in ml min^{-1}).

To investigate ambient mantle cavity pressures during AVC blood flow intervals, we examined individual swimming jets and corresponding vein flow pulses. For 6 randomly chosen animals, 10 SJs of pressure amplitudes > 1 kPa were randomly selected. MMP was determined for the entire SJ period (from minimum to minimum pressure, interval d in fig 4b), as was MMP during the time interval of forward blood flow in the vein (interval e in fig 4b). Also, mantle pressure was determined during periods of maximum flow in the vein (table 2).

$MMP_{control}$ and v_f have already been determined elsewhere for experiment 1 animals (Melzner, Bock, Pörtner, submitted b) and are listed in table 1. At least two 20 to 30 second MR image sequences were analyzed for each animal. Only MR image sequences during periods of resting

ventilation were considered for analysis, with at least 15 min of control v_f and MMP prior to and during MR image acquisition. Pulse rates in anterior vena cava (AVC), cephalic artery (CA) and afferent branchial vessels (aff BV) were determined and compared with ventilatory pressure pulse rates.

2.7 Statistics

Parameter changes during subsequent one minute periods in spontaneous exercise trials were analyzed using ANOVA in combination with Student - Newman - Keuls (SNK) post – hoc tests. Mean maximum parameter changes for all six animals in exercise periods were tested for significance using paired t-tests or ANOVA and SNK. Percentage values were arc sin transformed prior to ANOVA.

3. Results

3.1 Control conditions: venous flow and mantle pressure

Flow in the cuttlefish anterior vena cava (AVC) is tightly coupled to ventilatory movements. One blood flow pulse corresponds to one ventilatory pressure cycle. Fig. 2 shows a characteristic ventilatory mantle cavity pressure cycle (interval c) in combination with a vein flow pulse. Vena cava blood flow pulses are typically biphasic, consisting of a low amplitude peak (termed A in fig. 2) that is followed by a high amplitude peak (B in fig. 2). Both pulses are usually separated by a local flow minimum. Net forward flow in the gill heart direction can be found during 54% of the ventilatory cycle (flow peaks A+B in fig. 2). AVC minute volume (AVC_{MV}) amounts to 5.5 ml during phases of control ventilation (mean mantle pressures, $MMP_{control}$, of 0.02 kPa, ventilation frequencies, v_f, of 29.0 strokes min^{-1}), cephalic vein stroke volume (AVC_{SV}) amounts to 0.2 ml per blood pulse (see table 1).

Although both blood flow pulses last similarly long, pulse b provides 88% of total blood flow (see table 1) and will be referred to as the main blood pulse hereafter. Velocity profiles and mean maximum velocities under control conditions (see fig 2) are extremely constant in individual preparations, as is the phase relationship with rhythmic mantle cavity pressure pulses. A careful investigation of data from 8 experimental animals revealed that the major blood flow peak (B) is elicited exactly at the time of maximum pressure increase in the mantle cavity. Figure 3 illustrates the relationship between the phase angle of the maximum mantle cavity pressure increment (ϕ_1) and the phase angle of peak B start (ϕ_2) for each of these animals. The resultant linear regression is characterized by a slope that is not significantly different from one (i.e. $\phi_1 = 4.9 + 0.92(0.67 - 1.172)\phi_2$ (95% confidence interval for regression slope in brackets); $R^2 = 0.93$; $p<0.001$). Therefore we concluded that the coupling between both processes is tight and occurs at the same time point within each ventilation period. However, owing to differences in the shape of mantle cavity pressure pulses between animals (maximum slope occurs earlier or later in the ventilation period), these two processes shift along the regression line between approximately 45 and 150° of the ventilation period. Evaluation of the mean phase difference between both phase angles ($\phi_1 - \phi_2$) for all 8 animals revealed a phase shift (δ) of 1.2° (8.1 SD), which, during a ventilatory period of 2.1 s (at 29.0 ventilatory strokes min^{-1}), corresponds to a time difference of only 0.007 seconds. Fig. 2c provides the first derivative of the pressure traces from fig 2a, which illustrates nicely how well the start of pulse b start and maximum mantle cavity pressure increase coincide.

3.2 Venous flow and exercise

The tight coupling between mantle pressure pulses and AVC blood flow pulses remained valid under all conditions, even during spontaneous exercise, with mantle pressure amplitudes increasing 100-fold and higher.

Examples of three mantle cavity pressure pulses in combination with blood flow events in the AVC (all from animal #18) are displayed in fig 4. Figure 4a shows a typical control pulse with a pressure amplitude of 0.03 kPa, 4b an intermediate SJ with an amplitude of about 1.8 kPa, 4c the most extreme SJ observed in any of the investigated cuttlefish with an amplitude of close to 20 kPa. None of these pulses could abolish blood flow in the vein. Rather, fig 4b demonstrates that high AVC blood velocities can be maintained at maximum mantle pressure during complete overlap of mantle cavity pressure pulse and blood flow pulse. However, negative velocity (=backward blood flow towards the head) as witnessed in fig 4c (see also fig. 5b) can also frequently be observed during high amplitude SJs. The shape of blood flow pulses changes with exercise (fig 4b,c, 5b): Typically, there is only a single flow peak (B) present during exercise, i.e. peak A (see fig 4A) vanishes with increasing mantle cavity pressures. Table 2 reports mean pressure amplitudes for 60 randomly chosen SJs > 1 kPa pressure amplitude from 6 animals, with a mean SJ pressure amplitude of 3.9 kPa. This is equivalent to a MMP of 1.5 kPa over the entire mantle cavity pressure peak (i.e. interval d in fig 4b). Integrating mantle cavity pressure exclusively over the blood flow pulse interval (i.e. interval e in fig 4b) yielded a MMP of 1.6 kPa. This clearly indicates that the blood flow pulse always occurs during the SJ high pressure interval. This is remarkable, especially as MMPs encountered during blood flow were observed to range from 0.6 up to 7.6 kPa. At maximum flow in the AVC, mean pressure amounted to >2 kPa in the mantle cavity.

Figure 5a and b illustrate a short exercise sequence with high mantle cavity pressure cycles of amplitudes up to 5 kPa. This sequence is characteristic for all animals and demonstrates that during high mantle pressure phases, venous return is neither inhibited, nor significantly enhanced by mantle pressure. During high amplitude pressure cycles in fig 5b (which are due to swimming movements or escape jetting, Bone et al. 1994) $AVC_{av\ max\ V}$ does increase to some extent (from 7.2 cm s^{-1} during seconds 1 - 15 to 9.3 cm s^{-1} during seconds 16-36). However, the more crucial parameter with respect to oxygen supply via the blood, AVC_{MV}, does not change during the entire sequence displayed in 5b (5.6 ml min^{-1} during seconds 1-15, 5.8 ml min^{-1} during seconds 16-36, 6.2 ml min^{-1} during seconds 40-60).

Monitoring the effects of 1 – 2 minutes of vigorous exercise and subsequent recovery sequences from six randomly chosen animals over 30 minute periods revealed how blood volume flow is controlled. As the qualitative changes in hemodynamic parameters over time were fully comparable between animals, we decided to only show one typical series in detail (fig. 5c-f, obtained from animal #8, see also table 3). The most striking observation was that the increase in AVC_{MV} was delayed by about one minute in relation to the mantle cavity pressure peak (fig 5c). MMP quickly returned to control values (only mantle pressures after three minutes were significantly elevated above control values), while AVC_{MV} remained significantly elevated until after 8 minutes. Figs 5d-f suggest that these increases in blood flow are brought about by simultaneous increases in AVC_f, $AVC_{av\ max\ V}$ and AVC_{SV}.

Table 3 summarizes the main findings for all six investigated animals: 9.5-fold increases in MMP are followed by 2.2-fold increases in AVC_{MV}, however, with a mean time delay of 1.7 minutes. During periods with MMP > 0.13 kPa (exercise), AVC_{MV} was not found to be significantly different from control AVC blood minute volumes. Maximum increases in AVC blood minute volume are mediated by 1.5 - 1.6 fold increases in AVC_f and $AVC_{av\ max\ V}$, while AVC_{SV} was not significantly elevated. On average, blood minute volume remained significantly elevated for 4.2 minutes past the exercise period (tab 3b), although all time series (e.g. fig 5c) revealed a long phase (15-30 minutes) during which blood minute volume slowly approached control values.

Determining SJ frequencies and amplitudes within exercise intervals enabled us to estimate the amount of phosphagen used in the mantle musculature during high amplitude mantle contractions (using formula (5) determined in Melzner, Bock, Pörtner, submitted a). According to these estimates, all animals needed to break down phosphagen (PLA) in order to sustain the displayed levels of exercise. The highest estimate is for animal 21, which probably metabolized about 10% of its PLA reserves during 48 SJs during its exercise period. This animal also showed the highest factorial increase in blood flow of 2.7 and the longest post-exercise recovery period (12 minutes) characterized by significantly elevated AVC blood minute volumes.

All animals very likely used phosphagen reserves to fuel relatively few SJs (<50) during short periods of spontaneous exercise and increased blood flow thereafter, probably reflecting enhanced oxygen consumption while PLA levels were restored in the mantle muscle.

3.3 Magnetic resonance imaging (MRI)

The information on blood flow patterns in the AVC during rest is complemented by information from other vessels, obtained by use of MRI techniques. Fig 6a-h shows a control series of seven successive MRI images, fig 6J depicts the phasic flow information obtained from these images for the cephalic artery (CA), the AVC and the afferent and efferent branchial vessels (aBV, eBV), while fig 6i gives the mantle cavity pressure changes recorded simultaneously by use of an indwelling catheter and pressure transducer. Pulses in the CA originate from systemic heart contractions (and elastic properties of the vessel itself, Schipp 1987), those in the aff BV result from branchial heart contractions.

It appears, that each ventilatory pulse under resting conditions is not only coupled to one blood flow pulse in the AVC, but also to one branchial heart beat and one systemic heart beat. Pulse rates in all three vessels did not deviate significantly from one another nor from v_f (see table 1).

4. Discussion

4.1 Methodology

By use of *in vivo* MRI, we could simultaneously determine phasic blood flow patterns in several major vessels of cuttlefish acclimatized to 15°C. While this technique is able to non-invasively quantify flow patterns, it suffers from rather low time resolution of 0.82 s image^{-1} (= 73 possible

images min^{-1}). Maximum pulse frequencies of about 36 pulses min^{-1} can be resolved. At observed v_f and AVC_f of > 30 pulses min^{-1} in our experiment, it is thus not possible to accurately determine potential phase shifts between pulse cycles in different vessels. In addition and owing to constraints in time resolution, the influence of acutely elevated v_f on blood pulse frequencies in various vessels could not be determined.

Doppler measurements and pressure recordings did not suffer from such limited time resolution, thus we were able to accurately define phase relationships between blood flow in the AVC and associated pressure oscillations in the mantle cavities of cuttlefish. High variability in the AVC_{MV} data (see table 1) may have resulted from 1. occasional occurrence of slight Venturi effects with the result of artificially increased blood velocities (due to tight fittings of bridge and Doppler probe around the vessel, Figure 1), 2. a deviation of angle A (see methods) from 45° relative to the blood flow vector, or 3.(most likely) slight deviations of bridge position from the 180° relative to the vessel wall. Further optimization in bridge design (Figure 1) should further improve volume flow determinations.

Overall, techniques as applied here were minimally invasive, with just two sutures holding the low mass bridge setup. Animals did not seem to be disturbed by the presence of the sensors and usually settled quickly in the animal chamber during experimentation, with mantle cavity pressures and v_f being comparable to values obtained in experiment 1 (see table 1).

4.2 Venous return and mantle pressure

A number of studies could demonstrate that pressure oscillations in the large diameter AVC are correlated with ventilatory movements in octopods and squid (Johansen and Martin 1962, Smith 1962, Bourne 1982). While these early reports were based on venous pressure recordings in combination with visual observations of ventilatory movements, the present study focused on accurate determinations of phase relationships between ventilatory pressures and venous blood flow

patterns.We found a very tight coordination between ventilation and blood flow patterns in the cuttlefish *S. officinalis*. Short blood flow pulses in the AVC were consistently found during each ventilatory cycle at the point of maximum mantle pressure increase, regardless of the phase angle of maximum pressure increase in the mantle cavity. At first sight these findings correspond nicely to Johansen and Martin's (1962) conclusion of mantle pressure conveyance driving venous return in *O. dofleini*. However, the situation in cuttlefish is more complicated. Mean mantle pressures under resting conditions are about 0.02 kPa (15°C), pulse amplitudes are no greater than 0.04 kPa under such conditions (see Melzner, Bock, Pörtner, submitted b). At (putative) systolic pressures of 0.08 kPa in the cuttlefish AVC (Schipp and Fiedler, unpublished, mentioned in Schipp 1987) or diastolic pressures of 0.095 kPa in the branchial hearts (Fiedler 1992), it is virtually impossible that pressure conveyance from ventilatory mantle cavity pressure oscillations can be responsible for the observed blood flow pulses in the AVC, as ventilation pressures are generally lower under control conditions. Pulse shapes of blood flow do not resemble pressure pulse shapes at all, which also argues against a passively mediated pressure conveyance process. A recent ultrasound imaging study (King et al., 2005) revealed that the AVC is either compressed or does actively contract serially during each ventilatory cycle, forming a wave that could propagate blood towards the gills (see their supplemental video material on the jeb homepage, video1, sagittal view of the vessel). As transversal AVC views revealed a decrease in vessel circumference during each ventilation period (indicating active contraction of circular muscles rather than a passive compression of the vessel during the ventilation cycle systole; King, pers. communication), we favor the peristaltic blood transport scenario. A study of cuttlefish AVC preparations *in vitro* (Schipp, unpublished, in Schipp 1987b and Schipp, pers. communication) indicated that this vessel, unlike isolated octopus arm veins (Mislin and Kauffmann, 1948, Mislin 1950), is not characterized by a myogenic automatism under physiological conditions and does not display a Starling effect. The vessel wall contains extensively innervated circular and longitudinal muscles, indicating independent central control of vessel blood minute volume. Peristaltic contractions of the vessels circular muscles could not be elicited under normal physiological conditions, but were present in media containing acetylcholine (Schipp, 1987b, see above). As octopus arm vein peristaltic

action has been shown to be synchronized to ventilatory movements due to a central nervous reflex (Mislin, 1950), it would not be surprising if blood transport in the AVC were similarily coordinated in relation to ventilatory movements.

However, preliminary observations suggest involvement of further components in blood flow control: Gentle pressure exerted on the funnel of anaesthetized animals directly following surgery (thus with the Doppler probe already in place) can elicit the characteristic blood flow pulses in the vein as observed under control conditions (F. Melzner and C. Bock, unpublished observations), thereby possibly eliciting the central nervous reflex. In this case blood pulses may be elicited by compression of the muscular chamber located directly dorsal of the funnel roof. This muscular chamber forms the anterior end of the AVC and is characterized by the presence of several valves that prevent backflow of blood into those factors entering it (see Tompsett 1939, fig 48, M.CE. V.). Expansion of the funnel tube or movements of the funnel during the ventilatory cycle could potentially elicit flow pulses under *in vivo* conditions, especially during exercise (=large amounts of water passing through the funnel during jetting, see Shadwick 1994). The sagittal imaging ultrasound video of the AVC contractions by King and colleagues (see above) does, in fact, show cyclic movements of the funnel apparatus during each ventilatory period, which appear to be highly correlated with the waves passing over the AVC. Following this line of thought, the AVC would be passively compressed during subsequent vessel diastole, when mantle cavity pressures are highest (AVC blood pressure during diastole: 0 - 0.07 kPa, Schipp and Fiedler, unpublished in Schipp 1987), peak ventilation pressure amplitudes at rest in our experimental animals: 0.03-0.04 kPa). However, combining the advantages of ultrasound imaging studies with Doppler velocity or mantle cavity pressure measurements would be required to resolve the exact sequence of events in the AVC.

Pulsation rates in the CA and in the afferent branchial vessel did not deviate significantly from AVC_f, which suggests an integrated control of all of these patterns. Under truly resting ventilation patterns and at acclimation temperature high oxygen extraction rates from the ventilatory current of > 80% may be facilitated by a 1:1 ratio of ventilatory vs. blood flow pulses. Thus, each stroke volume of blood ejected into the gill vessels by the branchial hearts could potentially come into contact with a

fresh stroke volume of fully oxygenated seawater. Mislin (1966) also observed v_f not to differ significantly from systemic heart frequency (sh_f), although he noted that the coupling between both rates was not absolute, rather, rates could occasionally deviate from one another. King and colleagues (King et al. 2005) found mean heart and ventilation rates to differ significantly from one another, with sh_f and branchial heart frequency (bh_f) typically lower than v_f, although rates did match in 5 of 37 cases investigated.

Recent investigations of the cuttlefish ventilatory apparatus indicate that increases in oxygen flux through gill epithelia are achieved by increasing v_f and ventilatory stroke volume (v_{SV}) to a greater extent than blood minute volume. Temperature induced increases in metabolic rate by a factor of about 2 were sustained by a 21-fold increase in ventilatory power output (T = 14 - 23°C), while at the same time oxygen extraction rates from the ventilatory current dropped from >80% to about 40%. We suggested that this large range of adaptive flexibility is enabled by the low costs of the cuttlefish ventilation system (less than 2% of routine metabolic energy turnover are allocated to ventilation mechanics between 11-17°C; Melzner, Bock, Pörtner, submitted b). Thus, occasionally observed elevated v_f in relation to sh_f (see above) may be due to the need to increase oxygen diffusion gradients at gill epithelia at acutely elevated oxygen consumption rates (e.g. during specific dynamic action of food, hunting, social interaction, temperature change etc.). Such situations may go along with decreased oxygen extraction rates and enhanced oxygen supply to tissues.

However, with regard to the inactive, energy saving lifestyle of cuttlefish (Aitken et al. 2005), it is probably energetically advantageous to minimize ventilation volume by optimizing oxygen extraction from the ventilatory current whilst lying hidden under sand for the greater part of the day (Denton and Gilpin – Brown 1961). Under these resting conditions a common frequency of circulatory and ventilatory pulses may be helpful in attaining these high oxygen extraction rates.

King et al. (2005) concluded from their study that, apparently, two different systems oscillate at independent rates: The ventilatory system and the AVC on the one hand, the three hearts and contracting lateral venae cavae on the other. Our data also suggest that mantle cavity pressure

oscillations and AVC blood flow pulse rate match exactly in cuttlefish. Further, we would add to these conclusions that there is a constant phase relationship between the two. Under certain conditions (truly resting mantle cavity pressures, measurements in animals in a post absorptive state at acclimation temperature) rates of both systems match, likely in order to minimize energy expenditure and to increase oxygen extraction from the ventilatory stream. However, one question remains: why is one important element of the circulation apparatus (AVC) so tightly connected to ventilation rates, while the rest is able to operate at facultatively independent rates? The interfering influence of exercise may provide an answer to this question.

4.3 Spontaneous exercise

Previous laboratory studies (Melzner, Bock, Pörtner, submitted a) indicated that *S. officinalis* typically spend 1-3% of their time generating higher mantle cavity pressures, which are related to swimming, escape jetting and, presumably, other activities. We termed such non – ventilation related pressure oscillations > 0.2 kPa swimming jets (SJ). At present it is unclear how these patterns match with activity levels of this species of cuttlefish in the wild. However, a closely related species (*S. apama*, Australia) was found to be active for only 3% of a day time (Aitken et al., 2005). Resembling the octopod lifestyle (Mather and O'Dor, 1991), cuttlefish likely do not produce high pressures in their mantle cavities very often in their natural habitat.

However, in contrast to the situation in octopods (Wells et al. 1987), the results of the present study indicate that SJs do not stall venous return through the AVC. Wells et al (1987) observed cardiac arrest to occur in octopods during exercise runs that included propulsive jets. The authors suggested that even slow, jet propelled swimming with pressure amplitudes between 4 -8 kPa might be sufficient to stall venous return to the heart, which, when not being properly filled and stretched, does not contract. In cuttlefish, swimming jets with pressure amplitudes of up to 20 kPa, as observed in the present study, did not inhibit AVC blood flow. Rather, animals were able to maintain AVC_{MV} at pre –

exercise levels, although SJ pressures probably greatly exceeded venous blood pressures in AVC and lateral venae cavae, which are < 0.2 kPa in octopods (Wells and Smith 1987) and (presumably) < 0.1 kPa in cuttlefish (Fiedler 1992). We believe that peristaltic vein contractions cannot be responsible for blood flow pulses observed during exercise. Using *in vitro* vessel preparations of *O. vulgaris* AVC, Shadwick and Nilsson (1990) could demonstrate that the cephalopod AVC is designed to be a major capacitance element, characterized by a high volume compliance at low internal pressures. The authors found the vessel to change in volume at a rate of 7 * V_o kPa^{-1} between zero and one kPa internal pressure. This suggests that the vessel should, on the other hand, be easily compressed when outside pressure (=mantle cavity pressure) greatly exceeds internal blood pressure, which is most likely the case in our experimental cuttlefish. The arising conclusion is that there should not be a blood flow peak present during maximum exercise induced pressure in the mantle cavity, if peristalsis were the sole means of blood propulsion. Rather, we suggest that in the case of exercise, pressure conveyance from the ventilatory to the circulatory system must be responsible for the observed blood flow pulses. Owing to its structural organization and presence of several valves (see Tompsett 1939), pressurizing the AVC from the outside must result in blood flow directed towards the lateral venae cavae. Valves at the anterior AVC end prevent outflow of blood to the venous system of the head, a recently discovered valve at the posterior AVC end (King et al. 2005) prevents blood to flow back into the AVC from the lateral venae cavae. During exercise, flow in the AVC occurs exclusively during the high mantle pressure phases of observed SJs, flow pulse shape and pressure pulse shape are nearly identical. This argues for passively mediated blood transport in the case of exercise. The outlined scenario would be an elegant solution to assure continuity in venous return during exercise.

Blood volume flow did not increase during exercise, but rather remained at the pre – exercise level. After exercise AVC_{MV} increased with a 1.7 minutes delay compared to the maximum mantle cavity pressure peak (see table 3). Blood flow remained elevated for several minutes, independent of post exercise ventilation pressure, once short (but intense) exercise periods were terminated. This must be regarded as further evidence against the mantle pressure conveyance model of venous return under control conditions.

Although the AVC itself does not transport blood from the mantle (whose circular fibres are mainly responsible for pressure generation during exercise), it collects factors from the funnel apparatus and the collar flaps, which are engaged in ventilatory muscle contractions and during exercise as well (Bone et al. 1994). Increased AVC blood flow following termination of exercise likely depends on external signals associated with an increase in oxygen demand. *S. officinalis* was observed to frequently use mantle muscle phosphagen reserves (phospho-L-arginine, PLA) to sustain SJs, apparently owing to aerobic metabolism failing to provide sufficient amounts of energy for high intensity muscle work. All exercise events chosen in the present study (tab. 3b) were of such a magnitude that they negatively affected mantle muscle phosphagen reserves due to pressure generation above a threshold values of 2 kPa (Melzner, Bock, Pörtner, submitted a). For example, 23 SJs were counted in minutes three and four of the interval displayed in fig 5 (animal # 8). Using SJ amplitude and frequency information (see insert fig 5) it is possible to estimate the extent of phosphagen use (and concomitant inorganic phosphate [P_i] accumulation). Accordingly, the respective two minute exercise bout probably caused a P_i accumulation by about 1.5 μmol g ww^{-1} in the mantle muscle organ, which corresponds to > 4% of total mantle muscle PLA levels ([PLA] = 33.6 μmol g ww^{-1} in cuttlefish mantle muscle, Storey and Storey 1979). Elevated levels of blood flow likely provide the additional oxygen required to help restore original PLA levels in the mantle muscle and all other muscles involved in exercise.

However, approximately 10-fold increases in mean mantle cavity pressure are not paralleled by similar increases in blood minute volume through the AVC system. Mean maximum blood flow increases (see table 3a) by a factor of 2.2 were witnessed, the highest scope for blood volume flow was seen in animal # 21, where maximum post-exercise flow was 2.7 times the flow under control conditions (see table 2). This compares well with exercise induced blood flow increases in octopods. Wells et al. (1987) found mean increases in blood flow through the cephalic artery by a factor of two, maximum performing animals were characterized by a scope of 2.4 – 2.7 (animals x51 and x47, tab 2). Corresponding factorial aerobic scopes for the octopod range from 1.45 to 2.38 (Wells et al. 1983, Wells et al. 1987). No published determinations on *S. officinalis* factorial aerobic scopes for exercise

are available. However, tropical cuttlefish *S. apama* were characterized by an aerobic scope for exercise of 2.6 (Aitken and O'Dor 2004, measurements at zero and maximum sustainable speed at 20°C) and maximum increases in oxygen consumption during acute temperature change in *S. officinalis* were about twofold (between 14 and 23°C). Combining the available evidence, it appears that in both cephalopod taxa (octopods and cuttlefish), metabolic rate increases of between 2 - 3 are balanced by similar changes in cardiac output, rather than by increasing the arterial - venous hemocyanin oxygen saturation difference (i.e. a net decrease of venous oxygen reserve, as found in *S. officinalis* during hypoxic exposure (Johansen et al. 1982).

While mantle pressure quickly returned to resting ventilation values, AVC_{MV}, AVC_f and $AVC_{av\ max\ V}$ remained significantly elevated for several minutes. Obviously, an oxygen debt was being repaid. Elevated oxygen requirements upon the termination of exercise have been reported for both cuttlefish and octopod (*O. vulgaris*, Wells et al. 1983; *S. apama*, Aitken and O'Dor, 2004). For common octopus, the picture is especially clear: During a five minutes exercise period, both metabolic rate and blood flow are slowly adjusted to a maximum value, remain at a relatively constant elevated level during further exercise as well as during recovery from exercise, likely to repay an accumulated oxygen debt (Wells et al. 1983, 1987). The octopods with the highest scopes for blood flow of 2.4 - 2.7 (see above) were characterized by a twofold elevation in blood flow during recovery, suggesting that those blood flow levels observed during exercise actually represented maximum sustainable flow rates. Maximum factorial scopes of 2.7 observed for AVC blood flow in the cuttlefish *S. officinalis* compare well with cardiovascular scopes of octopods, and also with those of teleosts that live in similar bentho - pelagic habitats. Cod (*G. morhua*) is characterized by a cardiac scope (maximum / resting cardiac output) of 2.8 – 3.3, winter flounder (*P. americanus*) by one of 2.5 (Webber et al. 1998, Joaquim et al. 2004).

In conclusion, our results clearly show that venous return through the AVC is tightly coupled to the ventilatory cycle under control conditions and during exercise. We further demonstrated that greatly increased mantle cavity pressures during exercise do not stall venous return in cuttlefish and suggest that pressure conveyance enables AVC blood flow under exercise conditions. Under control

conditions, AVC volume flow is finely regulated and independent of mantle cavity pressure amplitudes. An observed matching of AVC_f, v_f, sh_f and bh_f under control conditions may be helpful in achieving high oxygen extraction rates, although further research needs to elaborate exact patterns of blood and water flow at gas exchange epithelia. Finally, factorial scopes of 2 to 3 for AVC blood flow during exercise match scopes reported for other cephalopods (*O. vulgaris*) with a comparable lifestyle (Wells and Wells 1991).

5. Acknowledgements

This study was carried out in support of the project: The cellular basis of standard and active metabolic rate in the free-swimming cephalopod, *Sepia officinalis* (NERC Grant PFZA/004). The authors wish to thank Timo Hirse for excellent technical support, Raymond and Marie - Paule Chichery (Université de Caen) for providing cuttlefish eggs in 2002 and 2003 and all student helpers that were engaged in raising the animals in our lab. Special thanks to Alison King for helpful and stimulating discussions on the subject of venous return in cephalopods.

6. References

AITKEN, J.P. AND O'DOR, R.K. (2004). Respirometry and swimming dynamics of the Australian cuttlefish *Sepia apama*. *Mar. Freshw. Behav. Physiol.* **37**, 217-234.

AITKEN, J. P., O'DOR, R. K. AND JACKSON, G. D. (2005). The secret life of the giant cuttlefish *Sepia apama* (Cephalopoda). Behaviour and energetics in nature revealed through radio acoustic positioning and telemetry (RAPT). *J. Exp. Mar. Biol. Ecol.* **320**, 77-91.

BERT, P. (1867). Mémoire sur la physiologie de la Seiche. *Mém. Soc. Sci phys. Nat. Bordeaux* **5**, 115.

BOCK, C., SARTORIS, F.J. AND PÖRTNER, H.O. (2002). *In vivo* MR spectroscopy and MR imaging on non anaesthetized marine fish : techniques and first results. *Magn. Reson. Imag.* **20**, 165-172.

BONE, Q., BROWN, E. R. AND TRAVERS, G. (1994). On the respiratory flow in the cuttlefish *Sepia officinalis*. *J. Exp. Biol.* **194**, 153-165.

BOURNE, G.B., REDMOND, J.T. AND JOHANSEN, K. (1978). Some aspects of heemodynamics in *Nautilus pompilius*. *J. Exp. Zool.* **205**, 63-70.

BOURNE, G. B. (1982). Blood pressure in the squid, *Loligo pealei*. *Comp. Biochem. Physiol.* **72**A, 23-27.

BOURNE, G. B. (1987). Hemodynamics in squid. *Experientia* 43, 500-502.

DENTON, E.J. AND GILPIN - BROWN, J.B. (1961). The effect of light on the buoyancy of the cuttlefish. *J. mar. biol. Ass. U.K.* **41**, 343-350.

DE WILDE, J. (1956). Koordination im Gefässsystem von *Octopus vulgaris*. *L. Pubbl. staz. zool. Napoli* **28**, 359-366.

FIEDLER, A. (1992). Die Rolle des venösen Füllungsdrucks bei der Autoregulation der Kiemenherzen von *Sepia officinalis* L. (Cephalopoda). *Zool.jb. Physiol.* **96**, 265-278.

HAASE, A. (1990). Snapshot FLASH MRI. Applications to T1, T2 and chemical shift imaging. *Magn. Reson. Med.* **13**, 77-89.

ISGROVE, A. (1909). Eledone. LMBC Memoirs, Liverpool University Press, 105 pp.
JOAQUIM, N., WAGNER, G.N. AND GAMPERL, A.K. (2004) Cardiac function and critical swimming speed of the winter flounder (*Pleuronectes americanus*) at two temperatures. *Comp. Biochem. Physiol. A* **138**, 277-285.

JOHANSEN, K. AND MARTIN, A. W. (1962). Circulation in the cephalopod, *Octopus dofleini*. *Comp.Biochem. Physiol.* **5**, 161-176.

JOHANSEN, K. (1965). Cardiac output in the large cephalopod *Octopus dofleini*. *J. Exp. Biol.* **42**, 475-480.

JOHANSEN, K., BRIX, O. AND LYKKEBOE, G. (1982b). Blood gas transport in the cephalopod, *Sepia officinalis*. *J. Exp. Biol.* **99**, 331-338.

KING, A.J., HENDERSON, S.M., SCHMIDT, M.H., COLE, A.G. AND ADAMO, S.A. (2005). Using ultrasound to understand vascular and mantle contributions to venous return in the cephalopod *Sepia officinalis* Linneaus. *J. Exp. Biol.* **208**, 2071-2082.

MADAN, J.J. AND WELLS, M.J. (1996). Cutaneous respiration in *Octopus vulgaris*. *J. Exp. Biol.* **199**, 2477-2483.

MATHER, J.A. AND O'DOR, R.K. (1991). Foraging strategies and predation risk shape the natural history of juvenile *Octopus vulgaris*. *Bull. Mar. Sci.* **49**, 256-269.

MARK, F. C., BOCK, C. AND PÖRTNER, H. O. (2002). Oxygen – limited thermal tolerance in Antarctic fish investigated by MRI and ^{31}P – MRS. *Am. J. Physiol.* **283**, R1254-R1262.

MELZNER, F., BOCK, C. AND PÖRTNER, H.O. Critical temperatures in the cephalopod *Sepia officinalis* investigated using *in vivo* ^{31}P NMR spectroscopy, *J. Exp. Biol.*, submitted a.

MELZNER F., BOCK C. AND PÖRTNER, H.O. Temperature dependent oxygen extraction from the ventilatory current and the costs of ventilation in the cephalopod *Sepia officinalis*. *J. Comp. Physiol.* B, submitted b.

MELZNER F., BOCK C. AND PÖRTNER, H.O. The circulatory system limits thermal tolerance in the cephalopod *Sepia officinalis*. *J. Comp. Physiol. B*, submitted, c.

MISLIN, H. AND KAUFFMANN, M. (1948). Der aktive Gefässpuls in der Armschrimhaut der Cephalopoden. *Rev. suisse Zool.* **55**, 267-271.

MISLIN, H. (1950). Nachweis einer reflektorischen Regulation des peripheren Kreislaufs der Cephalopoden. *Experientia* **6**, 467-468.

MISLIN, H. (1966). Ueber die Beziehungen zwischen Atmung und Kreislauf bei Cephalopoden (*Sepia officinalis* L.). Synchronregistrierung von Elektrokardiogramm (Ekg) und Atembewegungen am schwimmenden Tier. *Verh. Dtsch. Zool. Ges.* 175-181.

O'Dor, R. K. and Webber, D. M. (1986). The constraints on cephalopods: why squid aren't fish. *Can. J. Zool.* **64**, 1591-1605.

O'DOR, R. K. and WEBBER, D. M. (1991). Invertebrate athletes: trade-offs between transport efficiency and power density in cephalopod evolution. *J. Exp. Biol.* **160**, 93-112.

PIIPER, J. AND SCHEID, P. (1984). Model analysis of gas transport in fish gills. In: Hoar, W.S. and Randall, D.J. (eds.) Fish physiology.

PÖRTNER, H.O. (1994). Coordination of metabolism, acid-base regulation and haemocyanin function in cephalopods. In *Physiology of Cephalopod Molluscs: Lifestyle and Performance Adaptations*, eds. H.O. Pörtner R. K. O'Dor and D. L. Macmillan, pp. 131-148. Basel: Gordon and Breach.

SCHIPP, R. (1987a). The blood vessels of cephalopods. A comparative morphological and functional survey. *Experientia* **43**, 525-537.

SCHIPP, R. (1987b). General morphological and functional characteristics of the cephalopod circulatory system. An introduction. *Experientia* **43**, 474-477.

SHADWICK, R.E. AND NILSSON, E.K. (1990). The importance of vascular elasticity in the circulatory system of the cephalopod *Octopus vulgaris*. *J. Exp. Biol.* **152**, 471-484.

SHADWICK, R. E., O'DOR, R. K. AND GOSLINE, J. M. (1990). Respiratory and cardiac function during exercise in squid. *Can. J. Zool.* **68**, 792-798.

SHADWICK, R.E. (1994). Mechanical oraganization of the mantle and circulatory system of cephalopods. In *Physiology of Cephalopod Molluscs: Lifestyle and Performance Adaptations*, eds. H. O. Pörtner R. K. O'Dor and D. L. Macmillan), pp. 69-85. Basel: Gordon and Breach.

SMITH, L. S. (1962). The role of venous peristalsis in the arm circulation of *Octopus dofleini*. *Comp. Biochem. Physiol.* **7**, 269-275.

STOREY, K. B. AND STOREY, J. M. (1979). Octopine metabolism in the cuttlefish, *Sepia officinalis*: octopine production by muscle and ist role as an aerobic substrate for non-muscular tissues. *J. Comp. Physiol.* **131**, 311-319.

TOMPSETT, D.H. (1939). Sepia. LMBC Memoirs, Liverpool University Press, 184 pp.

SKRAMLIK, E.v. (1941). Über den Kreislauf bei den Weichtieren. *Ergebn. Biol.* **18**, 88-286.
WEBBER, D.M., BOUTILIER, R.G. AND KERR, S.R. (1998). Cardiac output as a predictor of metabolic rate in cod *Gadus morhua*. *J. Exp. Biol.* **204**, 3561-3570.

WELLS, M. J. (1979). The heartbeat of *Octopus vulgaris*. *J. Exp. Biol.* **78**, 87-104.

WELLS, M.J. (1983). Circulation in cephalopods. In Saleuddin, A.S.M. and Wilbur, K.M. (eds.): *The Mollusca* Vol 5, Physiology Part 2, pp. 239-290. Academic Press, New York.

WELLS, M.J. (1994). The evolution of a racing snail. In *Physiology of Cephalopod Molluscs: Lifestyle and Performance Adaptations*, eds. H. O. Pörtner R. K. O'Dor and D. L. Macmillan), pp. 1-11. Basel: Gordon and Breach.

WELLS, M. J. AND WELLS, J. (1982). Ventilatory currents in the mantle of cephalopods. *J. Exp. Biol.* **99**, 315-330.

WELLS, M. J. AND WELLS, J. (1983). The circulatory response to acute hypoxia in *Octopus*. *J. Exp. Biol.* **104**, 59-71.

WELLS, M. J. AND WELLS, J. (1985). Ventilation frequencies and stroke volumes in acute hypoxia in *Octopus*. *J. Exp. Biol.* **118**, 445-448.

WELLS, M. J. AND WELLS, J. (1986). Blood flow in acute hypoxia in a cephalopod. *J. Exp. Biol.* **122**, 345-353.

WELLS, M. J. AND WELLS, J. (1991). Is *Sepia* really an octopus? In Boucaud-Camou, E. (Ed.), La Seiche, 1st International symposium on the cuttlefish *Sepia*. Centre de publications, Universite de Caen. pp. 77-92.

WELLS, M. J. and SMITH, P. J. S. (1987). The performance of the octopus circulatory system: A triumph of engineering over design. *Experientia* **43**, 487-499.

WELLS, M.J., O'DOR, R.K., MANGOLD, K. AND WELLS, J. (1983). Oxygen consumption and movement by *Octopus*. *Mar. Behav. Physiol.* **9**, 289-303.

WELLS, M. J., DUTHIE, G. G., HOULIHAN, D. F., SMITH, P. J. S. AND WELLS, J. (1987). Blood flow and pressure changes in exercising octopuses (*Octopus vulgaris*). *J. Exp. Biol.* **131**, 175-187.

WELLS, M. J., HANLON, R. T., LEE, P. G. AND DIMARCO, F. P. (1988). Respiratory and cardiac performance in *Lolliguncula brevis* (Cephalopoda, Myopsida): the effects of activity, temperature and hypoxia. *J. Exp. Biol.* **138**, 17-36.

Figure captions

Figure 1: Schematic illustration of Doppler and bridge setup. A) Sagittal view of setup around the anterior vena cava (AVC). B) Transversal view of setup, showing bridge arms. C) Top view of sensor arrangement around the AVC. D = Doppler sensor with wiring (C), B = plastic bridge (7.5 mm width, 7.5 mm length, 6 mm height), A = bridge arms made of 0.5 mm diameter steel surrounded by PE tubing (8 mm total length), S = sutures to anchor bridge setup in place, HRM = head retractor muscles.

Figure 2: Control patterns of ventilation and blood flow in AVC. A) Pressure oscillations in the mantle cavity are due to ventilatory activity. One ventilation period extends from one pressure minimum to the next, all cyclic relationships are expressed in relation to the ventilation period (0 – 360°, see insert c). B) AVC blood velocity. Positive values indicate flow towards the lateral venae cavae and gill hearts, negative values reverse flow. Each blood flow pulse consists of two peaks of differing magnitude, usually separated by a local flow minimum, peak A (minor flow) and peak B (major flow, see inserts). Peak A can even display larger values (e.g. see fig 4a) than witnessed in this example. C) First derivative of the pressure curve displayed in A).

Figure 3: Phase relationships between phase angle of maximum mantle cavity pressure slope (ϕ_1 in ° phase) and of the main blood flow peak, peak B (ϕ_2 in ° phase) yielding a linear regression equation of $y = 0.92x + 4.9$ (R^2=0.93, $p<0.001$). As the 95% confidence interval for x includes 1 (i.e. $0.67 \leq x \leq 1.172$), it is straightforward to assume that the regression slope cannot differ significantly from one. Means and SD for 15 ventilation / blood flow pulses analyzed for each animal, with animal numbers included in the figure.

Figure 4: Correlated blood flow and mantle cavity pressure peaks during control (a), moderate (b) and most severe (c) exercise. AVC blood velocity in cm s^{-1} (red), mantle cavity pressure in kPa (blue).

Figure 5: Exercise effects on AVC blood flow. A) and B) A typical short exercise sequence (animal 18) as frequently encountered in all investigated animals. Top panels show mantle cavity pressure changes, lower panels AVC blood velocity (AVC_V). C) - F) Changes in AVC haemodynamic and ventilatory parameters during exercise and recovery in animal #8. One minute mean values and SD (obtained by averaging six ten second intervals); C = control, E = exercise. Symbols indicate levels significantly elevated above controls (=minute one values; ANOVA and Student - Newman - Keuls posthoc testing). C) mean mantle pressure (MMP) and AVC minute volume (AVC_{MV}). 23 SJs similar to those shown in fig 4A and 4B caused MMP to rise in minutes three and four, D) average maximum AVC blood velocity ($AVC_{av\ max\ V}$), E) AVC blood pulse frequency (AVC_f) (equivalent to v_f), F) AVC stroke volume (AVC_{SV}).

Figure 6: Magnetic resonance imaging (MRI) analyses of blood flow and blood pulse rates in major blood vessels under control conditions. A) - H): Series of seven consecutive MR images, shot in the transversal plane prior to forking of the AVC. Bright regions within images correspond to flow (=blood flow pulses); blood flow in efferent and afferent branchial vessels (affBV and effBV) and AVC is more clearly visible than pulsations in the cephalic artery (CA). Each image comprises flow information for 0.82 seconds. I) Mantle cavity pressures during acquisition of images. J) Flow information extracted from the seven images displayed above. Each symbol represents the mean flow intensity for 0.82 seconds in the respective vessels, data fitted by spline curves.

Table 1. Hemodynamic and ventilatory parameters under control conditions (14-15°C in experiment 1, 15°C in experiment 2).

Exp 2 parameter (N=8-10)	*Mean (SD)*
Mass (g)	231.7 (29.7)
MMP [Pa]	19.8 (7.6)
v_f [strokes min^{-1}]	29.0 (5.2)
AVC_f [strokes min^{-1}]	29.0 (5.2)
AVC_{MV}[ml min^{-1}]	5.5 (2.8)
AVC_{SV}[ml $stroke^{-1}$]	0.204 (0.11)
$AVC_{av\ max\ V}$[cm s^{-1}]	14.2 (7.1)
AVC net flow [% of cycle]	53.7 (4.5)
AVC pulse a duration [% of cycle]	26.4 (3.1)
AVC pulse b duration [% of cycle]	27.3 (3.4)
AVC flow pulse a [% of total flow]	11.7 (5.2)
AVC flow pulse b [% of total flow]	88.3 (4.8)
max slope MP time – start pulse b time [°phase shift]	1.2 (8.1)
Exp 1 parameter (N=5)	*Mean (SD)*
Mass (g)	104.2 (7.4)
MMP [Pa]	19.7 (5.3)
v_f [strokes min^{-1}]	31.6 (2.1)
AVC_f [strokes min^{-1}]	31.6 (2.1)
CA_f [strokes min^{-1}]	30.3 (1.5)
aff BV_f [strokes min^{-1}]	31.6 (2.1)

Table 2. Mantle cavity pressures during swimming jets (SJ). N = 60 SJs from 6 animals. MMP = mean mantle pressure = mantle cavity pressure integral during intervals d and e (see fig 4 and text for definition of intervals); MP at $AVC_{max\ V}$ = mantle cavity pressure at maximum AVC blood velocity.

Parameter	*Mean (SD; range)*
SJ amplitude (interval d) [kPa]	3.86 (3.11; 1.0-19.5)
MMP (interval d) [kPa]	1.49 (1.03; 0.4-6.9)
MMP (interval e) [kPa]	1.55 (1.06; 0.5-7.6)
MP at $AVC_{max\ V}$ [kPa]	2.01 (1.43; 0.6-6.9)

Table 3. Changes in blood flow induced by spontaneous exercise. Exercise periods were randomly chosen for six animals (replicates 8, 9, 13, 18, 19 and 21) in experiment 2. 30 minute periods of exercise and recovery were analyzed for maximum increases in haemodynamic and ventilatory parameters. Table 2A) provides control (minute 1), maximum (max) values and scopes for increases in each parameter. $AVC_{MV(exercise)}$ refers to blood flow during the $MMP_{(max)}$ minute interval; Δ time [min] is the time difference between MMP and AVC_{MV} maxima. Table 2B) gives frequencies and amplitudes of swimming jets (SJs) encountered during the respective exercise bouts. From these we calculated two variables (JI and JD) from which levels of inorganic phosphate (P_i) accumulation in the mantle muscle organ could be estimated ($\Delta[P_i]$ (μmol g^{-1} ww^{-1}) = 0.0335 JI + 0.1555 JD; see Melzner, Bock, Pörtner, submitted a for details). Phosphagen (PLA) use during high amplitude pressure generation was estimated from P_i accumulation (as PLA is split into L-arginine and P_i).

A

	Rep19	*Rep18*	*Rep21*	*Rep8*	*Rep9*	*Rep13*	*mean*	*SD*	*p*
1) $MMP_{(control)}$ [Pa]	22.6	19.9	20.6	24.0	25.5	24.3	22.8	2.2	
2) $MMP_{(max)}$ [Pa]	138.7	150.7	349.6	298.8	176.9	172.7	214.6	87.6	<0.002
Max scope [2/1]	6.1	7.6	17.0	12.5	6.9	7.1	9.5	4.3	
3) $AVC_{MV(control)}$ [ml min^{-1}]	8.2	2.5	7.5	2.1	3.0	3.2	4.4	2.7	
4) $AVC_{MV(exercise)}$ [ml min^{-1}]	9.4	3.3	2.8	2.2	5.1	3.5	4.4	2.6	N.S.
5) $AVC_{MV(max)}$ [ml min^{-1}]	17.2	4.3	20.4	4.0	7.7	6.0	9.9	7.1	<0.02
Max scope [5/3]	2.1	1.7	2.7	1.9	2.6	1.9	2.2	0.4	
Δ time [min] ($AVC_{MV(max)}$ - $MMP_{(max)}$)	2.0	1.0	2.0	1.0	2.0	2.0	1.7	0.5	
6) $v_{f\,(control)}$ [strokes min^{-1}]	27.3	25.7	24.8	30.9	27.8	27.9	27.4	2.1	
7) $v_{f\,(max)}$ [strokes min^{-1}]	46.6	46.7	43.1	42.6	48.0	40.2	44.5	3.0	<0.001
Max scope [7/6]	1.7	1.8	1.7	1.4	1.7	1.4	1.6	0.2	
8) $AVC_{av\ max\ v\ (control)}$ [cm s^{-1}]	23.9	5.5	21.9	5.2	9.7	9.2	12.6	8.2	
9) $AVC_{av\ max\ v\ (max)}$ [cm s^{-1}]	32.5	9.5	36.7	7.4	16.1	15.6	19.6	12.2	<0.006
Max scope [9/8]	1.4	1.7	1.7	1.4	1.7	1.7	1.6	0.2	
10) $AVC_{SV\ (control)}$ [ml $stroke^{-1}$]	0.30	0.10	0.30	0.07	0.11	0.10	0.16	0.11	
11) $AVC_{SV\ (max)}$ [ml $stroke^{-1}$]	0.40	0.09	0.52	0.11	0.19	0.15	0.24	0.17	N.S.
Max scope [11/10]	1.3	1.0	1.7	1.6	1.8	1.6	1.5	0.3	

B

	# of SJs with amplitudes between						*JI*	*JD*	*Δ[P_I] (μmol g^{-1} ww^{-1})*	*Δ PLA (% control)*	*Sig. elevated AVC_{MV} (min)*
	0.2 ≤ 1 kPa	*1 ≤ 2 kPa*	*2 ≤ 3 kPa*	*3 ≤ 4 kPa*	*4 ≤ 5 kPa*	*5 ≤ 6 kPa*					
rep19	10	9	3	0	0	0	7.5	0	+0.25	-0.75	1
rep18	11	5	3	0	1	0	12.0	0	+0.40	-1.20	2
rep21	13	12	3	8	10	2	91.5	2	+3.38	-10.05	12
rep8	3	9	7	2	1	1	34.5	1	+1.31	-3.90	6
rep9	15	15	2	0	0	1	10.5	1	+0.51	-1.51	2
rep13	16	7	3	2	0	0	14.5	0	+0.49	-1.45	2
mean									+1.06	-3.14	4.17

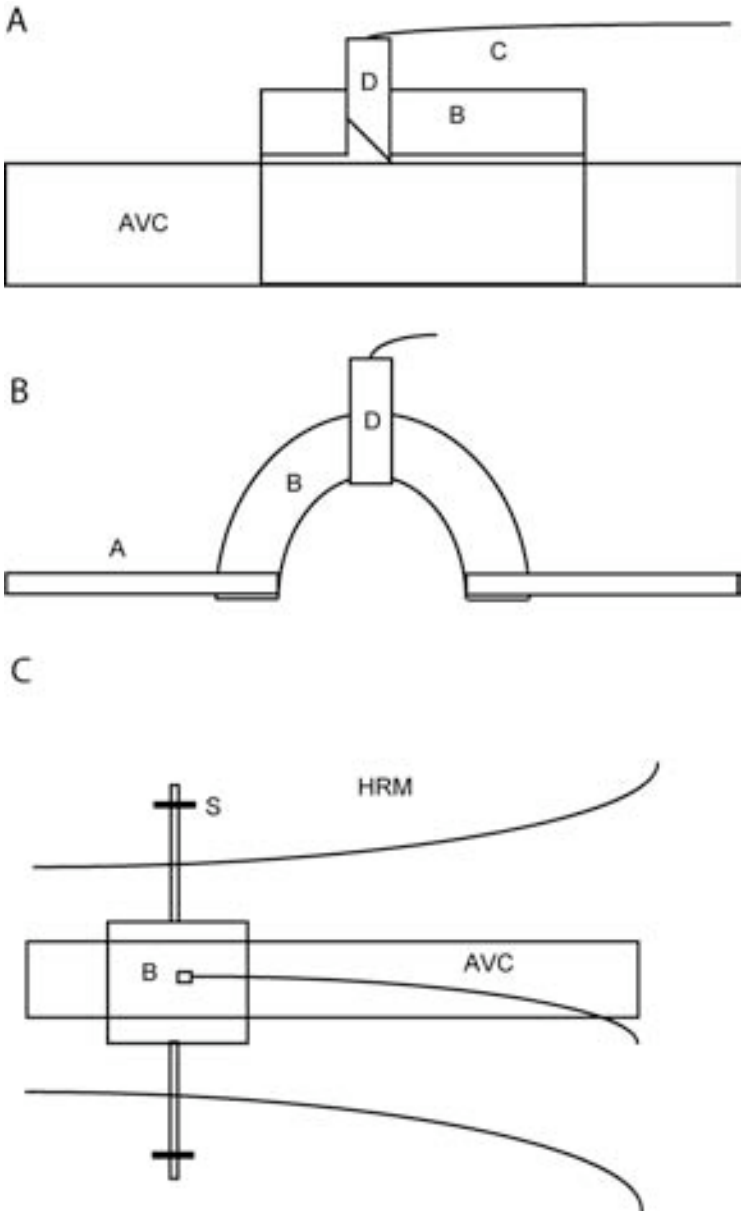

Figure 1

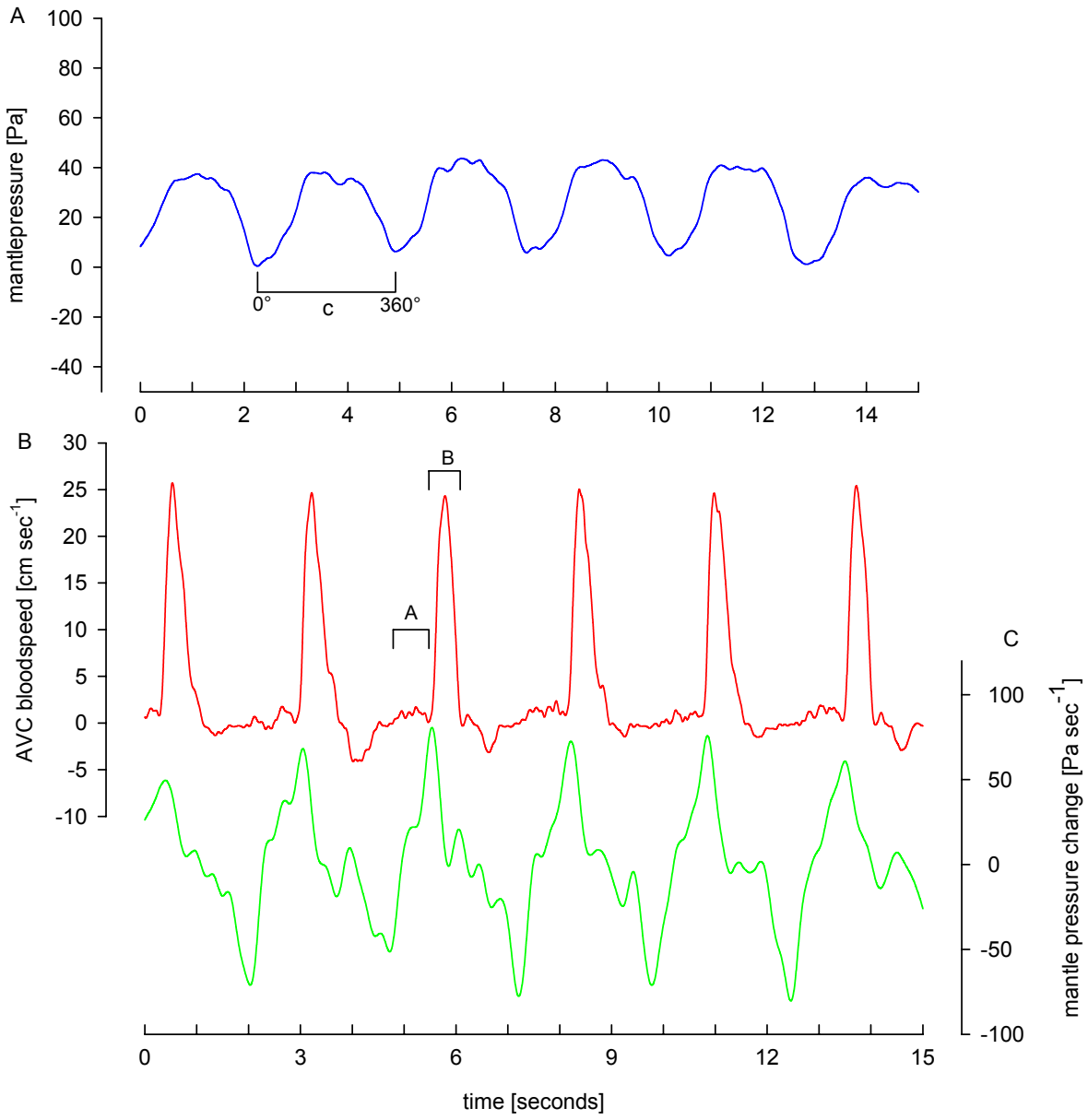
A
mantlepressure [Pa]
100
80
60
40
20
0
-20
-40
0°
c
360°
0
2
4
6
8
10
12
14
B
AVC bloodspeed [cm sec-1]
30
25
20
15
10
5
0
-5
-10
A
B
C
mantle pressure change [Pa sec-1]
100
50
0
-50
-100
0
3
6
9
12
15
time [seconds]

Figure 2

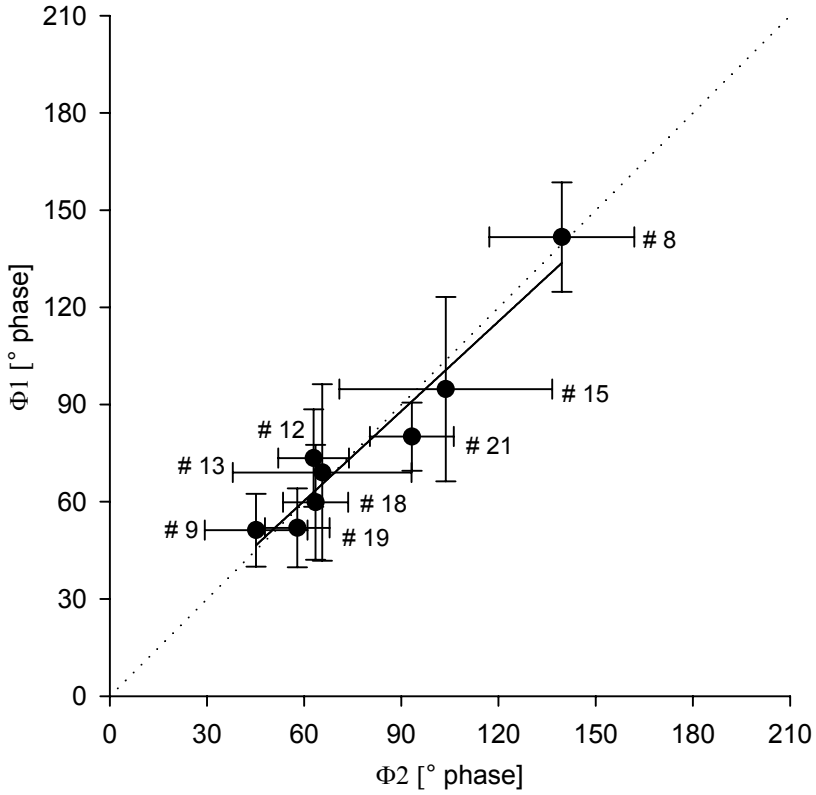
210
180
150
120
90
60
30
0
Φ1 [° phase]
0
30
60
90
120
150
180
210
Φ2 [° phase]
8
15
12
21
13
18
9
19

Figure 3

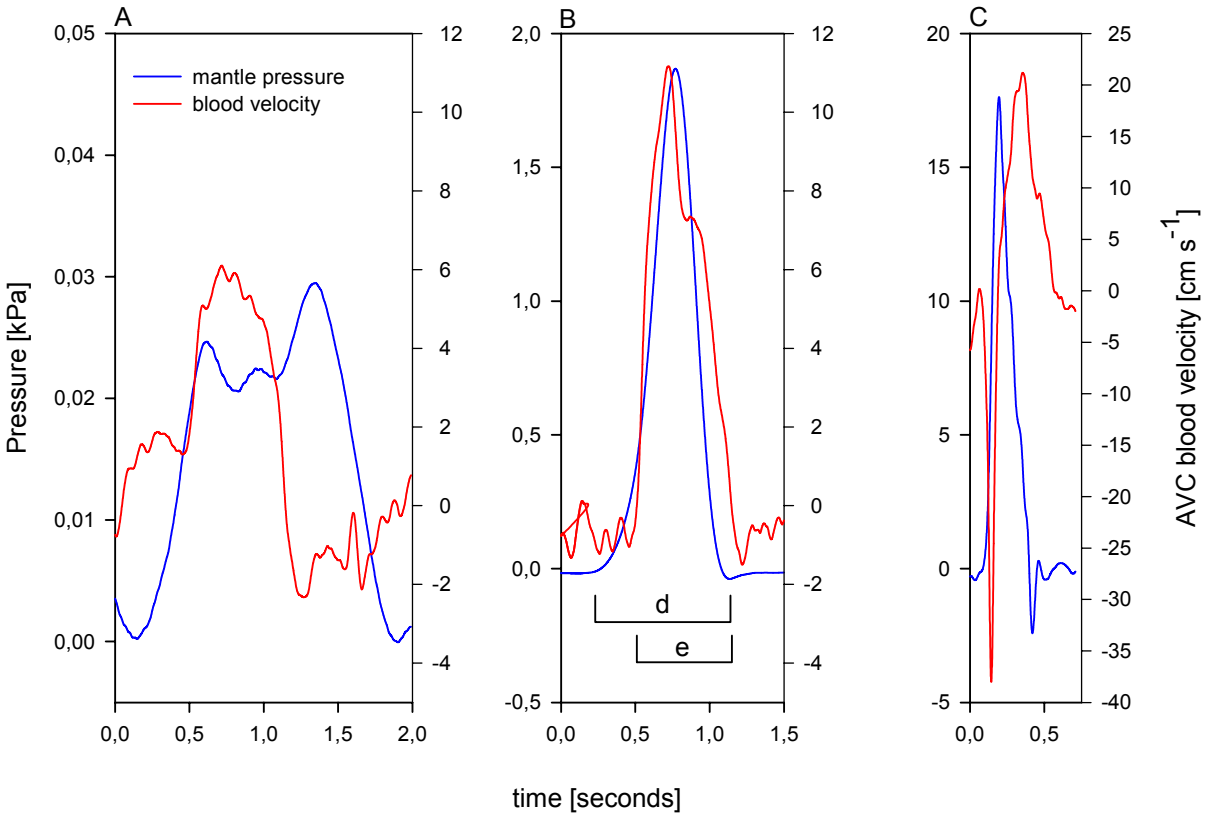
A
B
C
mantle pressure
blood velocity
Pressure [kPa]
AVC blood velocity [cm s-1]
time [seconds]
d
e
0,05
0,04
0,03
0,02
0,01
0,00
2,0
1,5
1,0
0,5
0,0
-0,5
20
15
10
5
0
-5
12
10
8
6
4
2
0
-2
-4
25
20
15
10
5
0
-5
-10
-15
-20
-25
-30
-35
-40
0,0
0,5
1,0
1,5
2,0

Figure 4

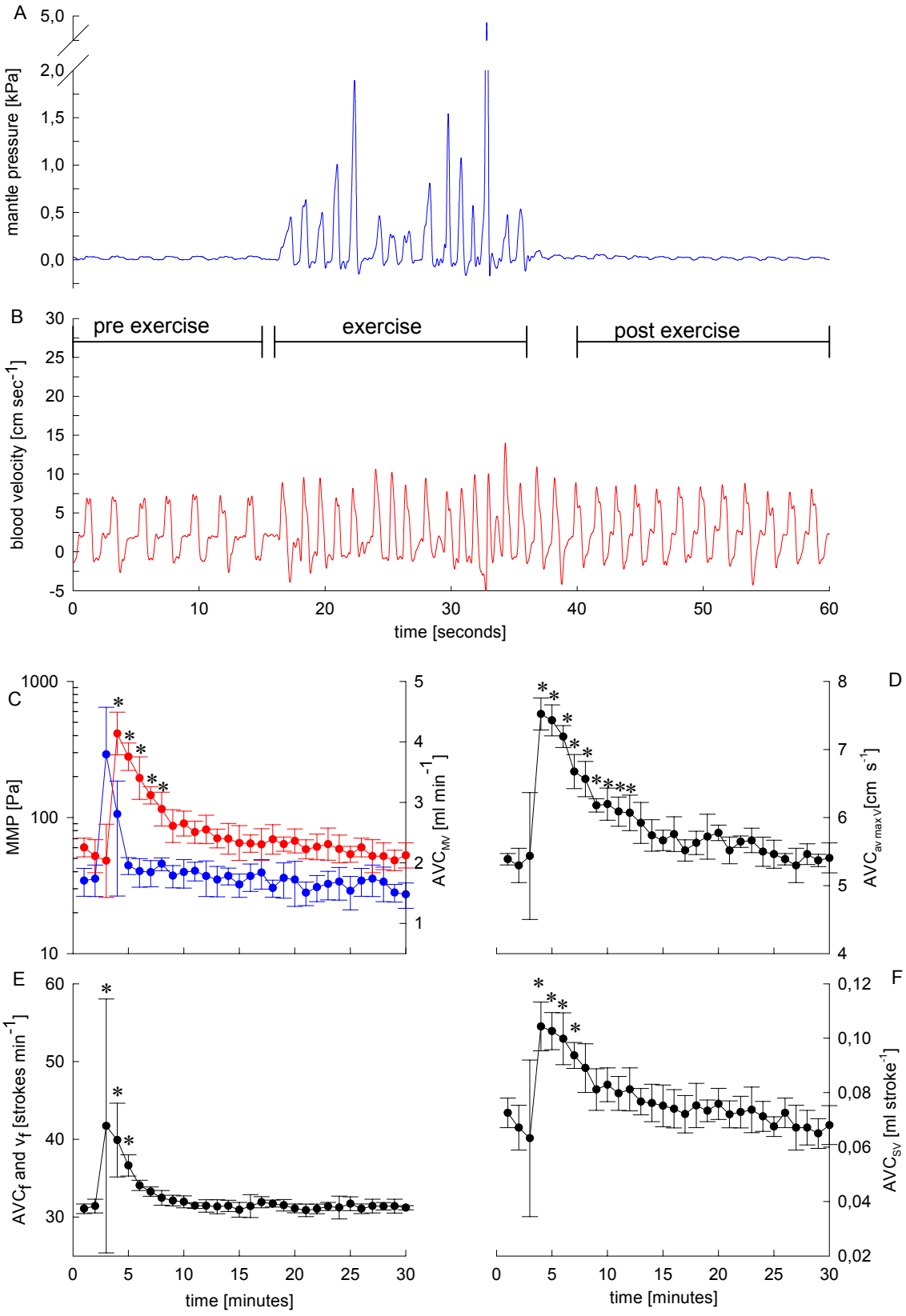
A
mantle pressure [kPa]
B
blood velocity [cm sec-1]
pre exercise
exercise
post exercise
time [seconds]
C
MMP [Pa]
AVCMV [ml min-1]
D
AVCav max V [cm s-1]
E
AVCf and vf [strokes min-1]
time [minutes]
F
AVCSV [ml stroke-1]
time [minutes]

Figure 5

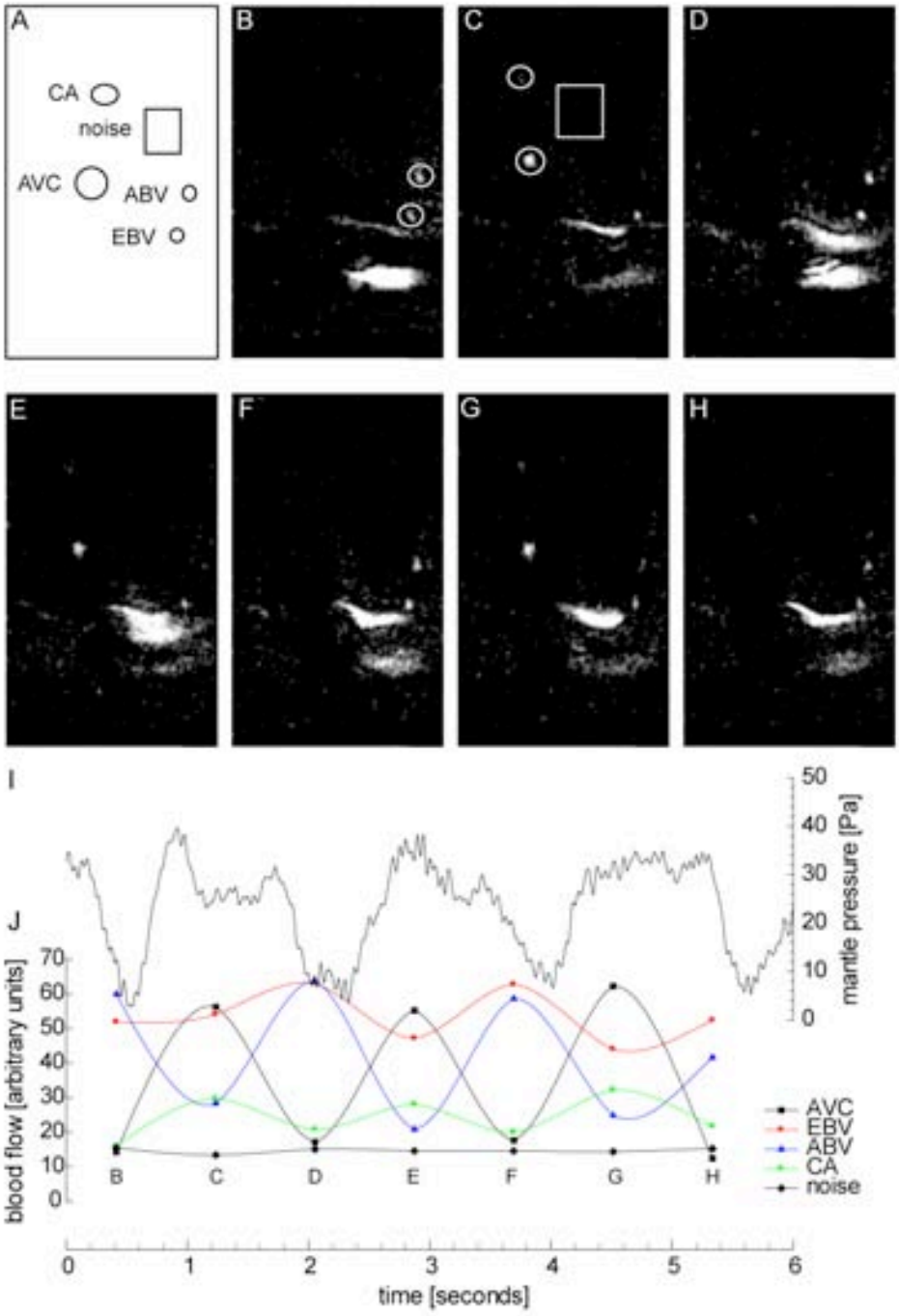
A
CA
noise
AVC
ABV
EBV
B
C
D
E
F
G
H
I
J
blood flow [arbitrary units]
mantle pressure [Pa]
time [seconds]
AVC
EBV
ABV
CA
noise

Figure 6

The circulatory system limits thermal tolerance in the cephalopod *Sepia officinalis*

Frank Melzner*, Christian Bock, Hans – O. Pörtner

Alfred Wegener Institute for Marine and Polar Research, Am Handelshafen 12, 27570 Bremerhaven, Germany

short title: circulation and ventilation in cuttlefish

Key words: cephalopoda, cuttlefish, venous return, thermal limits, ventilation, circulation, critical temperatures, anaerobic metabolism

* Author to whom correspondence should be addressed:
phone: +49-471-4831-1331; fax: +49-471-4831-1149;
email: fmelzner@awi-bremerhaven.de

1. Summary

It has recently been shown that the cuttlefish *Sepia officinalis* are limited by oxygen supply at approaching thermal extremes. By means of ^{31}P NMR spectroscopy, anaerobic metabolism was observed to supplement aerobic energy production in ventilatory mantle muscle at mean temperatures at 7 and 26.8°C, respectively. At temperatures of 11 and 23°C, routine metabolic rate (rmr) already started to drop below expected values, indicating a limitation of oxygen supply before the onset of anaerobic metabolism. It was hypothesized that circulatory capacity limitations were responsible for this mismatch. Therefore, the present study examined patterns of blood flow in the anterior vena cava (AVC), the most important cephalopod vein, with a Doppler flow probe. Accordingly, between 30 and 70% of cardiac output pass through the AVC between 11 and 23°C. AVC blood pulses are biphasic (consisting of peak A and B, with B providing >50 of total blood flow between 11 and 23°C) and are obligatorily coupled to ventilatory pressure oscillations in the mantle cavity at all temperatures tested. AVC minute volume (AVC_{MV}) increased 2.2-fold from control 15°C to 23°C. 1.6-fold increments in both, AVC blood pulse frequency (AVC_f) and AVC mean maximum pulse velocity ($AVC_{av\ max\ V}$) were shown to be responsible for the increase in minute volume. Above an AVC_f of 46-50 beats min^{-1}, occurring at 22-23°C, blood flow pulse shape changed dramatically (peak A provided the majority of flow) and $AVC_{av\ max\ V}$ could not be maintained at high levels, suggesting that mechanical constraints in vessel function cause an AVC_{MV} capacity limitation at temperatures > 23°C, that eventually results in an internal hypoxia. At temperatures below 11°C, AVC blood pulse shape detrimentally changed in a similar manner as observed at high temperatures (peak A dominance). In addition, constant AVC_{MV} between 11 and 8°C at decreasing rmr may indicate a temperature limitation of haemocyanin oxygen shuttling. In summary, the present study revealed, that as in their high – power teleost competitors, thermal tolerance in cephalopods becomes limited mainly by circulatory system mechanical design.

2. Introduction

An oxygen limitation of thermal tolerance has been proposed a universal principle for water breathing ectothermal animals (Pörtner 2001, 2002). In a recent report, we could demonstrate that, in fact, anaerobic metabolism needs to supplement aerobic metabolism of ventilatory muscle in laboratory raised cuttlefish *S. officinalis* when approaching both cold and warm extremes. Metabolic limitation of cellular function was first reflected in decreasing phosphagen levels (phospho - L - arginine, PLA) in the mantle muscle organ, thereby indicating critical temperatures (T_cs) at mean threshold temperatures of 7.0 and 26.8°C (Melzner, Bock, Pörtner, submitted a).

Consequently, we examined the cuttlefish ventilatory system in greater detail, trying to elucidate whether ventilatory muscle fatigue, as elicited by excessive ventilatory muscle power output in response to altered water convection requirements, may be the limiting factor setting T_cs. However, owing to low ventilation pressures and low ventilatory water volumes, ventilation costs (in % of routine metabolic rate, rmr) likely never exceed an upper boundary of 16% at the highest temperatures, and are extremely low (<1% rmr) at the lowest temperatures. In addition, model calculations demonstrated that ventilatory effort should always be sufficient to maintain the high arterial oxygen partial pressures witnessed under control conditions in *S. officinalis* (e.g. Johansen et al. 1982), which, presumably, are needed for full haemocyanin oxygen loading in the gills and for proper heart functioning (Melzner, Bock, Pörtner, submitted b). At the same time, rmr was shown to deviate from the expected exponential relationship with temperature (e.g. Hemmingsen 1960, O'Dor and Wells 1987) already between 11 and 8°C in the cold and between 23 and 26°C in the warm. In both cases, less oxygen was consumed than predicted indicating onset of metabolic depression due to endogenous hypoxia (Melzner, Bock Pörtner, submitted b,c, Pörtner et al., 2004). We therefore hypothesized, that the observed PLA use at T_cs is secondary to an insufficient capacity of the circulatory system to cover the oxygen demand of working ventilatory muscles, similar to findings in

various fish species (Heath and Hughes 1973, Mark et al. 2002, Lannig et al. 2004). The present study was designed to test this hypothesis.

Little is known about circulatory performance and blood flow in cephalopods and even less about its temperature dependence. No study has determined the integration of circulation, blood flow and corresponding ventilatory pressures in the mantle cavity. The present and a precursor study (Melzner, Bock, Pörtner, submitted d) are the first to qualify and quantify patterns of blood flow in a major cephalopod vein, the anterior vena cava (AVC). The only other investigations measuring blood flow in cephalopods are those of Wells and colleagues, focusing on cephalic artery flow in octopods during exercise and hypoxia (Wells and Wells 1986, Wells et al. 1987). We chose to study blood flow in the anterior vena cava (AVC) for several reasons:

(1) Placement of a Doppler – bridge arrangement on top of the AVC is minimally invasive. Access to the systemic heart and dorsal aorta (in contrast to fish, e.g. Webber et al. 1998) is more difficult (especially in cuttlefish, Tompsett 1939), and would require major surgery to place flow probes around the respective vessel (e.g. Wells and Wells 1986); (2) The AVC transports a large fraction of cardiac output (27-70%, see results). (3) The AVC drains organ systems, whose proper functioning is critical under all circumstances. This includes the brain and the collar flaps of the funnel apparatus, which generate the pressures driving expiration (Bone et al. 1994). It is thus unlikely to expect a redistribution of blood flow which favours other organs at the expense of reduced blood flow to the head. In fish blood flow is commonly observed to be restricted to certain organ systems during exercise or environmental stresses (e.g. the gastrointestinal system, Randall and Daxboeck 1982, Axelsson and Fritsche 1991). In contrast, flow to the brain is typically increased relative to control levels during acute environmental stresses (e.g. hypoxia in fish and turtles, Nilsson et al. 1994, Hylland et al. 1994). Thus, available comparative evidence suggests that the AVC likely is a very good indicator vessel to monitor a cephalopods' circulatory potential under stressful conditions. (4) Blood flow through the AVC was found to be closely correlated to pressure oscillations in the mantle cavity (Melzner, Bock, Pörtner, submitted d). This is especially important, as it allows monitoring the functional integration of both, circulation and ventilation, during acute temperature change. According to the hypothetical framework of our investigations (i.e. Pörtner 2002) we would expect a thermal

limitation of animal metabolism to occur first at the highest hierarchical levels of the oxygen transport system, the functional integration of the two major convection systems.

3. Material and Methods

3.1 Definitions

We will make use of the term ‚anterior vena cava (AVC)' instead of ‚cephalic vein', as the respective vein is called in the standard treatise on cuttlefish anatomy (Tompsett, 1939). This makes sense, as in the octopod literature, the homologous vessel is also termed AVC, while ‚cephalic vein' refers to a circular vein in the octopod head that collects factors from the arms (Isgrove 1909, Smith 1962).

Aerobic scope (AS) refers to increases in whole animal oxygen consumption above ‚routine metabolic rate' *sensu* Fry (1947), i.e. the difference between maximum and routine metabolic rate. Factorial aerobic scope (fAS) is used as maximum (aerobic) metabolic rate (mmr) divided by routine metabolic rate (rmr) (e.g. Farrell 1996). Factorial scopes for AVC blood flow and cardiac output (Q) follow the same reasoning (maximum rates of blood flow at mmr / rates of blood flow at rmr).

3.2 Animals

European cuttlefish (*Sepia officinalis*) used in the present study were grown from egg clusters trawled in the Bay of Seine (France) in May 2002, kindly provided to us by M.P. and R. Chichery. The animals were raised in a closed re-circulated aquaculture system ($20m^3$ total volume, protein skimmers, nitrification filters, UV – disinfection units) at the Alfred–Wegener–Institute on a diet of mysids (*Neomysis integer*) and brown shrimp (*Crangon crangon*) under a constant dark–light cycle (12 – 12) and constant temperature regime (15°C ±0.1°C). Water quality parameters were monitored three times per week. Concentrations of ammonia and nitrite were kept below 0.2 mg l^{-1}, nitrate concentrations below 80 mg l^{-1}. Salinity was maintained between 32 and 35‰, pH between 8.0 and

8.2. All animals were raised in the same $3m^3$ volume tank. Animal masses were 231.7 g (SD: 29.7g, N = 10 animals). Experiments were carried out between July and October 2003, thus with animals ranging in age between 14 and 17 months.

3.3 Experimental protocol

Experimental animals were starved for 24 hours, then transferred to the experimental setup. Surgery was conducted on the first day. Animals were equipped with a permanent catheter to record post-branchial ventilatory pressure in the mantle cavity and with a miniature Doppler sensor, fitted around the anterior vena cava (AVC) at a position slightly (2-3 mm) posterior of the ventral nerves (see Tompsett 1939). Surgery procedures, sensor design and experimental set-up have been described in detail in a previous report (Melzner, Bock, Pörtner, submitted d). Surgery was followed by an overnight acclimatization period within the experimental set-up at a constant 15°C (±0.1°C). *In vivo* ^{31}P - NMR – spectra showed that anaesthesia during surgery resulted in a transient accumulation of inorganic phosphate (P_i) in the cuttlefish mantle muscle organ, which could be fully reversed within 4-6 hours of recovery under control conditions (Melzner, Bock, Pörtner, submitted a). By use of programmable cryostats (Julabo, Germany) ambient water temperature was lowered continuously and automatically at a rate of 1°C h^{-1} on day two from 15 to 7°C (09:00-18:00 hours), and was brought back and maintained at the control temperature of 15°C for 10h (18:00-04:00 hours). On day three (07:00-19:00 hours) temperature was raised from 15 to 27°C. Both mantle cavity pressure and AVC blood flow were recorded continuously at a sampling rate of 100 – 400 Hz. Mantle cavity pressure and blood flow recordings obtained under control conditions from the same experimental animals between day 1 and day 2 (until 10:00 hours) were used for an in depth analysis of the integration of blood flow patterns and mantle cavity pressures at rest and under conditions of spontaneous exercise at 15°C (Melzner, Bock, Pörtner, submitted d). This enabled us to compare maximum blood flow levels elicited by spontaneous exercise and changing temperature.

3.4 Data analysis

All mantle cavity pressure and Doppler data were analyzed using Chart 5.0 software (AD Instruments, Australia). Ventilation frequency (v_f) and cephalic vein pulse frequency (AVC_f) were determined during the entire experimental period by automatically counting pressure or flow peaks. Voltage Doppler output was converted to velocities and volume flow using the Doppler equation ($V = (F_dC) (2F_0 \cos A)^{-1}$; with V = velocity in mm s^{-1}, F_d = Doppler shift frequency in kHz (the instrument was calibrated to 0.5 V phasic output = 1 kHz Doppler shift), C = velocity of sound in blood (1,565,000 mm s^{-1}), F_0 = transmitter frequency (20,000 kHz), A = angle between sound beam and velocity vector = 45°) and an average cephalic vein diameter of 2.8 mm (0.2 mm SD). Velocity profiles across the vessel hypotenuse were measured analogous to Webber et al. (1998) to calculate total blood flow from maximum blood velocity. Over the entire experiment, resting venous flow pulses were integrated to yield average blood minute volumes (AVC_{MV} in ml min^{-1}) and, in combination with AVC_f, stroke volumina (AVC_{SV} in ml blood $pulse^{-1}$). Also, average peak blood pulse velocities were determined ($AVC_{av\ max\ V}$ in cm s^{-1}). Positive velocities correspond to forward flow events (=flow in the gill direction), negative velocities to backward flow (=flow in the head direction). All parameters were determined for consecutive 10 minute periods, values were grouped in 1°C intervals and averaged (e.g. values from temperatures between 6.5 and 7.4°C were assigned to be 7°C).

Cardiac output (Q, ml kg^{-1} min^{-1}) was calculated to estimate the fraction of total blood flow passing though the AVC. Q estimates are based on the Fick principle, using a blood oxygen carrying capacity of 1.49 mmol l^{-1} as determined for *S. officinalis* from the English Channel population, and values for the amount of oxygen utilized from the blood (Ut, Ut = arterial – venous blood oxygen content / carrying capacity * 100) 80%, respectively (Johansen et al 1982). MO_2 values were calculated using a two factorial regression that incorporates temperature and animal mass, as obtained in a previous study that used animals from the same population under similar experimental conditions ($\ln MO_2 = -3.3 + 0.0945\ T - 0.215 \ln m$ ($R^2 = 0.93$), with T = temperature in °C, m = wet mass in g, MO_2 = routine metabolic rate in μmol O_2 g^{-1} min^{-1}, Melzner, Bock, Pörtner, submitted c).

Phase relationships of venous flow pulses relative to mantle cavity pressure pulses within representative sequences were analyzed in 6 animals, chosen because both recordings of mantle pressure and blood flow displayed very high quality (15 pressure and blood flow cycles were analyzed per animal at temperatures of 8, 11, 14, 15, 17, 20, 23 and 26°C). All phase comparisons were expressed in relation to the mantle cavity pressure period, with one full period (= one ventilatory stroke) corresponding to 360° phase and 0° and 360° defined to be minimum mantle cavity pressures. Typical blood pulses in the AVC under control conditions are biphasic: A minor flow peak (peak A) is followed by a major flow peak (peak B), which, at 15°C, contains 88% of total blood pulse flow. Analogous to our analyses under control conditions (Melzner, Bock, Pörtner, submitted d), we determined phase angles (ϕ) for the maximum mantle cavity pressure increase:

$$\phi_1 = T_{\text{max slope MP}} / v_p * 360° \quad (1)$$

and phase angles for the onset of main blood flow peaks start (termed peak B)

$$\phi_2 = T_{\text{start peak B}} / v_p * 360° \quad (2)$$

Phase shifts (δ) between both events were calculated for each of the six animals at each temperature:

$$\delta = \phi_1 - \phi_2 \quad (3)$$

with $T_{\text{max slope MP}}$ = time point of maximum mantle cavity pressure increment (=maximum slope of the pressure curve), measured (in s) from the start of the corresponding mantle cavity pressure period; $T_{\text{start peak B x,y,z}}$ = start of the main blood flow peak, measured (in s) from the start of the corresponding mantle cavity pressure period; v_p = duration of the respective mantle cavity pressure period (in s). Phase shifts were compared with those obtained under control conditions in our parallel study.

In addition, we investigated forward flow duration (=time interval with positive blood flow during each ventilation period) and the relative flow contributions of blood flow peaks A and B to total blood pulse flow for the same 6 animals (see fig 1, 3 and our companion paper for peak definitions). Again, 15 blood pulses were analyzed per animal and temperature.

3.5 Statistics

All statistics were performed using STATISTICA software (Statsoft, Version 5.1, 1997). Percent values (i.e. % contribution of peak A to blood pulse flow, % time of forward flow) were arcsine transformed prior to statistical treatment. One-way analysis of variance was performed on temperature grouped data, and, if appropriate, Student-Newman-Keuls (SNK) posthoc tests. Regression analysis and curve fitting was performed using SigmaPlot 9.0.

4. Results

The anterior vena cava (AVC) is the single most important vein in coleoid cephalopods, as it leads back all blood from the animals' head towards the gill apparatus. Table 1 gives (rough) Fick principle based estimates of the percentage values of cardiac output (Q) that pass through the AVC in a temperature range between 11 and 23°C. Using a value of 80% blood oxygen utilization, it appears that 27-47% (41-71%) of Q are being led through the AVC in the respective temperature range. At any constant Ut, the percent fraction of Q passing though the AVC initially increases with temperature, but remains fairly constant between 17 and 23°C at values of 66-71%.

Figure 1 depicts exemplary patterns of AVC blood flow and correlated ventilatory mantle cavity pressure pulses for a temperature range between 7 and 26°C (animal #19). As witnessed in a previous study under control conditions (15°C), each blood flow pulse is tightly coupled to one pressure pulse in the mantle cavity regardless of temperature, ventilation rate or mantle cavity pressure. Typical blood pulses in the AVC under control conditions were found to be biphasic (Figure 3): A minor flow peak (peak A) is followed by a major flow peak (peak B). The latter is tightly coupled in phase to ventilatory pressure oscillations in the mantle cavity in that it starts exactly at the phase angle of maximum mantle cavity pressure increase. Both peaks are usually separated by a local flow minimum (Figure 1).

Figure 2a suggests that the same holds true for all temperatures investigated in the present study. The phase shifts (δ) between ϕ_1 and ϕ_2 do not differ significantly from the phase shift observed under control conditions at 15°C (ANOVA: $F_{(7,40)}=1.94$; $p>0.08$). At 15°C δ did not differ significantly

from zero, indicating that both, maximum pressure slope and start of peak B, occur simultaneously within the ventilatory period. The data suggest that this principle pattern remains unchanged at all temperatures within the thermal tolerance window (Figure 2a), although there is a trend towards higher or lower δ at 8°C versus 26°C, respectively.

However, marked haemodynamic changes occurred in the AVC upon thermal change. First, the duration of the time interval of forward flow (in the gill heart direction) increased with respect to the ventilation period during both warming and cooling. While under control conditions, forward flow occurred during 54% of the ventilation period, this figure rose significantly to > 70% at 8°C, to > 80% at 23°C (ANOVA: $F_{(7,40)}$=8.6; p<0.001; SNK posthoc test results in fig 2b).

The second major change is related to blood volume flow distribution: Fig 3 depicts representative changes in blood flow distribution within blood pulses recorded from animal #19. For this figure, AVC blood velocity is expressed as % maximum pulse velocity to better illustrate differences between pulse shapes at varying temperatures. A black dot indicates the separation point between peaks A and B of each blood pulse. As pulse areas are proportional to blood flow, it appears that peak A is providing more flow to total pulse flow as temperatures deviate from control temperatures of 15°C (see also Figure 2c). Calculating the flow provided by peaks A and B for all animals confirms this observation: with rising and declining temperatures (15°C to 11°C, 15°C to 20°C), there is a clear trend towards more peak A flow during each blood pulse. This trend becomes significant at extreme temperatures of 8°C (44% of total pulse flow during peak A) and at 23 – 26°C (36 – 53% of total pulse flow during peak A) (ANOVA: $F_{(7,40)}$=20.4; p<0.001; SNK posthoc test results in fig 2c). Eventually, two separate peaks can originate from each AVC blood pulse in the warm (seen in 4 out of 6 animals), as the local minimum between peak A and B approaches a velocity of zero (see fig 1h, 26°C).

Figure 4 summarizes the main findings in anterior vena cava (AVC) haemodynamics obtained under conditions of acute temperature change for all N = 10 cuttlefish *S. officinalis* of 231 g mean wet mass. AVC_{MV} increases 4.7-fold from 3 to 14 ml min^{-1} between 7 and 23°, but stagnates thereafter (Fig 4c). A logistic regression (R^2=0.99) represents the data best and yields a maximum AVC_{MV} of 13.5 ml min^{-1} at a temperature of 23.9°C.

Changes in blood minute volume are brought about by concerted changes in maximum blood velocity ($AVC_{av\ max\ V}$), blood pulse frequency (AVC_f) and blood pulse stroke volume (AVC_{SV}). 5.9-fold increases in $AVC_{av\ max\ V}$ are witnessed between 7 and approximately 20°C (Fig 4a). Further warming leads to decreasing $AVC_{av\ max\ V}$ values. The dataset can be best represented by a four parameter Weibull peak regression ($R^2 = 0.99$), indicating a maximum velocity of 22.1 cm s^{-1} at 20.9°C. AVC_{SV} data (Figure 5d) can be best approximated by a three parameter Gaussian fit, which suggests a maximum stroke volume of 0.20 ml min^{-1} at temperatures close to control (15.3-15.7). Either warming or cooling results in decreased stroke volumina, with maximum decreases in relation to control values of about 50% observed at the highest temperatures (26°C). AVC_f (Figure 5c) increases exponentially ($R^2 = 0.97$) over the entire temperature range investigated (7-26°C). These changes in AVC_f are closely paralleled by changes in ventilation frequency (v_f) between 7 and 22°C. Both rates start to deviate from one another between 22° and 26°C, with ventilation frequency falling behind. In the following we will refer to the frequency at which both rates start to diverge as the ‚splitting frequency'. As pulse splitting is a consequence of gradually changing blood pulse shapes (see above, figs 2,3), AVC_f does not instantly double once a splitting frequency of 46 – 50 strokes min^{-1} is reached. Rather, occasional splitting between peaks A and B can be observed, with variability between animals being high.

5. Discussion

In general, cuttlefish estimated Q values of 30 – 90 ml min^{-1} kg^{-1} (11 vs. 23°C, table 1) are high in comparison with those observed in temperate teleosts (see Joaquim et al. 2004): E.g., in rainbow trout (acclimated to 10°C, 610 g mean mass), Q ranges from 27 ml kg^{-1} min^{-1} (resting) to 49 ml kg^{-1} min^{-1} (at U_{crit}, Thorarensen et al. 1996). Only the high power scombrids (tuna) surpass levels of cardiac output calculated for cuttlefish at 23°C, with resting Q well in excess of 100 ml kg^{-1} min^{-1} (Brill and Bushnell 2001). Active venous peristalsis (Mislin 1950, Smith 1962, King et al. 2005) in combination with three major blood pumps (branchial and systemic hearts) enable high blood perfusion rates in cuttlefish and cephalopods in general (Wells and Wells 1986, Wells et al. 1987).

The fact that between 40 and 70% of Q is passing through the anterior vena cava (AVC) indicates the important role of this vessel in the cuttlefish organism (table 1).

a) Temperature increase

From 15°C to high temperature extremes of 26°C, blood flow patterns (AVC_{MV}, fig 4c) very closely mimic patterns of change in routine metabolic rate (MO_2, see fig 5b and Melzner, Bock, Pörtner, submitted b,c). AVC_{MV} increased by a factor of 2.5 between 15°C and 23°C and levelled off thereafter. Oxygen consumption rate (MO_2) rose 2.1-fold in the same temperature interval and also remained at a constant level upon further heating to 26°C. It seems likely that stagnating metabolic rates are a consequence of maximum sustainable blood flow rates being reached between 23 and 26°C, analogous to the proposed circulatory and / or ventilatory capacity limitations witnessed in a crustacean (Frederich and Pörtner 2000) and in marine fish species (Heath and Hughes 1973, Mark et al. 2002, Lannig et al. 2004) subjected to acute warming.

The metabolic scope between 15 and 23°C is similar to the scope observed during spontaneous exercise at 15°C. Following short but intense spontaneous exercise periods under control conditions (Melzner, Bock, Pörtner, submitted d), animals elevated AVC_{MV} levels, on average, 2.2-fold above control flow levels to repay an accumulated oxygen debt. No animal was observed to increase blood flow more than 2.7-fold above control values, and, typically, blood flow remained elevated for several minutes in response to one or two minutes of facultative exercise periods, suggesting that such increases in AVC_{MV} represent maximum sustainable increments in response to exercise conditions. These findings are in line with similar maximum scopes for blood flow during exercise in an octopod (Wells et al. 1987). Further increases in blood flow above the levels observed may be sufficiently disadvantageous (e.g. potentially owing to vessel mechanics, see Shadwick and Nilsson 1990), and result in extended post-exercise recovery intervals instead.

Two haemodynamic variables were found to be responsible for exercise induced maximum increases in blood flow: both $AVC_{av\ max\ V}$ and AVC_f increased 1.6-fold. It appears likely that these factorial increases in haemodynamic variables (AVC_{MV}: 2.2-fold, AVC_{avmaxV}, AVC_f: 1.6-fold)

represent the typical ‚working range' available to the animal (acclimated to and exposed to 15°C) to master the various (daily) aerobic challenges (hunting, escaping, feeding, digesting). Extrapolating from the control temperature of 15°C, an upper temperature of 20 – 21.5°C could be sustained with the pattern of haemodynamic flexibility observed during recovery from exercise (see horizontal marks and blue symbols in fig 4a,b,c). Most strikingly, $AVC_{av\ max\ V}$ reaches a maximum in this temperature range. Obviously, further (slight) increases in blood volume flow beyond this temperature range are mediated exclusively by increasing AVC_f at greatly altered haemodynamic parameters. It is the temperature range beyond 20 - 21°C where peak A progressively gains importance, eventually resulting in a second blood pulse within each ventilatory period above the ‚splitting frequency' of 46 - 50 AVC strokes min^{-1}. $AVC_{av\ max\ V}$ can neither be increased, nor maintained under such conditions, resulting in stagnating blood flow starting at 23°C. Interestingly, Mislin (1966) found ventilation and systemic heart rates to be nearly identical in *S. officinalis* (as sampled from a Mediterranean population at Naples) between 14 and 24°C, but witnessed a progressing deviation between both processes at higher temperatures (with heart rates being consistently higher than v_f), indicating a functional disintegration of the two major convection systems. An *in vitro* study on the temperature dependence of branchial heart function adds another piece of information towards understanding the factors limiting cardiovascular performance during acute thermal stress: Fiedler (1992), working on animals from an Atlantic ocean population (Arcachon) of *S. officinalis*, found pressure amplitudes generated by perfused branchial hearts to increase by a factor of 2 between 15 and 22°C. Further warming did not increase pressure amplitudes anymore and at 26 – 27°C, cardiac arrhythmia could be observed. Thus, all available evidence to date suggests that the cuttlefish cardiovascular system can respond to rising metabolic rates with increased blood perfusion up to temperatures of 20-22°C. Thereafter, rates can be maintained over a limited temperature range, until finally, functional disintegration of the system occurs between 24 - 26°C. In line with the principle of symmorphosis, developed for the mammalian respiratory system (Taylor and Weibel 1981), major components of the circulatory system (AVC, branchial hearts) may be designed for similar workloads, and may, consequently, fail concomitantly once maximum workloads have been surpassed.

Summarizing events in the warm, we can distinguish two main phases: Phase 1 (fig 5, Pw1), encompassing the temperature range from control 15°C to 23°C, characterized by exponential increase in metabolic rate in concert with rising AVC_{MV}. Phase 2 (fig 5, Pw2) characterized by largely conserved metabolic rate at maximum AVC_{MV}. Significantly altered (detrimental) function of the AVC system (i.e. peak A dominance, pulse splitting, decreased maximum blood velocities) was witnessed in this temperature interval. Increasing rates of ventilatory power output (P_{out}, fig 5c) indicate some functional scope left in ventilation while circulatory scope is fully exploited. This phase ends with the onset of anaerobic metabolism in ventilatory muscle fibres (Pi accumulation, see fig 5c) (Melzner, Bock, Pörtner, submitted a,b).

b) Temperature decrease

While there are clear signs for a limitation of oxygen transport capacity in the warm, the situation is somewhat more complicated in the cold. We could previously identify a drop in routine metabolic rates below expected levels once temperatures reached 8°C (fig 5b and Melzner, Bock, Pörtner, submitted b), followed by the onset of anaerobic metabolism in mantle muscle tissues at a T_{c1} of 7.0°C (fig 5c and Melzner, Bock, Pörtner, submitted a). Analogous to the situation during warming, we find a significantly elevated contribution of peak A to total blood flow (fig 4b), as well as a trend towards an altered δ (fig 2c), indicating progressive disintegration of ventilatory and circulatory processes.

With MO_2 dropping by a factor of 1.7 between 11 and 8°C (Melzner, Bock, Pörtner, submitted c), we did not observe any changes in AVC_{MV} in the respective temperature interval. This may (at unaltered Ut) be indicative of redistribution in blood flow, favouring the head and funnel apparatus. Alternatively, oxygen transport in the cold may start to suffer in general as pH dependent haemocyanin oxygen unloading becomes more difficult: An *in vitro* oxygen binding study on cuttlefish (*S. officinalis*) haemocyanin suggested that from 20 to 10°C, oxygen isobars of a pH / saturation diagram (Pörtner 1990) shift to lower pH values and level off at higher levels of

haemocyanin oxygen saturation, forming a progressively increasing pH insensitive venous oxygen reserve (Zielinski et al. 2001): At 20°C and with a blood oxygen partial pressure of 4.3 kPa (see fig 3 in the respective publication), haemocyanin molecules are fully saturated with oxygen above an extracellular pH (pH_e) of 7.6. Saturation strongly declines between blood pH 7.65 and 7.4, to finally level off at about 20% (i.e. an Ut of 80%) below pH_e 7.2. At 10°C and the same PO_2, decreases in haemocyanin saturation with declining pH are less steep, and, in addition, values level off at about 40% saturation at pH values that are far lower (< pH 7.0) than those observed *in vivo* in cuttlefish lateral venae cavae (Johansen et al. 1982, pH_e values ranged from 7.4-7.6 at 17°C water temperature). Thus, at a (putative) pH_e of 7.4 and a vein PO_2 of 4.3 kPa, cuttlefish haemocyanin would be about 30% saturated (Ut = 70%) at 20°C, but more than 80% saturated (Ut= 20%) at 10°C, implying that more than three times the amount of blood needs to be circulated to support the organism with an equal amount of oxygen at low temperature.

In addition, the alpha stat hypothesis (Reeves, 1972) predicts pH_e values to be higher in the cold to ensure constant imidazole ionization (ΔpH = -0.017 units $°C^{-1}$). Howell and Gilbert (1976) suggested such a pattern to be relevant for squid blood. However, such a pattern of pH regulation would decrease Ut even more and, in consequence, further enhance blood perfusion requirements in the cold. Preliminary results indicate that, indeed, pH_e does significantly increase in the AVC upon acute temperature change from 17 to 11°C. However, Ut was not as dramatically reduced as suggested above: it (insignificantly) decreased from 75 to 62% (17°C pH_e: 7.96, 0.1 SD, Ut: 74.8%, 8% SD, PO_{2v} 1.3 kPa 0.6 kPa SD; 11°C: pH_e: 8.14, 0.07 SD, Ut: 62.2%, 21% SD, PO_{2v} 0.9 kPa 0.5 kPa SD; N=6 animals; Melzner, Langenbuch, Gutowska, Claireaux, Pörtner, unpublished *in vivo* results on *S. officinalis* from a Bay of Biscay population). However, there is a price the animal has to pay for high Ut values at low temperatures: Full haemocyanin deoxygenation at high pH and low temperature can only be achieved at low venous PO_2 values (see above and Zielinski et al. 2001).

Further cooling to 8°C likely worsens the situation. Maintaining a relatively high AVC_{MV} with regard to observed MO_2 values below 11°C may be the first indication of limited oxygen carrier function starting to impact whole animal performance. These limitations probably coincide with the above mentioned haemodynamic irregularities close to the lower critical temperature.

In summary, we can define two phases during progressive, acute cooling: Phase 1 (Pc1), extending from 15°C to 11°C, characterized by control – like haemodynamic and ventilatory patterns (fig 5), at exponentially declining MO_2 (fig 5b). This phase ends once stagnating AVC_{MV} indicate the onset of phase 2 (Pc2). From 11 to 8°C, MO_2 drops below expected values (fig 5b) at constant AVC_{MV}, with haemodynamic functioning significantly altered (peak A domination), eventually leading to anaerobic metabolism at 7°C, as characterized by significant [Pi] accumulation in ventilatory muscle fibres (Melzner, Bock, Pörtner submitted a).

c) Integration

Using spider crab (*Maja squinado*) as a model organism and building on previous work (as summarized in Pörtner 2001), Frederich and Pörtner (2000) developed a model of an oxygen limitation of thermal tolerance. Accordingly, an optimum temperature range, characterized by constantly high arterial PO_2s, is confined by threshold temperatures (pejus temperatures, T_{p1} in the cold, T_{p2} in the warm), beyond which progressively declining arterial PO_2s indicate a limitation of aerobic scope, until, finally critical temperatures (T_{c1} in the cold, T_{c2} in the warm) characterize the onset of anaerobic metabolism due to a loss of aerobic scope (for a recent update of the model see Pörtner et al., 2004). It was further proposed that aerobic scope is at its maximum in the optimum temperature range (cf. Pörtner et al., 2004) and that therefore, T_{p1} and T_{p2} would be of utmost ecological relevance in defining suitable habitat threshold temperatures. In addition, it was postulated that oxygen limitation mechanisms set in first at high levels of organismal complexity, chiefly at the (integrated) capacity of ventilatory and circulatory convection systems (Pörtner 2002). In the following, we will briefly discuss the vital model components and their applicability to the oxygen transfer patterns observed in the cuttlefish during acute temperature change.

1. *Limited oxygen availability causes transition to an anaerobic mode of energy production, both in the cold and in the warm.* This could be confirmed for the cuttlefish *S. officinalis*. Non-invasive, continuous ^{31}P NMR measurements during acute temperature change demonstrated that

starting beyond mean temperatures of 7.0 and 26.8°C, mantle muscle phospho - L – arginine (PLA) stores were progressively depleted to sustain energy supply (Melzner, Bock, Pörtner, submitted a).

2. *An oxygen limitation of thermal tolerance sets in at high levels of organismal complexity.* While in the spider crab with its open circulatory system, both ventilatory and circulatory capacity were suggested to become limiting for oxygen transfer at approaching thermal extremes (Frederich and Pörtner 2000), high power ectothermic vertebrates (fish) have improved thermal resistance of ventilation. High oxygen partial pressures in the gas exchange vessels of the gills result at all temperatures of the thermal tolerance window (e.g. Sartoris et al. 2003, North Sea cod, *Gadus morhua*). Mark et al. (2002) could demonstrate that ventilatory effort in Antarctic eelpout (*Pachycara brachycephalum*) increased exponentially over the entire temperature range studied. Accordingly, circulatory capacity limitations were identified to characterize temperature dependent oxygen limitation in both species (eelpout and cod, Mark et al. 2002, Lannig et al. 2004).

Competition between cephalopods and fish has led to the evolution of high power ecotypes with efficient ventilation and closed high-pressure circulation systems (Packard 1972, O'Dor and Webber 1986). It is thus not entirely surprising to find a similar shift in the role of oxygen transfer system components in thermal limitation of both groups. *S. officinalis* can increase ventilatory power output (P_{out}) over the entire temperature range investigated (see fig 5c) and is likely able to maintain high PO_2s in gill vessels to ensure proper haemocyanin oxygen loading and oxygen supply to cardiocirculation within wider thermal windows than supported by circulatory functions (Melzner, Bock, Pörtner, submitted b). Circulatory capacity limits are probably causative for the observed stagnating oxygen uptake rates at temperatures > 23°C (see fig 5b).

3. *Aerobic scope is at its maximum in an optimum temperature range, which may correlate with habitat threshold temperatures. Beyond the optimum range, a pejus range extends towards critical temperatures, both in the warm and in the cold, characterized by progressively declining aerobic scopes.* When acclimated to 15°C, the cuttlefish circulatory system is designed to elevate MO_2 by a factor of 2 – 2.5 above resting, regardless of the nature of the acute stimulant causing the increase in oxygen demand. Either exercise at 15°C (Melzner, Bock, Pörtner submitted d) or temperature change to 22-23°C evidently evoke the same maximum circulatory responses. A maximum v_f of 46.4 beats

min^{-1} was observed during recovery from exercise at 15°C (see fig 4b), while the present study indicated, that forced increases in oxygen demand due to increasing temperature result in blood pulse splitting above a v_f of 45-50 beats min^{-1} at 22-23°C. Once the splitting frequency is reached, $AVC_{av\ max\ V}$ and AVC_{MV} cannot be increased anymore. Therefore, we concluded that due to mechanical limitations in correlated ventilatory and circulatory mechanics, an upper ceiling for AVC_{MV}, and, concomitantly, maximum metabolic rate, exists that is independent of temperature between 15 and 23°C.

Fig 6a gives a schematic view of the conclusions arising from these findings: While the lower horizontal line indicates MO_2 at rmr at 15°C, the higher corresponds to those MO_2s that can maximally be sustained by the circulatory machinery. The differential between both lines is equivalent to the amount of metabolic rate and Q that the animal can allocate to the various oxygen sinks within the organism. As routine metabolic rate rises in its typical exponential fashion (see fig 6a, areas A and B), factorial aerobic scope (fAS) available for other activities progressively declines from a maximum at control 15°C (see fig 6b, fractions (A+B+C)/(A+B)), until, at approximately 23°C, the entire oxygen transport system needs to support routine metabolic rate and fAS becomes 1. Although it has yet to be elucidated, whether the rmr increment cannot be modified to sustain levels of activity beyond their predicted share (fig 6, area C): Cellular energy budget studies demonstrated that the percentage contribution of mitochondrial proton leakage to total cellular respiration increases with temperature in fish (Hardewig et al. 1999). As it could be shown that increased ATP demand is able to reduce the fraction of proton leakage on total cellular metabolism in mammal muscle (Rolfe et al. 1999), it therefore may be possible that some aerobic scope for activity can be generated in addition by increasing cellular efficiency (i.e. units ATP produced per unit oxygen), thus decreasing fraction B in fig. 6.

Following the rationale of precursor studies, 23°C would be defined the upper critical temperature (T_{c2a}), owing to the observed circulatory capacity limitations and the complete loss in fAS (Frederich and Pörtner 2000, Mark et al. 2002, Pörtner 2002). It is evident from the above analysis, that the subsequent critical temperature range is not characterized by residual aerobic scope for activity. Rather, fAS remains at 1 until anaerobic metabolism supports energy production in tissues of

immediate importance (i.e. ventilatory and circulatory muscles) at 26.8°C. In fig 6, this threshold temperature is termed T_{c2b}. Area D in fig 6 indicates the rising quantity of oxygen that the circulatory system cannot provide in the critical temperature range ('aerobic gap'). By means of an altered regional blood flow distribution (see introduction) in concert with metabolic depression (Hochachka and Somero 2000), common instruments available to animals to selectively channel limited resources into key processes of immediate importance to the organism, ventilatory and circulatory functions may be protected in the critical temperature range. In fact, changes in regional blood flow were observed in spider crab by Frederich et al. (2000) at low temperatures (favouring the head region), while at high temperatures, lactate accumulation in walking muscle prior to mitochondrial anaerobiosis in the muscle, hepatopancreas and heart may also be explained with an altered energy distribution within the organism. T_{c2b} indicates the limits in metabolic re – allocation, in that vital organs (e.g. ventilatory muscles) become progressively oxygen devoid and, subsequently, lose their functional integrity due to the accumulation of anaerobic end products and drops in the free energy for ATP hydrolysis.

According to fig 6 (thermal interval 15-27°C), the acclimation temperature of 15°C should be called the optimum temperature, as fAS is at its maximum value. The thermal range of 15 to 23°C, characterized by declining fAS, were to be called the 'pejus' range.

Recent evidence indicates that the finding of an optimum temperature at the long-term incubation temperature of the experimental animal group is not surprising. As most temperate fish species (e.g. Sidell 1980, Johnston, 1982, Rome et al. 1985, Johnston et al. 1998, Guderley and St-Pierre, 2002), *Sepia officinalis* can acclimate its metabolic rate and, likely, aerobic scope to altered temperature regimes (Melzner, Bock Pörtner, unpublished): Animals raised (and measured) at 20°C displayed comparable metabolic rate, as well as comparable v_f and AVC_f to animals raised at 15°C. Thus, cuttlefish can perform full metabolic compensation (*sensu* Precht 1958). By 'resetting' v_f and AVC_f to lower values, thermal acclimation to 20°C may 'conserve' factorial cardiovascular and aerobic scopes of >2. This is important for the particular mode of life of cephalopods, which forces these invertebrates to elevate blood flow 2-3-fold daily during digestion, as to sustain high rates of growth (e.g. Wells et al. 1983, Valverde and Garcia 2004). A 'resetting' of cardiac pacemaker rate to maintain scopes for performance has also been observed in fish species (Farrell and Jones 1992,

Lillywhite et al. 1999). With rates of change in habitat temperature in the English Channel of less than 3°C month^{-1} Boucaud-Camou and Boismery 1991, Wang et al. 2003), it is likely that *S. officinalis* is always able to adjust its fAS to the predominant water temperature. An adjustment in aerobic scope to a new thermal regime also implies a shift in the thermal tolerance window and therefore, of threshold temperatures (T_p and T_c), of the species, as demonstrated for the lugworm (Sommer et al. 1997). Therefore, to accurately determine temperature thresholds according to the outlined model assumptions (see above, Pörtner et al. 2004), aerobic scope has to be determined at a variety of acclimation temperatures. Studies performed on (salmonid) fish have indeed revealed a bell shaped curve of aerobic scope (for exercise) vs. acclimation temperature, with maximized aerobic scopes found in the natural thermal window of the species (Taylor et al 1996, Farrell 1996). More flexibility to threshold temperatures is added by the fact that multiple processes compete for the available oxygen the cardiovascular system can provide: Each exercise and the specific dynamic action of food (SDA) can 'consume' the entire aerobic scope of a cephalopod (Valverde and Garcia 2004, Wells et al. 1987). Accordingly, T_{c2a} in the cuttlefish may be considerably lower than 23°C when large meals are being digested simultaneously at an acute increase above acclimation temperature.

At low temperatures (15 to 7°C), assignment of model threshold temperatures (Pörtner et al. 2004) is more difficult. While the stagnation of rmr at temperatures >23°C correlated with fAS = 1 and defined T_{c2a}, it is unclear, whether the apparent deviation of rmr from the expected exponential relationship between 11 and 8°C (see fig. 5) also is an expression of a complete loss in AS. However, circumstantial evidence of progressively detrimental AVC function in concert with haemocyanin unloading problems (see above) indicate, that 11°C may characterize T_{c1a}. Observations of Richard (1971) confirm our conception: English Channel *S. officinalis* do not display physical activity once temperatures drop below 10°C, suggesting that, indeed, low blood oxygen partial pressures may be limiting performance at 10-11°C and below. In this light, the observed drop in metabolic rate may be regarded as a metabolic depression, likely in order to protect aerobic metabolism of circulatory and ventilatory muscles. The onset of anaerobic metabolism in vital ventilatory fibres eventually characterizes T_{c1b}.

In conclusion, cuttlefish from an English Channel population, laboratory raised at 15°C and 48 hours starved, can increase their metabolic rate exponentially between 11 and 23°C due to correlated increases in blood perfusion (AVC_{MV}). Beyond this thermal interval, T_{c1a} and T_{c2a} indicate a complete loss in aerobic scope. An interval of metabolic re-allocation, characterized by lower than expected metabolic rates (e.g. Hemmigsen 1960) extends from these natural threshold temperatures, until the onset of anaerobic metabolism in vital ventilatory muscle systems characterizes T_{c1b} and T_{c2b}. Within this interval, haemodynamic function of the anterior vena cava (AVC) – ventilatory system becomes progressively detrimental and, likely contributes to a developing internal, temperature related hypoxia.

6. References

ALSOP, D.H. and WOOD, C.M. (1997). The interactive effects of feeding and exercise on oxygen consumption, swimming performance and protein usage in juvenile rainbow trout *(Oncorhynchus mykiss*). *J. Exp. Biol.* **200**, 2337-2346.

AXELSSON, M. AND FRITSCHE, R. (1991). Effects of exercise hypoxia and feeding on the gastrointestinal blood flow in the Atlantic cod *Gadus morhua*. *J. Exp. Biol.* **158**, 181-196.

BONE, Q. AND BROWN, E. R. (1994). On the respiratory flow in the cuttlefish *Sepia officinalis*. *J. exp. Biol.* **194**, 153-165.

BOUCAUD – CAMOU, E. AND BOISMERY, J. (1991). The migrations of the cuttlefish (*Sepia officinalis*) in the English Channel. In: Boucaud-Camou, E. (Ed.), La Seiche, 1st International symposium on the cuttlefish *Sepia*. Center of publications, Universite de Caen. pp. 179-189.

BRILL, R.W. AND BUSHNELL, P.G. (2001). The cardiovascular system of tunas. In: Block, B.A. and Stevens, E.D. *Tuna: Physiology, Ecology and Evolution, vol 19*. Academic Press, San Diego, pp. 79-120.

FARRELL, A.P. AND JONES, D.R. (1992). The Heart. In: *Fish Physiology*, edited by Hoar, W.S., Randall, D.J. and Farrrell, A.P. San Diego, AP, vol 12A, 1-88.

FARRELL, A.P. (1996). Effects of temperature on cardiovascular performance. In: Wood, C.M. and McDonal, D.G. *Global Warming: Implications for freshwater and marine fish*. Soc. Exp. Biol. Sem. Ser. 61. Cambridge University Press, Cambridge, pp. 135-158.

FIEDLER, A. (1992). Die Rolle des venösen Füllungsdrucks bei der Autoregulation der Kiemenherzen von *Sepia officinalis* L. (Cephalopoda) (The role off venous filling pressue in autoregulation of the branchial hearts of *Sepia officinalis* L. (Cephalopoda)). *Zool. Jb. Physiol.* **96**, 265-278.

FREDERICH, M. AND PÖRTNER, H. O. (2000). Oxygen limitation of thermal tolerance defined by cardiac and ventilatory performance in spider crab, *Maja squinado*. *Am. J. Physiol.* **279**, R1531-R1538.

FREDERICH, M., DE WACHTER, B., SARTORIS, F. AND PÖRTNER, H.O. (2000). Cold tolerance and the regulation of cardiac performance and hemolymph distribution in *Maja squinado* (Crustacea: Decapoda). *Physiol. Biochem. Zool.* **73**, 406-415.

FRY, F.E.J. (1947). Effects of the environment on animal activity. *Univ. Toronto Student Biol. Series* **55**, 1-62.

GUDERLEY, H. AND ST-PIERRE, J. (2002). Going with the flow or life in the fast lane: contrasting mitochondrial responses to thermal change. *J. Exp. Biol.* **205**, 2237-2249.

HARDEWIG, I., PECK, L.S. AND PÖRTNER, H.O. (1999). Thermal sensitivity of mitochondrial function in the Antarctic Notothenioid Lepidonotothen nudifrons. *J. Comp. Physiol. B*, **169**, 597-604.

HEATH, A, G. AND HUGHES, G. M. (1973). Cardiovascular and respiratory changes during heat stress in the rainbow trout (*Salmo gairdneri*). *J. Exp. Biol.* **59**, 323-338.

HEMMIGSEN, A.M. (1960). Energy metabolism as related to body size and respiratory surfaces, and its evolution. *Rep. Steno Mem. Hosp. And Nordisk Insulin Laboratorium*. **9**, 6-110.

HOCHACHKA, P.W. AND SOMERO, G.N. (2002). *Biochemical Adaptation. Mechanism and process in physiological evolution*. Oxford University Press, Oxford, 466 pp.

HOWELL, B.J. AND GILBERT, D.L. (1976). pH - temperature dependence of the hemolymph of the squid, *Loligo pealei*. *Comp. Biochem. Physiol. A* **55**, 287-289.

HYLLAND, P., NILSSON, G. AND LUTZ, P. (1994). Time course of anoxia-induced increase in cerebral blood flow rate in turtles: Evidence for a role of adenosine. *J. Cereb. Blood Flow Metab.* **14**, 877-881.

JOAQUIM, N., WAGNER, G.N. AND GAMPERL, A.K. (2004) Cardiac function and critical swimming speed of the winter flounder (*Pleuronectes americanus*) at two temperatures. *Comp. Biochem. Physiol. A* **138**, 277-285.

JOHANSEN, K., BRIX, O. AND LYKKEBOE, G. (1982). Blood gas transport in the cephalopod, *Sepia officinalis*. *J. Exp. Biol.* **99**, 331-338.

JOHNSTON, I.A. (1982). Capillarisation, oxygen diffusion distances and mitochondrial content of carp muscles following acclimation to summer and winter temperatures. *Cell Tissue Res.* **222**, 325-337.

JOHNSTON, I.A., CALVO, J., GUDERLEY, H., FERNANDEZ, D. AND PALMER, L. (1998). Latitudinal variation in the abundance and oxidative capacities of muscle mitochondria in perciform fishes. *J. Exp. Biol.* **201**, 1-12.

KING, A.J., HENDERSON, S.M., SCHMIDT, M.H., COLE, A.G. AND ADAMO, S.A. (2005). Using ultrasound to understand vascular and mantle contributions to venous return in the cephalopod *Sepia officinalis* Linneaus. *J. Exp. Biol.* **208**, 2071-2082.

LANNIG, G., BOCK, C., SARTORIS, F. J. AND PÖRTNER, H. O. (2004). Oxygen limitation of thermal tolerance in cod, *Gadus morhua* L. studied by magnetic resonance imaging (MRI) and on-line venous oxygen monitoring. *Am. J. Physiol.* **287**, R902-R910.

LEE, C.G., FARRELL, A.P., LOTTO, A., MACNUTT, M.J., HINCH, S.G. AND HEALEY, M.C. (2003). The effect of temperature on swimming performance and oxygen consumption in adult sockeye (*Oncorhynchus nerka*) and coho (*O. kisutch*) salmon stocks. *J. Exp. Biol.* **206**, 3239-3251.

LILLYWHITE, H.B., ZIPPEL, K.C. AND FARRELL, A.P. (1999). Resting and maximal heart rates in ectothermic vertebrates. *Comp. Biochem. Physiol A* **124**, 369-382.

MARK, F. C., BOCK, C. AND PÖRTNER, H. O. (2002). Oxygen – limited thermal tolerance in Antarctic fish investigated by MRI and ^{31}P – MRS. *Am. J. Physiol.* **283**, R1254-R1262.

MELZNER, F., BOCK, C. AND PÖRTNER, H.O. Critical temperatures in the cephalopod *Sepia officinalis* investigated using *in vivo* ^{31}P NMR spectroscopy, *J. Exp. Biol.*, submitted a.

MELZNER F., BOCK C. AND PÖRTNER, H.O. Temperature dependent oxygen extraction from the ventilatory current and the costs of ventilation in the cephalopod *Sepia officinalis*. *J. Comp. Physiol. B.*, submitted b.

MELZNER F., BOCK C. AND PÖRTNER H.O. Allometry of thermal limitation in the cephalopod *Sepia officinalis*. *Comp. Biochem. Physiol. A*, submitted c.

MELZNER F., BOCK C. AND PÖRTNER H.O. Coordination between ventilatory pressure oscillations and venous return in the cephalopod *Sepia officinalis*. *J. Comp. Physiol. B,* submitted, d.

MISLIN, H. (1950). Nachweis einer reflektorischen Regulation des peripheren Kreislaufs der Cephalopoden. *Experientia* **6**, 467-468.

MISLIN, H. (1966). Ueber die Beziehungen zwischen Atmung und Kreislauf bei Cephalopoden (*Sepia officinalis* L.). Synchronregistrierung von Elektrokardiogramm (Ekg) und Atembewegungen am schwimmenden Tier. *Verh. Dtsch. Zool. Ges.* 175-181.

NILSSON, G.E., HYLLAND, P. AND LÖFMAN, C.O. (1994). Anoxia and adenosine induce increased cerebral blood flow rate in crucian carp *Am. J. Physiol.* **267**, R590-R595.

O'DOR, R.K. AND WEBBER, D.M. (1986). The constraints on cephalopods: why squid aren't fish. *Can. J. Zool.* **64**, 1591-1605.

O'DOR, R. K. AND WELLS, M. J. (1987). Energy and nutrient flow. In: Boyle, P. R. (ed.), *Cephalopod life cycles*, Comparative reviews. (Vol. 2) Academic Press, London, pp.109-133.

PACKARD, A. (1972). Cephalopods and fish: limits of convergence. *Biol. Rev.* **47**, 241-307.

PÖRTNER, H.O. (2001). Climate change and temperature dependent biogeography: oxygen limitation of thermal tolerance in animals. *Naturwissenschaften* **88**, 137-146.

PÖRTNER, H.O. (2002). Climate variations and the physiological basis of temperature dependent biogeography: systemic to molecular hierarchy of thermal tolerance in animals. *Comp. Biochem. Physiol. A* **132**, 739-761.

PÖRTNER, H.O., MARK, F.C. AND BOCK, C. (2004). Oxygen limited thermal tolerance in fish? Answers obtained by nuclear magnetic resonance techniques. *Respir. Physiol. Neurobiol.* **141**, 243-260.

PRECHT, H. (1958). Concepts of the temperature adaptation of unchanging reaction systems of cold-blooded animals. In: Prosser, C.L. (ed). *Physiological Adaptations*, Am. Physiol. Soc. Washington, D.C.

RANDALL, D.J. AND DAXBOECK, C. (1982). Cardiovascular changes in the rainbow trout (*Salmo gairdneri* Richardson) during exercise. *Can. J. Zool.* **60**, 1135-1140.

REEVES, R. B. (1972). An imidazole alphastat hypothesis for vertebrate acid –base regulation: tissue carbon dioxide content and body temperature in bullfrogs. *Respir. Physiol.* **14**, 219-236.

ROLFE, D.F.S., NEWMAN, J.M.B., BUCKINGHAM, J.A., CLARK, M.G. AND BRAND, M.D. (1999). Contributions of mitochondrial proton leak to respiration rate in working skeletal muscle and liver and to SMR. *Am. J. Phys.* **276**, C692-C699.

ROME, L.C., LOUGHNA, P.T. AND GOLDSPINK, G. (1985). Temperature acclimation: improved sustained swimming performance in carp at low temperatures. *Science* **228**, 194-196.

SARTORIS, F. J., BOCK, C., SERENDERO, I., LANNIG, G. AND PÖRTNER, H. O. (2003). Temperature – dependent changes in energy metabolism, intracellular pH and blood oxygen tension in the Atlantic cod. *J. Fish. Biol.* **62**, 1239-1253.

SHADWICK, R.E. AND NILSSON, E.K. (1990). The importance of vascular elasticity in the circulatory system of the cephalopod *Octopus vulgaris*. *J. Exp. Biol.* **152**, 471-484.

SIDELL, B.D. (1980). Response of goldfish (Carassius auratus L.) muscle to acclimation temperature: alterations in biochemistry and proportions of different fibre types. *Physiol Zool.* **53**, 98-107.

SMITH, L.S. (1962). The role of venous peristalsis in the arm circulation of *Octopus dofleini*. *Comp. Biochem. Physiol.* **7**, 269-275.

SOMMER, A. KLEIN, B. AND PÖRTNER, H.O. (1997). Temperature induced anaerobiosis in two populations of the polychaete worm *Arenicola marina* (L.). *J. Comp. Physiol. B* **167**, 25-35.

TAYLOR, C.R. AND WEIBEL, E.R. (1981). Design of the mammalian respiratory system. 1. Problem and strategy. *Respir. Physiol.* **44**, 1-10.

TAYLOR, S.E., EGGINTON, S. AND TAYLOR, E.W. (1996). Seasonal temperature acclimatisation of rainbow trout: cardiovascular and morphometric influences on maximal sustainable exercise level. *J. Exp. Biol.* **199**, 835-845.

THORARENSEN, H., GALLAUGHER, P:E: AND FARRELL, A.P. (1996). Cardiac output in swimming rainbow trout Oncorhynchus mykiss, acclimated to seawater. *Physiol. Zool.* **69**, 139-153.

TOMPSETT, D.H. (1939). Sepia. LMBC Memoirs, Liverpool University Press, 184 pp.

VALVERDE, J. C. AND GARCIA GARCIA, B. (2004). Influence of body weight and temperature on post – prandial oxygen consumption of common octopus (*Octopus vulgaris*). *Aquaculture* **233**, 599-613.

WANG, J., PIERCE, G.J., BOYLE, P.R., DENIS, V., ROBIN, J.P. AND BELLIDO, J.M. (2003). Spatial and temporal patterns of cuttlefish (*Sepia officinalis*) abundance and environmental influences – a case study using trawl fishery data in French Atlantic coastal, English Channel, and adjacent waters. *ICES J. Mar. Sci.* **60**, 1149-1158.

WEBBER, D.M., BOUTILIER, R.G. AND KERR, S.R. (1998). Cardiac output as a predictor of metabolic rate in cod *Gadus morhua*. *J. Exp. Biol.* **201**, 2779-2789.

WELLS, M.J. (1983). Circulation in cephalopods. In Saleuddin, A.S.M. and Wilbur, K.M. (eds.): *The Mollusca* Vol 5, Physiology Part 2, pp. 239-290. Academic Press, New York.

WELLS, M. J. AND WELLS, J. (1986). Blood flow in acute hypoxia in a cephalopod. *J. Exp. Biol.* **122**, 345-353.

WELLS, M.J., DUTHIE, G.G., HOULIHAN, D.F., SMITH, P.J.S. AND WELLS, J. (1987) Blood flow and pressure changes in exercising octopuses (*Octopus vulgaris*). *J. Exp. Biol.* **131**, 175-187.

ZIELINSKI, S., SARTORIS, F. AND PÖRTNER, H.O. (2001). Temperature effects on hemocyanin oxygen binding in an Antarctic cephalopod. *Biol. Bull.* **200**, 67-76.

Figure captions

Figure 1: Correlated patterns of flow in anterior vena cava (AVC) and of ventilatory mantle cavity pressures in a resting animal (#19) between 7 and 26°C. Mantle cavity pressure (blue) in Pa, AVC blood velocity (red) in cm s^{-1}. Note differences in x and y - axis scaling between 1A-D and 1E-H. The dotted line indicates zero blood velocity. Positive velocities indicate blood flow in the gill heart (proper) direction, negative velocities blood flow towards the head.

Figure 2: Haemodynamic parameters at selected temperatures. N = 6 animals, means ±SD. (A) Phase shift (δ) between phase angles of maximum mantle cavity pressure increase (ϕ_1) and phase angle of the main blood peak (peak B, see fig 3) start (ϕ_2) in °phase. (B) positive AVC blood flow duration in percent of the ventilatory period. (C) Contribution of blood peak A tot total blood pulse flow. C = control (15°C); asterisks indicate significant differences from controls; ANOVA and subsequent Student-Newman-Keuls (SNK) posthoc testing at $p < 0.05$.

Figure 3: Changes in blood flow pulse shape with temperature in a representative animal (#19). Blood velocity expressed as % of maximum pulse velocity. Black dots indicate separation between peaks A and B of each blood pulse. Areas left and right of these dots are proportional to peak A and B flow, respectively.

Figure 4: Haemodynamic and correlated ventilatory variables for all N = 10 animals subjected to acute temperature change. Means ±SE. (A) AVC average maximum blood velocity (cm s^{-1}). (B) AVC blood pulse rate (AVC_f black symbols) and ventilation rate (v_f white symbols) in strokes min^{-1}. Rates are identical below 22°C. (C) AVC minute volume (AVC_{MV}) in ml min^{-1}. (D) AVC stroke volume (AVC_{SV}) in ml $stroke^{-1}$. C = control temperature (15°C), horizontal lines and blue symbols (means ±SE) in A, B and C indicate maximum factorial increases of the respective haemodynamic variables

attained during recovery from exercise at 15°C (studied in the same animals; see Melzner, Bock, Pörtner submitted d), see text for further explanations. Curve fits: (A): Weibull 4 parameter (y=x0-b*((c-1)/c)^(1/c); 0; a*((c-1)/c)^((1-c)/c) * (abs((x-x0)/b+((c-1)/c)^(1/c))^(c-1)) * exp(-abs((x-x0)/b+((c-1)/c)^(1/c))^c+(c-1)/c))) with a =22.06, b=69.2, c=11.67, x0=21.0; R^2 = 0.99, p<0.001. (B): a) v_f: 2 factorial exponential fit (y=a*exp(b*x)) with a=11.9, b=0.06; R^2 = 0.99, p<0.001. b) AVC_f: 3 factorial exponential function (y=y0+a*exp(b*x)) with a=0.47, b=0.19, y0=20.1; R^2 = 0.97, p<0.001. (C): Lognormal function (y=y0+a*exp(-0,5*(ln(x/x0)/b)^2)) with a=10.3, b=0.3, x0=24.3, y0=2.9; R^2 = 0.99, p<0.001. (D): Gaussian fit (y=y0+a*exp(-,5*((x-x0)/b)^2)) with a=0.102, b=5.05, x0=15.45, y0=0.104; R^2 = 0.99, p<0.001.

Figure 5: Oxygen limitation of thermal tolerance in cuttlefish: summary of results. Mean values ±SE. (A) AVC_f, v_f and $AVC_{av\ max\ V}$, this study (B) AVC_{MV} (this study) and routine metabolism (MO_2) of 105 g cuttlefish (see Melzner, Bock, Pörtner submitted c) (C) ventilatory power output (P_{out}) of 105 g cuttlefish (see Melzner, Bock, Pörtner, submitted b) and inorganic phosphate content [P_i] of mantle muscle (see Melzner, Bock, Pörtner, submitted a). Bold vertical lines indicate temperatures at which anaerobic metabolism starts to support energy generation in ventilatory muscle (see Melzner, Bock, Pörtner, submitted a), dotted lines define intervals described in the text. T_{acclim} = long term acclimation temperature (15°C).

Figure 6: Schematic temperature tolerance model for cuttlefish subjected to acute temperature increase. (A) routine metabolic rate (bold blue line) or, equivalently, cardiac output (Q) vs. temperature, exponentially rising between 15 and 23°C, stagnating thereafter. The dotted blue line gives the expected development of rmr or Q beyond 23°C. The lower dotted horizontal line indicates rmr or Q at 15°C, the upper line maximum sustainable metabolic rate (mmr) or maximum sustainable Q (Q_{max}). I.e., the differential between both lines is equivalent to cardiac or aerobic scope. This can be consumed by either activity (area C), or by temperature dependent increases in rmr (area B). Evidently, aerobic scope is entirely consumed by B at 23°C, leaving no scope for C from this threshold temperature on. Fraction D is the amount of metabolic rate and Q that cannot be supplied to

ensure further exponentially rising rmr. (B) is a plot of (factorial) aerobic and factorial cardiac scopes for activity = (A+B+C)/(A+B) vs. temperature. Factorial aerobic scope (fAS) and factorial cardiac scope = 1 at 23 – 26.8°C. T_{acclim} (15°C) = acclimation temperature, T_{c2a} (23°C) = high critical temperature, i.e. fAS = 1 T_{c2b} (26.8°C) = onset of anaerobic metabolism in ventilatory muscles.

Table 1. AVC blood flow in relation to cardiac output at changing temperatures. Cardiac output estimates based on Fick's principle, using a blood oxygen carrying capacity of 1.49 mmol l^{-1} as determined for *S. officinalis* from the English Channel population as well as oxygen utilization values of 80% (Johansen et al 1982). MO_2 values were calculated using a two factorial regression obtained in a previous report (ln MO_2 = -3.3 + 0.0945 T – 0.215 ln m (R^2 = 0.93), with T = temperature in °C, m = wet mass in g, MO_2 = routine metabolic rate in μmol O_2 g^{-1} min^{-1}, Melzner, Bock, Pörtner, submitted c). Q = cardiac output [ml kg^{-1} min^{-1}]; AVC_{MV} = anterior vena cava minute volume [ml kg^{-1} min^{-1}]; Ut = utilization = difference between arterial and venous oxygen content, MO_2 = calculated oxygen consumption rates [μmol O_2 min^{-1} kg^{-1} $animal^{-1}$] for 231g wet mass animals.

T *[°C]*	*MO_2* *[μmol O_2 kg^{-1} min^{-1}]*	*Q* *[ml kg^{-1} min^{-1}]* *(80% Ut)*	*AVC_{MV}* *[ml kg^{-1} min^{-1}]*	*AVC_{MV}* *[% of Q]* *(80% Ut)*
11	33,1	29,5	12,1	40,9
12	36,3	32,5	16,9	52,1
13	40,0	35,7	21,8	61,1
14	44,2	39,5	26,5	66,9
15	48,1	43,0	23,9	55,6
16	53,1	47,4	27,9	58,8
17	58,5	52,3	35,7	68,1
18	64,3	57,4	38,9	67,6
19	70,7	63,2	44,4	70,2
20	77,8	69,5	48,0	69,0
21	85,4	76,3	53,8	70,5
22	94,1	84,1	55,1	65,5
23	103,3	92,3	60,7	65,7

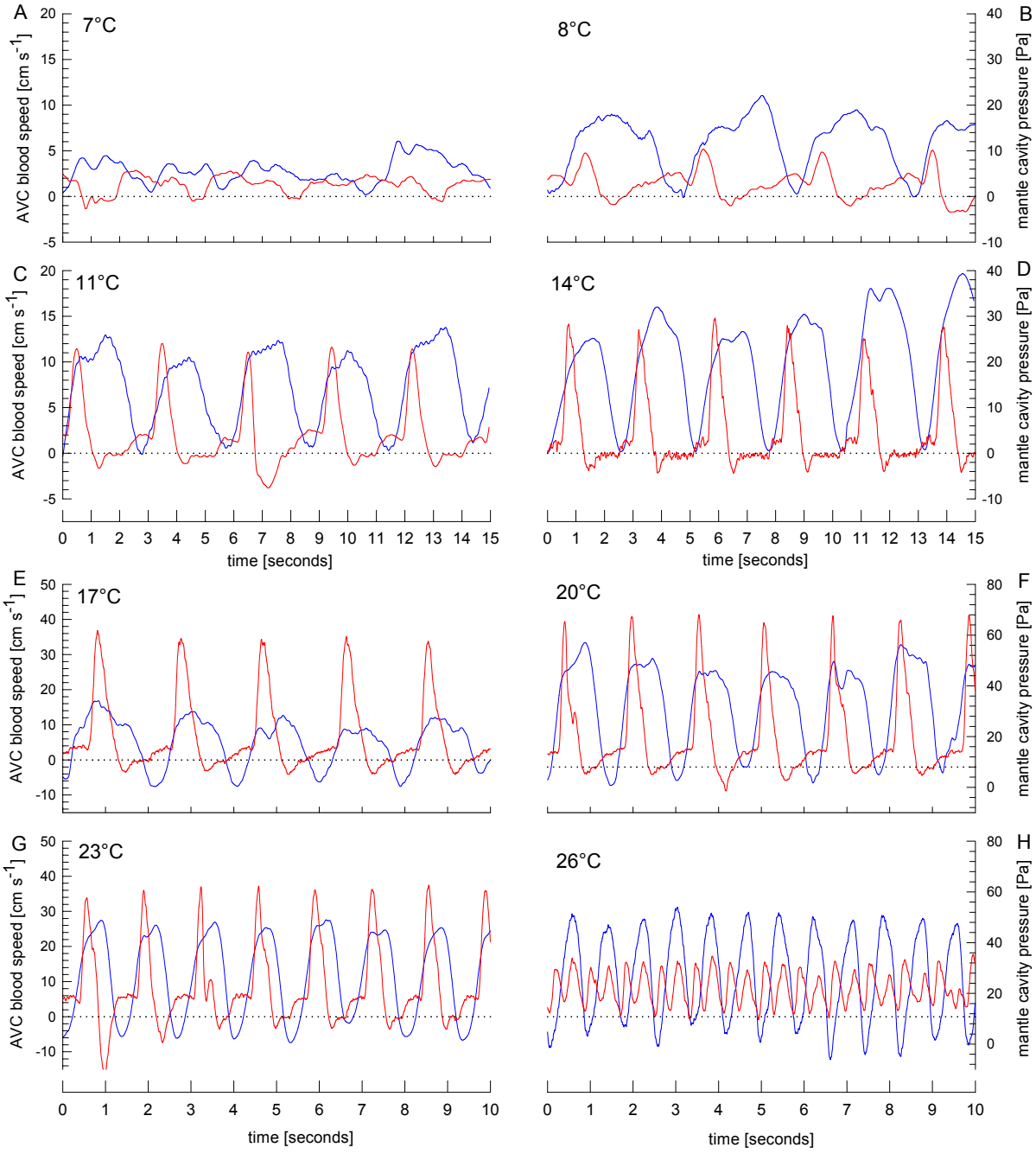
A
7°C
B
8°C
C
11°C
D
14°C
E
17°C
F
20°C
G
23°C
H
26°C
AVC blood speed [cm s-1]
mantle cavity pressure [Pa]
time [seconds]

Figure 1

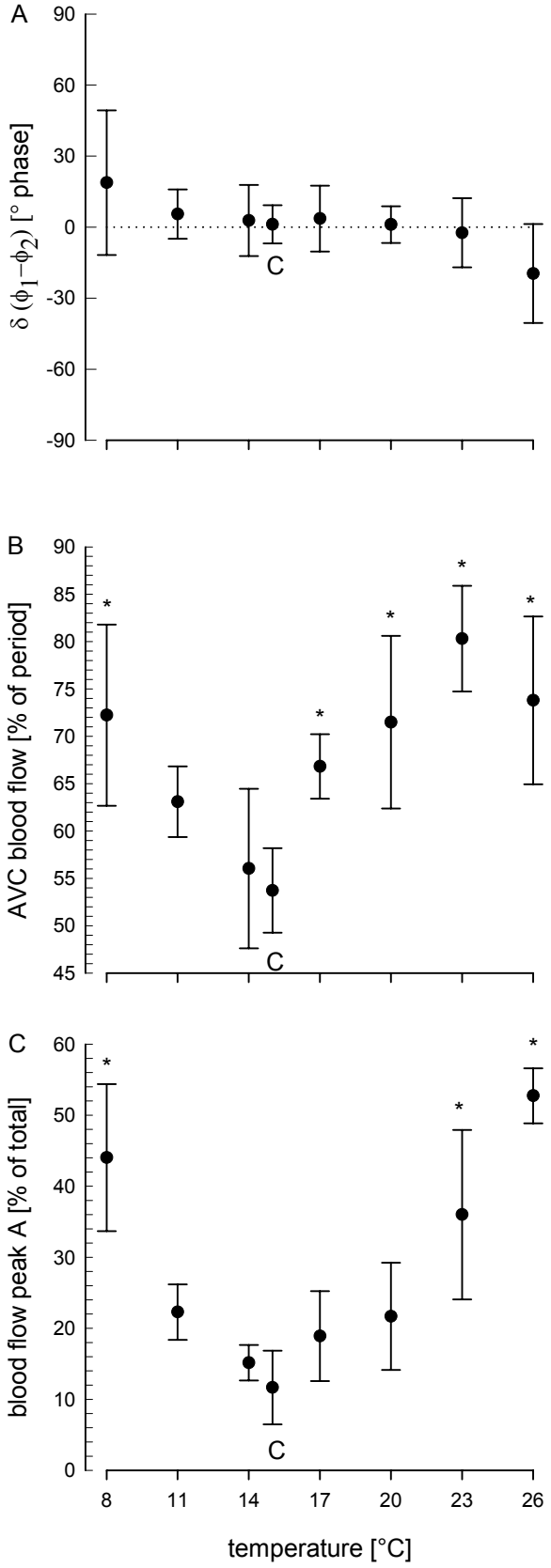
A
B
C
δ (ϕ1−ϕ2) [° phase]
AVC blood flow [% of period]
blood flow peak A [% of total]
temperature [°C]
C
*

Figure 2

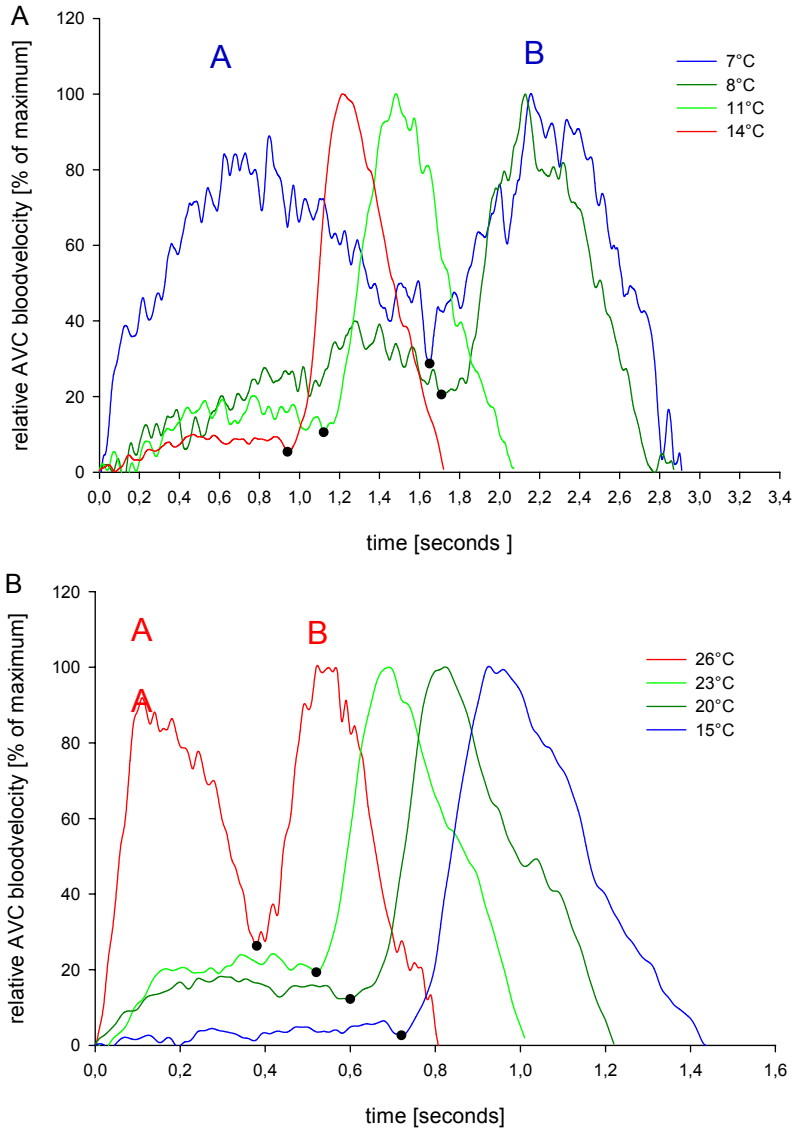
A
relative AVC bloodvelocity [% of maximum]
120
100
80
60
40
20
0
A
B
7°C
8°C
11°C
14°C
0,0 0,2 0,4 0,6 0,8 1,0 1,2 1,4 1,6 1,8 2,0 2,2 2,4 2,6 2,8 3,0 3,2 3,4
time [seconds]
B
relative AVC bloodvelocity [% of maximum]
120
100
80
60
40
20
0
A
A
B
26°C
23°C
20°C
15°C
0,0 0,2 0,4 0,6 0,8 1,0 1,2 1,4 1,6
time [seconds]

Figure 3

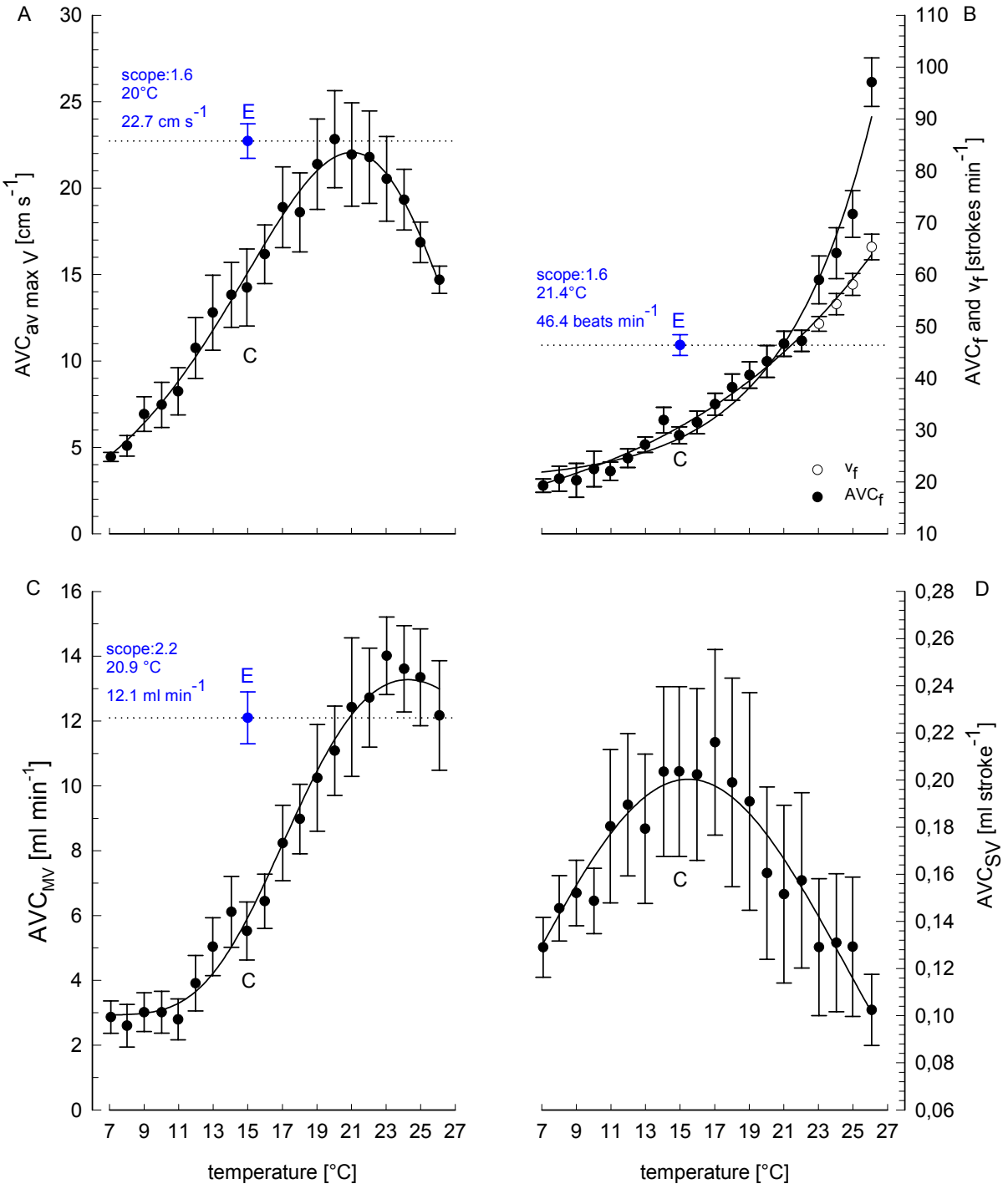
A
B
C
D
scope:1.6
20°C
22.7 cm s-1
E
C
AVCav max V [cm s-1]
scope:1.6
21.4°C
46.4 beats min-1
E
C
vf
AVCf
AVCf and vf [strokes min-1]
scope:2.2
20.9 °C
12.1 ml min-1
E
C
AVCMV [ml min-1]
C
AVCSV [ml stroke-1]
temperature [°C]
temperature [°C]

Figure 4

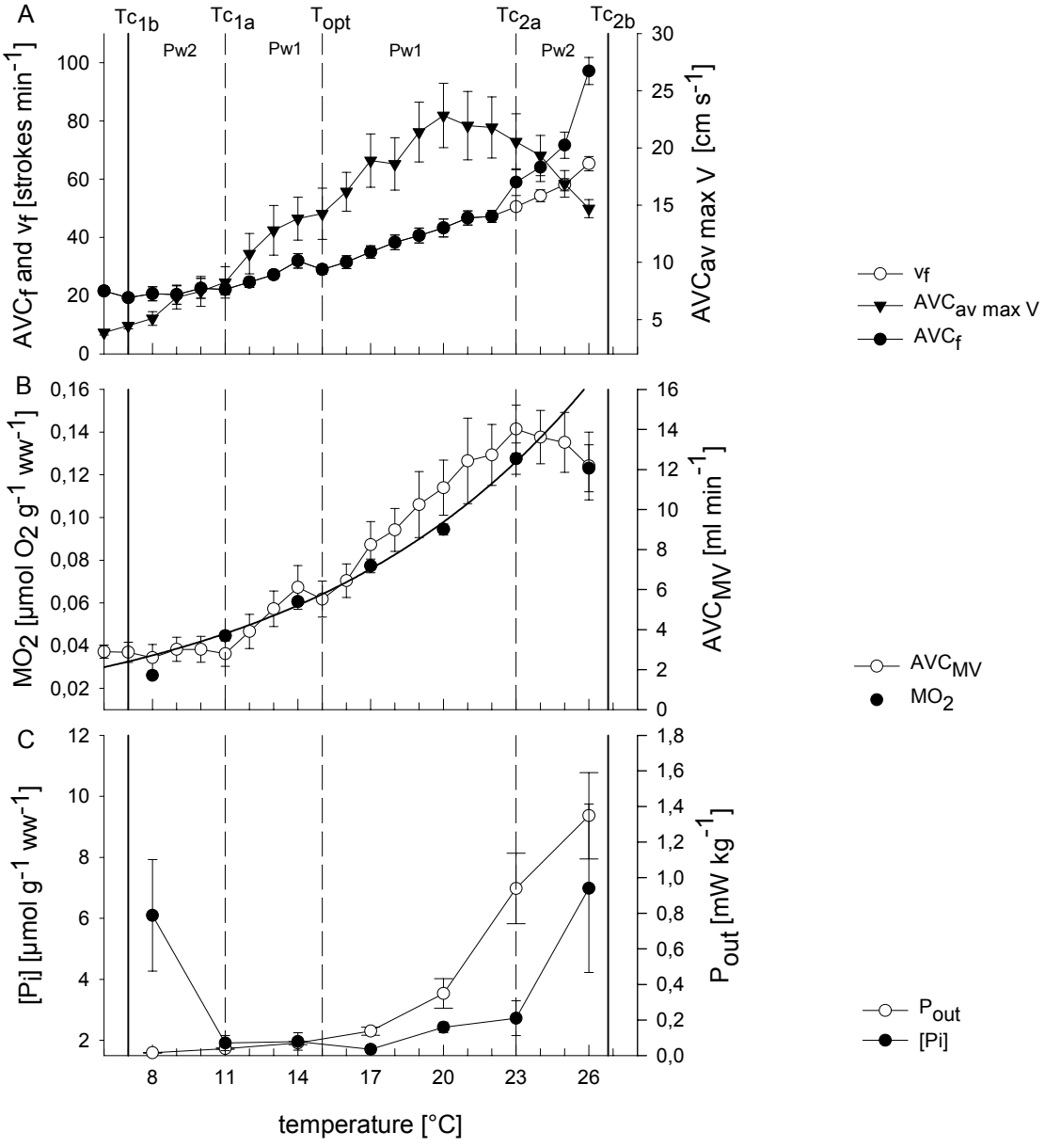
A
B
C
Tc1b
Tc1a
Topt
Tc2a
Tc2b
Pw2
Pw1
Pw1
Pw2
AVCf and vf [strokes min-1]
AVCav max V [cm s-1]
MO2 [µmol O2 g-1 ww-1]
AVCMV [ml min-1]
[Pi] [µmol g-1 ww-1]
Pout [mW kg-1]
temperature [°C]
vf
AVCav max V
AVCf
AVCMV
MO2
Pout
[Pi]

Figure 5

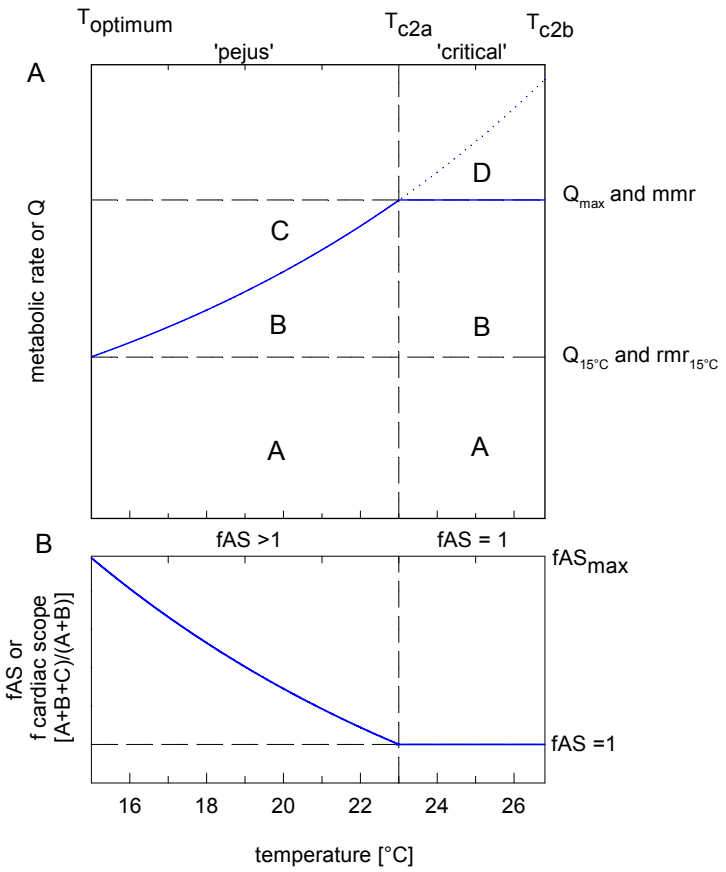
T optimum
T c2a
T c2b
'pejus'
'critical'
A
metabolic rate or Q
D
C
B
B
A
A
Q max and mmr
Q 15°C and rmr 15°C
B
fAS >1
fAS = 1
fAS max
fAS =1
fAS or
f cardiac scope
[A+B+C)/(A+B)]
16
18
20
22
24
26
temperature [°C]

Figure 6

4. Discussion

The present dissertation addressed the question, whether the cuttlefish *Sepia officinalis* L. (Mollusca, Cephalopoda) would suffer from limited oxygen supply once critical high or low temperature thresholds were reached. Such a phenomenon had previously been observed in several marine aquatic ectothermic animals (i.e. crustaceans, bivalve and gastropod molluscs, polychaete and sipunculid worms, teleosts) and resulted in the formulation of an ‚oxygen limitation of thermal tolerance' hypothesis (Zielinski and Pörtner, 1996, Sommer et al. 1997, Frederich et al. 2000, Pörtner, 2001, 2002, Mark et al. 2002, Lannig et al. 2004, Pörtner et al., 2004).

It was further proposed that oxygen limitation would set in at high hierarchical levels of systemic organization (Pörtner 2002), especially the integrated function of the main elements of convective oxygen transport of the organismic entity, i.e. the ventilatory and / or circulatory apparatus. Accordingly, the thermal window of individual cells and organels of an organism is ultimately wider than that of the multicellular unit, the organs, while the even higher unit, formed by the integration of functionally connected organs (for example, the circulatory system, consisting of blood pumps, muscular blood vessels with defined mechanical properties all of which are humorally, mechanically and neuronally integrated) has an even narrower thermal tolerance range. Analogous to a Gaussian error propagation system with an ever increasing amount of independent variables, more and more units with specific variabilities in performance, integrated into one system, contribute to a higher total ‚error'. In the case of whole organism thermal tolerance, a narrower thermal window of optimum performance would result. Functional integration of several vital system parts with differing optimum thermal performance ranges must result into the creation of a system with a narrower thermal tolerance range than each of its individual components. Figure 4.1 illustrates this principle:

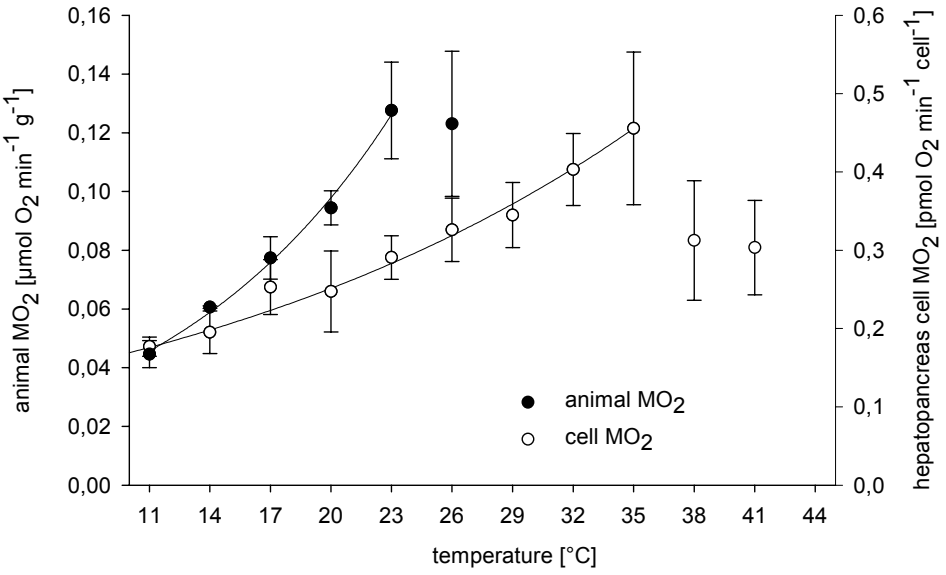

Figure 4.1. Whole animal vs. cellular oxygen consumption (MO_2) during warming. *S. officinalis* whole animal MO_2 data taken from publication 2, fig 4 for 105 g wet mass animals from the English Channel population. Cell MO_2 data: *S. officinalis* hepatopancreas cells from English Channel animals of 174 g mean wet mass (Trost, Hirse, Melzner, Pörtner, unpublished and Trost, 2003), means ± SD, n=4-6.

While respiration rate in isolated cuttlefish (*S. officinalis*) hepatopancreas cells follows an exponential relationship up to about 35°C, whereafter cellular function becomes impaired, whole animals from the same population can increase metabolic rate only up to 23°C. Apparently, upon integration of cells into a complex functional unit, thermal sensitivity of the whole unit has increased.

Dysfunctioning of highly integrated organ systems was found to be the first limiting factor determining organismic thermal tolerance windows in several taxa. For example, a failure of the ventilatory systems to oxygenate haemolymph developed progressively in a sipunculid worm and in a crustacean (Zielinski and Pörtner 1996, Frederich and Pörtner 2000), while a capacity limitation of the circulatory system was observed in teleosts (Mark et al. 2002, Lannig et al. 2004).

Therefore, a second aim of this dissertation was to investigate the functional characteristics of ventilatory and circulatory systems under conditions of thermal change. However, owing to the lack of data on cuttlefish ventilatory and circulatory function under control conditions, their basic characteristics had to be elaborated first. In the following sections, we will therefore first focus on the cuttlefish oxygen transfer system and its function under typical control conditions (15°C, at rest and during spontaneous exercise) and compare it to other cephalopod molluscs and teleosts that occupy similar ecological niches (see 4.1). In addition to material presented in publications 1, 2 and 4, some unpublished material on haemocyanin oxygen binding characteristics in cuttlefish will also be considered to elaborate the particular lifestyle adaptations this invertebrate employs to successfully compete in its habitat.

Acute thermal change experiments (section 4.2.1), as presented in publications 1, 2, 3 and 5 will be discussed with regard to similar experiments conducted with teleost species (Lannig et al. 2004, Mark et al. 2002). In addition, unpublished material on physiological characteristics of different temperature acclimation groups of cuttlefish (‚slow' temperature change, section 4.2.2) will be presented and discussed in relation to the velocity and magnitude of temperature changes in the natural habitat. Eventually, some concluding remarks on the importance of temperature as an abiotic stress factor for cuttlefish will follow (section 4.3).

4.1 Physiology of the cuttlefish oxygen transfer system

4.1.2 Resting conditions

‚Resting' probably is the predominant state of life in a cuttlefish. Recent investigations on activity modes of tropical cuttlefish (*Sepia apama*) in their natural habitat revealed that these animals spend up to 97% of a days time relatively motionless and hidden in rock crevices (Aitken et al. 2005). Foraging occurred during the remaining 3% of the day. Aitken and coworkers concluded from energetic considerations, that animals probably can feed to satiation within this restricted time interval,

indicating an energy efficient, sit–and-wait mode of predation. Indeed a lifestyle that resembles that of octopi, which also hide in dens and spend about 10% of a day's time foraging (Mather and O'Dor 1991). However, these lifestyles are completely different from those of the cuttlefish's pelagic decapod relatives, the constantly swimming oceanic squids (e.g. Nakamura 1991, O'Dor et al. 1994).

Despite several laboratory studies conducted on European cuttlefish (*S. officinalis*) over the past decades (e.g. see Hanlon 1990), there is surprisingly little quantitative information available on activity states and behaviour in the natural habitat. However, there are observations by Denton and Gilpin - Brown (1961b), reporting that juvenile animals are buried in sand (in a laboratory surrounding) for the greater part during daytime, whilst sitting on the sediment during night time to forage. Burrowing behaviours in sepiolid and sepioid cephalopods have often been described in laboratory surroundings (e.g. Boletzky and Boletzky 1970, Melzner, pers. obs.) and it is straightforward to assume that these (facultative) negatively buoyant predators spend a greater part of the day on the highly uniform seafloor in the English Channel (Bouchaud - Camou and Boismery 1991), avoiding predators and waiting for prey, whilst being covered by a protective sand layer.

a) *Ventilation mechanics*. A predominantly resting lifestyle has led to similar physiological adaptations in both octopi and cuttlefish (Wells and Wells, 1991: ‚Is *Sepia* really an octopus?'). While squid respire oxygen from a stream of water that also fuels swimming movements, octopods and cuttlefish have successfully decoupled their ventilatory water pumps from locomotory pumping systems (Wells 1990). By extracting high proportions (>50%) of dissolved oxygen, relatively small volumes of water have to be pumped through the mantle cavity (less than 3% of the animals' body mass per ventilatory stroke; Wells and Wells 1985, 1991), while during jet locomotion requirements go in the opposite direction: Jet propulsion is most efficient when a large volume of water is ejected at low velocity (O'Dor and Webber 1991). Thus, squid only extract 5-10% of dissolved oxygen from their ventilatory stream, while they eject 20-30% of their body mass (in seawater units) per jet (Wells and Wells 1991).

Experiments reported in publication 2 have revealed, that previous estimates of high oxygen extraction (EO_2) values in cuttlefish (Wells and Wells 1982, 1991) may even be underestimates. At a long term acclimation temperature of 15°C, cuttlefish of 105 g wet mass can extract 80% of dissolved oxygen from their ventilatory stream, thus only need to transport 22 ml water min^{-1}, which, at a ventilation rate (v_f) of 30 strokes min^{-1}, yields a ventilatory stroke volume of 0.7 ml $stroke^{-1}$. Combined action of the ventilatory muscles, the collar flaps of the funnel apparatus and the radial mantle muscle fibres (Bone et al. 1994a) generate this water current through the cuttlefish mantle cavity at relatively low mean pressures (MMP) of < 0.02 kPa. Low flow requirements and low MMP lead to a low power output (P_{out}) of the ventilatory system of 0.1-0.2 mW kg^{-1} animal, which results in very low cost for ventilation mechanics (v_C) in cuttlefish of 1 - 1.5% of routine energy expenditure (P_{tot}). These estimates are high estimates, as we used several pessimistic assumptions to calculate v_C (see publication 2 for a detailed discussion). It seems that, from an energetic point of view, cuttlefish

are well equipped to compete with flatfish which are also found in sandy bottom habitats of the English Channel. Not only do cuttlefish ventilation systems extract similar or even higher quantities of dissolved oxygen (see publication 2, Steffensen et al. 1982), *S. officinalis* also spends a lower fraction of routine energy expenditure for ventilation mechanics than fish. Common estimates for the costs of gill ventilation in fish range between 10 – 15 % rmr (Hughes 1973, Cameron and Cech 1970). The cuttlefish ventilation system is more cost efficient, because it is driven by a low pressure fluid dynamic pump (Vogel 1994) that operates at pressures nearly as low as those found in mussels (0.01-0.04 kPa, Jørgensen et al. 1988) and at significantly lower pressures than the buccal and opercular pumps of characteristic fish species (e.g. 0.2-0.3 kPa pressure amplitude in *Salmo salar* and *Squalus acanthias*, Perry and McKendry 2001). Minimizing costs for ventilation mechanics clearly suits the demands of an energy conserving sit-and-wait predator.

b) Circulation mechanics. Publication 4 presents experimental data that provide insight into how cuttlefish may achieve such a high gas exchange efficiency by coupling ventilatory to circulatory pumps. Several studies had previously demonstrated that the activity of circulatory components in some cephalopods is coordinated with ventilatory movements (e.g. Johansen and Martin 1962, Smith 1962, Bourne 1982). However, the phase relationships between both major convective oxygen carrier systems had not been investigated. For cuttlefish, no information on circulatory – ventilatory interactions was available at all, prompting us to investigate basic characteristics of the anterior vena cava (AVC) – flow and contractile system under control conditions, and, later, during thermal stress by use of a minute Doppler probe and mantle cavity pressure catheters (see publication 4, 5, and below).

Apparently, blood flow in this most important cuttlefish vein is strictly coupled to ventilatory pressure oscillations in a way, that short blood flow pulses in the vein are elicited exactly at the maximum increase in mantle cavity pressure (see fig. 2 in publication 4). Although ventilatory pressure curve shapes vary between individuals and for the same animal in that maximum slopes appear earlier or later in the ventilatory period, the tight connection between blood pulse start and maximum pressure increment was found to be obligatorily present in all records analyzed (see fig. 3 in publication 4). As mantle cavity pressure in cephalopods is directly correlated to respiratory water movements through the mantle cavity (e.g. Shadwick 1994), this apparent connection between circulatory and ventilatory systems might enable efficient gas exchange at the gills, by exactly timing blood flow within gill vessels and water flow around the latter. However, studies examining microcirculation of blood and water at the gill epithelia are lacking to date.

Our investigations using the *in vivo* magnetic resonance imaging (MRI) system (see fig 6. in publication 4) further substantiated the concept of a tight matching of ventilatory and circulatory perfusion rates: Under true resting conditions, not only the contractile veins (including the AVC), but also all three hearts beat at the very frequency of the ventilatory system, potentially improving oxygen extraction from the ventilatory current.

c) Oxygen transport in the blood. The efficiency of a counter current gas exchange system does not only depend on the precise shuttling of ventilatory water of defined oxygen partial pressures past the exchange surfaces, but also and to a great extent on PO_2 of blood entering and leaving the gills. The following formula can be used to approximate the average oxygen partial pressure gradient across the gill epithelia (ΔPO_2), pressure head for diffusion of oxygen into the blood (Piiper 1998, see also publication 2):

$$\Delta PO_2 = (0.5(PO_{2\,I} + PO_{2\,E})) - (0.5(PO_{2\,a} + PO_{2\,v})) \quad (1)$$

with $PO_{2\,I}$ (kPa) = inhalant water oxygen partial pressure; $PO_{2\,E}$ (kPa) = exhalant water oxygen partial pressure; $PO_{2\,a}$ (kPa) = arterial oxygen partial pressure; $PO_{2\,v}$ (kPa) = venous oxygen partial pressure. Exchange systems that maximize oxygen extraction (EO_2) from the ventilatory current must minimize $PO_{2\,E}$. Rearranging equation 1 gives:

$$PO_{2\,E} = (2*\Delta PO_2) - PO_{2\,I} + PO_{2\,a} + PO_{2\,v} \quad (2)$$

Thus, in order to minimize $PO_{2\,E}$, the right part of the equation has to be minimized as well. As $PO_{2\,I}$ ideally is constantly high at around 20 kPa in normoxic waters and as there is a driving force towards maximizing $PO_{2\,a}$ in cephalopods (see Johansen et al. 1982, Pörtner 1990b, publication 2), it is only the minimization of $PO_{2\,v}$ that can increase oxygen extraction. Judging from high oxygen extraction rates of 80% observed in *S. officinalis* under resting conditions at 15°C (see publication 2), one would therefore expect low oxygen partial pressures in venous vessels to be characteristic for this cephalopod ecotype.

Indeed, Johansen et al. (1982, English Channel population) found a mean $PO_{2\,v}$ of 3.5 kPa in the *S. officinalis* AVC, which is considerably lower than the 5.8 kPa measured in the same vessel in two squid species that are not characterized by high oxygen extraction rates (*Illex illecebrosus* and *Loligo pealei*, Pörtner et al. 1991). However, our results (Melzner, Langenbuch, Wolfram, Gutowska, Claireaux, Pörtner, unpublished) indicate that $PO_{2\,v}$ in the AVC can be even lower. Average PO_2 values of 1.3 kPa at a control temperature of 17°C were recorded in cannulated, resting Bay of Biscay animals (see table 4.1), illustrating yet another physiological feature enabling a high efficiency of gas exchange in cuttlefish.

In addition, haemocyanin oxygen binding characteristics support such low venous PO_2s. Figure 4.2 displays oxygen – binding properties of cuttlefish haemocyanin in a pH/saturation diagram as introduced by Pörtner (1990b) at an assay temperature of 17°C.

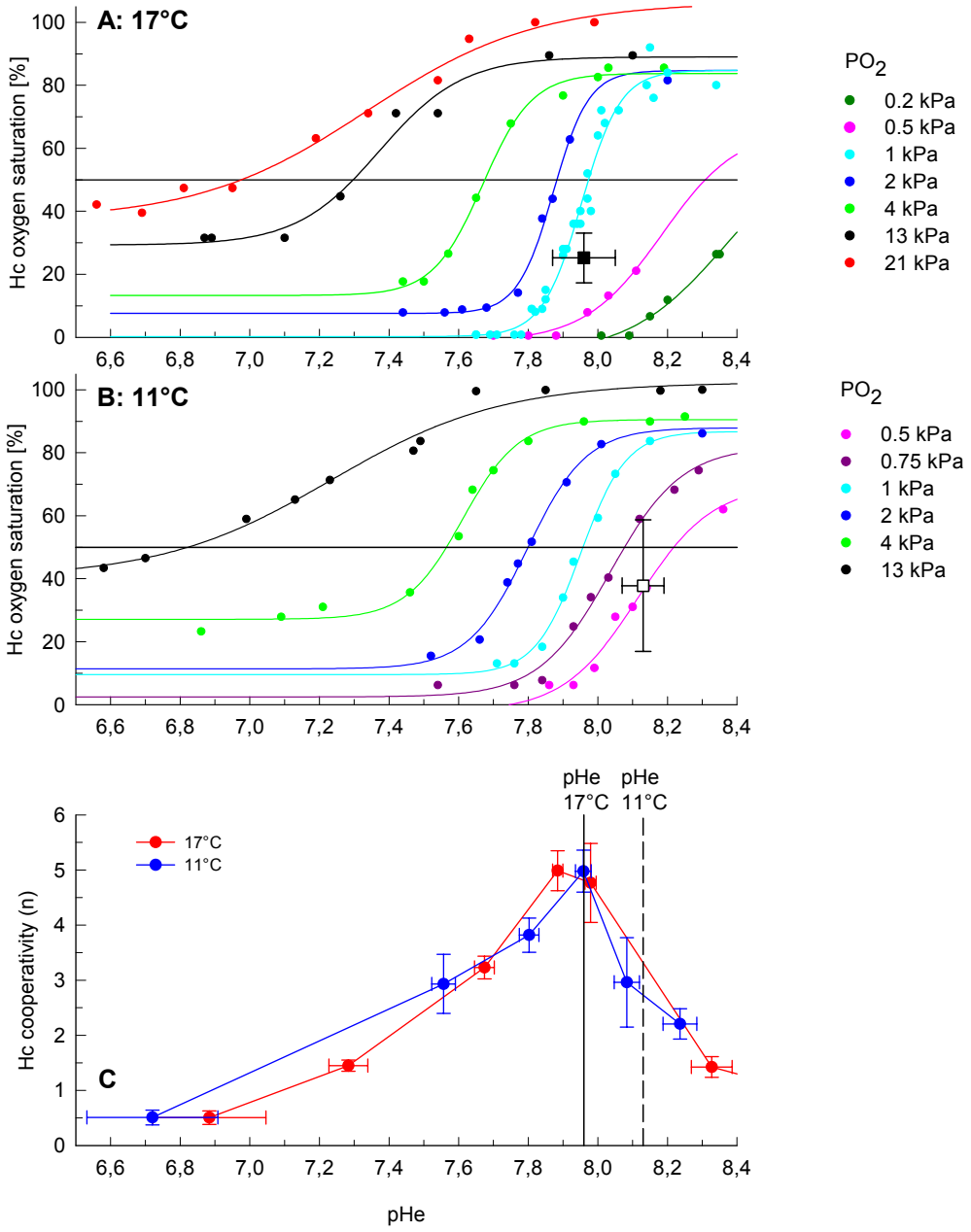

Figure 4.2. Relationships between pHe and PO_2 and oxygen binding as well as cooperativity in cuttlefish (*S. officinalis*) blood displayed in a pH/saturation diagram (Pörtner 1990b) at two different assay temperatures. (A) Hc saturation [%] in relation to pH and PO_2 at 17°C; (B) Hc saturation [%] in relation to pH and PO_2 at 11°C; (C) Changes in cooperativity (n_{50}, Hill coefficients) with pH and temperature. Oxygen isobar regressions are 4 factorial sigmoidal fits, the legend indicates oxygen partial pressures of the respective regressions. Inserts in (A) and (B) indicate *in vivo* pH and Hc saturation (means and SD) as measured in n=6 animals in the anterior vena cava (AVC) (see also table 1). Vertical lines in (C) indicate in vivo pH; Hill coefficients in (C) were calculated for each oxygen isobar between 40 and 60% saturation as in Pörtner (1990b).

At constant PO_2, transitions in haemocyanin (Hc) oxygenation with pH are displayed for a number of oxygen partial pressures between 0.2 and 21 kPa. As in the case of two squid species (*I. illecebrosus*, *L. pealei*, Pörtner 1990b), oxygen isobar curve shapes vary in a specific manner: With decreasing and increasing PO_2, sigmoidal isobar slopes become progressively greater around the point of inflection,

reaching a maximum in an intermediate PO_2 range. The steepest isobars are usually found in the region of *in vivo* blood pH. For Bay of Biscay cuttlefish, these are the 2 kPa isobar at a pH_{50} of 7.88 and the 1 kPa isobar at a pH_{50} of 7.98 (fig 4.2a). *In vivo* pH was found to be 7.96 in the AVC at 17°C (see table 4.1).

Table 4.1. *In vivo* (anterior vena cava, AVC) and *in vitro* blood oxygen binding parameters for *S. officinalis*, Bay of Biscay population at control (17°C) and acutely lowered (11°C, 8°C) temperatures.

	17°C; n=6	*11°C; n=6*	*8°C; n=2*	*p (17°C vs. 11°C)*
pHe	7.96 (0.09)	8.13 (0.06)	8.24	p<0.001)
S [%]	25.2 (7.9)	37.8 (20.9)	40.8	p>0.067
Ut [%]	74.8	62.2	59.2	
$PO_{2\,v}$ [kPa]	1.28 (0.64)	0.94 (0.32)	0.50 (0.27)	p>0.07
Bohr – coefficient (ΔP_{50} / Δ pH)	-1.32	-1.02	n.d.	

pHe = AVC blood pH, S = Haemocyanin (Hc) oxygen saturation, Ut = Hc oxygen utilization (in %) = arterial Hc oxygen saturation (estimated to be 100%, see Johansen et al. 1982) – venous Hc oxygen saturation (in %) , see publication 5; PO_{2v} = AVC venous oxygen partial pressure. Statistics: Paired t-tests between 17 and 11°C values; n.d. = not determined.

As the steepness of oxygen isobars is an indicator for the pH sensitivity of the pigment (i.e. Hc saturation change per unit pH), maximum steepness means that relatively small changes in pH suffice to liberate large fractions of haemocyanin bound oxygen into the blood. Maximum pH sensitivity ($\Delta S/\Delta pH$) encountered at a pH_{50} of 7.88 (2 kPa isobar) was found to be 368 $\%S\ pH^{-1}$. Therefore, a change in just 0.1 pH units in this pH range would liberate nearly 40% of all haemocyanin bound oxygen. However, this is only possible at relatively low venous oxygen partial pressures of 1 – 2 kPa. Cooperativity of the pigment (n_{50}), linearly correlated to pH sensitivity (Pörtner 1990b, Zielinski et al. 2001), is highest at pHe 7.88 and 17°C (see fig 4.2c). Our *in vitro* oxygen binding studies clearly suggest that high oxygen partial pressures in cuttlefish venous blood would decrease haemocyanin pH sensitivity and cooperativity, hampering efficient oxygen unloading. Thus, the respiratory pigment would largely contribute to oxygen transport at *in vivo* pH and relatively low venous PO_2 values.

In vertebrates, oxygen transport from the capillary into the cell (transcapillary diffusion) is considered to be the principle bottleneck, as mitochondrial membrane area is approximately 500 times greater than the aggregate surface area of red cell containing capillaries (Taylor et al. 1987). There are no haeme protein oxygen carriers present in the membrane, calling for a relatively high PO_2 gradient to drive oxygen flux (Honig 1992). It is straightforward to assume the same to be true for cephalopod molluscs. Although it is not exclusively the oxygen partial pressure difference between extra- and intracellular media, but also a multifactorial oxygen conductance terminus (see Honig 1992 and references therein for details) that determines oxygen flux into the cell, $PO_{2\,v}$ may still be a prime

indicator for aerobic scope or metabolic potential of a given species. As for decapod cephalopods studied so far, there are some obvious relationships between blood $PO_{2\,v}$, whole animal metabolic rate and haemocyanin oxygen binding properties (see table 4.2):

Table 4.2. Oxygen isobars from pH/saturation diagrams with the highest pH sensitivity and cooperativity (n_{50}) vs. animal routine metabolic rates (rmr) for different decapod cephalopods.

Species	*PO_2 [kPa] (at pH_{50}) of steepest isobar*	*In vivo $PO_{2\,v}$ [kPa]*	*n_{50} at pH*	*MO_2 [µmol O_2 g^{-1} min^{-1}] 50 g wet mass animals*
I. illecebrosus	7.9 (7.4) (1)	5.8 (3)	10.6 (7.4) (1)	0.34 (4)
L. pealei	3.7 (7.65) (1)	5.8 (3)	6.1 (7.65) (1)	0.23 (5)
S. officinalis	2.0 (7.88) (2)*	1.3 (2)*	5.0 (7.88) (2)*	0.07 (6)

Data: (1) Pörtner 1990b; (2) Melzner, Langenbuch, Wolfram, Gutowska, Claireaux, Pörtner, fig. 2 and unpublished data; (3) Pörtner et al., 1991; (4) DeMont, 1981; (5) Macy, 1980; (6) Melzner, Bock, Pörtner, publication 3, two – factorial regression for MO_2 (routine). pH_{50} = pH value at 50% Hc saturation for the respective oxygen isobars. All in *vitro* and *in vivo* data obtained at 15°C, except for * = 17°C. n_{50} = Hill coefficients, maximum values for each species displayed.

From the pelagic, constantly swimming squid *I. illecebrosus* to the nekto – benthic cuttlefish *S. officinalis*, routine metabolic rate declines by a factor of roughly five. Correlated, PO_2s of steepest isobars in the ph/saturation diagram progressively decline, as do cooperativity (Hill coefficients, n_{50}) and *in vivo* $PO_{2\,v}$ in the AVC. Thus, a progressive trend towards low PO_{2v} and an optimization of blood pigment function at low PO_2 may provide the basis for high oxygen extraction rates in the less active decapods. On the other hand, the very same characteristics may also prevent cuttlefish from displaying higher metabolic rates, as diffusion is hampered by a low 'driving force', i.e. a low oxygen partial pressure difference across the cell membrane, as is caused by low PO_{2v}.

d) <u>*Summary.*</u> Compared to their pelagic decapod relatives, cuttlefish 'live in the slow lane', as they are resting for large fractions of the day. Several physiological characteristics of *S. officinalis* support such an energy conserving lifestyle. Decoupling of the ventilatory from the locomotory water flow resulted in the establishment of a very cost-efficient ventilation system, characterized by low pressures driving low volumes of water. Low ventilatory volumes can be realized as cuttlefish extract 80% of dissolved oxygen from the ventilatory water. This likely is a consequence of precise hydrodynamic coupling of ventilatory and circulatory perfusion systems, low venous oxygen partial pressures and concomitant modifications in haemocyanin function.

4.1.3 Aerobic challenges

In order to investigate the impact of thermal challenges on the cuttlefish oxygen distribution system, it is important to consider maximum aerobic performance under control temperatures. Three

main processes force cephalopods to display grossly elevated metabolic rates at constant temperature, steady state aerobic exercise (hunting, social interactions), recovery from escape behavior and elevated oxygen requirements following large meals, the specific dynamic action of food (SDA).

a) Exercise. Jet propulsion is an inherently inefficient mode of locomotion when compared with the undulatory mode of fin swimming in teleosts (O'Dor and Webber 1986, 1991, Vogel 1994). The cuttlefish ecotype escapes this limitation mainly by hardly moving at all (see above and Aitken et al. 2005) and, when moving, by combining low pressure jet propulsion with thrust generation by undulatory movements of their prominent fins (Aitken and O'Dor, 2004) while using their cuttlebone for buoyancy regulation (Denton and Gilpin – Brown, 1961 a,b, Webber et al. 2000).

Under resting conditions (publication 1), cuttlefish displayed elevated mantle cavity pressure amplitudes (MMPA), related to spontaneous exercise, for approximately 3% of the experimental time, a figure that is close to activity levels found in tropical *S. apama* in the natural habitat (Aitken et al 2005). Escape or swimming jets (SJs) of pressure amplitudes up to 12 kPa (publication 1) and 17 kPa (publication 4) were witnessed occasionally, being fuelled in part by the net use of phosphagen (phospho-L-arginine, PLA) stores in the thick layers of central, circular muscle bundles (publication 1). Not only does oxygen extraction from the ventilatory current decrease during such high pressure swimming jet phases (see fig 2, publication 2), SJs also interacts with blood flow in the anterior vena cava (AVC) (see fig 4 in publication 4). The high jet pressures, encountered during exercise in the mantle cavity, compress this thin capacitance vessel. However, owing to a sophisticated arrangement of valves, blood flow is not inhibited (as in octopods, Wells et al. 1987), but rather led in the proper direction towards the branchial hearts. In publication 4, exercise and recovery time – series, and their influence on blood flow through the AVC were also studied. Short, but intensive exercise periods resulted in steep increases in blood flow shortly after termination of 1-2 minute exercise periods. AVC minute volume (AVC_{MV}) increased by a mean maximum factor of 2.2. Similar exercise related factorial scopes for blood flow increments were about 2 in *O. vulgaris* (Wells et al. 1987). Magnitudes of factorial scopes for blood flow in these two cephalopod ecotypes are comparable to maximum factorial aerobic scopes during exercise (i.e., maximum aerobic metabolic rate / routine metabolic rate) of between two and three (Wells et al. 1983a, 1987 Aitken and O'Dor 2004), suggesting that these factorial scopes are mainly supported by the respective increase in blood flow during an exercise challenge. Therefore, increasing oxygen utilization (Ut) from the blood, as observed during hypoxia in cuttlefish (Johansen et al. 1982), probably only plays a minor role during exercise bouts.

b) Specific dynamic action of food (SDA). Cephalopods are the fastest growing marine invertebrates known (Forsythe and Van Heukelem 1987). *S. officinalis* of approximately 100 g wet mass are able to ingest 10% of their body mass on a daily basis at 23°C, while growing at a rate of 4% of their own body mass per day (Melzner et al. 2005). Unfortunately, nothing is known about the aerobic costs of digestion in cuttlefish, the specific dynamic action of food (SDA). However, some information is available for the octopod *O. vulgaris*. Several authors found maximum increases in

metabolic rate with feeding of 2-3 times routine metabolism, occurring 1-2 hours after feeding to satiation (Wells et al. 1983, Valverde and Garcia 2004, Katsanevakis et al. 2005). The shorter duration of the SDA response in *O. vulgaris* (<10h, Wells et al. 1983, Katsanevakis et al. 2005) than in fish (e.g. 24-36h, Jobling 1981) is believed to be the basis for the high growth rates encountered, and thus for the particular, semelparous, ‚live fast, die young' life – cycle strategy that is characteristic for cephalopods in general (Wells et al. 1983b, Katsanevakis et al. 2005). The sharp 2-3 fold increase in MO_2 just one or two hours after a meal reflects a similar aerobic scope as during exercise.

At comparable feeding and growth rates in both octopi and cuttlefish (Mangold and von Boletzky 1973, Forsythe et al. 1994, Melzner et al. 2005), it is straightforward to assume that cuttlefish face similar digestive challenges as octopods. As oxygen extraction from venous blood is already as high as 75% in cuttlefish (see table 1), there is little room for an increase in oxygen demand, unless by an increase in blood flow. Thus, as seen during exercise, elevated oxygen demands are probably met by tantamount increases in relative blood perfusion. At high daily food intake and high daily growth rates, cephalopods thus very likely constantly need to use considerable parts of their cardiac and aerobic scopes to cope with food processing: Wells et al. (1983b) simulated growth rates observed in the natural habitat by feeding 250-1000g octopi one crab of 20 g per day for several days. Average oxygen consumption rates increased by a factor of 2-3 with respect to oxygen consumption rates under starving conditions. Wells et al. (1983a,b) concluded from their study that it is feeding state and not physical activity that largely determines oxygen requirements of an octopus.

c) Summary. Both physical activity and the effects of feeding can increase aerobic metabolic rate in octopods and, likely, cuttlefish by a factor of 2-3. At Hc oxygen utilization (Ut, see table 4.1) being already very high, it is probably the tantamount increases in blood perfusion provide the extra quantity of oxygen during such situations. As short SDA periods are a reflect a lifestyle characterized by rapid growth rates, it is likely the oxygen demand of digestion that shape the maximum performance characteristics of the cardiovascular system of cuttlefish and octopods. However, it follows that with both, exercise and SDA being dependent on extra oxygen provided by elevated cardiovascular performance (i.e. increases in cardiac output), neither process can reach its maximum aerobic rate when they compete for the oxygen available from the circulatory system.

The (likely) additive character of aerobic challenges and their dependence on cardiovascular performance, as well as the fact, that cuttlefish and octopods likely always and continuously devote a significant quantity of their cardiovascular capacity to the excessive demands of SDA, should be borne in mind when the effects of acute thermal change are being discussed in the next section.

4.2 Oxygen limitation of thermal tolerance

4.2.1 ‚Fast' ambient temperature change

Publications 1, 2, 3 and 5 explored the effects of acute temperature changes (at an average rate of 1 °C h^{-1}) on mantle muscle energy status, ventilatory and circulatory performance and routine metabolic rate. All studies used the same experimental protocol: Following 24 h of starvation, animals had to undergo surgery (if necessary) on experimental day 1, were kept within the experimental setup to acclimate during the remainder of the day, cooled down at an average rate of 1°C h^{-1} on day 2, brought back to and kept at control temperature (15°C) during the night, and were heated at 1°C h^{-1} during day 3. All of these experiments were performed on cultured animals originating from the English Channel. Some additional material highlighting the crucial role of the blood oxygen carrier haemocyanin, obtained on wild caught animals from the Bay of Biscay, will also be considered in the discussion. Figure 4.3 illustrates the major findings from all acute temperature change experiments:

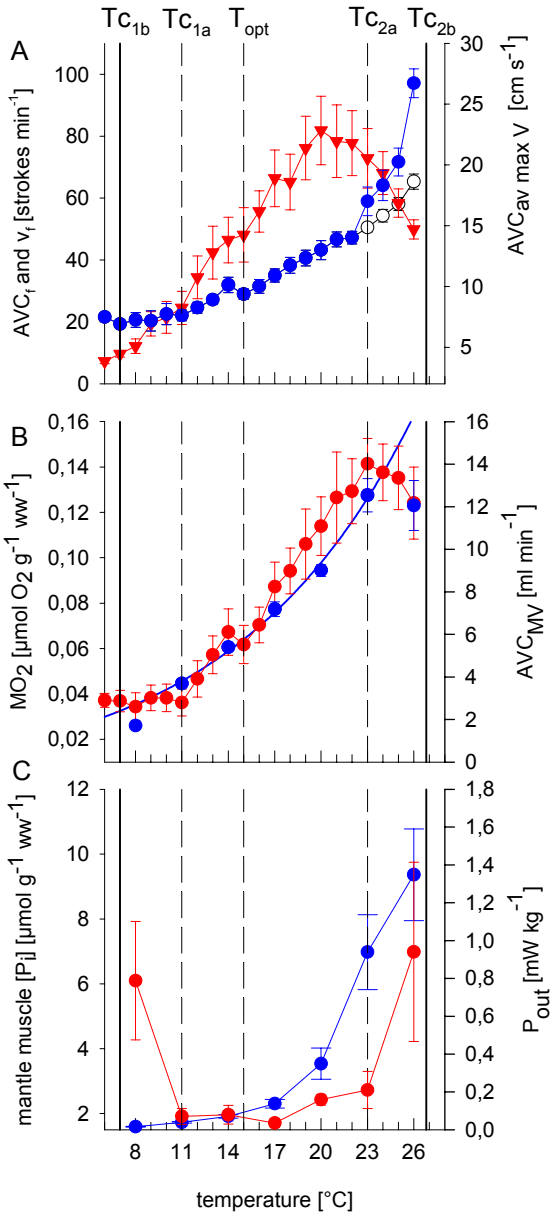

Fig 4.3 (equivalent to figure 5 in publication 5): Oxygen limitation of thermal tolerance in cuttlefish: summary of results. Mean values ±SE. (A) anterior vena cava pulse frequency (AVC_f), ventilatory frequency (v_f) and AVC average maximum blood velocity ($AVC_{av\ max\ V}$), (B) AVC minute volume (AVC_{MV}) and routine metabolic rate (MO_2) of 105g cuttlefish (C) ventilatory power output (P_{out}) of 105 g cuttlefish and inorganic phosphate content [P_i] of mantle muscle. T_{opt} = optimum and acclimation temperature (15°C), $T_{c1a,2a}$ = critical temperatures. T_{c1b} and T_{c2b} indicate the onset of anaerobic metabolism in ventilatory muscle tissues (see fig 4.4 and section c) for a discussion of threshold temperatures).

a) <u>*Decreasing temperature.*</u> In publication 1 we were able to demonstrate that temperature reduction does eventually result in a progressive transition to anaerobic metabolism in cuttlefish mantle tissue once a mean temperature of 7.0°C is being reached. *In vivo* ^{31}P NMR spectroscopic measurements clearly showed that phospho-L-arginine (PLA) stores were used to complement routine aerobic metabolism. PLA use results in an accumulation of inorganic phosphate in muscle cells (see fig 4.3c). Combined changes in cellular phosphagen status lead to progressively declining free energy of ATP hydrolysis values, the driving force for any ATPase mediated cellular process and to time limited survival. Publication 2 revealed that routine metabolic rate (MO_2 in fig 4.3b) deviates from the expected exponential pattern between 11 and 8°C, suggesting a limitation of aerobic metabolism at

higher temperatures already. Such a deviation to lower MO_2 beyond a low threshold temperature was typical for all experimental animals, regardless of body mass (15 – 495 g wet mass range studied; publication 3). This drop in oxygen consumption rate was not related to a failure of the ventilatory apparatus, as model calculations indicate that observed ventilatory effort is always able to provide the PO_2 gradients across gill epithelia required to support efficient haemocyanin oxygenation (publication 2). Significant changes in AVC blood flow mechanics occur: From 11 to 8°C, blood flow peak A contribution to total pulse flow (see publications 4, 5 for terminology) rose significantly above control patterns (Fig. 2b in publication 5). In addition, there was a trend towards an altered phase relationship between ventilatory pressure cycles and AVC blood flow pulses (Fig. 2c in publication 5). It is unclear, whether these changes in haemodynamics and ventilatory – circulatory integration are detrimental to the proper functioning of the oxygen transport chain. Surely they do correlate with the observed deviations of routine metabolic rate encountered in the same temperature interval. AVC minute volume (AVC_{MV}) stagnated in the very same temperature range (11 to 8°), despite decreasing routine metabolic rate. Literature data on the temperature sensitivity of haemocyanin function (Zielinski et al. 2001) and a separate data set on *in vivo* PO_2 in cuttlefish AVC (Johansen et al. 1982) suggested that low temperature may hamper haemocyanin unloading and decrease Ut, thus greatly increasing blood perfusion requirements (see publication 5 for a detailed discussion). However, determination of *in vivo* blood pH, haemocyanin oxygen saturation (S) and PO_2, in combination with *in vitro* studies on the thermal sensitivity of haemocyanin oxygen binding, led to a different picture (see figure 4.2 and table 4.1), due to higher pH values seen in cold exposed cuttlefish *in vivo*: Between 17 and 11°C, Ut does decrease from 75% to 62%, thus not as dramatically as estimated in publication 5. Still, blood perfusion has to be increased by roughly 20% at constant oxygen demand to compensate for these lower Ut values.

Apart from these minor changes in Ut, the major threat to organismic thermal tolerance in the cold probably are the low oxygen partial pressures encountered in the AVC and, likely, in the capillary bed as well. As they are already low at 17°C (1.3 kPa), they further drop down below 1 kPa at 11°C (table 4.1). For two animals, a mean PO_{2v} of 0.5 kPa was found at 8°C. Owing to the observed (and expected, Reeves 1972) upward shift in pH with declining temperature (table 4.1), maintenance of low oxygen partial pressures is the only means of liberating significant fractions of haemocyanin bound oxygen at low temperatures. Thus, high Ut, caused by proper haemocyanin unloading in the tissues, comes at the expense of very low venous PO_2. Whether the observed AVC oxygen partial pressures suffice to drive oxygen diffusion and match oxygen demand is questionable. Insufficient oxygen supply may result beyond 11°C, eventually leading to the onset of anaerobic metabolism.

Oxygen partial pressures in mammalian red muscle cells at rest range between 0.7 and 5 kPa and intracellular oxygen gradients are shallow owing to the presence of myoglobin (Mb). However, minimum intracellular PO_2 required for maximum cytochrome turnover in red muscle ranges between 0.04 and 0.07 kPa. Owing to large mitochondrial surface areas in relation to capillary diffusion areas,

oxygen diffusion gradients from cytosol to mitochondria are lower than 0.01 kPa (Clark et al. 1987, Gayeski and Honig 1986, 1988, Gayeski et al. 1987). As Honig and colleagues (1992) concluded from their studies, it is the PO_2 gradient between capillary and cytosol that is rate limiting for oxygen transfer. In marine teleosts, where venous PO_2 is the diffusion pressure head for the systemic heart, threshold PO_{2v} values of approximately 1 – 3.3 kPa have been identified to limit cardiac performance during exercise and at T_{c2} (Steffensen and Farrell 1998, Lannig et al. 2004). Venous oxygen partial pressures in fish swum to fatigue or subjected to hypoxia ranged between 0.8 - 2 kPa (Kiceniuk and Jones 1977, Lai et al.1990, Forster 1985). For invertebrates, there is only one record available relating extracellular PO_2 to intracellular anaerobiosis: Cold exposure and hypoxia in the peanut worm (*Sipunculus nudus*) result in a transition to an anaerobic mode of energy production, once coelomic fluid PO_2 reaches threshold values of about 0.5 - 0.7 kPa (Pörtner et al. 1985, Pörtner and Zielinski 1996).

Information on intracellular PO_2 and on oxygen diffusion gradients required to sustain adequate fluxes of oxygen into cells is neither available for cephalopods, nor for other molluscs. However, while the measured cuttlefish PO_{2v} values are in excess of those required for maximum cytochrome c oxidase turnover at all temperatures (see above), it is uncertain, whether exercising ventilatory muscle fibres at very low temperatures can maintain intracellular PO_2 (PO_{2i}) high enough: Kindig et al. (2003) found PO_{2i} to be approximately 10% less than extracellular PO_2 (PO_{2e}) in single isolated myocytes under resting conditions (several PO_{2e} tested in myoglobin deficient *Xenopus laevis* cells). Intensive contractile activity resulted in a sharp decline of PO_{2i}. Final steady state PO_{2i} under exercise conditions was dependent on PO_{2e}: At a PO_{2e} of 2.7 kPa, PO_{2i} levelled off at 0.4 kPa during increased contractile activity. At similar extra- to intracellular PO_2 differences for cuttlefish working ventilatory (myoglobin-less) muscle cells (PO_{2v} being equivalent to PO_{2e}), PO_2 values could become limiting for mitochondrial ATP synthesis at very low temperatures (8°C).

In conclusion, there is a good evidence that haemocyanin functional properties change with decreasing temperature in a way that buffer only very low blood PO_2 values in the tissues (< 1kPa at <11°C) and support only low rates of oxygen consumption. In addition, haemodynamic patterns in the AVC also start to deviate from control conditions below temperatures of 11°C, indicating a progressing disintegration of ventilatory and circulatory circuits. Cooling below 8°C leads to a progressive reliance of mantle muscle on anaerobic energy production, as pressure heads for oxygen diffusion might drop below critical values required for sufficient oxygen flux to mitochondrial cytochrome c oxidase.

b) *Increasing temperature.* Similar to the effect of cooling, warming also caused transition to anaerobic metabolism in cuttlefish mantle muscle beyond 26.8°C (publication 1). As spontaneous exercise did not contribute to phosphagen (PLA) utilization, an energetic limitation of constantly working (ventilatory) radial mantle muscle fibres was proposed to limit systemic oxygen transport (and vice versa). However, similar to the situation in the cold, routine metabolic rate (MO_2 in fig 4.3b)

started to deviate from the expected relationship already between 23 and 26°C (see publication 2), indicating that ventilatory failure probably resulted from capacity limitations first in other vital oxygen transfer system components. Stagnating oxygen consumption rates beyond 23°C (animals >100g body mass) to 26°C (animals <100g body mass) were found in all animals between 15 and 495 g body wet mass (publication 3) and likely indicate metabolic depression in response to oxygen limitation.

Correlated ventilatory and circulatory changes during warming have been discussed in greater detail in publication 5. Briefly, manifold increases in ventilatory power output (P_{out}, see fig 4.3c) were observed between 15 and 26°C. By dropping oxygen extraction (EO_2) and increasing ventilatory perfusion of the gills with more water, the ventilatory apparatus is probably always able to establish oxygen diffusion gradients across the gill epithelia as needed to ensure high PO_{2a} values of >14 kPa and full Hc oxygenation (publication 2). In contrast, the circulatory system already suffered from capacity limitation at lower temperatures: both AVC_{MV} and metabolic rate stagnates at about 23°C. Increased AVC blood velocity ($AVC_{av\ max\ v}$) and blood pulse rate (AVC_f) contributed to a 2.5 fold increase in AVC_{MV} between 15 and 23°C (publication 5), while MO_2 rose 2.2 fold in the same temperature interval. As Ut is already very high in cuttlefish blood (> 70%, see above and Johansen et al. 1982), temperature dependent increments in oxygen demand are likely provided by tantamount increases in blood perfusion rather than by changing haemocyanin oxygen shuttling properties. Haemodynamic patterns in the AVC at maximum blood flow at 20-23°C matched those observed under recovery from exercise surprisingly well (see publication 4), leading us to conclude that the *S. officinalis* circulatory system is designed in mechanical terms to sustain 2 – 2.5 fold increases in metabolic rate, regardless of the nature of the specific aerobic challenge (exercise, recovery, SDA or acute thermal change). Oxygen demand beyond maximum sustainable rates led to a progressive disintegration of correlated ventilatory and circulatory convection systems (publication 5): The ventilatory system depends on steadily rising ventilation frequency (v_f) to increase perfusion of the gills, which, on the other hand, negatively affects the correlated AVC blood pulse mechanics. Starting at temperatures of 20-21, $AVC_{av\ max\ V}$ can not be increased any more, while from 23°C on, peak A dominance, pulse splitting and decreasing $AVC_{av\ max\ V}$ result in stagnating AVC_{MV} despite rising AVC_f. In accordance with the principle of symmorphosis (Taylor and Weibel 1981), other cuttlefish circulatory organs have been observed to functionally disintegrate at about the same temperature as the AVC – ventilatory system (Mislin 1966, Fiedler 1992). Between 23 and 26.8, metabolic depression (e.g. Hochachka 1986) occurs, as routine MO_2 ranges below predicted rates (publication 2). At an average temperature of 26.8°C, all 5 animals investigated in publication 1 (using the *in vivo* ^{31}P NMR experimental set-up) were exploiting PLA reserves to supplement aerobic metabolism of radial mantle muscle fibres during ventilatory work. Eventually, levels of Gibb's free energy for ATP hydrolysis were calculated to drop below critical values of – 45 kJ mol^{-1} in phase $B_{extreme}$, likely causing decreasing ventilatory pressure in the mantle cavity due to radial fibre fatigue (see fig 6 in publication

1). In conclusion, an oxygen limitation of radial fibre metabolism is a secondary process caused by stagnating blood perfusion rates.

c) *Threshold temperatures*

Using the terminology and concepts introduced by Frederich and Pörtner (2000, see introduction), further modified by Pörtner (2001, 2002) and Pörtner et al. (2004), thermal thresholds for the European cuttlefish *Sepia officinalis* can be defined for the acute warming scenario. Briefly, key characteristics of the model are:

1) An optimum temperature range, characterized by maximum aerobic scope (AS_{max})
2) Pejus temperatures (T_{p1}, T_{p2}), characterized by transition from optimum to pejus ranges on both sides of the thermal spectrum; Aerobic scope (AS) is falls below AS_{max}.
3) Critical temperatures (T_{c1}, T_{c2}), characterized by a loss in aerobic scope and an onset of transition to an anaerobic mode of energy production.

Maximum scope for AVC_{MV} increases during exercise at 15°C and during warming from 15 to 23°C were found virtually identical. The cuttlefish circulatory system, acclimated to 15°C, is thus characterized by a set maximum blood perfusion capacity. Maximum blood perfusion rates in the AVC are reached with similar adjustments in AVC_f and $AVC_{av\ max\ V}$, both during recovery from exercise at 15°C and under resting conditions at 23°C. Apparently, v_f (and, correlated, AVC_f) must not increase above a critical frequency of about 46-50 cycles min^{-1} in animals acclimated to 15°C, as functional disintegration of the tightly connected ventilatory and circulatory systems occurs beyond this frequency (‚splitting frequency', publication 5). Therefore, it seems that mechanical properties of integrated circulatory and ventilatory systems determine maximum blood flow rates independent of (acutely modulated) ambient temperature, at least for temperatures above 15°C (again: exclusively for animals acclimated to 15°C). A fixed and constant upper ceiling for blood perfusion is proposed for cuttlefish between 15 and 23°C (termed Q_{max}) that is able to sustain maximum metabolic rates (mmr). Figure 4.4 schematically illustrates the consequences.

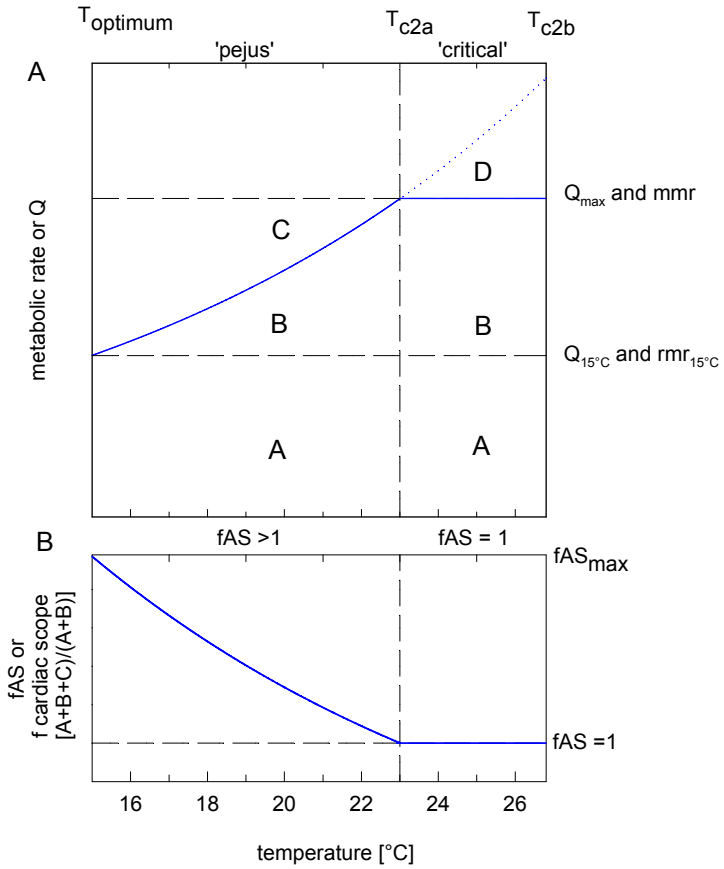

Fig 4.4. Schematic temperature tolerance model for cuttlefish subjected to acute temperature increase. Letters A-D refer to areas enclosed by the lines surrounding them. (A) routine metabolic rate (bold blue line) or, equivalently, cardiac output (Q) vs. temperature. The dotted blue line gives the expected development of rmr or Q beyond 23°C. The lower dotted horizontal line indicates rmr or Q at 15°C, the upper line maximum sustainable metabolic rate (mmr) or maximum sustainable Q (Q_{max}). (B) is a plot of factorial aerobic and factorial cardiac scope for activity. Factorial aerobic scope (fAS) = (A+B+C)/(A+B). Aerobic scope (AS *sensu* Fry 1947) corresponds to areas (C+B+A)-(B+A), i.e. area C. Factorial aerobic scope and cardiac scope = 1 at 23 – 26.8°C. $T_{optimum}$ (15°C) = optimum and acclimation temperature with AS and fAS at maximum values, T_{c2a} = critical temperature, fAS = 1, T_{c2b} = onset of anaerobic metabolism in mantle muscle; pejus interval = 15 – 23°C, critical interval = 23 –26.8°C. See text.

While the lower horizontal line in fig. 4.4a corresponds to routine metabolic rate and Q at 15°C, the upper one corresponds to maximal metabolic rate (mmr) that can be supported by the circulatory machinery (Q_{max}) at and beyond 15°C. The differential between both (equivalent to areas B+C) corresponds to the amount of metabolic energy and Q that can be allocated to the various oxygen sinks within the organism. As routine metabolic rate rises in its typical exponential fashion (areas A+B), progressively less oxygen is available for other aerobic activities (area C), thus, factorial aerobic scope (fAS, areas (A+B+C) / (A+B), fig 4.4b) or aerobic scope (AS, areas (A+B+C) - (A+B), fig 4.4b) decline progressively. The vertical line at 23°C characterizes the point at which routine metabolism consumes all aerobic energy, as Q_{max} is being reached, thus areas (A+B+C) = areas (A+B), i.e. fAS is 1. Beyond 23°C (T_{c2a}), Q and metabolic rate stagnate at highest levels at fAS = 1. Area D reflects the rising quantity of oxygen that the circulatory system cannot provide ('aerobic gap'). Therefore, there are two distinct phases between 15 and 26°C (fig. 4.4b): The interval of fAS > 1 (15-23°C) and the interval of AS = 1 (23-26.8°C). According to the definitions summarized above (1 to 3), the acclimation temperature of 15°C (T_{acclim}) would be the temperature of maximum aerobic

scope (fAS_{max}), therefore be called optimum temperature (T_{opt}), while the interval between fAS > 1 and < fAS_{max} would be the 'pejus' interval. It is important to note, that there is no optimum range (at least not in the 15 –26.8°C range), as fAS changes continuously with temperature.

In publication 1, we have assigned 26.8°C the critical temperature. However, as no residual aerobic scope is left at 23°C already (i.e. fAS = 1, see fig 4.3, 4.4), this threshold had to be lowered. Therefore, two natural thresholds could be identified, T_{c2a}, characterized by fAS reaching one, and T_{c2b}, characterized by the onset of anaerobic metabolism in ventilatory mantle muscle tissues at largely unaltered fAS. These temperatures enclose a 'critical interval of metabolic re-allocation'. Within this interval, it must be an altered regional blood flow distribution, likely in combination with metabolic depression (Hochachka 1986, Hochachka and Somero 2002) that protects those organs that are most important during short term aerobic stresses (i.e. ventilatory and circulatory organs, neuronal tissues). Such an altered blood flow and, therefore, oxygen and nutrient distribution within the body, was observed in several organisms (e.g. crustaceans, fish, turtles) in response to exercise or environmental stressors (Randall and Daxboeck 1982, Axelsson and Fritsche, Nilsson et al. 1994, Hylland et al. 1994, Frederich et al. 2000). Owing to the drastic decreases in the Gibb's free energy of ATP hydrolysis in radial mantle muscle fibres at T_{c2b}, this thermal threshold indicates time limited survival of the species (i.e. in the range of minutes to hours): It is this process of radial fibre fatigue, which subsequently results in a functional failure of the ventilatory apparatus (i.e. declining ventilation pressures, publication 1), further worsening the situation of the circulatory system and vice versa. Thus, a series of negative feedback processes is eventually leading to a complete failure of the oxygen transfer chain and the death of the animal (personal observation). Whether the critical range of fAS = 1 (23-26.8°C) already is an ‚incipient lethal temperature range' (*sensu* Fry 1971) for *S. officinalis*, or whether the acclimation potential of the species is sufficient (in terms of phenotypic plasticity and speed of acclimation) to reach a new cardiovascular and metabolic steady state (see also 4.2.2) yet remains to be established.

As we have no information available on maximum cardiovascular capacity and maximum (exercise or SDA - induced) metabolic rates of cuttlefish in the cold, it is impossible to test the thermal tolerance model characteristics 1 – 3 (see above) for temperatures below 15°C. However, a natural thermal threshold temperature was identified, as metabolic rate deviated from the expected exponential relationship with temperature (O'Dor and Wells 1987) between 8 and 11°C (see publication 2). This pattern of metabolic depression may well be due to oxygen limitations below a lower T_{c1a} of 11°C. Owing to potentially detrimental changes in haemodynamics, haemocyanin oxygen transport and PO_{2v}, occurring in the respective interval (see above), it is tempting to postulate a critical thermal range between 11 and 7°C, before a T_{c1b} characterizes the onset of anaerobic metabolism in the mantle musculature at 7°C (publication 1). Richard (1971) reported English Channel cuttlefish *S. officinalis* to be active only at temperatures > 10°C, indicating that the T_{c1a} of 11°C (see fig. 4.3) could indeed correspond to a loss in aerobic scope. Venous oxygen partial

pressures < 1 kPa thus are probably too low as diffusion heads to support increased oxygen fluxes during activity at temperatures < 10-11°C.

In summary, in a temperature interval of 11 – 23°C, rmr of 15°C acclimated cuttlefish of 104 – 495g wet mass follows an exponential relationship (see publication 3 for cuttlefish < 100g) enabled by tightly correlated ventilatory and circulatory convection systems. Lower than expected routine metabolic rates at temperatures beyond this interval (both, in the cold and in the warm) are the first indication of an organismic oxygen deprivation and likely correspond to a loss in aerobic scope, i.e. fAS = 1. Therefore these thresholds were termed critical temperatures (T_{c1a} = 11°C, T_{c2a} = 23°C). Important muscle groups (radial mantle fibres), however, can operate aerobically beyond critical temperatures. Anaerobic metabolism in these fibres sets in at T_{c1b} = 7.0°C and T_{c2b} = 26.8°C. On either side of the temperature window, these two threshold temperatures, T_{ca} and T_{cb}, comprise a 'critical interval of metabolic re-allocation', which, presumably, is characterized by alterations in oxygen distribution within the organism to support organs and muscles of immediate importance.

However, it has to be noted that the elaborated thermal thresholds are exclusively valid for 24 - 48 h food – deprived, 15°C long - term acclimated cuttlefish of body mass > 100 g and that they will not allow any conclusions on the thermal tolerance window of the species in the natural habitat. At least not before thermal acclimation effects on cuttlefish metabolism have been discussed in section 4.2.2.

d) common trends in high power marine ectotherms Fish and cephalopods are the only marine ectothermic animals that have evolved closed, high pressure circulatory systems and a high power mode of life (Packard 1972). While, generally, cephalopods are characterized by higher metabolic rates and higher cardiac output (Q) than fish (O'Dor and Webber 1986), factorial aerobic and cardiac scopes are roughly comparable between temperate species of comparable lifestyle (publication 4, Wells et al. 1988, Joaquim et al. 2004, Webber et al. 1998). Convergent developments towards high power life styles and the ability to increase metabolism by similar factors have also led to similar bottlenecks in the oxygen transfer chain: Generally, closed circulatory systems require more power than ventilatory systems, both in molluscs and fish (e.g. Bourne et al. 1990 for an intra - molluscan comparison). For example, the *S. officinalis* circulatory convection system consumes more than twice the amount of power than the ventilatory system does (table 4.3), largely due to elevated blood pressure needed to propel blood through low diameter vessels. These differences in pressure between ventilatory and circulatory systems are not compensated for by a higher oxygen transport capacity of Hc containing blood with respect to seawater (thus, lower system flow):

Table 4.3. Power requirements of cuttlefish *S. officinalis* fluid convection systems at 20°C:

S. officinalis 20°C	*Q (ml / min kg)*	*p (Pa)*	*P_{out} (mW / kg)*
circulation	70 (1)	1225 (2)	1.47
ventilation	620 (3)	60 (3)	0.62

Power output (mW kg^{-1} animal mass) required by ventilatory and circulatory convection systems. P_{out} = system power output; p = mean system pressure (Pa); Q = mean system flow (ml min^{-1} kg^{-1}) Power output estimated using P_{out} = p Q (O'Dor and Webber 1991). (1) cf. publication 5; (2) Schipp 1987, mean Aorta cephalica pressure; (3) cf. publication 2 table 1.

Fish ventilatory and circulatory convection systems are characterized by similar factorial differences in p and Q (Farrell and Jones 1992, Steffensen et al. 1982, Perry and McKendry 2001, Driedzic 1988). Although the principle of symmorphosis suggests that excess capacity of any system component of the oxygen transfer apparatus is being avoided (Taylor and Weibel 1981), it is quite straightforward to assume that this principle may be even more relevant for those components that are already ‚expensive' per se, i.e. the blood pumps. In addition, circulatory systems in both, fish and cephalopods, consist of a multitude of highly integrated subsystems (multiple contractile organs and vessels, multiple humoral and neuronal effectors etc.), while ventilatory systems typically are structured and regulated in a much simpler fashion (Wells 1983, Wood and Perry 1985, Schipp, 1987a,b, Farrell and Jones 1992, Bone et al. 1994a,b).

Based on these considerations and according to the concept of a hierarchy of thermal tolerance mechanisms (Pörtner 2002), it is not surprising to find the cardiovascular system to be the first system component to become limiting for oxygen transport during acute thermal change. As shown for the cuttlefish *S. officinalis* (see above), temperate teleost ventilatory systems are typically able to maintain high arterial PO_2 over the entire temperature range studied (e.g. Sartoris et al. 2003 for cod *Gadus morhua*), while the capacity of the circulatory system becomes limiting, both in the cold and in the warm (Lannig et al. 2004, *G. morhua*). Especially during acute warming, patterns of change in metabolic rate are very similar in cuttlefish and temperate teleosts: Both rainbow trout (*Oncorhynchus mykiss* Heath and Hughes 1973) and cod (4°C acclimated North Sea cod, Fischer 2003) show exponentially increasing metabolic rates that stagnate once a high threshold temperature is being surpassed. In the case of rainbow trout, this threshold is correlated with stagnating heart rates (Heath and Hughes 1973). For cod, it has been demonstrated that oxygen consumption rates correlate linearly with cardiac output during exercise (Webber et al 1998, but see also Brodeur et al. 2001). Given the same holds true for cardiac output during temperature increase, the threshold temperature Fischer (2002) identified would correlate with stagnating cardiac output, and thus exactly mirror the situation observed in *S. officinalis* beyond the T_{c2a}.

4.2.2 ‚Slow' ambient temperature change: Thermal acclimation

Typical thermal challenges in the natural habitat of the European cuttlefish *S. officinalis* in the English Channel and the Bay of Biscay are considerably less than the acute rate of 1°C h^{-1} imposed on animals in the present experiments. Typically, average rates of change in temperature are about 3°C $month^{-1}$, i.e. 0.1°C day^{-1} (fig. 4.6, Wang et al. 2003), thus potentially allowing animals to slowly adjust to seasonally varying thermal regimes. The following section will consider such seasonal acclimation effects.

Thermal acclimation of metabolic machinery and body structure is an expression of phenotypic plasticity common to most ectothermic animals in order to conserve functional integrity of metabolism, motor and growth performance at seasonally altered habitat temperatures (e.g. Fry and Hart 1948, Guderley and St-Pierre 2002, Johnston and Temple 2002, Gamperl and Farrell 2004). It may involve changes in muscle protein composition (Langfeld et al. 1991), muscle capillary densities (Johnston, 1982), muscle contractile properties (Johnston et al. 1985), and adjustments in enzyme concentrations or capacities and kinetic properties (e.g. Lehmann 1970, Sidell et al. 1973, Cai and Adelman 1989, Lucassen et al. 2003). Mitochondria, as the source for aerobically generated energy, are a primary target of thermal acclimation (Guderley and St-Pierre 2002). Cold acclimation leads to compensatory increased mitochondrial proliferation in fish muscle (Jankowsky and Korn 1965, Tyler and Sidell 1984), for example, with total tissue volume of mitochondria found to be three times higher in 5°C than in 25°C acclimated fish (striped bass, *Morone saxatilis*, Egginton and Sidell 1989). Thus, reduced enzymatic turnover rates at colder temperatures (Somero 1997) are compensated for by increased enzyme concentration and/or capacities and animal metabolic rate can be maintained at a comparable level at the new body temperature. Mwangangi and Mutungi (1994) observed oxygen consumption rates in nile tilapia (*Oreochromis niloticus*) acclimated to 20.5°C to be higher than those of 26.5 acclimated animals at any given test temperature (20, 25, 30°C). These differences were mirrored by higher citrate synthase (CS) activities in glycolytic and oxidative muscles in the 20.5°C acclimation group at a given assay temperature. As CS activity in tissues is commonly regarded as an indicator for mitochondrial proliferation (either in mitochondrial volume density (Tyler and Sidell 1984, Egginton and Sidell 1989) or for mitochondrial (intrinsic) capacity (St-Pierre et al. 1998), higher whole animal oxygen consumption rates in the 20.5°C vs. 26.5°C acclimation group are most probably causally linked to enhanced mitochondrial oxygen demand.

Full metabolic compensation, i.e. equal metabolic rates at control and acclimation temperature (Q_{10} = 1; type 2 adaptation, Precht 1958) stands against a complete lack of compensation, i.e. metabolic rate drops (rises) with decreasing (increasing) temperature (Q_{10} of 2 - 3; type 4 adaptation, Precht 1958). Type 4 adaptation has previously been suggested for cephalopod organisms (O'Dor and Wells 1987). However, these conclusions are based exclusively on oxygen consumption data for octopods (Borer and Lane 1971, Van Heukelem 1976, Wells et al. 1983). Only specimens of one species were raised under differing temperature regimes during the entire lifecycle (i.e. *Octopus maya*,

Q_{10} for MO_2 = 1.6; animals raised at 20 and 30°C, Van Heukelem 1976). None of these studies determined Q_{10} values for MO_2 during acute temperature change (e.g. at 0.5-2°C h^{-1}) compared to the effect of a long term (months rather than weeks) acclimation period to various temperatures. Yet, this is an absolute prerequisite for distinguishing between acclimation modes.

Consequently, and in addition to the investigation of acute temperature changes in 15°C acclimated animals, routine oxygen consumption (MO_2), ventilation frequencies (v_f) and mean ventilation pressures (MMP) were measured in cuttlefish raised at 20°C and acutely exposed to temperature changes, in order to accurately define the acclimation mode of cuttlefish. In contrast to the above mentioned study (O'Dor and Wells, 1987), the present investigations on cuttlefish (*S. officinalis*; English Channel population), show clear signs of metabolic compensation in this cephalopod:

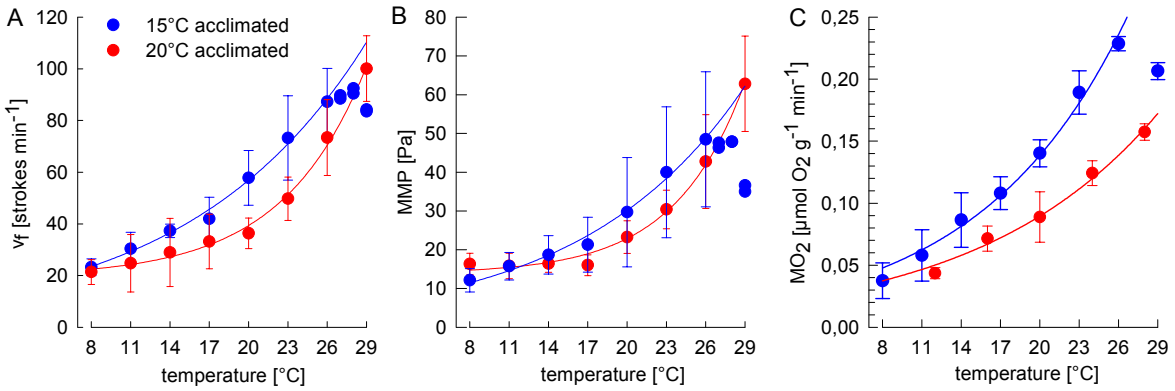

Figure 4.5: Effects of acclimation temperature on thermal tolerance of cuttlefish. Warm acclimated (WA = red symbols, 20°C; 5A, B: 104g, 5C: 12g) and cold acclimated (CA = blue symbols, 15°C: 1A, B 104 g wetmass, 1C: 10 g wetmass) animals. N = 5 animals at each temperature step, except for temperatures >26°C in WA animals (N=2), experiments with CA animals were terminated once significant inorganic phosphate accumulation in the mantle muscle organ occurred). A) Ventilation frequency (v_f), B) mean mantle cavity pressure (MMP), C) oxygen consumption rate (MO_2) or routine metabolic rate (rmr). Data was best represented by exponential fits (see table 4.5 below): y = y0 + a*exp(b*x) or y = a*exp(b*x). Comparison of linear plots of log transformed MO_2 data from both acclimation groups revealed that slopes could not be considered different from each other (test for heterogeneity of slopes: $F_{(1,51)}$ = 2.9; p>0.09). Subsequent ANCOVA revealed significant differences in oxygen consumption rates with acclimation temperature (ANCOVA, independent variable: acclimation temperature, dependent variable: MO_2, covariable: test temperature; $F_{(1,52)}$ = 74.7; p<0.001).

Table 4.4. Regression parameters for datasets displayed in figure 4.5.

	MMP (CA)	*MMP (WA)*	*v_f (CA)*	*v_f (WA)*	*MO_2 (CA)*	*MO_2 (WA)*
y0		13.77				
a	6.02	0.21	13.03	7.45	0.0235	0.0209
b	0.081	0.19	0.074	0.088	0.0887	0.0727
R^2	0.990	0.993	0.993	0.964	0.990	0.988
F	$F_{(1,5)}$ = 520	$F_{(2,5)}$ = 387	$F_{(1,5)}$ = 726	$F_{(1,6)}$ = 161	$F_{(1,5)}$ = 508	$F_{(1,3)}$ = 259
p	<0.001	<0.001	<0.001	<0.001	<0.001	<0.001

Routine metabolic rates for animals of 12 g body mass, raised at 15°C are consistently higher than those raised at 20°C at all test temperatures (see fig. 4.5c). Direct comparison of MO_2 values of cold acclimated animals (CA) at 14 and 20°C with those of warm acclimated (WA) at 20°C reveals that in CA animals, oxygen demand significantly increases between 14°C and 20°C, while WA metabolic rate does not differ significantly from the CA rate at 14°C (see ANOVA and SNK results in fig. 4.5). This indicates that complete thermal acclimation (type 2, Precht 1958) is taking place in the European cuttlefish *Sepia officinalis*. In concert with comparable metabolic rates found at both acclimation temperatures, v_f (table 4.5) of WA animals at 20°C did not differ significantly from that of CA animals at 15°C.

Table 4.5: Temperature acclimation in cuttlefish *Sepia officinalis*.

	ventilation frequency (v_f) *ANOVA: $F_{(2,12)} = 14.4$; $p < 0.001$*			*oxygen consumption (MO_2)* *ANOVA: $F_{(2,12)} = 10.5$; $p < 0.001$*		
SNK results	14 CA	20 CA	20 WA	14 CA	20 CA	20 WA
14 CA	X	<0.001	<0.84	X	<0.005	<0.85
20 CA	<0.001	X	<0.002	<0.005	X	<0.003
20 WA	<0.84	<0.002	X	<0.85	<0.003	X

ANOVA and subsequent Student – Newman –Keuls tests (SNK, if applicable) between 14 and 20°C test temperatures of cold acclimated (CA, 15°C) and 20°C test temperature of warm acclimated (WA, 20°C) animals. No significant differences were detected when comparing mean mantle cavity pressures (MMP; ANOVA: $F_{(2,12)} = 1.9$, $p>0.05$). Significant differences marked red.

Available evidence suggests that an acute temperature increase from 15 to 20°C would initially cause a significant rise in rmr according to the characteristic Q_{10} relationship (see publication 3), while during prolonged exposition to such an altered temperature regime, acclimation would probably ‚reset' metabolic rate as well as ventilatory and correlated cardiovascular variables (see publications 4, 5) to the original resting values at 15°C. But then: what would the functional significance of such an acclimatory response be? A first reason could be the maintenance of an energetical and mechanical optimum in correlated ventilatory and cardiovascular (i.e.AVC) function at acclimation temperature. In publication 5, we could demonstrate that AVC_{SV} is at its maximum at the long term acclimation temperature of 15°C (publication 5, fig 4). In addition, two other haemodynamic variables (peak A contribution to total flow, time of ventilatory period spent with forward blood flow) were characterized by minima at this temperature (publication 5, fig 2). Thus it appears that long term acclimation to a specific temperature can result in functional optimization of ventilatory pressure oscillations and anterior vena cava (AVC) blood flow. Similar findings have been reported for cardiovascular parameters in teleosts: For example, both isometric force and pumping capacity of *in vitro* perfused hearts of the burbot (*Loto lota*) were optimized at an acclimation temperature of 1°C with respect to acutely altered test temperatures (Tiitu and Vornanen 2002). Another likely reason for a ‚resetting' of cardiovascular variables is to conserve haemodynamic, and, in consequence, aerobic scope. Publications 4 and 5 developed the concept of an upper mechanical

threshold for proper anterior vena cava (AVC) function, witnessing a functional disintegration of correlated AVC and ventilatory movements once v_f surpassed a frequency of about 50 strokes min^{-1} (‚splitting frequency'). Although it is somewhat speculative to assume a similar upper cardiovascular working limit to be present in WA animals, there is some support for a similar hypothesis in the fish literature: For example, warm acclimation in goldfish (*C. auratus*, 10°C and 25°C) resulted in a resetting of intrinsic cardiac pacemaker activity to a lower rate, conserving scope for increases in heart frequency (h_f) (Morita and Tsukuda 1994). ‚Resetting' is necessary, as most teleost fish appear to have a fixed upper limit for maximum h_f, set at about 120 strokes min^{-1} (Farrell 1991, exception: tuna, Blank et al. 2002, 2004). In rainbow trout (*O. mykiss*) acclimated to 12°C, limiting heart frequencies are being reached at a temperature of 24°C (Heath and Hughes, 1973, Brodeur et al. 2001). Brodeur et al. (2001) and Webber et al. (1998) elaborated a tight linear correlation between h_f and MO_2 in salmonid and gadid teleosts during aerobic challenges. Obviously, resetting of h_f to a lower baseline value upon warm acclimation may be crucial for conserving aerobic scope. However, studies performed mainly on salmonid teleosts acclimated to a variety of test temperatures demonstrated that aerobic scope for exercise cannot be maintained constant for all temperatures, rather, temperature ranges with maximized aerobic scope could be identified (Keen and Farrell 1994, Taylor et al. 1996a,b, Farrell 1996, 2002). Typically for these high performance teleosts, factorial cardiac scopes can be maintained over a wide temperature window, whereas acclimation to high temperatures (greater than 15-20°C) results in decreased factorial cardiac scopes (see Farrell 2002 for a review).

Whether acclimation of cuttlefish to a relatively high temperature of 20°C results in a 1:1 conservation of aerobic scope for exercise and SDA remains to be investigated in more detail. However, between the acclimation temperature of 20°C and an acute test temperature of 28°C, animals were able to increase metabolic rate by a factor of 1.8. As there was no plateau in rmr reached within the thermal range studied in this acclimation group, it remains speculative whether WA animals have a similar metabolic scope as CA animals, which could increase rmr by a factor of 2.7 between acclimation temperature (15°C) and 26°C (differences in thermal thresholds with respect to fig. 4.3 originate from the comparatively small body size of animals used for the acclimation comparison, see also publication 3). Clearly, ‚resetting' of rmr enables WA animals to follow an exponential rmr relationship to higher temperatures of (at least) 28°C, while CA animals of comparable body mass could only increase rmr exponentially to 26°C (fig. 4.5c). These differences between acclimation groups are mirrored by changes in ventilation system parameters: WA animals can increase both v_f and MMP exponentially to 29°C, while CA animals are characterized by stagnating v_f and MMP beyond 26°C. Obviously, WA animals are not experiencing onset of anaerobic metabolism and correlated changes in radial fibre Gibb's free energy of ATP hydrolysis as early as CA animals. Thus, thermal acclimation can shift the thermal window of *S. officinalis* to higher temperatures. Whether tolerance to lower temperatures is decreased in WA compared to CA animals, remains to be

established. In the lugworm (*Arenicola marina*) such a parallel shift of both, high and low, critical temperatures has been observed in the course of seasonal acclimatization (Sommer at al. 1997).

Marine and freshwater fish typically acclimate rapidly to a new temperature regime: Sidell et al. (1973) showed cytochrome c oxidase and succinic dehydrogenase activities in goldfish (*Carassius auratus*) white muscle to adjust to new steady state activities following 3 - 4 weeks of exposure to temperatures lowered or raised by 10°C. Lucassen et al. (2003) determined stable and elevated citrate synthase activities in eelpout (*Zoarces viviparus*) liver following a 10 day acclimation period to 6.5° C lower temperatures. Cardiovascular parameters are also subject to rapid change during thermal acclimation: 3 – 4 weeks of exposure to a 10°C temperature drop resulted in an increase in relative ventricular mass by 20-40% in rainbow trout (*Oncorhynchus mykiss*), helping to maintain pressure development and Q in the cold (Farrell et al. 1988). Heart rate (h_f) of rainbow trout acclimated to 8 and 18° C for 3 weeks followed a Q_{10} relationship of 1.5 (Keen and Farrell 1994), while acute changes in temperature typically produce Q_{10} values for h_f of about 2.0 (e.g. Graham and Farrell 1985). In summary, available evidence indicates that temperate teleosts manage to acclimate metabolic machinery (tissue enzyme concentrations, mitochondrial densities) and cardiovascular system parameters (heart ultrastructure, heart functional characteristics, see Gamperl and Farrell 2004 for a review) to changes by up to 10°C within one month. Given temperate *S. officinalis* are characterized by a similar or even faster acclimation velocity than found in fish species, they should be able to always fully acclimate to the respective average habitat temperatures. As fig. 4.6b demonstrates, rates of change in average sea surface temperatures (SST, 1989-1998) in the natural habitats of both, English Channel and southern Bay of Biscay *S. officinalis* populations never exceed and are usually lower than 3° C per month (Wang et al. 2003):

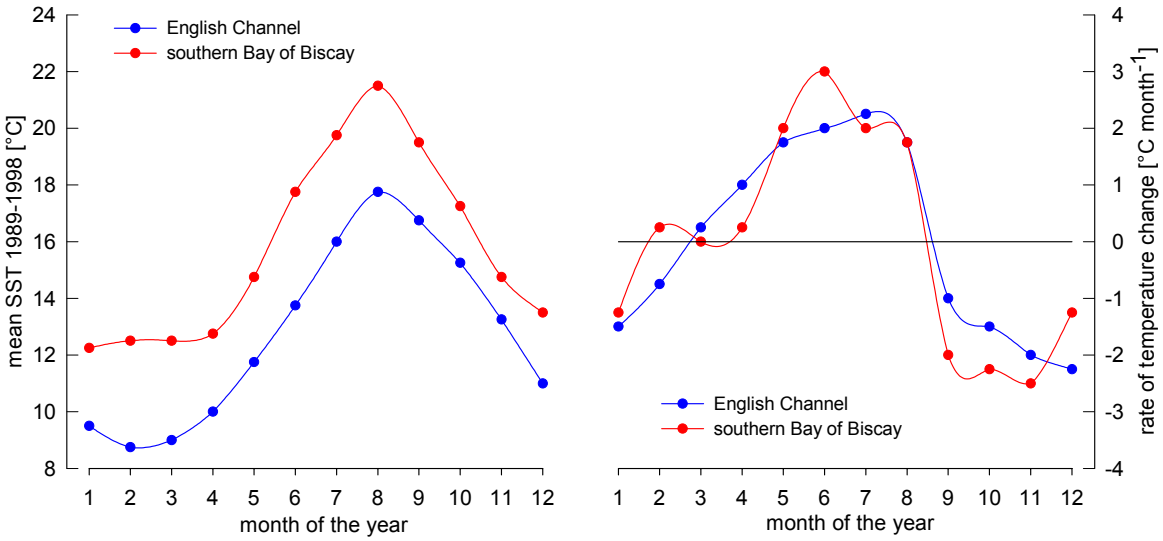

Fig 4.6. Mean sea surface temperatures (SST) in cuttlefish habitats in the English Channel (ICES subdivision 7d and 7e) and the southern Bay of Biscay (ICES subdivisions 8a and 8b) from 1989 – 1998 (Wang et al. 2003, fig. 3). (A) Mean SST, (B) mean rates of change in SST in °C month^{-1}. Month of the year: 1 = january, 12 = december. Rate of change for month 5 = mean temperature month 5 - mean temperature month 4. Boucaud - Camou and Boismery (1991) report sea bottom temperatures for the English Channel habitat to range between 10 and 17.5°C.

Thus, cuttlefish are likely able to adjust their thermal window and optima close to oscillating seasonal habitat temperatures. Whether they are also able to conserve cardiovascular and metabolic scopes for activity (i.e. SDA and aerobic scope for exercise) over the entire seasonal thermal cycle (fig 4.6a), is unclear at present, but may be an important prerequisite of the particular cephalopod life style: Growth rates in the field are high, even during the winter months. A fast SDA response, enabled by cardiovascular and metabolic scopes of 2-3, likely are the basis for English Channel and Bay of Biscay cuttlefish reaching a final body mass of 2000 - 2500 g in just about 1 - 2 years time (Gauvrit et al. 1997, LeGoff and Daguzan 1997, Dunn 1999).

4.3 Conclusions

A number of conclusions result from experiments carried out within this dissertation. When subjected to acute warming and cooling rates by 1°C h^{-1}, European cuttlefish *Sepia officinalis*, laboratory raised at 15°C, experience an oxygen limitation of thermal tolerance, as indicated by a progressive transition to anaerobic metabolism in ventilatory muscle systems. As found in teleosts (Mark et al. 2002, Sartoris et al. 2003, Lannig et al. 2004) and predicted by Pörtner (2002), an initial limitation in oxygen transfer capacity sets in at high levels of systemic complexity. Both in the warm and in the cold, detrimental changes in cardiovascular dynamics were observed in the major cuttlefish vein, the anterior vena cava (AVC). While impaired haemocyanin functioning may contribute to hamper oxygen transport in the cold, stagnating metabolic rates in the warm correlate with stagnating blood flow levels. A set of natural threshold temperatures (T_{c1a}, T_{c2a}, see above) prior to critical temperatures was identified at both sides of the temperature spectrum, characterized by routine metabolic rates dropping below expected values. But do such threshold temperatures, determined in acute thermal change (i.e. at rates of 1-2 °C h^{-1}) experiments, have any relevance in that they could predict the natural thermal window of the species, as proposed for other temperate marine ectotherms (*Maja squinado* Frederich and Pörtner 2000, *G. morhua*, Lannig et al. 2004)? Figure 4.7 illustrates why such an attempt would fail for the English Channel cuttlefish population:

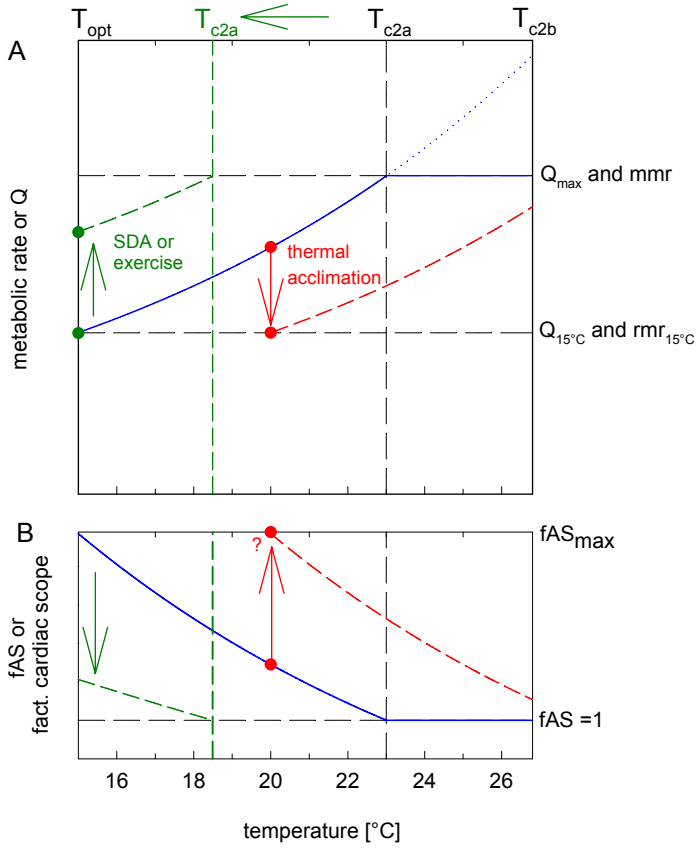

Fig 4.7. Effects of thermal acclimation, SDA of food and exercise on threshold temperatures between 15 and 27°C. The figure is virtually identical to fig. 4.4 (see above). (A) The green dotted curve illustrates the case of an animal whose metabolic rate has been significantly elevated due to the specific dynamic action of food (SDA) or due to exercise, reaching the threshold mark of factorial aerobic scope (fAS) = 1 at 18.5°C already. The red curve illustrates, how aerobic scope can be 'resetted' upon acclimation to a higher (20°C) temperature. T_{c2} shifts to a higher temperature in this case (not illustrated). (B) Corresponding (putative) changes in factorial aerobic scope (fAS).

The threshold temperatures elaborated in publications 1,2,3 and 5 are valid for animals >100g wet mass that

(1) were acclimated to 15°C and (2) have been starved for 24 - 48 h. As to (1), the results of the present investigation indicate that cuttlefish have the ability to fully acclimate to a new thermal regime. As the red curve in fig 4.7a illustrates, a resetting of routine metabolic rate and cardiac output (Q) upon warm acclimation results in elevated tolerance of higher temperatures. Therefore, cuttlefish likely have a different set of thermal threshold temperatures at each acclimation temperature in the natural habitat. Point (2) reflects a constraint unlikely to be effective in the natural habitat. As discussed above, acute temperature tolerance is a direct function of scope for increased blood flow, i.e. cardiac output (Q). As SDA and aerobic scope for exercise are also functions of Q, the following equation (3) describes the distribution of Q within the cuttlefish organism:

$$Q_{max} - (Q_{rmr15°C} + Q_T + Q_E + Q_{SDA} + Q_X) \geq 0 \quad (3)$$

with Q_{max} = maximum cardiac output = approximately 2-3 * $Q_{rmr15°C}$ in cephalopods, $Q_{rmr15°C}$ = Q needed to sustain rmr at 15°C, Q_T = temperature dependent Q increment, Q_E = exercise dependent Q increment, Q_{SDA} = SDA related Q increment, Q_X = Q for unidentified oxygen sinks. Thus, different aerobic sinks ‚compete' for the same limited ‚resource', i.e. cardiac output (Q). There is, however, still some uncertainty regarding the degree of additivity of aerobic sinks (see publication 5, Alsop and Wood 1997, Rolfe et al. 1999). At critical temperatures (T_{c2a}) determined in the acute warming experiments, $Q_E + Q_{SDA} + Q_X = 0$, and, therefore, Q_T exploits Q_{max}. On the other hand, previous workers have demonstrated that Q_{SDA} must be at constantly high levels in the natural habitat to sustain the fast growing mode of life in cephalopods (see above, O'Dor and Wells 1987). Therefore, figure 4.7 probably illustrates a more realistic case of an oxygen limitation of cuttlefish metabolism (green curve): With a substantial Q_{SDA} component present that ‚uses' more than 50% of available cardiac scope at 15°C (Wells et al. 1983b), Q_T is reduced and, as rmr rises with a Q_{10} of 2.5, a T_{c2a} is being reached at a temperature of about 18.5°C already, as compared to 23°C with $Q_{SDA} = 0$. With Q_E contributing significantly, T_{c2a} could be further lowered. These considerations illustrate the requirement to maintain optimum temperature close to ambient temperature.

T_{c2a} and T_{c2b} most likely are quite variable, as they shift readily with acclimation. However, owing to the potentially high contribution of SDA to average Q, it is evident that even minor thermal changes of 1-2°C day^{-1} can have considerable impact on cuttlefish performance (i.e. growth, reproduction) in the natural habitat and require instant onset of acclimation.

While the present study could elucidate some of the basic systemic mechanisms that contribute to oxygen and capacity limited thermal tolerance in a cephalopod model organism, it is not able to make predictions on the species natural thermal window. To construct such tolerance windows for the cuttlefish *Sepia officinalis*, more information on the actual physiological performance of animals acclimated to a variety of temperatures is necessary. Based on the present findings, identifying the acclimation temperature range in which aerobic and cardiac scopes are being maximized should correlate with the natural thermal window of the population, as could be demonstrated for fish species (Farrell 1996). As a wider implication from the present work the hypothesis was elaborated that the

thermal optimum closely follows ambient temperature fluctuations. This hypothesis should also be tested in the field and it should be investigated to what extent other, more hypometabolic animals like the spider crabs or cod would also be subject to the same dynamics of seasonal temperature acclimatization

5. References

ABBOT, N.J. AND BUNDGAARD, M. (1987). Microvessel surface area, density and dimensions in brain and muscle of the cephalopod *Sepia officinalis*. *Proc. R. Soc. Lond. B* **230**, 459-482.

AITKEN, J.P. AND O'DOR, R.K. (2004). Respirometry and swimming dynamics of the Australian cuttlefish *Sepia apama*. *Mar. Freshw. Behav. Physiol.* **37**, 217-234.

AITKEN, J. P., O'DOR, R. K. AND JACKSON, G. D (2005). The secret life of the giant cuttlefish *Sepia apama* (Cephalopoda): Behaviour and energetics in nature revealed through radio acoustic positioning and telemetry (RAPT). *J. Exp. Mar. Biol. Ecol.* **320**, 77-91.

ALSOP, D.H. and WOOD, C.M. (1997). The interactive effects of feeding and exercise on oxygen consumption, swimming performance and protein usage in juvenile rainbow trout (*Oncorhynchus mykiss*). *J. Exp. Biol.* **200**, 2337-2346.

AXELSSON, M. AND FRITSCHE, R. (1991). Effects of exercise hypoxia and feeding on the gastrointestinal blood flow in the Atlantic cod *Gadus morhua*. *J. Exp. Biol.* **158**, 181-196.

BALLANTYNE, J.S., HOCHACHKA, P.W. AND MOMMSEN, T.P. (1981). Studies on the metabolism of the migratory squid, *Loligo opalescens*: enzymes of tissues and heart mitochondria. *Mar. Biol. Lett.* **2**, 75-85.

BARTOL, I.K. (2001). Role of aerobic and anaerobic circular mantle muscle fibers in swimming squid: electromyography. *Biol. Bull.* **200**, 59-66.

BERT, P. (1867). Mémoire sur la physiologie de la Seiche. *Mém. Soc. Sci phys. Nat. Bordeaux* **5**, 115.

BLANK, J.M., MORRISSETTE, J.M, DAVIE, P.S. AND BLOCK, B.A. (2002). Effects of temperature, epinephrine and Ca^{2+} on the hearts of yellowfin tuna (*Thunnus albacares*). *J. Exp. Biol.* **205**, 1881-1888.

BLANK, J.M., MORRISSETTE, J.M, LANDEIRA-FERNANDEZ, A.M., BLACKWELL, S.B., WILLIAMS, T.D. AND BLOCK, B.A. (2004). *In situ* cardiac performance of Pacific bluefin tuna hearts in response to acute temperature change. *J. Exp. Biol.* **207**, 881-890.

BOCK, C., SARTORIS, F., WITTIG, R-M. AND PÖRTNER, H. O. (2001). Temperature-dependent pH regulation in stenothermal antarctic and eurythermal temperate eelpout (Zoarcidae): an *in vivo* NMR study. *Polar Biol.* **24**, 869-874.

BOCK, C., SARTORIS, F.J. AND PÖRTNER, H.O. (2002). *In vivo* MR spectroscopy and MR imaging on non anaesthetized marine fish : techniques and first results. *Magn. Reson. Imag.* **20**, 165-172.

BOLETZKY, S.v. (1983). *Sepia officinalis*. In: Boyle, P.R. (ed.). *Cephalopod life cycles. Vol 1*. Academic Press, London, pp.31-52.

BOLETZKY, S.v. AND BOLETZKY, M.V.v. (1970). Das Eingraben in Sand bei *Sepiola* und *Sepietta* (Mollusca, Cephalopoda). *Rev. suisse Zool.* **77**: 536-548.

BONE, Q., PULSFORD, A., CHUB, A.D. (1981). Squid mantle muscle. *J. mar. biol. Ass. U.K.* **61**, 327-342.

BONE, Q., BROWN, E. R. AND TRAVERS, G. (1994a). On the respiratory flow in the cuttlefish *Sepia officinalis*. *J. Exp. Biol.* **194**, 153-165.

BONE, Q., BROWN, E. R. AND USHER, M. (1994b). The structure and physiology of cephalopod muscle fibres. In *Cephalopod Neurobiology* (ed. N.J. Abbot, R. Williamson and L. Maddock), pp. 301-329. Oxford: Oxford University Press.

BORER, K.T. AND LANE, C.E. (1971). Oxygen requirements of *Octopus briareus* Robson at different temperatures and oxygen concentrations. *J. Exp. Mar. Biol. Ecol.* **7**, 263-269.

BOUCAUD – CAMOU, E. AND BOISMERY, J. (1991). The migrations of the cuttlefish (*Sepia officinalis*) in the English Channel. In: Boucaud-Camou, E. (Ed.), La Seiche, 1st International symposium on the cuttlefish *Sepia*. Center of publications, Universite de Caen. pp. 179-189.

BOURNE, G.B., REDMOND, J.T. AND JOHANSEN, K. (1978). Some aspects of haemodynamics in *Nautilus pompilius*. *J. Exp. Zool.* **205**, 63-70.

BOURNE, G. B. (1982). Blood pressure in the squid, *Loligo pealei*. *Comp. Biochem. Physiol.* **72**A, 23-27.

BOURNE, G.B., REDMOND, J.R. AND JØRGENSEN, D.D. (1990). Dynamics of the molluscan ciculatory system: open versus closed. *Physiol. Zool.* **63**: 140-166.

BOUTILIER, R.G., HEMING, T.A., IWAMA, G.K. (1984). Appendix: Physicochemical parameters for use in fish respiratory physiology. In Hoar, W.S. and Randall, D.J. (eds). *Fish Physiology.* Vol 10a, Academic Press.
BRETT, J.R. (1944). Some lethal temperature relations of Algonquin Park fishes. *Univ. Toronto Studies Biol. Ser.* **52**, 1-49.

BURTON, R. F. (2002). Temperature and acid-base balance in ectothermic vertebrates: the imidazole alphastat hypothesis and beyond. *J. Exp. Biol.* **205**, 3587-3600.

BRETT, J.R. (1946). Rate of gain of heat tolerance in goldfish (*Carassius auratus*). *Univ. Toronto Studies Biol. Ser.* **52**, 1-49.

BRETT, J.R. (1952). Temperature tolerance in young Pacific salmon genus *Oncorhynchus*. *J. Fish. Res. Board Can.* **9**, 265-323.

BRETT, J.R. (1958). Implications and assessment of environmental stress. In: Larkin, P.A. (ed): *Investigations of Fish-power problems*, H.R. Mac Millan Lectures in Fisheries, Univ. of Brit. Columbia, pp.69-83

BRETT, J.R. AND ALDERDICE, D.F. (1958). The resistance of cultured young chum and sockeye salmon to temperatures below 0°C. *J. Fish. Res. Board Can.* **15**, 805-813.

BRODEUR, J.C., DIXON, D.G. AND MCKINLEY, R.S. (2001). Assessment of cardiac output as a predictor of metabolic rate in rainbow trout. *J. Fish. Biol.* **58**, 439-452.

BRIDGES, C.R., BICUDO, J.E.P.W. AND LYKKEBOE, G. (1979). Oxygen content measurement in blood containing haemocyanin. *Comp. Biochem. Physiol.* A **62**, 457-462.

BRIX, O., LYKKEBOE, G., JOHANSEN, K. (1981). The significance of the linkage between the Bohr and Haldane coefficients in cephalopod bloods. *Respir. Physiol.* **44**, 177-186.

BRIX, O., BÅRGARD, A., CAU, A., COLOSIMO, A, CONDO, S.G., GIARDINA, B. (1989). Oxygen binding properties of cephalopod blood with special reference to environmental temperatures and ecological distribution. *J. Exp. Zool.* **252**, 34-42.

CAI, Y.J. AND ADELMANN, I.R. (1990). Temperature acclimation in respiratory and cytochrome c oxidase activity in common carp (*Cyprinus carpio*). *Comp. Biochem. Physiol*. **95**A, 139-144.

CAMERON, J. N. AND CECH, J.R. (1970). Notes on the energy cost of gill ventilation in teleosts. *Comp. Biochem. Physiol.* **34**, 447-455.

CLARK, A., CLARK, P.A.A., CONNETT, R.C. GAYESKI, T.E.J., HONIG, C.R. (1987). How large is the drop in PO_2 between cytosol and mitochondria? *Am. J. Physiol.* **256**, C583-C587.

COMBS, C. A. AND ELLINGTON, W. R. (1997). Intracellular sodium homeostasis in reaction to the effective free-energy change of ATP hydrolysis: studies of crayfish muscle fibers. *J. Comp. Physiol. B* **167**, 563-569.

CURTIN, N.A. AND WOLEDGE, R.C. (1988). Power output and force velocity relationships of live fibers from white myotomal muscle of the dogfish, *Scyliorhinus canicula*. *J. Exp. Biol.* **140**, 187-197.

CURTIN, N.A., WOLEDGE, R.C. AND BONE, Q. (2000). Energy storage by passive elastic structures in the mantle of *Sepia officinalis*. *J. Exp. Biol.* **203**, 869-878.

DEMONT, M.E. AND O'DOR, R.K. (1984). The effects of activity, temperature and mass on the metabolism of the squid *Illex illecebrosus*. *J. Mar. Biol. Ass. U.K.* **64**, 535-543.

DENIS, V. AND ROBIN, J.P. (2001). Present status of French Atlantic fishery for cuttlefish (*Sepia officinalis*). *Fish. Res.* **182**, 1-12.

DENTON, E.J. AND GILPIN-BROWN, J.B. (1961a). The buoyancy of the cuttlefish, *Sepia officinalis* (L.). *J. mar. Biol. Ass. U.K.* **41**, 319-342.

DENTON, E.J. AND GILPIN - BROWN, J.B. (1961b). The effect of light on the buoyancy of the cuttlefish. *J. mar. Biol. Ass. U.K.* **41**, 343-350.

DE WACHTER, B., SARTORIS, F. AND PÖRTNER, H.O. (1997). The anaerobic endproduct lactate has a behavioural and metabolic signalling function in the shore crab. *J. Exp. Biol.* **200**, 1015-1024.

DE WILDE, J. (1956). Koordination im Gefässsystem von *Octopus vulgaris*. *L. Pubbl. staz. zool. Napoli* **28**, 359-366.

DOUMEN, C. AND ELLINGTON, W. R. (1992). Intracellular free magnesium in the muscle of an osmoconforming marine invertebrate: measurement and effect of metabolic and acid-base pertubations. *J. Exp. Zool.* **261**, 394-405.

DRIEDZIC, W.R. (1988). Matching of cardiac oxygen delivery and fuel to supply to energy demand in teleosts and cephalopods. *Can. J. Zool.* **66**, 1078-1083.

DUNN, M.R. (1999). Aspects of the stock dynamics and exploitation of cuttlefish, *Sepia officinalis* (Linnaeus, 1758), in the English Channel. *Fish. Res.* **40**, 277-293.

EGGINTON, S. AND SIDELL, B.D. (1989). Thermal acclimation induces adaptive changes in subcellular structure of fish skeletal muscle. *Am. J. Phys.* **256**, R1-R9.

FARRELL, A.P. (1991). From hagfish to tuna – a perspective on cardiac function. *Phys. Zool.* **64**, 1137-1164.

FARRELL, A.P. (1996). Effects of temperature on cardiovascular performance. In: Wood, C.M. and McDonald, D.G. Global Warming: Implications for freshwater and marine fish. Soc. Exp. Biol. Sem. Ser. 61. Cambridge University Press, Cambridge, pp. 135-158.

FARRELL, A.P. (2002). Cardiorespiratory performance in salmonids during exercise at high temperature: insights into cardiovascular design limitations in fishes. *Comp. Biochem. Physiol.* **132**A, 797-810.

FARRELL, A.P. AND JONES, D.R. (1992). The heart. In: Hoar, W.S., Randall, D.J. and Farrell, A.P. *Fish Physiology, Vol 12a. Cardiovascular Systems*. Academic Press, New York, pp. 1-88.

FARREL, A.P. AND CLUTTERHAM, S.M. (2003). On-line venous oxygen tensions in rainbow trout during graded exercise and at two acclimation temperatures. *J. Exp. Biol*. **206**, 487-497.

FARRELL, A.P., HAMMONS, A.M., GRAHAM, M.S. AND TIBBITS, G.F. (1988). Cardiac growth in rainbow trout, *Salmo gairdneri*. *Can. J. Zool.* **66**, 2368-2373.

FARRELL, A.P., GAMPERL, A.K., HICKS, J.M.T., SHIELS, H.A. AND JAIN, K.E. (1996). Maximum cardiac performance of rainbow trout (*Oncorhynchus mykiss*) at temperatures approaching their upper lethal limit. *J. Exp. Biol.* **199**, 663-672.

FIEDLER, A. (1992). Die Rolle des venösen Füllungsdrucks bei der Autoregulation der Kiemenherzen von *Sepia officinalis* L. (Cephalopoda). *Zool.jb. Physiol.* **96**, 265-278.

FINKE, E., PÖRTNER, H.O., LEE, P.G. AND WEBBER, D.M. (1996). Squid (*Lolliguncula brevis*) life in shallow waters: oxygen limitation of metabolism and swimming performance. *J. Exp. Biol.* **199**, 911-921.

FISCHER. T. (2002). The effects of climate induced temperature change on cod (*Gadus morhua*): linking ecological and physiological investigations. Ph.D. Dissertation, University of Bremen.

FORSTER, M.E. (1985). Blood oxygenation in shortfinned eels during swimming and hypoxia: Influence of the Root effect. *N.Z.J. Mar. Freshwater Res.* **19**, 247-251.

FORSYTHE, J.W. AND VAN HEUKELEM, W.F. (1987). Growth. In: Boyle, P.R. (Ed.) *Cephalopod life cycles, Vol. 2, Comparative reviews*, Academic Press, London, pp. 135–156.

FORSYTHE, J.W., DERUSHA, R.H. AND HANLON, R.T. (1994). Growth, reproduction and life span of *Sepia officinalis* (Cephalopoda: Mollusca) cultured through seven consecutive generations. *J. Zool. Lond.* **233**, 175-192.

FREDERICH, M. AND PÖRTNER, H. O. (2000). Oxygen limitation of thermal tolerance defined by cardiac and ventilatory performance in spider crab, *Maja squinado*. *Am. J. Physiol.* **279**, R1531-R1538

FREDERICH, M., DE WACHTER, B., SARTORIS, F. AND PÖRTNER, H.O. (2000). Cold tolerance and the regulation of cardiac performance and hemolymph distribution in *Maja squinado* (Crustacea: Decapoda). *Physiol. Biochem. Zool.* **73**, 406-415.

FRY, F.E.J., BRETT, J.R. AND CLAWSON, G.H. (1942). Lethal limits of temperature for young goldfish. *Rev. Can. Biol.* **1**, 50-56.

FRY, F.E.J., HART, J.S. AND WALKER, K.F. (1946). Lethal temperature relations for a sample of young speckled trout. *J. Fisheries Res. Board Can.* **23**, 1121-1134.

FRY, F.E.J. (1947). Effects of the environment on animal activity. *University of Toronto Studies Biology Series* **55**, 1-62.

FRY, F.E.J. (1971). The effect of environmental factors on the physiology of fish. In: Hoar and Randall (eds.) *Fish Physiology, Vol 6: Environmental relations and behavior*. Academic Press, New York, pp. 1-98.

FRY, F.E.J. AND HART, J.S. (1948). The relation of temperature to oxygen consumption in the goldfish. *Biol. Bull.* **94**, 66-77.

GAMPERL, A.K AND FARRELL, A.P. (2004). Cardiac plasticity in fishes: environmental influences and intraspecific differences. *J. Exp. Biol.* **207**, 2539-2550.

GAUVRIT, E., LE GOFF, R. AND DAGUZAN, J. (1997). Reproductive cycle of the cuttlefish, *Sepia officinalis* (L.) in the northern part of the Bay of Biscay. *J. Moll. Stud.* **63**, 19-28.

GAYESKI, T.E.J. AND HONIG, C.R. (1986). O_2 gradients from sarcolemma to cell interior in a red muscle at maximal VO_2. *Am. J. Physiol.* **251**, H789-H799.

GAYESKI, T.E.J. AND HONIG, C.R. (1988). Intracellular PO_2 in long axis of individual fibers in working dog gracilis muscle. *Am. J. Physiol.* **254**, H1179-H1186.

GAYESKI, T.E.J., CONNETT, R.J. AND HONIG, C.R. (1987). Minimum intracellular PO_2 for maximum cytochrome turnover in red muscle *in situ*. *Am. J. Physiol.* **252**, H906-H915.

GRAHAM, M. AND FARRELL, A.P. (1985). The seasonal intrinsic cardiac performance of a marine teleost. *J. Exp. Biol.* **118**, 173-183.

GUDERLEY, H., AND ST-PIERRE, J. (2002). Going with the flow or life in the fast lane: contrasting mitochondrial responses to thermal change. *J. Exp. Biol.* **205**, 2237-2249.

HAASE, A. (1990). Snapshot FLASH MRI. Applications to T1, T2 and chemical shift imaging. *Magn. Reson. Med.* **13**, 77-89.

HANLON, R.T. (1990). Maintenance, rearing and culture of teuthoid and sepioid squids. In:Gilbert, D.L., Adelman, Jr., W.J. (eds). *Squids as experimental animals*. Plenum Press, New York, pp. 35-62.

HEATH, A, G. AND HUGHES, G. M. (1973). Cardiovascular and respiratory changes during heat stress in the rainbow trout (*Salmo gairdneri*). *J. Exp. Biol.* **59**, 323-338.

HOCHACHKA, P.W. (1986). Defense strategies against hypoxia and hypothermia. *Science* **231**, 234-241.

HOCHACHKA, P.W. (1994). Oxygen efficient design of cephalopod muscle metabolism. In *Physiology of Cephalopod Molluscs: Lifestyle and Performance Adaptations*, eds. H.O. Pörtner R. K. O'Dor and D. L. Macmillan, pp. 61-67. Basel: Gordon and Breach.

HOCHACHKA, P.W. AND SOMERO, G.N. (2002). *Biochemical Adaptation. Mechanism and process in physiological evolution*. Oxford University Press, Oxford, 466 pp.

HOCHACHKA, P.W., FRENCH, C.J, AND MEREDITH, J. (1978). Metabolic and ultrastructural organization in *Nautilus* muscles. *J. Exp. Zool.* **205**, 51-62.

HOCHACHKA, P.W., MOMMSEN, T.P., STOREY, J.M., STOREY, K.B., JOHANSEN, K. AND FRENCH, C.J. (1983). The relationship between arginine and proline metabolism in cephalopods. *Mar. Biol. Lett*. **4**, 1-21.

HOFF, J.G. AND WESTMAN, J.R. (1966). The temperature tolerance of three marine species of fish. *J. Marine Res.* **24**, 131-140.

HONIG, C.R., CONNETT, R.J. AND GAYESKI, T.E.J. (1992). O_2 transport and its interaction with metabolism; a systems view of aerobic capacity. *Med. Sci. Sports Exerc.* **24**, 47-53.

HOULIHAN, D.F., DUTHIE, G., SMITH, P.J., WELLS, M.J. AND WELLS, J. (1986). Ventilation and circulation during exercise in *Octopus vulgaris*. *J. Comp. Physiol. B* **156**, 683-689.

HOWELL, B.J. AND GILBERT, D.L. (1976). pH - temperature dependence of the hemolymph of the squid, *Loligo pealei*. *Comp. Biochem. Physiol. A* **55**, 287-289.

HUGHES, G. M. (1973). Respiratory responses to hypoxia in fish. *Amer. Zool.* **13**, 475-489.

HULME, M., BARROW, E.M., ARNELL, N.W., HARRISON, P.A., JOHNS, T.C. AND DOWNING, T.E. (1999). Relative impacts of human – induced climate change and natural climate variability. *Nature*, **397**, 688-691.

HYLLAND, P., NILSSON, G. AND LUTZ, P. (1994). Time course of anoxia-induced increase in cerebral blood flow rate in turtles: Evidence for a role of adenosine. *J. Cereb. Blood Flow Metab.* **14**, 877-881.

JANKOWSKY, H.D. AND KORN, H. (1965). The influence of acclimation temperature on the mitochondrial content of fish muscle. *Naturwissenschaften* **52**, 642-643.

JANSEN, M. A., SHEN, H., ZHANG, L., WOLKOWICZ, P.E. AND BALSCHI, J. A. (2003). Energy requirements for the Na^+ gradient in the oxygenated isolated heart: effect of changing the free energy of ATP hydrolysis. *Am. J. Physiol.* **285**, H2437-H2445.

JOAQUIM, N., WAGNER, G.N. AND GAMPERL, A.K. (2004) Cardiac function and critical swimming speed of the winter flounder (*Pleuronectes americanus*) at two temperatures. *Comp. Biochem. Physiol. A* **138**, 277-285.

JOBLING, M. (1982). A study of some factors affecting rates of oxygen consumption of plaice, *Pleuronectes platessa* L. *J. Fish. Biol.* **20**, 501-516.

JØRGENSEN, C.B. AND RIISGÅRD, H.U. (1988). Gill pump characteristics of the soft clam *Mya arenaria*. *Mar. Biol.* **99**, 107-109.

JOHANSEN, K. and MARTIN, A. W. (1962). Circulation in the cephalopod, *Octopus dofleini*. *Comp.Biochem. Physiol.* **5**, 161-176.

JOHANSEN, K., BRIX, O. AND LYKKEBOE, G. (1982). Blood gas transport in the cephalopod, *Sepia officinalis*. *J. Exp. Biol.* **99**, 331-338.

JOHNSTON, I.A. AND TEMPLE, G.K. (2002). Thermal plasticity of skeletal muscle phenotype in ectothermic vertebrates and its significance for locomtory behaviour. *J. Exp. Biol.* **205**, 2305-2322.

JOHNSTON, I.A. (1982). Capillarisation, oxygen diffusion distances and mitochondrial content of carp muscles following acclimation to summer and winter temperatures. *Cell Tissue Res.* **222**, 325-337.

JOHNSTON, I.A., SIDELL, B.D., AND DRIEDZIC, W.R. (1985). Force – velocity characteristics and metabolism of carp muscle fibres following temperature acclimation. *J. Exp. Biol.* **119**, 239-249.

KAMMERMEIER, H., SCHMIDT, P. AND JÜNGLING, E. (1982). Free energy change of ATP-hydrolysis: a causal factor of early hypoxic failure of the myocardium? *J. mol. Cell. Cardiol.* **14**, 267-277.

KATSANEVAKIS, S. PROTOPAPAS, N., MILIOU, H. AND VERRIOPOULOS, G. (2005). Effect of temperature on specific dynamic action in the common octopus, *Octopus vulgaris* (Cephalopoda). *Mar. Biol.* **146**, 733-738.

KEEN, J.E. AND FARRELL, A.P. (1994). Maximum prolonged swimming speed and maximum cardiac performance of rainbow trout, *Oncorhynchus mykiss*, acclimated at two different water temperatures. *Comp. Biochem. Physiol.* **108**A, 287-295.

KICENIUK, J.W. AND JONES, D.R. (1977). The oxygen transport system in trout (*Salmo gairdneri*) during sustained exercise. *J. Exp. Biol.* **69**, 247-260.

KIER, W.M AND SMITH, K.K. (1985). Tongues, tentacles and trunks: the biomechanics of movement in muscular hydrostats. *Zool. J. Linnean Soc.* **83**, 307-324.

KINDIG, CA, HOWLETT,R.A. AND HOGAN, M.C. (2003). Effect of extracellular PO_2 on the fall in intracellular PO_2 in contracting single myocytes. *J. Appl. Physiol.* **94**, 1964-70.

KING, A.J., HENDERSON, S.M., SCHMIDT, M.H., COLE, A.G., ADAMO, S.A. (2005). Using ultrasound to understand vascular and mantle contributions to venous return in the cephalopod *Sepia officinalis* Linneaus. *J. Exp. Biol.* **208**, 2071-2082.

KOST, G. J. (1990). PH standardization for phosphorus – 31 magnetic resonance heart spectroscopy at different temperatures. *Magn. Res. Med.* **14**, 496-506.

LAI, N.C., GRAHAM, J.B. AND BRUNETT, L. (1990). Blood respiratory properties and the effect of swimming on blood gas transport in the leopard shark, *Triakis semifasciata*, during exercise: the role of the pericadioperitoneal canal. *J. Exp. Biol.* **151**, 161-173.

LANGFELD, K.S., CROCKFORD, T.C. AND JOHNSTON, I.A. (1991). Temperature acclimation in the common carp: force-velocity characteristics and myosin subunit composition of slow muscle fibres. *J. Exp. Biol.* **155**, 291-304.

LANNIG, G., BOCK, C., SARTORIS, F. J. AND PÖRTNER, H. O. (2004). Oxygen limitation of thermal tolerance in cod, *Gadus morhua* L. studied by magnetic resonance imaging (MRI) and on-line venous oxygen monitoring. *Am. J. Physiol.* **287**, R902-R910.

LEE, P.G. (1994). Nutrition in cephalopods: fueling the system. In: H.O. Pörtner R. K. O'Dor and D. L. Macmillan (eds.). *Physiology of Cephalopod Molluscs: Lifestyle and Performance Adaptations*. Basel: Gordon and Breach, pp. 35-52.

LE GOFF, R. AND DAGUZAN, J. (1991). Growth and life cycles of the cuttlefish *Sepia officinalis* L. (Mollusca: Cephalopoda) in south Brittany (France). *Bull. Mar. Sci.* **49**, 341-348.

LEHMANN, J. (1970). Veränderungen der Enzymaktivitäten nach einem Wechsel der Adaptationstemperatur, untersucht am Seitenrumpfmuskel des Goldfisches (*Carassius auratus*). *Int. Rev. Hydrobiol.* **55**, 763-781.

LUCASSEN, M, SCHMIDT, A., ECKERLE, L.G. AND PÖRTNER, H.O. (2003). Mitochondrial proliferation in the permanent vs. temporary cold: enzyme activities and mRNA levels in Antarctic and temperate zoarcid fish. *Am. J. Physiol.* **258**, R1410-R1420.

MACY, W.K. (1980). The ecology of the common squid, *Loligo pealei* LeSueur, 1821, in Rhode Island waters. Ph.D. Dissertation, University of Rhode Island, 236 pp.

MANGOLD, K. (1966). *Sepia officinalis* de la Mer Catalane. *Vie Milieu* **17**, 961-1012.

MANGUM, C.P. (1990). Gas transport in the blood. In: Gilbert, D.L., Adelman jr, W.J., Arnold, J.M. (eds.) *Squid as experimental animals*. Plenum Publishing Corporation, New York, pp. 443-468.

MARK, F. C., BOCK, C. AND PÖRTNER, H. O. (2002). Oxygen – limited thermal tolerance in Antarctic fish investigated by MRI and ^{31}P – MRS. *Am. J. Physiol.* **283**, R1254-R1262.

MATHER, J.A. AND O'DOR, R.K. (1991). Foraging strategies and predation risk shape the natural history of juvenile *Octopus vulgaris*. *Bull. Mar. Sci.* **49**: 245-269.

MELZNER, F., FORSYTHE, J.W., LEE, P.G., WOOD, J.B., PIATKOWSKI, U. AND CLEMMESEN, C. (2005). Estimating recent growth in the cuttlefish *Sepia officinalis*: are nucleic acid based indicators for growth and condition the method of choice? *J. Exp. Mar. Biol. Ecol.* **317**, 37-51.

MESSENGER, J. B., NIXON, M. AND RYAN, K. P. (1985). Magnesiumchloride as an anaesthetic for cephalopods. *Comp. Biochem. Physiol. C* **82**, 203-205.

MILLER, K. (1994) Cephalopod haemocyanins. A review of structure and function. In: H.O. Pörtner R. K. O'Dor and D. L. Macmillan (eds.). *Physiology of Cephalopod Molluscs: Lifestyle and Performance Adaptations*. Basel: Gordon and Breach, pp. 101-120.

MILLIGAN, B. J., CURTIN, N. A. AND BONE, Q. (1997). Contractile properties of obliquely striated muscle from the mantle of squid (*Alloteuthis subulata*) and cuttlefish (*Sepia officinalis*). *J. Exp. Biol.* **200**, 2425-2436.

MISLIN, H. AND KAUFFMANN, M. (1948). Der aktive Gefässpuls in der Armschrimhaut der Cephalopoden. *Rev. suisse Zool.* **55**, 267-271.

MISLIN, H. (1950). Nachweis einer reflektorischen Regulation des peripheren Kreislaufs der Cephalopoden. *Experientia* **6**, 467-468.

MISLIN, H. (1966). Ueber die Beziehungen zwischen Atmung und Kreislauf bei Cephalopoden (*Sepia officinalis* L.). Synchronregistrierung von Elektrokardiogramm (Ekg) und Atembewegungen am schwimmenden Tier. *Verh. Dtsch. Zool. Ges.* 175-181.

MOMMSEN, T.P. AND HOCHACHKA, P.W. (1981). Respiratory and enzymatic properties of squid heart mitochondria. *Eur. J. Biochem.* **120**, 345-350.

MOMMSEN, T.P., BALLANTYNE, J., MACDONALD, D., GOSLINE, J. AND HOCHACHKA, P.W. (1981). Analogues of red and white muscle in squid mantle. *Proc. Natl. Acad. Sci. USA* **78**, 3274-3278.

MOON, T.W. AND HULBERT, W.C. (1975). The ultrastructure of the mantle musculature of the squid, *Symplectoteuthis oualaniensis*. *Comp. Biochem. Physiol. B* **52**, 145-149.

MORITA, A. AND TSUKUDA, H. (1994). The effect of thermal acclimation on the electrocardiogram of goldfish. *J. Therm. Biol*. **19**, 343-348.

MWANGANI, D.M. AND MUTUNGI, G. (1994). The effects of temperature acclimation on the oxygen consumption and enzyme activity of red and white muscle fibres isolated from the tropical freshwater fish *Oreochromis niloticus*. *J. Fish. Biol.* **44**, 1033-1043.

NAKAMURA, Y. (1991). Tracking the mature female of flying squid, *Ommastrephes bartrami*, by an ultrasonic transmitter. *Bull. Hokkaido Nat. Fish. Res. Inst.* **55**: 205-208.

NILSSON, G.E., HYLLAND, P. AND LÖFMAN, C.O. (1994). Anoxia and adenosine induce increased cerebral blood flow rate in crucian carp *Am. J. Physiol.* **267**, R590-R595.

O'DOR, R.K. AND WELLS, M.J. (1978). Reproduction vs. somatic growth: Hormonal control in *Octopus vulgaris*. *J. Exp. Biol.* **77**, 15-31.

O'DOR, R.K. AND WEBBER, D.M. (1986). The constraints on cephalopods: why squid aren't fish. *Can. J. Zool.* **64**, 1591-1605.

O'DOR, R. K. AND WELLS, M. J. (1987). Energy and nutrient flow. In: Boyle, P. R. (ed.), *Cephalopod life cycles*, Comparative reviews. (Vol. 2) Academic Press, London, pp. 109-133.

O'DOR, R. K. AND WEBBER, D. M. (1991). Invertebrate athletes: trade – offs between transport efficiency and power density in cephalopod evolution. *J. Exp. Biol.* **160**, 93-112.

O'DOR, R.K., HOAR, J.A., WEBBER, D.M., CAREY, F.G., TANAKA, S., MARTINS, H.R. AND PORTEIRO, F.M. (1994). Squid (*Loligo forbesi*) performance and metabolic rates in nature. *Mar. Freshw. Behav. Physiol.* **25**: 163-177.

PACKARD, A. (1972). Cephalopods and fish: limits of convergence. *Biol. Rev.* **47**, 241-307.

PACKARD, A. AND TRUEMAN, E.R. (1974). Muscular activity of the mantle of *Sepia* and *Loligo* (Cephalopoda) during respiratory movements and jetting, and its physiological interpretation. *J. Exp. Biol.* **61**, 411-419.

PASCUAL, E. (1978). Crecimiento y alimentacion de tres generacions de *Sepia officinalis*. *Investigationes Pesqa* **42**, 15-22.

PAULIJ, W.P., BOGAARDS, R.H. AND DENUCE, J.M. (1990). Influence of salinity on embryonic development and the distribution of Sepia officinalis in the Delta Area (South Western part of the Netherlands). *Mar. Biol.* **107**, 17-23.

PAULIJ, W.P. HERMAN, P.M.J., ROOZEN, M.E.F. AND DENUCE, J.M. (1991). The influence of photoperiodicity on hatching of *Sepia officinali*s. *J. Mar. Biol. Ass. U.K.* **71**, 665-678.

PERRY, S.F. AND MCKENDRY, J.E. (2001). The relative roles of external and internalCO_2 versus H^+ in eliciting the cardiorespiratory responses of *Salmo salar* and *Squalus acanthias* to hypercarbia. *J. Exp. Biol.* **204**, 3963-3971.

PIIPER, J. (1998). Branchial gas transfer models. *Comp. Biochem. Physiol.* **119**A, 125-130

PÖRTNER, H.O. (1990a). Determination of intracellular buffer values after metabolic inhibition by fluoride and nitrilotriacetic acid. *Respir. Physiol.* **81**, 275-288.

PÖRTNER, H.O. (1990b). An analysis of the effects of pH on oxygen binding by squid (*Illex illecebrosus, Loligo pealei*) haemocyanin. *J. Exp. Biol.* **150**, 407-424.

PÖRTNER, H.O. (1994). Coordination of Metabolism, acid-base regulation and haemocyanin function in cephalopods. In *Physiology of Cephalopod Molluscs: Lifestyle and Performance Adaptations*, eds. H.O. Pörtner R. K. O'Dor and D. L. Macmillan, pp. 131-148. Basel: Gordon and Breach.

PÖRTNER, H.O. (2001). Climate change and temperature dependent biogeography: oxygen limitation of thermal tolerance in animals. *Naturwissenschaften* **88**, 137-146.

PÖRTNER, H.O. (2002a). Climate change and temperature dependent biogeography: systemic to molecular hierarchies of thermal tolerance in animals. *Comp. Biochem. Physiol.* **132A**, 739-761.

PÖRTNER, H. O. (2002b). Environmental and functional limits to musclular exercise and body size in marine invertebrate athletes. *Comp. Biochem. Physiol. A* **133**, 303-321.

PÖRTNER, H.O., HEISLER, N. AND GRIESHABER, M.K. (1985). Oxygen consumption and mode of energy production in the intertidal worm Sipunculus nudus L: definition and characterization of the critical PO_2 for an oxyconformer. *Respir. Physiol.* **59**, 361-377.

PÖRTNER, H.O., WEBBER, D.M., BOUTILIER, R.G. AND O'DOR, R.K. (1991). Acid-base regulation in exercising squid (*Illex illecebrosus, Loligo pealei*). *Am. J. Physiol.* **261**, R239-R246.

PÖRTNER, H.O., WEBBER, D.M., O'DOR, R.K. AND BOUTILIER, R.G. (1993). Metabolism and energetics in squid (*Illex illecebrosus, Loligo pealei*) during muscular fatigue and recovery. *Am. J. Physiol.* **265**, R157-R165.

PÖRTNER, H. O., FINKE, E. AND LEE, P. G. (1996), Metabolic and energy correlates of intracellular pH in progressive fatigue of squid (*L. brevis*) mantle muscle. *Am. J. Physiol.* **271**, R1403-R1414.

PÖRTNER, H.O., MARK, F.C. AND BOCK, C. (2004). Oxygen limited thermal tolerance in fish? Answers obtained by nuclear magnetic resonance techniques. *Respir. Physiol. Neurobiol.* **141**, 243-260.

PRECHT, H. (1958). Concepts of the temperature adaptation of unchanging reaction systems of cold-blooded animals. In: Prosser, C.L. (ed). *Physiological Adaptations*, Am. Physiol. Soc. Washington, D.C.

RANDALL, D.J. AND DAXBOECK, C. (1982). Cardiovascular changes in the rainbow trout (*Salmo gairdneri* Richardson) during exercise. *Can J. Zool.* **60**, 1135-1140.

REEVES, R. B. (1972). An imidazole alphastat hypothesis for vertebrate acid –base regulation: tissue carbon dioxide content and body temperature in bullfrogs. *Respir. Physiol.* **14**, 219-236

RICHARD, A. (1971). Contribution à l'étude expérimentelle de la croissance et de la maturation sexuelle de *Sepia officinalis* L. (Mollusque Céphalopode). Ph.D. Dissertation, Univ. Lille, 264 pp.

ROLFE, D.F.S., NEWMAN, J.M.B., BUCKINGHAM, J.A., CLARK, M.G. AND BRAND, M.D. (1999). Contribution of mitochondrial proton leak to respiration rate in working skeletal muscle and liver to smr. *Am J. Phys.* **276**, C692-C699.

SACKTOR, B. (1976). Biochemical adaptations for flight in the insect. *Biochem. Soc. Symp.* **41**, 111-131.

SARTORIS, F. J., BOCK, C., SERENDERO, I., LANNIG, G. AND PÖRTNER, H. O. (2003). Temperature – dependent changes in energy metabolism, intracellular pH and blood oxygen tension in the Atlantic cod. *J. Fish. Biol.* **62**, 1239-1253.

SCHIPP, R. (1987a). The blood vessels of cephalopods. A comparative morphological and functional survey. *Experientia* **43**, 525-537.

SCHIPP, R. (1987b). General morphological and functional characteristics of the cephalopod circulatory system. An introduction. *Experientia* **43**, 474-477.

SENOZAN, N.M., AVINC, A. AND UNVER, Z. (1988). Hemocyanin levels in *Octopus vulgaris* and the cuttlefish *Sepia officinalis* from the Aegean Sea. *Comp. Biochem. Physiol.* **91**A, 581-585.

SHADWICK, R.E. (1994). Mechanical oraganization of the mantle and circulatory system of cephalopods. In *Physiology of Cephalopod Molluscs: Lifestyle and Performance Adaptations*, eds. H. O. Pörtner R. K. O'Dor and D. L. Macmillan), pp. 69-85. Basel: Gordon and Breach.

SHADWICK, R.E. AND NILSSON, E.K. (1990). The importance of vascular elsticity in the circulatory system of the cephalopod *Octopus vulgaris*. *J. Exp. Biol.* **152**, 471-484.

SHADWICK, R. E., O'DOR, R. K. AND GOSLINE, J. M. (1990). Respiratory and cardiac function during exercise in squid. *Can. J. Zool.* **68**, 792-798.

SHELFORD, V.E. (1931). Some concepts of bioecology. *Ecology* **12**, 455-467.

SIDELL, B.D. (1980). Response of goldfish (*Carassius auratus* L.) muscle to acclimation temperature: alterations in biochemistry and proportions of different fibre types. *Physiol. Zool.* **53**, 98-107.

SIDELL, B.D., WILSON, F.R., HAZEL, J AND PROSSER, C.L. (1973). Time course of thermal acclimation in goldfish. *J. comp. Physiol.* **84**, 119-127.

SKRAMLIK, E.v. (1941). Über den Kreislauf bei den Weichtieren. *Ergebn. Biol.* **18**, 88-286.

SMITH, L. S. (1962). The role of venous peristalsis in the arm circulation of *Octopus dofleini*. *Comp. Biochem. Physiol.* **7**, 269-275.

SOMERO, G.N. (1997). Temperature relationships: from molecules to biogeography. In: Dantzler, W.H. (ed) Handbook of Physiology, section 13, vol. 2, Oxford University Press, Oxford, pp. 1391-1444.

SOMMER, A. KLEIN, B. AND PÖRTNER, H.O. (1997). Temperature induced anaerobiosis in two populations of the polychaete worm *Arenicola marina* (L.). *J. Comp. Physiol. B* **167**, 25-35.

STEFFENSEN, J.F. AND FARRELL, A.T. (1998). Swimming performance, venous oxygen tension and cardiac performance of coronary ligated rainbow trout, *Oncorhynchus mykiss*, exposed to progressive hypoxia. *Comp. Biochem. Physiol. A* **119**, 585-592.

STEFFENSEN, J. F., LOMHOLT, J. P., JOHANSEN, K. (1982). Gill ventilation and O_2 extraction during graded hypoxia in two ecologically distinct species of flatfish, the flounder (*Platichthys flesus*) and the plaice (*Pleuronectes platessa*). *Env. Biol. Fish.* **2**, 157-163.

ST-PIERRE, J. CHAREST, P.M. AND GUDERLEY, H. (1998). Relative contribution of quantitative and qualitative changes in mitochondria to metabolic compensation during seasonal acclimatisation of rainbow trout, *Oncorhynchus mykiss*. *J. Exp. Biol.* **201**, 2961-2970.

STOREY, K.B. AND STOREY, J.M. (1978). Energy metabolism in the mantle muscle of the squid, *Loligo pealeii*. *J. Comp. Physiol.* **123**, 169-175.

STOREY, K. B. AND STOREY, J. M. (1979). Octopine metabolism in the cuttlefish, *Sepia officinalis*: octopine production by muscle and its role as an aerobic substrate for non-muscular tissues. *J. Comp. Physiol.* **131**, 311-319.

STOREY, K.B. AND STOREY, J.M. (1983). Carbohydrate metabolism in cephalopod molluscs. In: Hochachka, P.W. (ed.) *The Mollusca Vol. 1.* Academic Press, New York, London, pp. 91-136.

TAYLOR, C.R. AND WEIBEL, E.R. (1981). Design of the mammalian respiratory system. 1. Problem and strategy. *Respir. Physiol.* **44**, 1-10.

TAYLOR, C.R., KARAS, R.H., WEIBEL, E.R. AND HOPPELER, H. (1987). Adaptive variation in the mammalian respiratory system in relation to energy demand. *Resp. Physiol.* **69**, 1-127.

TAYLOR, E.W., EGGINTON, S., TAYLOR, S.E. AND BUTLER, P.J. (1996a). Factors which may limit swimming performance at different temperatures. In: Wood, C.M. and McDonald, D.G. *Global Warming: Implications for freshwater and marine fish*. Soc. Exp. Biol. Sem. Ser. 61. Cambridge University Press, Cambridge, pp. 105-133.

TAYLOR, S.E., EGGINTON, S. AND TAYLOR, E.W. (1996b). Seasonal temperature acclimatisation of rainbow trout: cardiovascular and morphometric influcences on maximal sustainable exercise level. *J. Exp. Biol.* **199**, 835-845.

TIITU, V. AND VORNANEN, M. (2002). Regulation of cardiac contractility in a cold stenothermal fish, the burbot *Lota lota* L. *J. Exp. Biol.* **205**, 1597-1606.

TOMPSETT, D.H. (1939). *Sepia*. LMBC Memoirs, Liverpool University Press, 184 pp.

TROST, M. (2003). Ökophysiologische Untersuchungen zur Temperaturtoleranz von *Sepia officinalis*. Abschlussbericht 'Jugend forscht', 15 pp.

TUCKER, V.A. (1967). A method for the measurement of oxygen content and dissociation curves on microliter blood samples. *J. Appl. Physiol.* **23**, 407-410.

TYLER, S. AND SIDELL, B.D. (1984). Changes in mitochondrial distribution and diffusion distances in muscle of goldfish upon acclimation to warm and cold temperatures. *J. Exp. Zool.* **232**, 1-9.

VALVERDE, J.C. AND GARCIA, B.G. (2004). Influence of body weight and temperature on post prandial oxygen consumption of common octopus (*Octopus vulgaris*). *Aquaculture* **233**, 599-613.

VAN DIJK, P. L. M., TESCH, C., HARDEWIG, I. AND PÖRTNER, H. O. (1999). Physiological disturbances at critically high temperatures: a comparison between stenothermal antarctic and eurythermal temperate eelpouts (zoarcidae). *J. Exp. Biol.* **202**, 3611-3621.

VAN HEUKELEM, W.F. (1976). Growth, bioenergetics and life-span of *Octopus cyanea* and *Octopus maya*. Ph.D. Dissertation, University of Hawaii, 224 pp.

VOGEL, S. (1994). Life in moving fluids: the physical biology of flow. Princeton University Press, 467 pp.

WANG, J., PIERCE, G.J., BOYLE, P.R., DENIS, V., ROBIN, J.P. AND BELLIDO, J.M. (2003). Spatial and temporal patterns of cuttlefish (*Sepia officinalis*) abundance and environmental influences – a case study using trawl fishery data in French Atlantic coastal, English Channel, and adjacent waters. *ICES J. Mar. Sci.* **60**, 1149-1158.

WEBBER, D. M. AND O'DOR, R. K. (1986). Monitoring the metabolic rate and activity of free – swimming squid with telemetered jet pressure. *J. Exp. Biol.* **126**, 205-224.

WEBBER, D.M., BOUTILIER, R.G. AND KERR, S.R. (1998). Cardiac output as a predictor of metabolic rate in cod *Gadus morhua*. *J. Exp. Biol.* **204**, 3561-3570.

WEBBER, D.M., AITKEN, J.P. AND O'DOR, R.K. (2000). Costs of locomotion and vertic dynamics of cephalods and fish. *Physiol. Biochem. Zool.* **73**, 651-662.

WELLS, M.J. (1983). Circulation in cephalopods. In Saleuddin, A.S.M. and Wilbur, K.M. (eds.): *The Mollusca* Vol 5, Physiology Part 2, pp. 239-290. Academic Press, New York.

WELLS, M. J. (1990). Oxygen extraction and jet propulsion in cephalopods. *Can. J. Zool.* **68**, 815-824.

WELLS, M. J. AND WELLS, J. (1982). Ventilatory currents in the mantle of cephalopods. *J. Exp. Biol.* **99**, 315-330.

WELLS, M. J. AND WELLS, J. (1983). The circulatory response to acute hypoxia in *Octopus*. *J. Exp. Biol.* **104**, 59-71.

WELLS, M. J. AND WELLS, J. (1985). Ventilation frequencies and stroke volumes in acute hypoxia in *Octopus*. *J. Exp. Biol.* **118**, 445-448.

WELLS, M. J. and SMITH, P. J. S. (1987). The performance of the octopus circulatory system: A triumph of engineering over design. *Experientia* **43**, 487-499.

WELLS, M. J. AND WELLS, J. (1991). Is *Sepia* really an octopus? In Boucaud-Camou, E. (Ed.), La Seiche, 1st International symposium on the cuttlefish *Sepia*. Centre de publications, Universite de Caen. pp. 77-92.

WELLS, M.J., O'DOR, R.K., MANGOLD, K. AND WELLS, J. (1983a). Oxygen consumption and movement by *Octopus*. *Mar. Behav. Physiol.* **9**, 289-303.

WELLS, M.J., O'DOR, R.K., MANGOLD, K. AND WELLS, J. (1983b). Feeding and metabolic rate in *Octopus*. *Mar. Behav. Physiol.* **9**, 305-317.

WELLS, M. J., DUTHIE, G. G., HOULIHAN, D. F., SMITH, P. J. S. AND WELLS, J. (1987). Blood Flow and Pressure Changes in Exercising Octopuses (*Octopus vulgaris*). *J. Exp. Biol.* **131**, 175-187.

WELLS, M. J., HANLON, R. T., LEE, P. G. AND DIMARCO, F. P. (1988). Respiratory and Cardiac Performance in *Lolliguncula brevis* (Cephalopoda, myopsida): the Effects of Activity, Temperature and Hypoxia. *J. Exp. Biol.* **138**, 17-36.

WOOD, C.M. AND PERRY, S.F. (1985). Respiratory, circulatory, and metabolic adjustments to exercise in fish. In: Gilles, R. (ed). Circulation, Respiration and Metabolism. Current comparative approaches. Springer, Berlin, pp. 2-22.

WITTENBERG, J.B. AND WITTENBERG, B.A. (1990). Mechanisms of cytoplasmatic hemoglobin and myoglobin. *Ann. Rev. Biophys. And Chem.* **19**, 217-241.

ZIELINSKI, S. AND PÖRTNER, H. O. (1996). Energy metabolism and ATP free - energy change of the intertidal worm *Sipunculus nudus* below a critical temperature. *J. Comp. Physiol. B* **166**, 492-500.

ZIELINSKI, S., LEE, P.G. AND PÖRTNER, H.O. (2000). Metabolic performance of the squid *Lolliguncula brevis* (Cephalopoda) during hypoxia: an analysis of the critical PO_2.

ZIELINSKI, S., SARTORIS, F. AND PÖRTNER, H.O. (2001). Temperature effects on hemocyanin oxygen binding in an Antarctic cephalopod. *Biol. Bull*. **200**, 67-76.

Frank Melzner
Bgm. Martin-Donandt Platz 32
27568 Bremerhaven

Bremerhaven, den 05. Juli 2005

Erklärung gem. § 5 (1) Nr. 3 PromO

Ich erkläre hiermit,

1. dass ich mich vor dem jetzigen Promotionsverfahren keinem anderen Promotionsverfahren unterzogen habe

und

2. dass ich außer dem jetzt laufenden Promotionsverfahren auch kein anderes beantragt habe.

(Frank Melzner)